JCMK

JOURNAL OF CLINICAL MEDICINE OF KAZAKHSTAN

Recognised for exellence 5 star

Online ISSN 2313-1519
Print ISSN 1812-2892
www.clinmedkaz.org

№23 (2) 2026

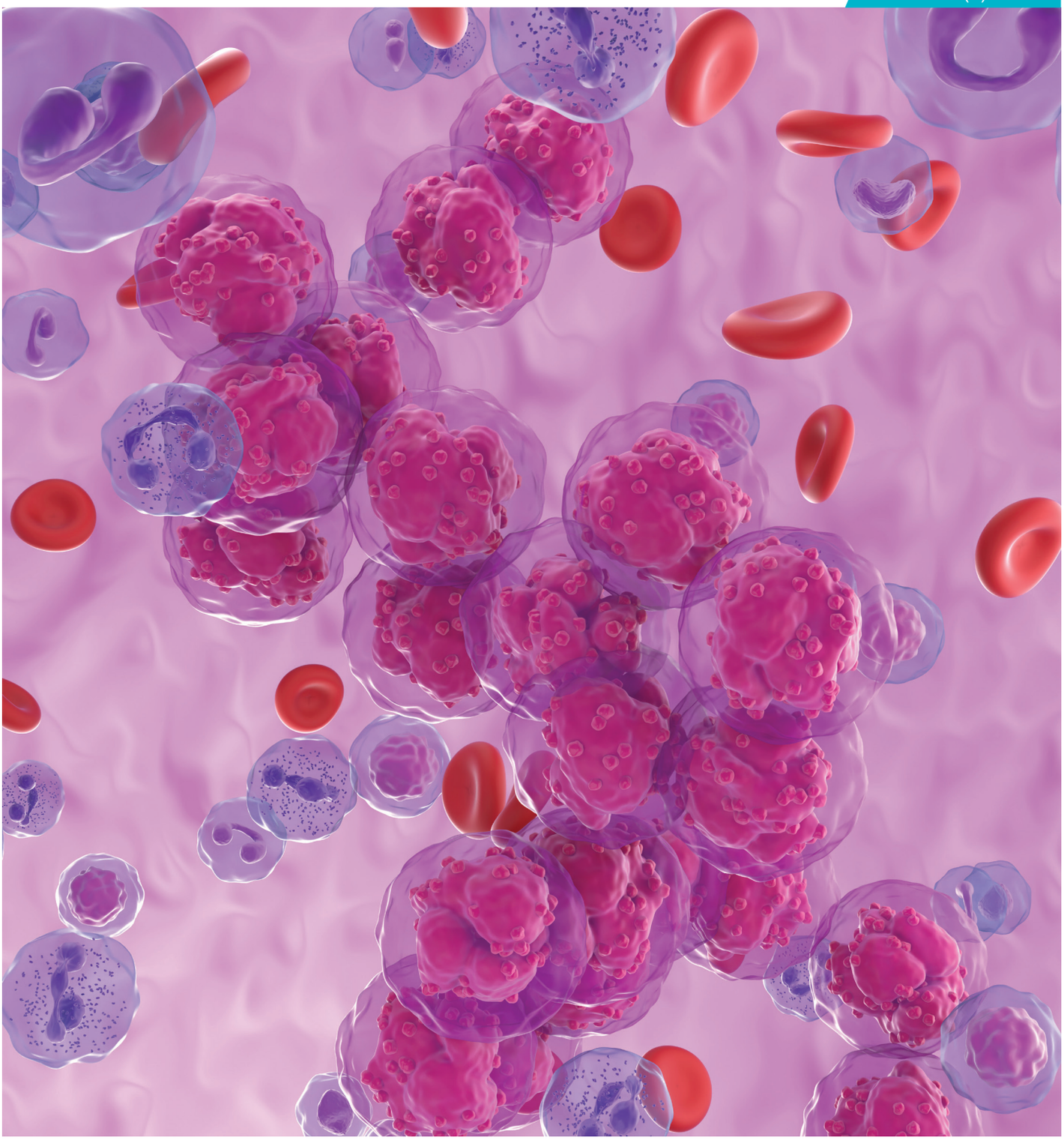

16-Year Epidemiologic Study of Chronic Myeloid Leukemia in Azerbaijan: Clinical and Molecular Insights

> See page 6 and 18

Cytogenetic Characteristics and Treatment Outcomes of Congenital Acute Leukemia in Children in Kazakhstan: Retrospective Study

> See page 51 and 56

Impact of Nanocellulose-Based Biocomposite Implantation on Rodent Behavior in the Elevated Plus Maze Test

> See page 104 and 108

JCMK
JOURNAL OF CLINICAL MEDICINE OF KAZAKHSTAN

Online ISSN 2313-1519
Print ISSN 1812-2892
№23 (2) 2026
Published since 2004.

EFQM Recognised for exellence 5 star
TÜV CERT Management system as per ISO 9001:2000

EDITORIAL

FOUNDER and HONORED EDITOR
Abay Baigenzhin (Kazakhstan).
Scopus ID: 55484939900
https://orcid.org/0000-0002-7703-5004

EDITOR-IN-CHIEF
Abduzhappar Gaipov (Kazakhstan)
Scopus ID: 54415462800
https://orcid.org/0000-0002-9844-8772

ASSOCIATE EDITORS
Sinan Kardes (Turkey)
Scopus ID: 56734551700
https://orcid.org/0000-0002-6311-8634
Ashish Jaiman (India)
Scopus ID: 24724727300
https://orcid.org/0000-0002-4625-0107
Mathias Hossain Aazami (Iran)
Scopus ID: 55947317200
https://orcid.org/0000-0002-4787-8676
Petar Jovan Avramovski (Macedonia)
Scopus ID: 36544785300
https://orcid.org/0000-0003-2816-3365
Gulzhanat Aimagambetova (Kazakhstan)
Scopus ID: 57192414078
https://orcid.org/0000-0002-2868-4497
Alpamys Issanov (Canada)
Scopus ID: 57212149985
https://orcid.org/0000-0002-8968-2655

EXECUTIVE SECRETARY
Yekaterina Dotsenko (Kazakhstan)

PRODUCTION AND PRINTING MANAGER
Bekzad Pulatov (Kazakhstan)

EDITORIAL BOARD

Yasin Uzuntarla (Turkey)
Scopus ID: 56676428600
https://orcid.org/0000-0002-5021-3763
Sakir Ahmed (India)
Scopus ID: 57198883927
https://orcid.org/0000-0003-4631-311X
Manarbek Askarov (Kazakhstan)
Scopus ID: 26026792700
https://orcid.org/0000-0003-4881-724X
Zulfiya Orynbayeva (USA)
Scopus ID: 23490020700
https://orcid.org/0000-0002-7401-2165
Rimantas Benetis (Lithuania)
Scopus ID: 9268082500
https://orcid.org/0000-0001-8211-9459
Galina Fedotovskikh (Kazakhstan)
Scopus ID: 6601949785
https://orcid.org/0000-0003-2416-7385
Ospan Mynbaev (Russian Federation)
Scopus ID: 6602811094
https://orcid.org/0000-0002-9309-1938
Selman Unverdi (Turkey)
Scopus ID: 24478207600
https://orcid.org/0000-0003-1902-2675
Dinara Galiyeva (Kazakhstan)
Scopus ID: 57212506227
https://orcid.org/0000-0002-9769-1690
Talgat Nurgozhin (Kazakhstan)
Scopus ID: 6505537260
https://orcid.org/0000-0002-8036-604X
Jakhongir Alidjanov (Germany)
Scopus ID: 55781386400
https://orcid.org/0000-0003-2531-4877
Praveen Kumar Potukuchi (USA)
Scopus ID: 57144489700
https://orcid.org/0000-0003-0649-6089
Dmitriy Viderman (Kazakhstan)
Scopus ID: 56480667000
https://orcid.org/0000-0002-6007-9326
Natalya Glushkova (Kazakhstan)
Scopus ID: 55804914400
https://orcid.org/0000-0003-1400-8436

ADVISORY BOARD

Turgut Teke (Turkey)
Kubes Jiri (Czech Republic)
Yaroslav Tolstyak (Ukraine)
Rustam Mustafin (Bashkortostan, Russian Federation)
Adem Kucuk (Turkey)
Yana Sotskaya (Ukraine)
Ainura Dzhangaziyeva (Kyrgyz Republic)
Mehtap Tinazli (Turkey)
Yulia Lunitsyna (Russian Federation)
Yuksel Ersoy (Turkey)
Rikhsi Sabirova (Uzbekistan)
Nurdin Mamanov (Kyrgyz Republic)
Mariya Derbak (Ukraine)
Anatoliy Kolos (Kazakhstan)
Vitaliy Koikov (Kazakhstan)
Almagul Kushugulova, (Kazakhstan)
Marlen Doskali (Japan)
Kakharman Yesmembetov (Germany)
Nelya Bissenova (Kazakhstan)
Gauri Bapayeva (Kazakhstan)
Bagdat Imasheva (Kazakhstan)
Galiya Shaimardanova (Kazakhstan)
Nasrulla Shanazarov (Kazakhstan)
Adilzhan Albazarov (Kazakhstan)
Elmira Chuvakova (Kazakhstan)
Zhannat Taubaldieva (Kazakhstan)
Aidos Konkayev (Kazakhstan)
Samat Saparbayev (Kazakhstan)
Olga Ulyanova (Kazakhstan)
Galiya Orazova (Kazakhstan)
Natavan Aliyeva (Azerbaijan)
Jamilya Saparbay (Kazakhstan)
Lina Zaripova (Kazakhstan)
Olimkhon Sharapov (Uzbekistan)

AIMS AND SCOPE OF THE JOURNAL

Journal "Clinical Medicine of Kazakhstan" (ISSN 1812-2892) is a multi-field dedicated peer-reviewed medical journal. The main thematic scope – publication of materials on medical science and practice, education and healthcare organization. Joint Stock Company "National Scientific Medical Center" publishes the journal bimonthly in a year (in February, April, June, August, October, and December).

All articles sent to editors undergo double-blind review. Manuscripts are judged by two experts exclusively on the basis of their contribution to initial data, ideas and their presentations. Editors accept articles for consideration and publication at no cost. Detailed information is available in the section Information for authors at the end of this material.

The Journal of "Clinical Medicine of Kazakhstan" to the full extent is wedded to initiative of open access and ready to provide free access to full texts of articles, as soon as they will be published and available in the Internet (www.clinmedkaz.org).

Journal was registered in the Ministry of Information of the RK on 05.04.2004 and currently included to the list of Publications, approved by the Committee for Control of Education and Science of the Ministry of Education and Science of the Republic of Kazakhstan for publication of the main outcomes of scientific activity.

The journal is indexed in such international scientific-information bases as Scopus, Index Copernicus International, Google Scholar, CrossRef. DOAJ.

JOURNAL OF CLINICAL MEDICINE OF KAZAKHSTAN
Scientific and practical journal

JCMK JOURNAL OF CLINICAL MEDICINE OF KAZAKHSTAN
Editorial Office: Journal of Clinical Medicine of Kazakhstan
Ave Abylay-khan #42, 010009, Astana, Kazakhstan. Phone: +7(7172) 577411
Fax: +7(7172) 232927 E-mail: editor@clinmedkaz.org Web Adress: www.clinmedkaz.org

NATIONAL SCIENTIFIC MEDICAL CENTER JSC, ASTANA CITY,
REPUBLIC OF KAZAKHSTAN

SURGERY AND TRANSPLANTATION

The key activities of these departments of NSMC are reconstructive surgery, transplantation, innovative minimally invasive approaches, microsurgical correction, cell-based therapy of various surgical diseases.
New types of minimally invasive surgical technologies, video-endoscopic and microsurgical techniques, mini-thoracoscopic operations, chemoembolization of tumors were implemented that fundamentally change the approaches to the treatment of many surgical diseases and reduce the time of hospitalization of the patients.

JOURNAL OF CLINICAL MEDICINE OF KAZAKHSTAN (E-ISSN 2313-1519)
Letter to Editor DOI: https://doi.org/10.23950/jcmk/18325

ST-elevation Myocardial Infarction and Alcohol Mixed with Energy Drink

Vitorino Modesto dos Santos[1], Kin Modesto Sugai[2], Rafael Campos Nunes[3]

[1]*Department of Medicine, Catholic University, Brasilia-DF, Brazil*
[2]*Postgraduate Course of Management, Technology, and Information Security, University of Brasilia, Brasilia-DF, Brazil*
[3]*Computer Science BSc Undergraduate at the University of Brasilia, Brasilia-DF, Brazil*

Received: 2026-03-21.
Accepted: 2026-04-07.

This work is licensed under a Creative Commons Attribution 4.0 International License

J Clin Med Kaz 2026; 23(2): 4-5

Corresponding author:
Vitorino Modesto dos Santos.
E-mail: vitorinomodesto@gmail.com.
ORCID: 0000-0002-7033-6074.

Abstract

Myocardial infarction with ST-elevation related to alcohol mixed with the energy drink has been a challenging condition more frequently among young males under the age of 45 years. Energy drinks are proinflammatory risk factors even in the absence of classical risk factors, and healthcare professionals should pay special attention to this specific factor during the medical history, especially when diagnosing some acute cardiovascular disorders in younger patients. This diagnostic hypothesis is reinforced in cases of myocardial infarction in the absence of the traditional risk factors, and effective measures should be implemented and closely monitored. The purpose of this letter is to comment on some new literature about the challenging issue.

Keywords: alcohol, energy drink, AMED, STEMI, myocardial infarction.

Dear *Journal of Clinical Medicine of Kazakhstan* Editors,

Episodes of myocardial infarction (MI) with ST-elevation (STEMI) related to alcohol and energy drinks consumption (EDC) may occur in patients under the age of 45, as recently described by Dondurmaci E and colleagues in this Journal [1]. The 19-year-old man without medical antecedents had precordial pain after two days of caffeine energy drinks with alcohol; his electrocardiogram (ECG) revealed ST elevation in the D1, AVL, V5, and V6 leads, and the coronary angiography showed a 99% thrombotic lesion in the distal circumflex artery branch. The result of urine toxicological screening was negative. He initially underwent intracoronary heparin and glyceryl trinitrate (in bolus), followed by the routine schedule with enoxaparin, acetylsalicylic acid, clopidogrel, atorvastatin, and metoprolol, resulting in a good outcome [1]. The follow-ups over two months revealed normal electrocardiograms and echocardiograms. The authors commented on the education of young people and a reduction in energy drinks [1]. The objective of the letter is to present some new bibliographic data on a global concern [2-7]. A 31-year-old asthmatic man with excessive EDC had chest pain, and the inferior STEMI with an elevated troponin and persistent coronary artery spasm (CAS) refractory to vasodilators, besides right coronary artery and first diagonal branch balloon angioplasty [2]. Initially improved, he presented with hyper eosinophilic syndrome (HES) confirmed by organ biopsies and responsive to corticosteroids; the authors highlighted that STEMI from CAS is an uncommon component of HES, which usually demands the multidisciplinary management [2]. The authors commented on the role of early diagnosis and control of HES in patients with unexplained MI, mainly if related to an EDC, and in the absence of atherosclerotic risk factors. A 26-year-old previously healthy man had an electrocardiographic diagnosis of atrial fibrillation and rapid ventricular response; his blood tests showed elevated thyroid-stimulating hormone and normal free thyroxine levels, with no structural heart disease on chest images [3]. No intracardiac thrombus was seen, and the urine screening test was positive for Amphetamine; the patient returned to the sinus rhythm before the cardioversion procedure that was chosen. The authors emphasized the scarce data about the commonest arrhythmias by the use of the drug, the need to assess the relationship between stimulant medications and atrial fibrillation, and guidelines for prescriptions to patients with some risk for developing atrial fibrillation [3]. In

Malaysia, EDs are often premixed with sexual stimulants and have caused arrhythmias, coronary vasospasm, prolonged QTc interval, spontaneous coronary artery dissection, MI with or without obstructive coronary artery disease (MINOCA), besides cases of cardiac arrest [4]. A 33-year-old male smoker had a sudden transient loss of consciousness, urinary incontinence, chest discomfort, and palpitation after consuming the sexual stimulant Kopi Jantan with coffee, as utilized during the last two years, with increased amounts two months before this event [4]. The ECG showed atrial flutter, and echocardiography revealed normal cardiac chambers; his diagnosis was atrial flutter with rapid ventricular response secondary to ED ingestion; he was successfully managed by intravenous amiodarone in addition to synchronized cardioversion. He was discharged with verapamil to maintain the sinus rhythm with outpatient ambulatory [4]. A 27-year-old male non-smoker had sudden-onset central crushing chest pain radiating to the back, profuse sweating, and vomiting after two years of Kopi Jantan drinks; there was neither use of recreational drugs nor other supplements or herbs, nor family cardiovascular disease [4]. As the ECG revealed ST elevations in leads I, AVL, and V2-V6, he underwent intravenous streptokinase, which resulted in the complete resolution of the ST-segment elevations; other investigations (urine toxicology, autoimmune disease, and infection screening) were negative. Coronary angiography revealed a non-obstructive stenosis in the left anterior descending artery, and as his diagnosis was MINOCA, the acute thrombotic occlusion resolved with thrombolysis; he was discharged on dual antiplatelets and remained well in outpatient clinic follow-ups [4]. A 28-year-old African male with no cardiovascular risk factors had an 8-hour retrosternal chest pain 4 hours after taking 1250 cc of an ED (caffeine, taurine, sugar, and glucuronolactone) [5]. As the electrocardiogram and echocardiogram showed an anterolateral STEMI, and the catheterization revealed a 100% thrombotic occlusion of the proximal left anterior descending artery, his prompt management with success was revascularization and a drug-eluting stent [5]. Considering the overall data indicative of an increasing incidence of ED-associated coronary involvements, the authors called attention to the need to limit the consumption of the beverages. A 19-year-old man with gastro-esophageal reflux presented with acute chest pain and had the electrocardiographic and biochemical diagnosis of STEMI, but heart images were normal [6]. He had neither important family medical history nor obvious risk factors for coronary heart disease; he denied smoking and illicit drug use, but had ingested a large volume of ED in the week before admission. Therefore, the authors strongly believed that this could be the origin of the sudden coronary event, manifested by the central, dull thoracic pain radiating to the right arm, being well-responsive to both the sublingual glyceryl trinitrate and the diamorphine [6]. Aspirin, clopidogrel, ACE inhibitor, and a β-blocker were prescribed to continue on discharge; in the two-month follow-up, he was totally EDs abstinent and had no further thoracic pains [6]. In fact, distinct risk factors are associated with young-onset MI in comparison to older patients, and more attention is necessary on susceptibility factors and preventive measures search [7]. As an example, the very young South Asian people developing early coronary arterial disease, who have many novel evolving risk factors associated with an MI, and need intervention [7]. To reduce morbidity and mortality, one must consider the well-known markers like lipoprotein A, dyslipidemias, or stress, and new risks like periodontitis, micro- or nanoplastics, and ED [7].

New prospective studies may reveal novel risk factors for increased young AMIs, and case reports of STEMIs in young people enhance the awareness of potentially underrecognized triggers of the acute coronary events in patients without traditional cardiovascular risk factors. The data discussed should serve as a key message for physicians, mainly during history taking, risk assessment, and selection of the management options in younger patients with STEMIs.

Author Contributions: Conceptualization, V. M. S, K. M. S., R. C. N.; investigation, V. M. S., K. M. S., R. C. N.; verification, V K. M. S., R. C. N.; writing – original draft preparation, K. M. S., R. C. N.; writing – review and editing, V. M. S. The authors have read and agreed to the published version of the manuscript.

Disclosures: The authors have no conflicts of interest.

Acknowledgments: None.

Funding: None.

Data availability statement: Not applicable.

Artificial Intelligence (AI) Disclosure Statement: The authors declare no AI Tools used for preparation of this work.

References

1. Dondurmaci E, Özkorkmaz E, Sakalli S, Polat E. Young Patient Presenting with ST-elevation Myocardial Infarction (STEMI) Following Alcohol Mixed with Energy Drink (AMED). *J Clin Med Kaz.* 2026; 23(1): 97-99. https://doi.org/10.23950/jcmk/17818.
2. Czaja MP, Mantha Y, Canales ML, Chilton RJ. Hypereosinophilic Syndrome Presenting as Coronary Artery Spasm and ST-Segment Elevation Myocardial Infarction. *JACC Case Rep.* 2025;30(30):105308. https://doi.org/10.1016/j.jaccas.2025.105308.
3. Karakayali M, Omar T. New Onset Atrial Fibrillation due to Amphetamine Use in a Young Patient. *SSHS*. 2021;3(1): 45-49. https://dergipark.org.tr/tr/download/article-file/1508059.
4. Othman MK, Yusof Z, Mohd Rossli NI, Mohd Fauzi MH, W Isa WYH. Adverse Cardiovascular Events Associated with Kopi Jantan. *Cureus*. 2024;16(1):e52344. https://doi.org/10.7759/cureus.52344.
5. Pallangyo P, Bhalia SV, Komba M, Mkojera ZS, Swai HJ, Mayala HA, et al. Acute Myocardial Infarction Following the Consumption of Energy Drink in a 28-Year-Old Male: A Case Report. *J Investig Med High Impact Case Rep.* 2023;11:23247096231168811. https://doi.org/10.1177/23247096231168811.
6. Scott MJ, El-Hassan M, Khan AA. Myocardial infarction in a young adult following the consumption of a caffeinated energy drink. *BMJ Case Rep*. 2011;2011:bcr0220113854. https://doi.org/10.1136/bcr.02.2011.3854.
7. Ranjan A, Agarwal R, Mudgal SK, Bhattacharya S, Kumar B. Young hearts at risk: Unveiling novel factors in myocardial infarction susceptibility and prevention. *J Family Med Prim Care.* 2024;13(4):1200-1205. https://doi.org/10.4103/jfmpc.jfmpc_1639_23.

JOURNAL OF CLINICAL MEDICINE OF KAZAKHSTAN (E-ISSN 2313-1519)
Original Article DOI: https://doi.org/10.23950/jcmk/18009

16-Year Epidemiologic Study of Chronic Myeloid Leukemia in Azerbaijan: Clinical and Molecular Insights

Aytan Shirinova[1], Chingiz Asadov[1], Aypara Hasanova[1], Zohra Alimirzoyeva[1]

[1]*National Hematology and Blood Transfusion Center, Baku, Azerbaijan*

Received: 2026-01-18.
Accepted: 2026-02-24.

This work is licensed under a Creative Commons Attribution 4.0 International License

J Clin Med Kaz 2026; 23(2): 6-18

Corresponding author:
Aytan Shirinova.
E-mail: medicolisto@yahoo.com.
ORCID: 0000-0002-2525-3069.

Abstract

Background: Chronic myeloid leukemia (CML) is a myeloproliferative neoplasm with a global incidence of 0.5–2 per 100,000 population. However, comprehensive epidemiologic data from Azerbaijan remain limited.

Methods: A retrospective nationwide cohort study was conducted at the National Hematology and Blood Transfusion Center, the sole hematology referral center in Azerbaijan. All patients diagnosed with CML between 2008 and 2023 were included. Demographic, clinical, molecular, and treatment data were extracted from medical records. Descriptive analyses assessed temporal trends, age and sex distribution, seasonal and geographic patterns, ABO/Rh blood groups, kinase domain mutations, treatment response, and survival.

Results: Study included 766 patients , with a female predominance (54%) and the highest disease burden observed in individuals aged 50–59 years. CML incidence increased from 0.31 to 0.86 per 100,000 population between 2008 and 2023, while prevalence rose more than twelve-fold. Following the introduction of tyrosine kinase inhibitors (TKIs), five-year overall survival exceeded 80%. Most patients resided in the Absheron region, suggesting possible environmental or industrial influences. New diagnoses were more frequent during summer months (29.6%). Blood group A was more prevalent among patients compared with controls (40.3% vs 35.4%). First-line imatinib achieved optimal molecular responses in approximately 80% of patients, while 15% experienced treatment failure. Among 115 patients tested, T315I was the most common BCR-ABL mutation.

Conclusions:: This nationwide CML analysis from Azerbaijan reveals a rising disease burden, female predominance, and favorable survival outcomes with TKI therapy. The findings emphasize the need for sustained access to molecular diagnostics and support national strategies for equitable CML care.

Keywords: chronic myeloid leukemia; epidemiology; Azerbaijan; molecular mutations; treatment response.

Introduction

Chronic myeloid leukemia (CML) is a myeloproliferative neoplasm characterized by the presence of the Philadelphia chromosome, resulting from a reciprocal translocation between chromosomes 9 and 22, which creates the BCR-ABL1 fusion oncogene. This molecular alteration drives constitutive tyrosine kinase activity and uncontrolled proliferation of myeloid precursors [1]. Globally, CML accounts for about 15% of adult leukemia, with an annual incidence ranging between

0.5 and 2 per 100,000, depending on local diagnostic infrastructure, registry coverage, and population demographics [2, 3].

Historically, most studies have documented a modest male predominance in CML, with a male-to-female ratio typically between 1.2–1.7 [4]. Nevertheless, some regional data have shown a female predominance in certain ethnic or geographic populations [5][6]. Age distribution generally peaks between 40 and 60 years, although the introduction of tyrosine kinase inhibitors (TKIs) has dramatically changed outcomes, extending life expectancy and transforming CML into a chronic, manageable disease [7].

In Azerbaijan, epidemiological data remain sparse apart from limited reports on leukemia incidence in general [6]. Given Azerbaijan's unique industrial and environmental landscape, regional studies are crucial to detect possible influences on leukemia occurrence. Local analyses are therefore essential to identify patterns in gender distribution, age at diagnosis, Sokal risk stratification, and molecular features, which could influence both public health policy and clinical treatment approaches. In addition, factors such as seasonal diagnosis trends, ABO/Rh blood group associations, and molecular mutations in TKI-resistant patients are poorly described in this population.

Global Context and Rationale: Over the past two decades, the treatment landscape of chronic myeloid leukemia has been revolutionized by tyrosine kinase inhibitors (TKIs) [1,7]. Imatinib, the first-generation TKI, transformed CML from a fatal disease into a chronic, controllable condition. Subsequent second- and third-generation TKIs such as nilotinib, dasatinib, bosutinib, and ponatinib have further improved response depth, durability, and outcomes, particularly among patients harboring resistant clones [1]. Despite these advances, the emergence of ABL kinase domain mutations remains a key mechanism of therapeutic resistance. Among these, the T315I mutation is clinically the most relevant, conferring high-level resistance to first- and second-generation TKIs and often necessitating treatment with third-generation agents such as ponatinib. Evaluating the frequency of such mutations provides essential insight into molecular resistance profiles within a population and informs national treatment strategies.

In addition to molecular mechanisms, several epidemiological and biological factors have been proposed to influence CML occurrence and presentation. These include environmental exposures, population-level variations in blood group distribution, and possible seasonal patterns in diagnosis. ABO and Rhesus blood group antigens have been hypothesized to modulate immune and inflammatory responses, which could contribute to leukaemogenesis, whereas seasonal variation may reflect environmental, infectious, or behavioral influences affecting detection rates. Assessing these variables in a nationwide cohort helps to contextualize disease characteristics and identify potential avenues for future research.

This study aimed to characterize the epidemiology of chronic myeloid leukemia (CML) in Azerbaijan using nationwide data collected over a 16-year period (2008–2023). The primary objective was to describe national trends in incidence, prevalence, and survival outcomes within a unified healthcare system. Secondary aims were to explore demographic and regional patterns—including gender distribution, age at diagnosis, and geographic clustering—as well as to assess treatment responses and common resistance-associated molecular mutations among patients receiving tyrosine kinase inhibitors. By focusing on these core outcomes, the study provides a structured overview of disease burden and treatment effectiveness across the Azerbaijani CML population.

Methods

This study was conducted following best practices for observational epidemiologic research, ensuring methodological transparency and reproducibility. Detailed descriptions of the study design, patient selection, diagnostic procedures, data collection, and statistical analysis are provided below to allow independent replication of all steps undertaken.

Study Design and Setting

This was a nationwide retrospective cohort study designed to evaluate the epidemiology, clinical characteristics, treatment response, and survival outcomes of patients diagnosed with chronic myeloid leukemia (CML) in Azerbaijan over a 16-year period (2008–2023).

The study was conducted at the National Hematology and Blood Transfusion Center (NHBTC) in Baku, which serves as the country's only authorised tertiary reference centre for the diagnosis, treatment, and follow-up of patients with CML.

Within the national healthcare system, patients with suspected hematologic malignancies are referred to the NHBTC from regional hospitals and outpatient clinics. At this centre, diagnostic confirmation is performed using standardized cytogenetic and molecular testing, including BCR–ABL1 detection by quantitative RT-PCR and karyotyping. All confirmed cases are registered in the national CML database.

The NHBTC also coordinates the national tyrosine kinase inhibitor (TKI) distribution programme under the Ministry of Health. Treatment initiation, response monitoring, mutation testing, and long-term follow-up are therefore centralized at this institution. This structure ensures uniform diagnostic criteria, standardized treatment protocols, and near-complete national coverage of CML cases.

Although a small proportion of patients may initially seek diagnostic confirmation or second opinions abroad, these individuals are routinely re-registered at the NHBTC upon return to continue therapy within the national programme. Consequently, the registry is considered representative of nearly all CML cases nationwide. Some degree of under-diagnosis in remote regions cannot be entirely excluded; however, its impact is likely minimal because molecular and cytogenetic testing have been routinely available through the central programme since 2008.

Follow-up was defined from the date of initial CML diagnosis (first documented positive BCR-ABL1 test or bone marrow confirmation) to the date of last recorded clinical visit, death, or 31 December 2023, whichever occurred first. Patients alive at the end of this period were censored at their last documented follow-up. Survival analyses therefore reflect observation intervals ranging from 1 month to 16 years, depending on the year of diagnosis.

Patient Population

All patients with a confirmed diagnosis of chronic myeloid leukaemia (CML) between 1 January 2008 and 31 December 2023 were included in the registry-based cohort. Diagnosis was established according to World Health Organization (WHO) criteria [13], requiring detection of the BCR-ABL1 fusion transcript by quantitative RT-PCR and/or the presence of the Philadelphia chromosome on karyotyping.

Inclusion criteria: Confirmed diagnosis of CML with documented BCR-ABL1 positivity, age ≥ 18 years at diagnosis (paediatric cases were registered separately but excluded from adult analyses), availability of complete baseline demographic and clinical data.

Exclusion criteria: Patients with incomplete diagnostic confirmation (missing cytogenetic or molecular data), patients who were initially misclassified or referred with other myeloproliferative neoplasms, patients lost to follow-up immediately after diagnosis with no treatment or outcome data available.

During the study period, a total of 812 patients with confirmed CML were identified in the national registry. After applying the predefined inclusion and exclusion criteria, 766 patients fulfilled all eligibility requirements and were included in the final analysis.

A total of 766 patients fulfilled these criteria and were included in the main analysis.

Of these, 249 patients had adequate serial molecular monitoring data to evaluate treatment response to first-line imatinib according to ELN guidelines. Patients without consistent quantitative BCR-ABL1 measurements were not included in this sub-analysis to avoid measurement bias. Similarly, 115 patients underwent ABL kinase domain mutation testing due to clinical or molecular evidence of TKI resistance; this subset reflects all cases with available stored samples and formal resistance evaluation during the study period.

The remaining patients continued first-line or subsequent-line TKI therapy (nilotinib, dasatinib, or bosutinib) under standard national protocols but were excluded from those sub-analyses due to insufficient longitudinal molecular data or absence of resistance work-up.

To evaluate the distribution of ABO blood groups and Rhesus factor among patients with CML, a control population was used for comparison. Anonymized data from 7,086 healthy blood donors were obtained from the NHBTC Blood Bank database. Controls were matched to patients by sex and broad age categories (±10 years) to minimize demographic bias. This control cohort represents the general healthy donor population in Azerbaijan and serves as the national reference for blood group distribution.

Data Collection

Demographic data comprised age, sex, and place of residence. Clinical data included Sokal risk category at diagnosis, disease phase (chronic, accelerated, or blast crisis), hematologic parameters (hemoglobin, leukocyte counts, platelet counts, basophil percentages), treatment responses to tyrosine kinase inhibitors, and molecular analyses (including ABL kinase domain mutations in patients with treatment resistance). Seasonal patterns and ABO/Rh blood group distributions were also extracted from the patient records.

Outcome Measures

The primary outcome was to describe the epidemiological profile of CML in Azerbaijan, including incidence, prevalence, age and gender distribution, regional distribution, seasonal patterns, and treatment responses. Secondary outcomes included evaluation of survival trends before and after TKI therapy and analysis of molecular resistance patterns.

Genetic and Molecular Analysis

Molecular testing for BCR-ABL1 transcript quantification was performed using real-time quantitative PCR at baseline and during follow-up according to ELN guidelines. ABL kinase domain mutation analyses were performed in patients who demonstrated suboptimal response or resistance to imatinib (n=115), using PCR amplification and pyrosequencing techniques. Confirmatory testing was performed at Ankara ATQ Biotechnology Laboratories for less common variants.

Follow-up for Outcomes: All outcome measures were evaluated over the defined follow-up period, beginning at the date of confirmed CML diagnosis and ending at death, last clinical contact, or 31 December 2023, whichever occurred first. Patients alive at the last available follow-up were treated as censored observations in survival analyses. Overall survival and treatment-response outcomes were therefore calculated within observation intervals ranging from 1 month to 16 years, depending on year of diagnosis and completeness of follow-up data.

Statistical Analysis

Descriptive statistics were used to summarize demographic, clinical, and molecular characteristics. Continuous variables are presented as medians with interquartile ranges (IQR), and categorical variables as counts and percentages. Incidence and prevalence rates were standardized to national population data from the State Statistical Committee of Azerbaijan for each calendar year.

Incidence and prevalence rates reported in this study are crude population-based rates. Age-standardized rates were not calculated because the primary objective was to describe national trends using complete registry data rather than to perform international comparative analyses. Annual incidence and prevalence rates were calculated with 95% confidence intervals using Poisson distribution methods.

Survival analyses were performed using the Kaplan–Meier method. Follow-up was defined from the date of diagnosis to death, last clinical contact, or 31 December 2023, whichever occurred first. Patients alive at last follow-up or lost to follow-up were censored at the date of their last documented clinical contact and were included in the analysis up to the time of censoring. Median overall survival (OS) and progression-free survival (PFS) were estimated with 95% confidence intervals (CIs) using Greenwood's formula. One-, three-, and five-year overall survival probabilities were also estimated. Survival curves were compared using the log-rank test, with p-values reported descriptively.

Annual mortality incidence rates were summarized, and the average annual percent change (AAPC) was calculated using log-linear regression. The AAPC and its 95% confidence interval were derived from the regression slope, and statistical significance was assessed using two-sided p-values.

Comparisons across categorical variables were analyzed using chi-square (χ^2) tests. For analyses involving multiple categorical comparisons, such as seasonal distribution and ABO/Rh blood-group frequencies, results were adjusted using the Holm–Bonferroni correction to control for multiple testing. All results are expressed descriptively or as effect estimates with 95% CIs.

Multivariable modeling was not performed because several key confounding variables—including comorbidity profiles, treatment adherence, socioeconomic indicators, and environmental exposure data—were not consistently available across the national registry, particularly for earlier years of the cohort. The study was therefore designed as a primarily descriptive national epidemiological analysis.

All analyses were performed using SPSS Statistics version 26.0 (IBM Corp., Armonk, NY, USA) and independently cross-checked by two investigators to ensure reproducibility.2.7 Treatment Response Assessment

Treatment response to imatinib was assessed according to the European LeukemiaNet (ELN) 2020 criteria. Optimal molecular response was defined as BCR-ABL1 ≤ 10 % at

3 months, ≤ 1 % at 6 months, and ≤ 0.1 % (major molecular response, MMR) at 12 months. Patients who did not achieve these milestones, lost a previously achieved response, or developed BCR-ABL kinase-domain mutations conferring resistance (e.g., T315I, F359C/V) were categorised as imatinib-resistant. For descriptive subgroup analyses, patients were stratified by achievement of early molecular response (EMR) and major molecular response (MMR) to explore trends in long-term outcomes.

Ethical Considerations

The study protocol was approved by the Institutional Ethics Committee of the National Hematology and Blood Transfusion Center. All analyses were performed on anonymized data extracted from the center's registry in accordance with the Declaration of Helsinki. Written informed consent was obtained from all patients at the time of enrollment for data collection and future research purposes.

Results

Gender Distribution of CML Patients

A total of 766 patients with chronic myeloid leukemia were included in the study cohort. As illustrated in Figure 1, there was a slight female predominance, with females comprising 54% of cases and males 46%.

Temporal Trends in CML Incidence

The incidence of chronic myeloid leukemia demonstrated an overall increasing trend in Azerbaijan between 2008 and 2023 (Figure 2). In 2008, the recorded incidence was 0.31 per 100,000 population, rising to 0.86 per 100,000 in 2023. The most pronounced growth occurred between 2010 and 2011, with incidence nearly doubling from 0.42 to 0.83 per 100,000.

When stratified by gender, female incidence generally exceeded that of males across most years. Female incidence ranged from 0.15 per 100,000 in 2009 to a peak of 0.58 per 100,000 in 2022. Male incidence varied between 0.14 per 100,000 in 2008 and 0.46 per 100,000 in 2021. These patterns align with the overall observed female predominance in the cohort.

Annual incidence rates with 95% confidence intervals were calculated for each year and sex. Among females, incidence ranged from 0.27 per 100,000 (95% CI: 0.12–0.42) in 2008 to 1.15 per 100,000 (95% CI: 0.85–1.44) in 2022. Among males, incidence ranged from 0.29 per 100,000 (95% CI: 0.13–0.46) in 2009 to 1.16 per 100,000 (95% CI: 0.86–1.46) in 2016. Confidence intervals for all annual rates were calculated using Poisson methods.

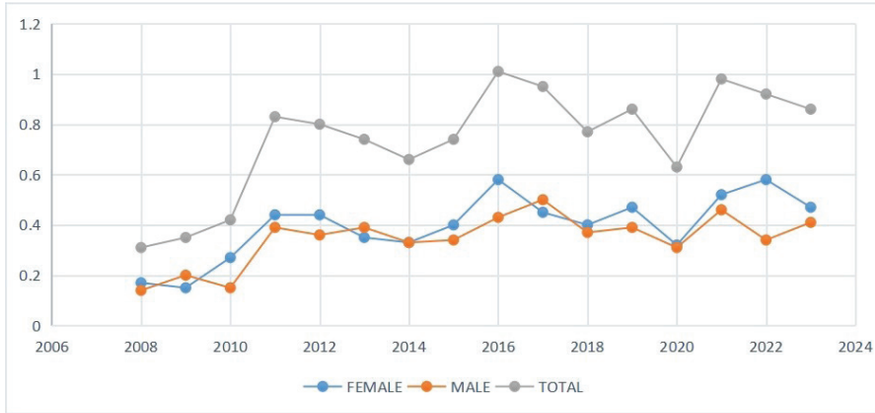

Figure 1 – Incidence of CML by years

The figure shows annual incidence rates of CML stratified by sex (female and male) and total population. Trends demonstrate year-to-year variation with generally higher total incidence driven by contributions from both sexes. Female and male incidence rates follow similar temporal patterns, with fluctuations observed across the study period.

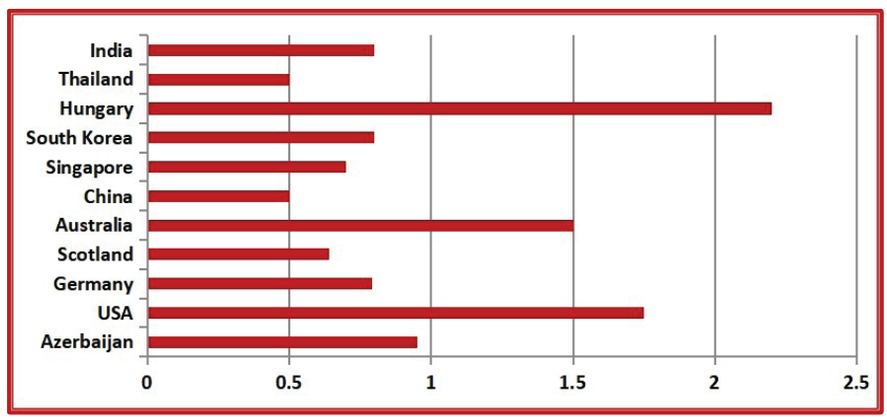

Figure 2 – Incidence of CML among different countries

The figure compares reported CML incidence rates among different countries, highlighting international variability in disease burden. Differences may reflect population structure, diagnostic practices, and registry coverage.

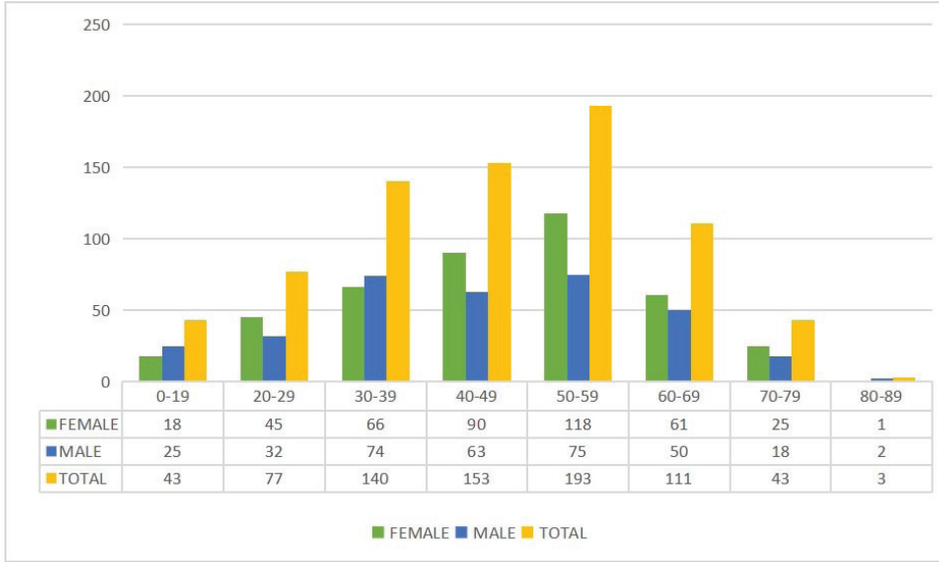

Figure 3 – Age-gender distribution

The figure illustrates the distribution of CML cases across age groups stratified by sex. The highest number of cases was observed in middle-aged and older adults, with comparable patterns between females and males across most age categories.

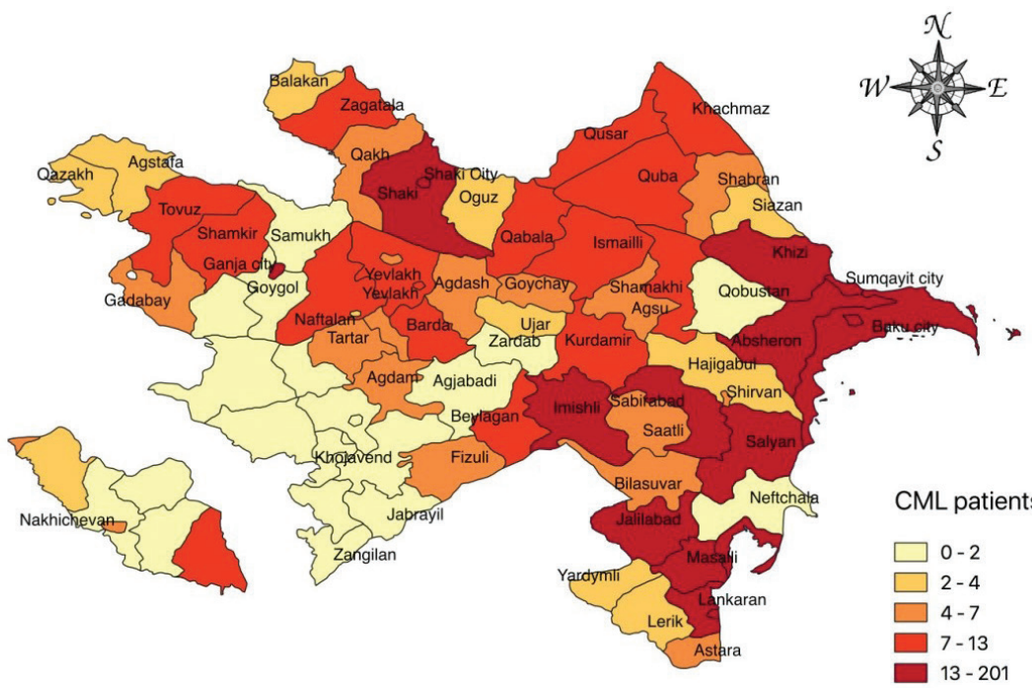

Figure 4 – Distribution of CML patients among regions of Azerbaijan

The map illustrates the regional distribution of CML patients in Azerbaijan, with darker shading indicating a higher number of cases. Variation across regions likely reflects differences in population density, referral patterns, and access to specialized hematology services.

International Comparison of CML Incidence

Figure 3 presents an international comparison of chronic myeloid leukemia incidence, allowing contextualization of the Azerbaijani data within a global epidemiological framework. In Azerbaijan, the incidence was approximately 0.9 per 100,000, similar to that reported in Germany and South Korea. In contrast, the incidence was notably higher in Hungary (2.3 per 100,000), Australia (1.5 per 100,000), and the United States (1.7 per 100,000). Lower incidence rates were observed in Thailand (0.4 per 100,000) and China (0.5 per 100,000).

Prevalence Trends in CML

The prevalence of chronic myeloid leukemia in Azerbaijan showed a consistent and notable rise over the period 2008–2023 (Figure 4). The total number of patients living with CML increased from 99 in 2008 to 1,219 in 2023, representing a more than twelve-fold increase over sixteen years.

When stratified by sex, the number of prevalent female cases grew from 43 in 2008 to 617 in 2023, while male prevalent cases increased from 56 to 602 during the same period. The consistently higher cumulative number of female

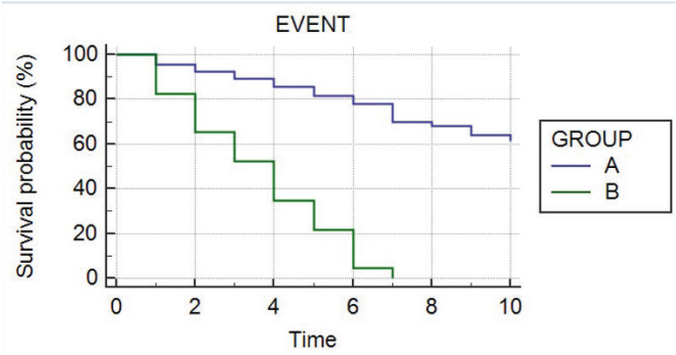

Figure 5 – Kaplan–Meier Survival Curves Comparing CML Patients Treated Before and After Introduction of TKI Therapy

Kaplan–Meier curves illustrate event-free survival over time for two study groups (Group A and Group B). Group A demonstrates a consistently higher survival probability throughout the follow-up period compared with Group B.

patients supports the female predominance observed in this cohort.

Annual prevalence rates with 95% confidence intervals were also calculated for each year and sex. Among females, prevalence increased from approximately 0.97 per 100,000 (95% CI: 0.68–1.30) in 2008 to 12.13 per 100,000 (95% CI: 11.16–13.12) in 2023. Among males, prevalence increased from approximately 1.29 per 100,000 (95% CI: 0.96–1.67) in 2008 to 11.95 per 100,000 (95% CI: 11.02–12.92) in 2023. Confidence intervals for all annual prevalence rates were calculated using Poisson methods.

Number of Newly Diagnosed CML Patients

Figure 5 illustrates the annual number of patients newly diagnosed with chronic myeloid leukemia from 2008 to 2023. Over this sixteen-year period, there was a general upward trend in new diagnoses, with some year-to-year fluctuations.

In 2008, 27 new CML cases were identified (12 female, 15 male). The number of new diagnoses rose sharply to 76 cases in 2011, followed by a stable period where annual new diagnoses ranged between 63 and 99 cases from 2012 to 2023. The highest annual count was recorded in 2021 with 98 new cases.

Age and Gender Distribution of CML Patients

Analysis of age groups (Figure 6) revealed the highest disease burden in the 50–59 age group, with female predominance evident in several decades. Most patients were diagnosed between the ages of 30 and 69 years, accounting for approximately 72% of the total cohort, with clear peaks in the 50–59 and 40–49 age groups. Specifically, the highest burden was observed in patients aged 50–59 years, accounting for 193 cases (118 female and 75 male). Although age categories are presented in decades starting from 0–19 years, only patients aged 18 years and older were included in the study. Therefore, the 0–19 group represents only patients aged 18–19 years.

In younger age groups (under 30 years), the incidence of CML was substantially lower, with only 43 cases in the 0–19 group and 77 cases in the 20–29 group. Likewise, the prevalence sharply declined after age 70, reflecting both lower life expectancy and lower disease detection in advanced age.

Female predominance was apparent in several key age brackets, particularly in the 50–59 group (118 females vs. 75 males) and 40–49 group (90 females vs. 63 males), supporting the gender pattern noted in the overall cohort.

Geographic Distribution of CML Patients

Figure 7 illustrates the geographic distribution of chronic myeloid leukemia patients across the administrative regions of Azerbaijan. The map shows a clear concentration of CML cases in the Absheron economic region, including Baku and Sumgayit, which reported the highest burden (up to 201 cases) and are indicated in dark red.

Moderate case densities (7–13 patients) were observed in districts such as Ganja, Mingachevir, and parts of Lankaran, while low-prevalence areas (0–2 patients) were mainly located in rural western and southern regions, including parts of Qazakh and Zangilan.

Seasonal Patterns of CML

Table 1 presents the distribution of chronic myeloid leukemia (CML) diagnoses across the four seasons in Azerbaijan. The highest proportion of cases occurred during summer (June–August) (29.6 %), followed by spring (March–May) (25.4 %), autumn (September–November) (23.5 %), and winter (December–February) (21.5 %).

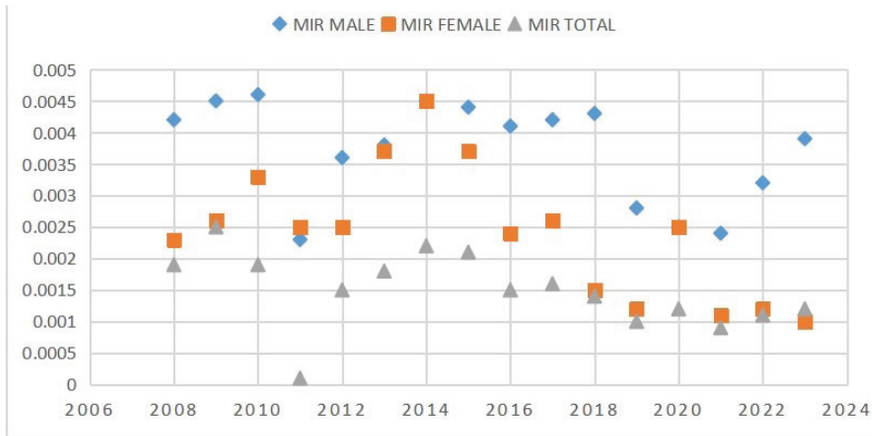

Figure 6 – Mortality rate of CML patients.

The figure presents annual mortality rates of CML stratified by sex (male and female) and for the total population. Male mortality rates were consistently higher than female rates across most years, while overall mortality demonstrated temporal fluctuations during the study period.

Table 1 Distribution of Disease Phase and Sokal Risk Groups among CML Patients

Category	Subcategory	Male, n (%)	Female, n (%)	Total, n (%)	P value
Disease phase	Chronic	290 (80.6)	322 (79.3)	612 (79.9)	0.63
	Accelerated	60 (16.7)	75 (18.5)	135 (17.6)	
	Blast crisis	10 (2.7)	9 (2.2)	19 (2.5)	
Sokal risk group	Low	79 (22.2)	105 (25.5)	184 (24.0)	0.41
	Intermediate	220 (62.0)	255 (62.0)	475 (62.0)	
	High	56 (15.8)	51 (12.5)	107 (14.0)	

This table summarizes the distribution of chronic myeloid leukemia patients by disease phase and Sokal risk category, stratified by sex. Most patients were diagnosed in the chronic phase, and the majority belonged to the intermediate Sokal risk group, with similar distributions observed between male and female patients.

Table 2 Comparison of Imatinib Responders and Resistant Patients

Variable	Imatinib responders (n = 651)	Imatinib resistant (n = 115)	OR	95% CI	p-value
Age, years	Range: 4–84; mean: 47.3	Range: 16–80; mean: 45.3	-	-	-
Sex distribution	Male: 42.0%; Female: 58.0%	Male: 55.7%; Female: 44.3%	1.74	1.16–2.61	0.007
Disease phase	Chronic: 84.8% Accelerated: 15.2% Blast crisis: 0%	Chronic: 78.3% Accelerated: 16.5% Blast crisis: 5.2%	1.55	0.94–2.55	0.080
Sokal risk group	Low: 51.9% Intermediate: 40.4% High: 7.7%	Low: 30.4% Intermediate: 58.3% High: 11.3%	2.51	1.27–4.95	0.008

Odds ratios were calculated comparing resistant versus responder groups. Confidence intervals were derived using standard logistic methods. This table presents demographic and disease-related variables in patients who achieved an optimal response to first-line imatinib (n = 651) and those who were classified as imatinib-resistant (n = 115). Age distribution was comparable between the two groups, with similar mean ages (47.3 vs. 45.3 years). A significantly higher proportion of males was observed among imatinib-resistant patients compared with responders (55.7% vs. 42.0%), corresponding to an odds ratio (OR) of 1.74 (95% CI: 1.16–2.61; p = 0.007). Regarding disease phase at diagnosis, resistant patients more frequently presented with advanced phases, including accelerated phase and blast crisis (21.7% vs. 15.2% in responders), although this difference did not reach statistical significance (OR: 1.55; 95% CI: 0.94–2.55; p = 0.080). Risk stratification according to the Sokal score showed a significantly higher proportion of intermediate- and high-risk patients in the imatinib-resistant group. The odds of resistance were significantly increased among patients with higher Sokal risk (OR: 2.51; 95% CI: 1.27–4.95; p = 0.008).

Association of ABO Blood Groups and Rhesus factor with CML

Table 2 summarises the distribution of ABO blood groups and Rhesus factor among patients with CML and among healthy controls. Blood group A was more frequent among patients (40.3 %) than among controls (35.4 %), whereas blood group B was less common (14.6 % vs 20.2 %). Blood group A was significantly more frequent among CML patients than controls, and this association remained statistically significant after Bonferroni correction for multiple ABO group comparisons (adjusted p = 0.024). The proportions of groups O and AB were similar between the two populations.

Regarding Rhesus factor, Rh-positive individuals predominated in both groups (about 92 % of patients and 90 % of controls).

Table 3 Distribution of BCR-ABL Kinase Domain Mutations among Imatinib-Resistant Patients by Gender

Mutation	Male, n (%)	Female, n (%)	Total, n (%)
E255K	1 (7.1)	0 (0.0)	1 (5.3)
F359C	2 (14.3)	1 (20.0)	3 (15.8)
F317L (TTA)	1 (7.1)	0 (0.0)	1 (5.3)
F317L (TTG)	1 (7.1)	1 (20.0)	2 (10.5)
F359V	2 (14.3)	1 (20.0)	3 (15.8)
Y253H	2 (14.3)	0 (0.0)	2 (10.5)
T315I	5 (35.7)	2 (40.0)	7 (36.8)

This table presents the frequency and distribution of BCR–ABL1 kinase domain mutations in imatinib-resistant patients, stratified by sex. The T315I mutation was the most frequently detected mutation in both male and female patients.

Disease Phase and Risk Group Distribution

Table 3 summarizes the distribution of disease phases and risk groups among CML patients according to Sokal classification. Risk stratification was performed using the Sokal scoring system, as this was the only risk model consistently applicable throughout the entire 2008–2023 dataset. Variables required for the ELTS score (EUTOS Long-Term Survival) were not uniformly available for earlier cases; thus, the Sokal score was adopted for standardization and longitudinal comparability. At presentation, the majority of patients were diagnosed in the chronic phase (79.9%), with 80.6% of males and 79.3% of females falling into this category. The accelerated phase was identified in 17.6% of patients overall (16.7% male and 18.5% female), while only 2.5% presented in blast crisis (2.7% male and 2.2% female).

Risk stratification by the Sokal scoring system revealed that 24% of patients were classified as low risk, 62% as intermediate risk, and 14% as high risk. The proportion of low-risk patients was slightly higher among women (25.5%) compared to men (22.2%). Conversely, high-risk disease was marginally more frequent among males (15.8%) than females (12.5%).

Table 4 Distribution of BCR-ABL Kinase Domain Mutations by Disease Phase and Sokal Risk Group

Group	Patients with mutations, n	Proportion (%)	p-value
Disease phase			
Chronic phase	10	11.1	
Accelerated phase	5	26.3	
Blast crisis phase	4	66.7	0.0008
Sokal risk group			
Low risk	5	14.3	
Intermediate risk	12	17.9	
High risk	2	15.4	0.890

This table shows the proportion of patients harboring BCR–ABL1 kinase domain mutations according to disease phase and Sokal risk category. Mutation frequency increased significantly with disease progression, being highest in blast crisis, while no significant association was observed between mutation frequency and Sokal risk group.

Hematologic Parameters across Disease Phases

Table 4 presents hemoglobin levels and leukocyte counts stratified by disease phase among CML patients.

In terms of hemoglobin levels, the majority of patients in the chronic phase had moderate anemia, with 47.7% having hemoglobin between 7.1–10 g/dL and 27.1% between 10.1–12 g/dL. Severe anemia (Hb 4–7 g/dL) was present in 8.7% of chronic-phase patients. Among patients in the accelerated phase, 67.4% had hemoglobin above 7 g/dL, while 10.4% had severe anemia. In blast crisis, severe anemia was more frequent, with nearly half (47.4%) of patients showing hemoglobin levels in the 4–7 g/dL range.

Regarding leukocyte counts, chronic-phase patients most commonly had counts between 21–100 x 10^9/L, representing 20.1% in the 21–50 range and 20.9% in the 51–100 range. Very high leukocyte counts (>300 x 10^9/L) were seen in only 13.5% of chronic-phase patients. In contrast, 26.7% of patients in the accelerated phase and 42.1% in blast crisis had extremely elevated leukocyte counts above 100 x 10^9/L, consistent with disease progression.

Table 5 details the distribution of basophil percentages and platelet counts among chronic myeloid leukemia patients, stratified by disease phase.

In chronic-phase patients, the majority had basophil percentages between 0–1 % (57.0%) or 2–7% (36.6%), with only 3.4% showing basophil counts above 8%. In contrast, patients in the accelerated phase showed a shift toward higher basophil levels, with 8.9% having basophils between 8–20% and 7.0% exceeding 21%. Among those in blast crisis, elevated basophil percentages were common, with 42.1% in the 8–20% category and 21% above 21%, reflecting progressive disease activity.

Regarding platelet counts, most chronic-phase patients had counts in the normal-to-moderately elevated range (150–450 x 10^9/L in 67.3%, 451–1000 x 10^9/L in 15.0%). Thrombocytosis exceeding 1000 x 10^9/L was seen in 7.9% of chronic-phase patients. In the accelerated phase, 57.0% had platelet counts of 150–450 x 10^9/L, while 18% showed elevated counts between 451–1000 x 10^9/L. Notably, in blast crisis, 10.5% of patients presented with severe thrombocytopenia (<20 x 10^9/L), indicating advanced marrow failure.

Survival of CML Patients Before and After TKI Therapy

Figure 8 presents the Kaplan–Meier survival analysis comparing chronic myeloid leukemia patients treated before the introduction of tyrosine kinase inhibitors (TKIs) (Group B, green curve) and those treated after TKI availability (Group A, blue curve).

Patients receiving TKI therapy (Group A) demonstrated markedly improved survival outcomes, with an estimated 5-year survival probability exceeding 80% and maintaining above 60% even at 10 years of follow-up. In contrast, patients managed before TKI availability (Group B) showed a steep decline in survival, with median survival below 4 years and 10-year survival approaching 0%. The difference between the two survival curves was statistically significant according to the log-rank test ($p < 0.001$).

In the TKI-treated cohort, the estimated overall survival was approximately 95% at 1 year, 89% at 3 years, and 81% at 5 years. Median overall survival was not reached during the observation period.

In contrast, the pre-TKI cohort showed substantially lower survival, with estimated survival of approximately 84% at 1 year, 53% at 3 years, and 23% at 5 years. The median overall survival in the pre-TKI group was approximately 3.5–4 years. The difference between survival curves was statistically significant according to the log-rank test ($p < 0.001$).

CML Mortality Trends Over Time

Figure 9 shows annual mortality incidence rates (MIR) for chronic myeloid leukemia patients in Azerbaijan from 2008 to 2023, stratified by sex. Overall, the mortality rate has declined over the study period, reflecting improvements in early diagnosis, monitoring, and treatment with tyrosine kinase inhibitors.

In the early observation years (2008–2011), the total mortality incidence rate ranged between 0.002 and 0.0045, with similar patterns across males and females. Peak mortality was observed around 2010–2014, where MIR values for males approached 0.0045 and for females reached 0.004. After 2015, a steady downward trend was evident, with the total MIR stabilizing below 0.0015 after 2020.

The mortality incidence rate (MIR) increased from 0.057 to 0.165 per 100,000 population between 2008 and 2016, after which it stabilized and showed a modest decline. Log-linear regression demonstrated an average annual percent change (AAPC) of +7.0% per year (95% CI: 4.0–9.0; $p < 0.001$).

First-Line Imatinib Response in CML Patients

Table 6 summarizes treatment responses to first-line imatinib therapy among 249 patients with chronic myeloid leukemia. At the 3-month evaluation, 198 patients (79.5%) achieved an optimal response, defined as BCR-ABL1 ≤ 10%, while 12 patients (4.8%) showed a suboptimal response (BCR-ABL1 > 10%). A total of 39 patients (15.7%) failed to achieve complete hematologic remission (CHR) at this time point.

At 6 months, 195 patients (78.3%) achieved BCR-ABL1 ≤ 1%, fulfilling criteria for optimal response, whereas 16 patients (6.4%) remained suboptimal (BCR-ABL1 > 1%), and 38 patients (15.3%) had BCR-ABL1 levels above 10%, indicating treatment failure.

By 12 months, 200 patients (80.3%) achieved major molecular response (MMR, BCR-ABL1 ≤ 0.1%), while 9 patients (3.6%) continued to show suboptimal response. In contrast, 40 patients (16.1%) failed treatment with BCR-ABL1 > 1% at 12 months.

ABL Kinase Domain Mutation Analysis

Mutation analysis of the ABL kinase domain was performed in 115 patients with chronic myeloid leukaemia who showed suboptimal response or resistance to imatinib. Fourteen distinct mutations were detected, most commonly affecting the P-loop and ATP-binding regions. The T315I mutation was the predominant variant, followed by substitutions at codons F359, Y253, E255, and F317.

A detailed list of all mutations, including nucleotide and amino-acid changes, is provided in Table 8. Several uncommon variants were confirmed by pyrosequencing in an external reference laboratory (Ankara ATQ Biotechnology Laboratories).

BCR-ABL Kinase Domain Mutations in Imatinib-Resistant Patients

BCR–ABL1 kinase domain mutation analysis was performed in 115 patients with suspected resistance or suboptimal response. Among these, 19 patients (16.5%) were found to harbor mutations. When expressed relative to the entire cohort of 766 patients, the overall mutation prevalence was 2.5%.

Among mutation-positive cases, the most frequent mutation was T315I, detected in 7 patients (36.8%), followed by F359C and F359V in 3 patients each (15.8%), Y253H and F317L (TTG) in 2 patients each (10.5%), and E255K and F317L (TTA) in 1 patient each (5.3%).

Comparison of Responders vs. Imatinib-Resistant Patients

Table 7 compares clinical characteristics between patients who responded to imatinib therapy (n=651) and those who were resistant (n=115).

Among imatinib responders, the median age was 47.3 years (range 4–84), with a female predominance (58% female, 42% male). In contrast, the imatinib-resistant group had a median age of 45.3 years (range 16–80) and a male predominance (55.7% male, 44.3% female).

Phase distribution showed that most responders were in chronic phase (84.8%), with 15.2% in accelerated phase and none in blast crisis. For the imatinib-resistant group, 78.3% were in chronic phase, 16.5% in accelerated phase, and 5.2% in blast crisis, indicating more advanced disease among resistant patients.

Risk stratification by the Sokal score revealed that among responders, 51.9% were low risk, 40.4% intermediate risk, and 7.7% high risk. Conversely, imatinib-resistant patients had a higher proportion of intermediate (58.3%) and high-risk (11.3%) profiles, with only 30.4% classified as low risk.

Characteristics of BCR-ABL Mutations in Imatinib-Resistant Patients

Table 8 provides a detailed breakdown of mutation characteristics among imatinib-resistant CML patients. The overall mutation detection rate was higher in patients over the age of 50 years (20.45%) compared to those under 50 years (14.08%), with a p-value of 0.045.

Mutation frequency was also higher in males (24.5%) than in females (7.8%), a difference observed . Among mutation-positive patients, T315I remained the predominant variant, detected in seven males (35.7 %) and two females (40 %). When calculated relative to the entire group of imatinib-resistant patients, this corresponded to approximately 9 % of males and 3 % of females overall.

Distribution of Detected Mutations by Disease Phase and Risk Group

Figure 20 shows how BCR-ABL mutations among imatinib-resistant patients were distributed according to disease phase and Sokal risk categories.

By disease phase, mutations were identified in approximately 11 % of patients in the chronic phase, 26 % in the accelerated phase, and 67 % in blast crisis.

By Sokal risk group, mutations were found in 15.4% of high-risk patients, 17.9% of intermediate-risk patients, and 14.3% of low-risk patients, without a difference.

Discussion

This study provides the first comprehensive epidemiological evaluation of chronic myeloid leukemia in Azerbaijan over a 16-year period. The variability in CML incidence across different countries likely reflects differences in genetic background, environmental exposures, population age structure, diagnostic infrastructure, and reporting standards [2]. For example, previous studies have reported CML incidence rates of around 1.5 per 100,000 in the United Kingdom [8], 1.2–1.5 per 100,000 in Italy [9], and about 1 per 100,000 in Japan [10].Placing Azerbaijan's incidence within this international context suggests it is in the mid-range globally, consistent with patterns observed in other upper-middle-income countries with developing hematology services. Continued improvement of cancer registries and diagnostic capacity will be essential to fully understand national trends.

The upward trend in prevalence likely reflects both increasing annual diagnoses and improved survival with tyrosine kinase inhibitor (TKI) therapy, which has transformed CML into a chronic, manageable condition [11]. These findings indicate a growing long-term care burden in Azerbaijan.

Although the national population increased from about 8 million in 2008 to nearly 10 million in 2023, all prevalence estimates were standardized per 100,000 population; therefore, the rise cannot be explained by population growth alone. It more likely reflects improved survival and accumulation of long-term treated patients.

Compared internationally, CML prevalence in Azerbaijan remains lower than in some Western European regions, such as Lombardy, Italy [12], likely due to differences in registry maturity, diagnostic access, and population age structure.

Risk group analyzing results are consistent with international patterns in which most patients are diagnosed in the chronic phase and classified into intermediate-risk groups, though the relatively low proportion presenting in blast crisis highlights the benefits of improved early detection and treatment access in this population [13]. The use of the Sokal score rather than more contemporary prognostic systems such as the ELTS score represents a limitation of the present study. Complete data required for ELTS calculation were not consistently available in the earlier years of the national registry, and therefore Sokal scoring was used to ensure uniformity across the full 16-year cohort. Future analyses of more recent patient subsets, where complete variables are available, may allow incorporation of ELTS-based risk stratification to improve contemporary prognostic assessment and international comparability.

The hematologic parameters highlight typical disease evolution in CML, with increasing basophilia and a trend toward thrombocytopenia as patient progress from chronic phase to blast crisis. These patterns illustrate typical hematologic features of CML at various stages, with lower

hemoglobin and higher leukocyte burdens observed in advanced phases [14,15].

One of the most striking features was a slight female predominance, contrary to the modest male predominance described in many global studies [17]. A similar female predominance has been noted in some local studies on leukemia in Azerbaijan [6]. The observed female predominance in this national cohort may reflect complex biological and sociocultural factors. Hormonal influences on immune modulation and tyrosine-kinase inhibitor metabolism, as well as differences in health-seeking behavior and occupational exposure, could contribute to the observed pattern. Estrogens have been shown to modulate hematopoietic stem and progenitor cell function, potentially influencing disease incidence and progression [18]. However, these explanations remain speculative and should be regarded as hypothesis-generating. Future mechanistic and population-based studies are needed to clarify the biological and environmental underpinnings of gender-related variations in CML. This finding should be interpreted with caution. Differences in healthcare access, referral patterns, health-seeking behavior, or occupational exposure profiles between men and women may contribute to the observed distribution and cannot be excluded. Because the present study was observational and registry-based, it was not designed to evaluate biological mechanisms underlying sex differences. Therefore, speculative explanations related to hormonal influences on hematopoiesis cannot be supported by the current data. Future population-based studies incorporating detailed occupational, environmental, and healthcare utilization variables will be necessary to clarify the determinants of sex-specific patterns in CML. The consistent increase in both incidence and prevalence observed across the study period is likely related to improved molecular diagnostics, greater disease awareness, and stronger referral pathways [19]. However, a true increase in CML burden cannot be ruled out, potentially associated with environmental exposures, lifestyle factors, and aging of the population, and deserves further monitoring [20].

Geographic mapping revealed that most CML cases were concentrated in the Absheron economic region, particularly Baku and Sumgayit. This is unsurprising given population density and proximity to advanced hematology centers. However, it is also notable that Absheron is an area with substantial industrial activity and documented air pollution [21]. Airborne pollutants, including benzene and particulate matter, have previously been associated with leukemogenesis [22, 23]. The observed geographic clustering is therefore consistent with the possibility of environmental or population-related influences on disease distribution. Nevertheless, this study was observational and descriptive in design and cannot establish a causal relationship between environmental exposures and CML occurrence. The higher case concentration in Absheron may also reflect population density, referral patterns, or healthcare accessibility. Future prospective studies incorporating quantitative environmental exposure assessment and individual-level risk factor data are needed to clarify potential associations.

Seasonal diagnostic patterns were also observed, with a higher proportion of diagnoses in summer and a lower rate in winter. This pattern should be interpreted with caution, as CML is a chronic myeloproliferative disorder with an insidious onset, making true biological seasonality unlikely. The observed distribution more plausibly reflects seasonal differences in healthcare utilization, infection-related laboratory testing, or healthcare-seeking behavior, which may lead to incidental detection of hematologic abnormalities [24]. Therefore, the seasonal variation likely represents differences in diagnostic timing rather than underlying disease biology. This should be considered a limitation of the present study, and larger prospective investigations incorporating detailed clinical and healthcare utilization data will be needed to clarify these findings.

An association between ABO blood group distribution and CML was observed, with a higher frequency of blood group A among patients compared with controls. However, this finding should be interpreted cautiously. As this was an observational, registry-based analysis, the association cannot be considered causal or definitive. Potential confounding factors, population structure, or referral patterns may have influenced the observed distribution. Therefore, the blood group association should be regarded as preliminary and hypothesis-generating, requiring independent validation in larger population-based cohorts.

Age distribution showed that most patients were diagnosed between 40 and 69 years, peaking in the 50–59 decade, which is consistent with global CML epidemiology [25]. The repeated finding of female predominance across several age brackets deserves closer study, as hormonal, environmental, or occupational exposures could all contribute.

The mutation findings in this study are generally consistent with international experience, with T315I and F359C/V emerging as the most frequent variants. However, these results should be interpreted with caution, as mutation testing was performed in a subset of 115 patients, representing those with treatment resistance or suboptimal response. This limited sample may not fully capture the true population distribution of ABL kinase-domain variants in Azerbaijan. Expanded molecular screening and longitudinal surveillance will be required to define mutation epidemiology more comprehensively.

In addition, BCR–ABL1 transcript subtype information (e.g., p190, p210, e13a2, e14a2) was not consistently available in the registry and was therefore not included in the analysis. This limits detailed baseline prognostic assessment and evaluation of treatment selection strategies. Future registry updates should incorporate systematic transcript-type recording to enhance prognostic modeling.

Treatment response to first-line imatinib was encouraging, with nearly 80% of patients achieving major molecular response by one year, consistent with international data [26]. Nevertheless, about 15% of patients showed suboptimal or failed responses, underlining the necessity of early molecular monitoring and the availability of second- and third-generation TKIs [27]. Mutation testing revealed a range of BCR-ABL kinase domain mutations among resistant cases, with T315I being the most common, similar to international experience [28]. Expanding mutation testing facilities and second-line treatment options will be critical for optimal disease control.

Lastly, survival analyses confirmed the enormous benefit of TKIs, with 5-year survival above 80% compared to a pre-TKI median survival of less than four years. These results highlight the importance of sustained access to these therapies to continue improving outcomes for Azerbaijani patients with CML [27, 29].

Detailed subgroup survival analyses from this national cohort, including sex-based comparisons, have been reported separately to provide more focused prognostic evaluations.

In summary, this study lays the foundation for understanding CML epidemiology in Azerbaijan. Ongoing efforts should prioritize strengthening registry data, expanding molecular testing, addressing possible environmental risk factors, and ensuring equitable access to care across both urban and rural areas.

Limitations

This study has several limitations to consider. Its retrospective design may introduce information bias and limit the completeness of clinical records, particularly from the earlier years of the observation period. Molecular analyses for BCR-ABL kinase domain mutations were conducted only in a subset of patients with imatinib resistance, potentially underestimating the overall mutation prevalence. Although geographic clustering was observed in industrial regions, this study did not directly collect detailed environmental exposure data, limiting causal conclusions about pollution and CML. Seasonal diagnosis patterns could also be influenced by healthcare utilization rather than true seasonal disease variation.

However, as the National Hematology and Blood Transfusion Center is the only hematology reference center in Azerbaijan, this dataset is likely to represent nearly the entire population of CML patients in the country, which strengthens the generalizability of these findings. Future prospective, multicenter collaboration could further validate and enrich these results.

Conclusion

This comprehensive epidemiological study provides the first nationwide description of chronic myeloid leukemia in Azerbaijan, leveraging data from the country's sole hematology reference center. The findings reveal unique gender patterns, with a slight female predominance, as well as an increasing incidence and prevalence trend over the study period. Geographic clustering of cases in the Absheron region and seasonal variations in diagnosis highlight the importance of further investigations into possible environmental and healthcare utilization factors.

Treatment responses to first-line imatinib were comparable to international standards, although approximately 15% of patients showed suboptimal or failed responses, emphasizing the need for continuous molecular monitoring and access to second- and third-generation TKIs. The notable survival benefit associated with TKI therapy underscores the value of sustaining investments in modern hematology infrastructure.

Finally, this large single-center dataset, which effectively reflects the CML population nationwide, provides a robust basis for health planning and public policy. Establishing a comprehensive national leukemia registry could further validate these findings and support policy planning. Future work should focus on exploring environmental risk factors, expanding regional diagnostic capabilities, and strengthening support for long-term disease monitoring and equitable care across Azerbaijan. This study provides a robust foundation for health system planning and public health initiatives.

Author Contributions: Conceptualization, A.S. and C.A.; methodology, A.S., C.A. and A.H.; validation, A.S. and Z.A.; formal analysis, A.S. and A.H.; investigation, A.S., C.A. and Z.A.; resources, C.A.; data curation, A.S. and A.H.; writing – original draft preparation, A.S.; writing – review and editing, A.S., C.A., A.H. and Z.A.; visualization, A.S.; supervision, C.A.; project administration, A.S.; funding acquisition, Not applicable. All authors have read and agreed to the published version of the manuscript.

Disclosures: The authors have no conflicts of interest.

Acknowledgments: The authors would like to thank the staff of the National Hematology and Blood Transfusion Center for their invaluable assistance in data collection and patient care. We also express our gratitude to the patients and their families, whose participation made this study possible.

Funding: None.

Data availability statement: All raw data underlying the findings of this study can be obtained from the corresponding author upon reasonable request.

Artificial Intelligence (AI) Disclosure Statement: AI- The authors declare no AI Tools used for preparation of this work.

References

1. Jabbour E, Kantarjian H. Chronic myeloid leukemia: 2025 update on diagnosis, monitoring, and treatment. *American Journal of Hematology.* 2023;98(1):95–109. https://doi.org/10.1002/ajh.27443
2. Chaulagain P, Poudel A, Aryal S, Sainatham C, Lutfi F. Global trends of burden of chronic myeloid leukemia based on socio-demographic index (SDI): a comparative epidemiological study. *Blood.* 2024;144(Suppl 1):7918. https://doi.org/10.1182/blood-2024-210443
3. Smith A, Howell D, Patmore R, Jack A, Roman E. Incidence of haematological malignancy by sub-type: a report from the Haematological Malignancy Research Network. *British Journal of Cancer*. 2011;105(11):1684–1692. https://doi.org/10.1038/bjc.2011.450
4. Karantanos T, Jain T, Moliterno AR, Jones RJ, DeZern AE. Sex-related differences in chronic myeloid neoplasms: from the clinical observation to the underlying biology. *International Journal of Molecular Sciences*. 2021;22(5):2595. https://doi.org/10.3390/ijms22052595
5. Ohyashiki K. Clinical epidemiology [in Japanese]. *Nihon Rinsho*. 2001;59(12):2416–2420.
6. Asadov Ch, Alimirzayeva Z, Kerimov A. Epidemiology of leukemia in Azerbaijan. Baku: Xazar Universitesi Nesriyyati; 2012.
7. Hochhaus A, Larson RA, Guilhot F, Radich JP, Branford S, Hughes TP, Baccarani M, Deininger MW, Cervantes F, Fujihara S, Ortmann CE, Menssen HD, Kantarjian H, O'Brien SG, Druker BJ. Long-term outcomes of imatinib treatment for chronic myeloid leukemia. *New England Journal of Medicine.* 2017;376(10):917–927. https://doi.org/10.1056/NEJMoa1609324
8. Li J, Smith A, Crouch S, Oliver S, Roman E. Estimating the prevalence of hematological malignancies and precursor conditions using data from the Haematological Malignancy Research Network (HMRN). *Cancer Causes & Control.* 2016;27(8):1019–1026. https://doi.org/10.1007/s10552-016-0780-z
9. Ferlay J, Steliarova-Foucher E, Lortet-Tieulent J, Rosso S, Coebergh JWW, Comber H, Forman D, Bray F. Cancer incidence and mortality patterns in Europe: estimates for 40 countries in 2012. *European Journal of Cancer*. 2013;49(6):1374–1403. https://doi.org/10.1016/j.ejca.2012.12.027
10. Au WY, Caguioa PB, Chuah C, Hsu SC, Jootar S, Kim DW, Kweon IY, O'Neil WM, Saikia TK, Wang J. Chronic myeloid leukemia in Asia. *International Journal of Hematology*. 2009;89(1):14–23. https://doi.org/10.1007/s12185-008-0230-0
11. Szczepanek E, Chukwu O, Kamińska M, Wysogląd H, Cenda A, Zawada M. Long-term outcomes of patients with chronic myeloid leukemia who commenced treatment with imatinib: a 20-year single-centre experience. *Leukemia & Lymphoma.* 2022;63(9):2213–2223. https://doi.org/10.1080/10428194.2022.2068000
12. Maas CCHM, van Klaveren D, Ector GICG, Posthuma EFM, Visser O, Westerweel PE, Janssen JJWM, Blijlevens NMA, Dinmohamed AG. The evolution of the loss of life expectancy in patients with chronic myeloid leukaemia: a population-based study in the Netherlands, 1989–2018. *British Journal of Haematology.* 2022;196(5):1219–1224. https://doi.org/10.1111/bjh.17989
13. Jabbour E, Kantarjian H. Chronic myeloid leukemia: 2022 update on diagnosis, therapy, and monitoring. American Journal of Hematology. 2022;97(9):1236–1256. doi.org/10.1002/ajh.26642
14. Turhan AG. Chronic myelogenous leukaemia: recent progress in biology and therapeutic strategies [in French]. *Bulletin du Cancer.* 2005;92(1):75–82.
15. Baccarani M, Pileri S, Steegmann JL, Müller M, Soverini S, Dreyling M; ESMO Guidelines Working Group. Chronic myeloid leukemia: ESMO Clinical Practice Guidelines for diagnosis, treatment and follow-up. *Annals of Oncology.* 2012;23(Suppl 7):vii72–vii77. https://doi.org/10.1093/annonc/mds228
16. Usui N. Molecular targeted treatment—new treatment strategy for patients with chronic myeloid leukemia [in Japanese]. Rinsho Byori (Japanese Journal of Clinical Pathology). 2004;52(2):136–144.
17. Shirinova A, Asadov C, Hasanova A, Alimirzoyeva Z. Unique gender-related characteristics and differences of chronic myeloid leukemia patients in Azerbaijan: a retrospective cohort study. *Cureus*. 2025;17(10):e94677. https://doi.org/10.7759/cureus.94677
18. Illing A, Liu P, Ostermay S, Schilling A, de Haan G, Krust A, Amling M, Chambon P, Schinke T, Tuckermann JP. Estradiol increases hematopoietic stem and progenitor cells independent of its actions on bone. *Haematologica*. 2012;97(8):1131–1135. https://doi.org/10.3324/haematol.2011.052456
19. Steliarova-Foucher E, O'Callaghan M, Ferlay J, Masuyer E, Rosso S, Forman D, Bray F, Comber H. The European Cancer Observatory: a new data resource. *European Journal of Cancer.* 2015;51(9):1131–1143. https://doi.org/10.1016/j.ejca.2014.01.027
20. Lin Q, Mao L, Shao L, Zhu L, Han Q, Zhu H, Jin J, You L. Global, regional, and national burden of chronic myeloid leukemia, 1990–2017: a systematic analysis for the Global Burden of Disease Study 2017. *Frontiers in Oncology.* 2020;10:580759. https://doi.org/10.3389/fonc.2020.580759
21. Aliyeva G, Salamzadeh S. Air pollution and its effects in Baku: a public health perspective. *Azerbaijan Medical Journal.* 2018;54(2):45–50.
22. Smith MT. Advances in understanding benzene health effects and susceptibility. *Annual Review of Public Health.* 2010;31:133–148. https://doi.org/10.1146/annurev.publhealth.012809.103646
23. Turner MC, Andersen ZJ, Baccarelli A, Diver WR, Gapstur SM, Pope CA 3rd, Prada D, Samet J, Thurston G, Cohen A. Outdoor air pollution and cancer: an overview of the current evidence and public health recommendations. *CA: A Cancer Journal for Clinicians*. 2020;70(6):460–479. https://doi.org/10.3322/caac.21632
24. Hassan J, Adil SO, Haider Z, Zaheer S, Anwar N, Nadeem M, Ansari SH, Shamsi T. Seasonal variations in hematological disorders: a 10-year single-center experience. *International Journal of Laboratory Hematology.* 2021;43(1):93–98. https://doi.org/10.1111/ijlh.13337
25. Bower H, Björkholm M, Dickman PW, Höglund M, Lambert PC, Andersson TM. Life expectancy of patients with chronic myeloid leukemia approaches the life expectancy of the general population. *Journal of Clinical Oncology.* 2016;34(24):2851–2857. https://doi.org/10.1200/JCO.2015.66.2866
26. Hughes TP, Hochhaus A, Branford S, Müller MC, Kaeda JS, Foroni L, Druker BJ, Guilhot F, Larson RA, O'Brien SG, Rudoltz MS, Mone M, Wehrle E, Modur V, Goldman JM, Radich JP, on behalf of the IRIS investigators. Long-term prognostic significance of early molecular response to imatinib in newly diagnosed chronic myeloid leukemia: an analysis from the International Randomized Study of Interferon and STI571 (IRIS). *Blood*. 2010;116(19):3758–3765. https://doi.org/10.1182/blood-2010-03-273979

27. Druker BJ, Talpaz M, Resta DJ, Peng B, Buchdunger E, Ford JM, Lydon NB, Kantarjian H, Capdeville R, Ohno-Jones S, Sawyers CL. Efficacy of a specific BCR-ABL tyrosine kinase inhibitor in chronic myeloid leukemia. *New England Journal of Medicine.* 2001;344(14):1031–1037. https://doi.org/10.1056/NEJM200104053441401
28. Soverini S, Hochhaus A, Nicolini FE, Gruber F, Lange T, Saglio G, Pane F, Mueller MC, Ernst T, Rosti G, Porkka K, Baccarani M, Cross NCP, Martinelli G. BCR-ABL kinase domain mutations and resistance to first- and second-generation tyrosine kinase inhibitors. *Blood*. 2011;118(15):4010–4015. https://doi.org/10.1182/blood-2010-12-326405
29. Goldman JM, Melo JV. Chronic myeloid leukemia—advances in biology and new approaches to treatment. *New England Journal of Medicine.* 2003;349(15):1451–1464. https://doi.org/10.1056/NEJMra020777

JOURNAL OF CLINICAL MEDICINE OF KAZAKHSTAN (E-ISSN 2313-1519)
Original Article DOI: https://doi.org/10.23950/jcmk/18438

The Region-Specific Landscape of Sensitization to Respiratory Allergens in the Population of Kazakhstan Accord Based on Molecular Diagnostics

Nurlan R. Utelbayev[1], Marina A. Morenko[1], Aleksandr N. Pampura[2], Kseniya V. Shnayder[1], Madina R. Gatauova[1], Nadezhda A. Mayevskaya[1], Zhanat N. Abdikadyr[3], Adil A. Zhamankulov[1], Yerlan Suleimenov[4], Alexey Balas[4]

[1]*Department of Pediatric Diseases №1, Astana Medical University (AMU), Astana, Kazakhstan*
[2]*Scientific Research Institute of Pediatrics (SRIP) named after Academician Yu. E. Veltishchev. Federal State Budgetary Educational Institution of Higher Education "Russian National Research Medical University named after N. I. Pirogov" of the Ministry of Health of the Russian Federation, Russia, Moscow*
[3]*Department of Epidemiology and Biostatistics, Astana Medical University, Astana, Kazakhstan*
[4]*OLYMP Clinical Diagnostic Laboratory LLP, Astana, Kazakhstan*

Received: 2025-12-12.
Accepted: 2026-04-13.

This work is licensed under a **Creative Commons Attribution 4.0 International License**

J Clin Med Kaz 2026; 23(2): 19-30

Corresponding author:
Nurlan Utelbayev.
E-mail: utelbayev.n@amu.kz.
ORCID: 0009-0007-9995-5884.

ABSTRACT

Introduction: Allergic diseases still remain one of the most common and widespread chronic pathologies of our time, affecting up to 40% of the population. Due to its unique environment, which presents a combination of steppe, desert and mountain ecosystems, the Republic of Kazakhstan is of particular interest for studying regional sensitization features. The use of molecular diagnostic methods, such as ImmunoCAP ISAC, makes it possible to detect sensitization at the level of individual allergenic components and form personalized therapy strategies.

Aim: Evaluate epidemiological and regional features of sensitization to respiratory allergens in Kazakhstan for the period 2021-2024 using component allergy diagnostics.

Methods: The study embraces 4,745 patients with clinical manifestations of allergic diseases (allergic rhinitis, bronchial asthma, atopic dermatitis) who were tested against the ISAC panel (21 inhaled allergens). Descriptive statistics, Pearson's $\chi 2$ criterion, Monte Carlo simulation, and Fisher's exact criterion were used.

Results: During the observation period, the median number of sensitizations increased more than sixfold (from 18.0 in 2021 to 113.0 in 2024), indicating an increase in allergic load. The most frequently detected components were rFel d 1 (34.7%), rPhl p 1 (23.0%), nArt v1 (22.8%) and rBet v1 (21.5%).

Significant regional differences were identified ($p = 0.001$): weeds (Ambrosia, Artemisia) prevailed in the southern regions, tree allergens (Betula, Alnus) prevailed in the northern regions, polysensitization prevailed in the central and eastern regions, and a combination of steppe and household allergens prevailed in the western regions. Gender differences did not demonstrate any statistical significance ($p > 0.05$).

Conclusion: The study revealed a substantial increase in sensitization in Kazakhstan and a confirmed geographical stratification of the allergenic spectrum. The results obtained emphasize the need for introduction of regionally adapted diagnostic panels, development of personalized allergen-specific immunotherapy (ASIT) regimens and system monitoring of molecular profile of sensitization for realization of personalized medicine principles.

Keywords: sensitization, allergens, ImmunoCAP ISAC, Kazakhstan, component-resolution diagnostics, allergen-specific immunotherapy, epidemiology of allergy, regional peculiarities.

Introduction

Allergic diseases are currently regarded as one of the most significant medical and social health problems worldwide. According to the World Health Organization (WHO), allergic disorders are detected in 20–30% of the population in industrialized countries, while in some regions the prevalence reaches up to 40%. The frequency and structure of allergic diseases largely depend on climatic, environmental, and botanical characteristics of a given territory, which determine the spectrum of aeroallergens and shape the pattern of sensitization in the population.

Kazakhstan is located at the intersection of steppe, desert, semi-desert, and mountainous ecosystems and is characterized by pronounced climatic and geographic diversity. The territory of the country includes arid, sharply continental, and mountainous zones, each with a specific composition of vegetation and distinct pollen exposure patterns. Such environmental heterogeneity creates conditions for the formation of a wide spectrum of inhalant allergens and contributes to the development of polysensitization in the population [1–3].

In Central Asian countries, pollen allergens from trees, grasses, and weeds belonging to the families Betulaceae, Poaceae, Asteraceae, and Amaranthaceae play a leading role in the structure of respiratory allergy. Among tree allergens, the most clinically relevant are species of the genera Betula (birch), Alnus (alder), and Corylus (hazel), which predominate in northern and eastern regions characterized by more humid and moderately continental climates. Pollen from grasses of the family Poaceae, including Phleum pratense (timothy grass), is widely distributed in steppe and forest-steppe zones and represents one of the most common causes of seasonal allergic rhinitis. In arid and semi-desert regions, weed species predominate, particularly Artemisia (mugwort), Ambrosia (ragweed), and Salsola (saltwort), which are considered major sources of aeroallergens under continental climate conditions. Pollen of Artemisia and representatives of the family Amaranthaceae is regarded as one of the main factors in the development of pollinosis in Central Asia and Eastern Europe [4–6].

Previous epidemiological studies have demonstrated that the structure of sensitization significantly depends on climatic conditions, vegetation patterns, and the degree of urbanization. In regions with dry continental climates, sensitization to weed pollen is more frequently observed, whereas in northern and forest-steppe areas reactions to tree pollen predominate. These differences emphasize the need for region-specific data when evaluating sensitization patterns and planning allergen-specific immunotherapy.

In recent years, significant progress in the study of allergic diseases has been associated with the introduction of component-based molecular allergodiagnostics. The ImmunoCAP ISAC technology allows detection of specific IgE not only to allergen extracts but also to individual molecular components, making it possible to distinguish primary sensitization from cross-reactivity and to identify clinically relevant allergens

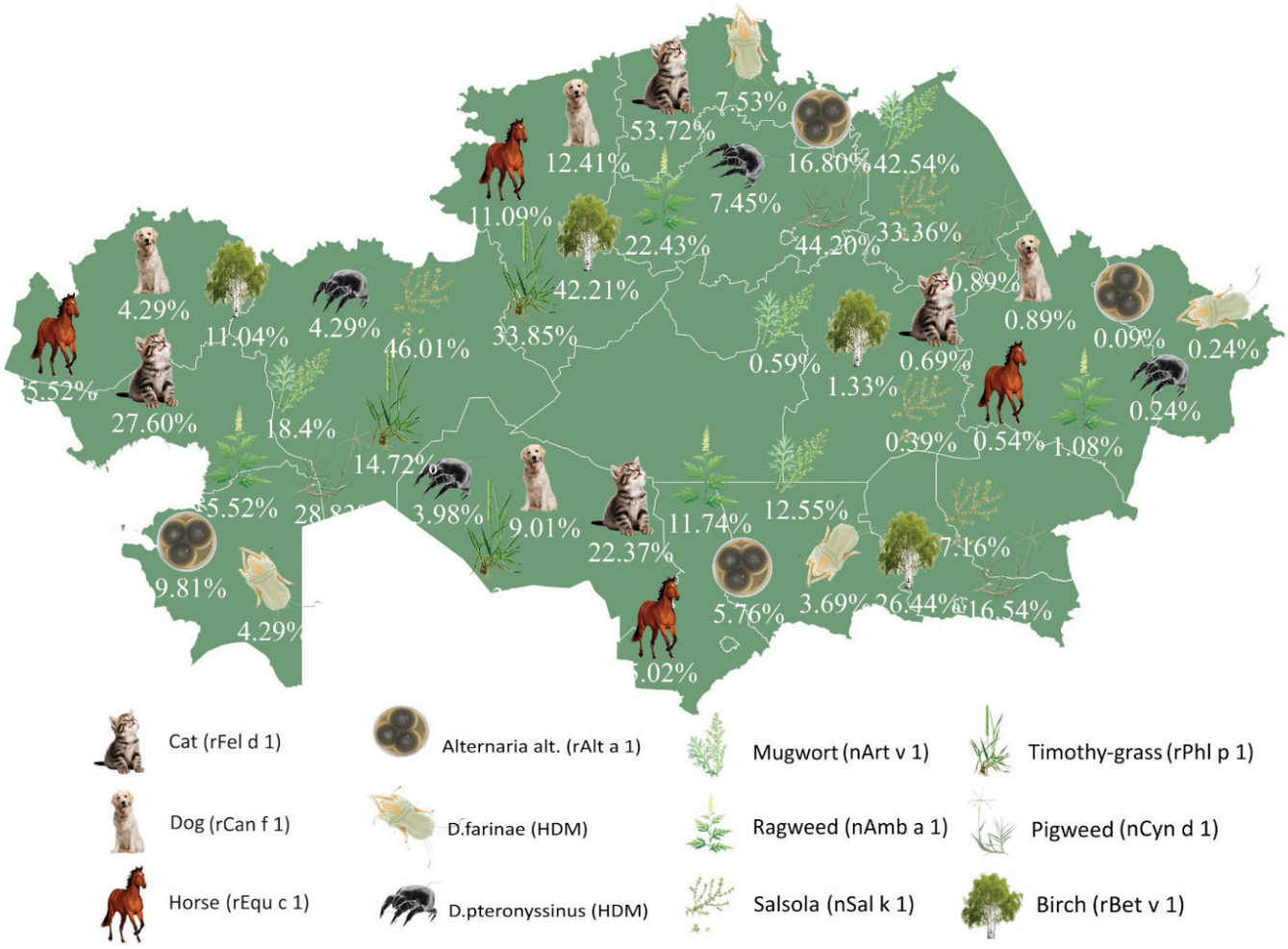

Figure 1 –The landscape of sensitization spectrum of Republic of Kazakhstan

[26, 27]. This approach is particularly important in regions with high floristic variability, where conventional diagnostic methods may not accurately reflect the true structure of sensitization.

Objective. To evaluate the structure of sensitization to inhalant allergens among patients from different regions of Kazakhstan between 2021 and 2024 using component-based molecular allergy diagnostics.

Methods

Study design and population

A retrospective, multicenter, observational study was conducted to evaluate the structure of molecular sensitization in patients from the Republic of Kazakhstan using component-resolved molecular allergodiagnostics.

Laboratory data obtained between January 2021 and December 2024 were included in the analysis. The final sample consisted of 4745 patients who underwent testing using the ImmunoCAP ISAC method.

Patients were referred for component-resolved diagnostics by allergists, pediatricians, pulmonologists, dermatologists, and general practitioners due to suspected IgE-mediated allergic diseases, presence of polysensitization, discrepancy between clinical manifestations and extract-based diagnostics, severe or systemic reactions, as well as during planning of allergen-specific immunotherapy (AIT). Thus, the study cohort represents a clinically selected population rather than a population-based sample.

Inclusion and exclusion criteria

Inclusion criteria:

1. Age of the patient from 1 to 80 years.
2. Availability of testing performed using the ImmunoCAP ISAC method during the period from January 2021 to December 2024.
3. Availability of a valid result of molecular allergy diagnostics with the possibility of analyzing inhalant allergen components.
4. Availability of the minimum required set of demographic data: age, sex, region, and year of testing.
5. Availability of a unique anonymized identifier allowing exclusion of repeated tests of the same patient.
6. Examination of the patient in medical institutions of the Republic of Kazakhstan / availability of data attributable to the population of the Republic of Kazakhstan.

Exclusion criteria:

1. Repeated testing of the same patient; only the first result was included in the analysis.
2. Incomplete laboratory data.
3. Incomplete or logically inconsistent demographic data.
4. Inability to perform unambiguous regional stratification of the patient.
5. Technically incorrect test results, including pre-analytical and analytical errors, as well as invalid internal controls.
6. Absence of results for key analyzed inhalant allergen components.
7. Age outside the established study range.

Molecular allergodiagnostic method

Molecular sensitization was assessed using the ImmunoCAP ISAC microarray platform (Thermo Fisher Scientific, Uppsala, Sweden), which allows semi-quantitative detection of specific IgE antibodies to 112 allergen components.

Serum samples were analyzed according to the manufacturer's instructions. Results were expressed in ISU-E (ISAC Standardized Units). The positivity threshold was defined as ≥ 0.3 ISU-E. Sensitization levels were interpreted as follows: 0.3–1 ISU-E — low level, 1–15 ISU-E — moderate level, 15 ISU-E — high level. Interpretation of molecular profiles was performed taking into account biochemical properties of allergens and known mechanisms of cross-reactivity.

Clinical stratification

Complete clinical data on confirmed diagnoses (allergic rhinitis, bronchial asthma, atopic dermatitis, food allergy, etc.) were not available for the entire study cohort.

The analysis was based on anonymized laboratory data extracted from the database of a clinical diagnostic laboratory and included only results of component-resolved molecular allergodiagnostics together with basic demographic parameters (age, gender, region of residence).

Due to complete data depersonalization, individual verification of clinical diagnoses, as well as the retrieval and analysis of medical records for each of the 4,745 patients at the level of healthcare institutions across the Republic of Kazakhstan, were not feasible from both organizational and ethical perspectives.

Therefore, the present study has primarily a laboratory-epidemiological design and is aimed at analyzing the structure of molecular sensitization rather than clinical phenotyping of patients.

Statistical analysis

Statistical analysis was performed using Microsoft Excel software (Microsoft Corp., USA).

The analysis was predominantly descriptive and aimed at evaluating the prevalence of molecular sensitization and comparing the frequency of detection of allergen components and panallergen families.

Quantitative values of specific IgE (ISU-E) were analyzed as continuous variables. Because of non-normal distribution, data were described using median (Me) and interquartile range (IQR).

Categorical variables (presence or absence of sensitization) were presented as absolute values and relative frequencies n (%). The prevalence of sensitization was calculated using the formula: $P (\%) = n / N \times 100$, where n is the number of patients with a positive result and N is the total number of examined patients (4745).

Comparison of proportions between allergen groups and panallergen families was performed using Pearson's χ^2 test. When expected values in contingency tables were less than 5, Fisher's exact test was applied. The level of statistical significance was set at $p < 0.05$.

Since the analysis had a predominantly descriptive epidemiological character, correction for multiple comparisons was not performed; statistically significant differences were interpreted taking into account clinical and biological plausibility.

The analysis was performed using a complete-case approach; missing values were not imputed.

Ethical considerations

The study protocol was approved by the local ethics committee of NJSC "Astana Medical University", Astana,

Kazakhstan. The study was based on retrospective analysis of anonymized laboratory data obtained from the database of "OLYMP Clinical Diagnostic Laboratory LLP" (Kazakhstan). Personal data were not available to the investigators. According to current legislation and local regulations, analysis of anonymized data did not require individual informed consent or additional ethical approval. The study was conducted in accordance with the principles of the Declaration of Helsinki.

Results

A total of 4745 patients were included in the study: 364 were examined in 2021, 371 in 2022, 854 in 2023, and 3156 in 2024. An increase in the number of examined patients was observed over the study period, most pronounced in 2024, which may be related to increased awareness of molecular allergodiagnostics, improvement of diagnostic methods, and growing clinical interest in polysensitization [13, 14].

Since the distribution of quantitative variables was non-normal, the data were described using median (Me) and interquartile range (Q1–Q3): 2021 — Me = 18.0 (Q1–Q3: 10.5–49.0); 2022 — Me = 25.0 (11.0–52.0); 2023 — Me = 34.0 (18.5–87.5); 2024 — Me = 113.0 (61.0–280.5), max = 1009, as shown in Table 1.

Table 1 Descriptive statistics of overall sensitization analysis

Indicators	ME	$Q_1 - Q_3$	n	MIN	MAX
2021	18,00	10,50 – 49,00	55	1,00	159,00
2022	25,00	11,00 – 52,00	55	0,00	182,00
2023	34,00	18,50 – 87,50	55	0,00	295,00
2024	113,00	61,00 – 280,50	55	1,00	1009,00

The use of the median as a measure of central tendency ensures robustness of the analysis in the presence of asymmetric distributions, while the interquartile range reflects the variability of the sample.

At the same time, a progressive increase in both the interquartile range and the maximum values was observed, indicating changes in the distribution shape and an expansion of the variability range across the respective cohorts. Since the analysis was based on independent patient samples, these differences should be interpreted as inter-cohort variations reflecting differences in the composition of the examined groups, rather than as temporal trends at the individual level.

For analytical convenience, all identified allergens were conditionally grouped into three main categories: epidermal allergens, pollen allergens and indoor allergens.

Among epidermal allergens, the highest sensitization frequency was observed for the major cat allergen components rFel d 1 (34.7%) and Fel d 4 (10.2%).

Sensitization to major dog allergens was less frequent: rCan f 1 was detected in 9.1% of patients and rCan f 6 in 6.0%. The third most common epidermal allergen was the horse allergen rEqu c 1, detected in 6.8% of examined individuals. The lowest sensitization rates among epidermal allergens were observed for rodent allergens (mouse and hamster), not exceeding 2% of cases (Figure 2).

With regard to pollen allergens, the highest sensitization rates were detected for major components of timothy grass — rPhl p 1 (23.0%), rPhl p 2 (2.8%), rPhl p 4 (12.6%), rPhl p 5

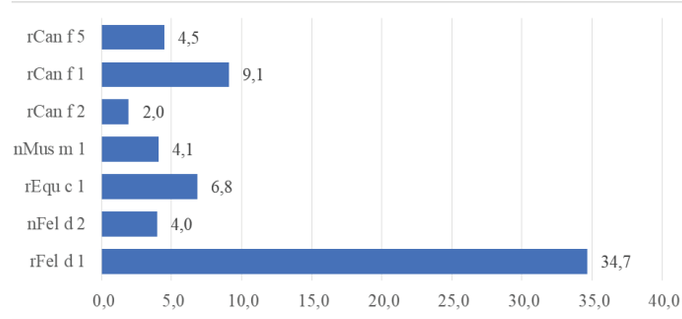

Figure 2 – Spectrum of sensitization to epidermal allergens (%)

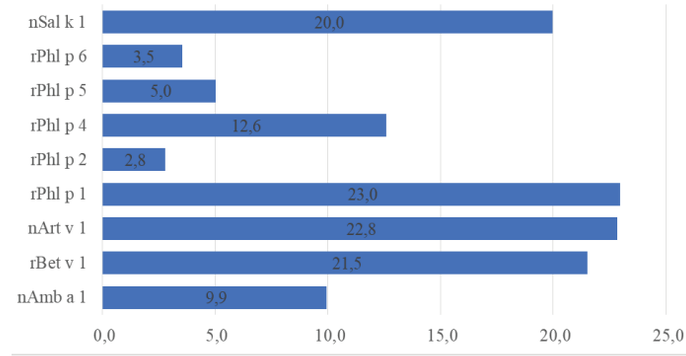

Figure 3 – Spectrum of pollen sensitization (%)

(5.0%), and rPhl p 6 (3.5%); mugwort — nArt v 1 (22.8%); birch — rBet v 1 (21.5%); bermuda grass — nCyn d 1 (20.3%); and saltwort — nSal k 1 (20.0%).

Sensitization to the major allergen components of annual mercury — rMer a 1 was detected in 17.5% of patients, and to alder — rAln g 1 in 13.4%.

The identified components included allergens derived from trees, grasses, and weed pollen (Figure 3).

Regarding indoor allergens, the highest frequency of sensitization was observed for house dust mites, including Dermatophagoides pteronyssinus — nDer p 1 (4.4%) and Dermatophagoides farinae — nDer f 1 (4.5%).

With respect to fungal allergens, the most prevalent component was Alternaria alternata — rAlt a 1 (9.9%), whereas Aspergillus fumigatus (rAsp f 1, rAsp f 3, rAsp f 6) and Cladosporium herbarum were detected in 2–3% of cases (Figure 4).

Thus, the sensitization profile was characterized by a combination of high-frequency components (rFel d 1, rPhl p 1,

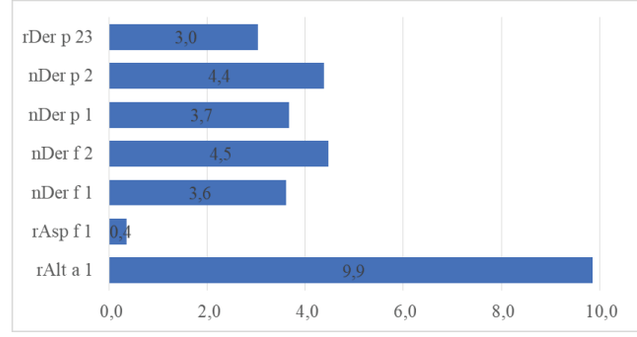

Figure 4 – Spectrum of sensitization to indoor allergens (%)

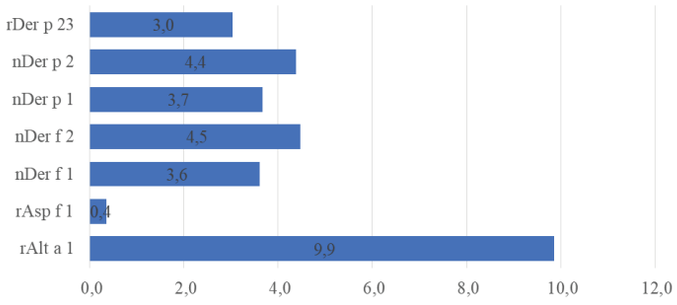

Figure 5 – Dominant molecular allergen components

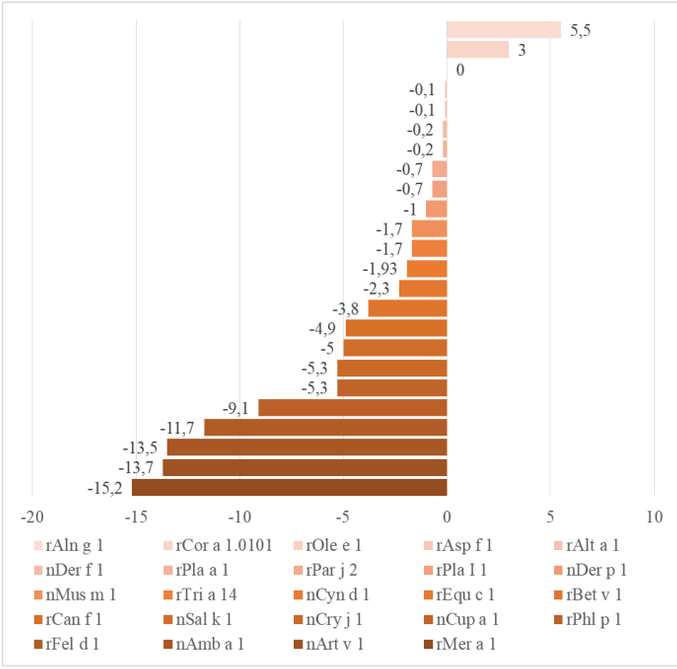

Figure 6 – Changes of sensitization to allergen components (percentage points)

rBet v 1, nArt v 1) and a wide range of less prevalent allergens, which can be visually demonstrated by the Pareto chart shown in Figure 5.

Differences in sensitization frequency to individual allergen components were observed between yearly patient cohorts. The corresponding data are presented in Table 2, with visualization shown in Figure 6.

For comparative analysis of the sensitization structure, the results are presented as the proportion of sensitized patients (%) and the difference between 2021 and 2024 expressed in percentage points (pp), which allows comparison of independent samples without interpreting the observed differences as temporal changes.

The largest differences between yearly cohorts for pollen allergens were observed for the following components: annual mercury (rMer a 1): −15.2 percentage points (from 32.7% to 17.5%); mugwort (nArt v 1): −13.7 pp (from 36.5% to 22.8%); timothy grass (rPhl p 1): −9.1 pp (from 32.1% to 23.0%); ragweed (nAmb a 1): −13.5 pp (from 20.9% to 7.4%).

Relatively stable values were observed for birch (rBet v 1), where the difference was −3.8 pp (from 25.3% to 21.5%), as well as for bermuda grass (nCyn d 1), for which the sensitization

Table 2 Changes in sensitization to allergen components by year (percentage points)

Allergen		2021	2022	2023	2024	Change (p.p.)
Ragweed *Ambrosia artemisiifolia*	nAmb a 1	20,9	18,3	10,5	7,4	-13,5
Birch *Betula verrucosa*	rBet v 1	25,3	26,4	17,1	21,5	-3,8
Cypress *Cupressus sempervirens*	nCup a 1	11,3	13,2	5,7	6	-5,3
Salsola (saltwort) *Salsola kali*	nSal k 1	25	27,7	23,1	20	-5
Bermuda grass *Cynodon dactylon*	nCyn d 1	8	7,1	11,8	6,07	-1,93
Alder *Alnus glutinosa*	rAln g 1	7,9	8,1	8,1	13,4	5,5
Plane tree *Platanus acerifolia*	rPla a 1	0,3	0,5	0,1	0,1	-0,2
Plantain *Plantago lanceolata*	rPla I 1	2,2	2,5	1,3	1,5	-0,7
Mugwort *Artemisia vulgaris*	nArt v 1	36,5	31,2	23,7	22,8	-13,7
Wall pellitory *Parietaria officinalis*	rPar j 2	1,4	2,3	0,6	0,7	-0,7
Annual mercury *Mercurialis annua*	rMer a 1	32,7	29,7	17,8	17,5	-15,2
Wheat *Triticum aestivum*	rTri a 14	4,9	7,1	4,8	3,2	-1,7
Olive tree *Olea europaea*	rOle e 1	0,5	1	0,4	0,5	0
Hazel *Corylus avellana*	rCor a 1.0101	9,3	10,7	10,7	12,3	3
Timothy grass *Phleum pratense*	rPhl p 1	32,1	30,5	20,3	23	-9,1
Japanese cedar *Cryptomeria japonica*	nCry j 1	10,7	15,5	5,2	5,4	-5,3
Alternaria alternata	rAlt a 1	10	9,9	0	9,9	-0,1
Aspergillus fumigatus	rAsp f 1	0,5	1,3	0	0,4	-0,1
D.farinae (HDM)	nDer f 1	3,8	3,6	3,6	3,6	-0,2
D. pteronyssinus (HDM)	nDer p 1	4,7	4,6	3,1	3,7	-1
Cat	rFel d 1	43,7	46,2	34,7	32	-11,7
Horse	rEqu c 1	9,1	9,1	7,3	6,8	-2,3
Mouse	nMus m 1	5,8	2,8	4	4,1	-1,7
Dog	rCan f 1	14	10,7	8,3	9,1	-4,9

frequency remained close to 20% in all cohorts. Some tree pollen allergens demonstrated higher values in 2024 compared with 2021, including rAln g 1 (+5.5 pp) and rCor a 1.0101 (+3.0 pp).

For animal-derived allergens, the highest sensitization frequency in all cohorts was observed for cat allergen rFel d 1. The proportion of sensitized patients was 43.7% in 2021, 46.2% in 2022, 34.7% in 2023, and 32.0% in 2024, corresponding to a difference of −11.7 pp between 2021 and 2024. Sensitization to dog allergen rCan f 1 decreased from 14.0% to 9.1% (−4.9 pp).

Among fungal allergens, the most pronounced difference was observed for Alternaria alternata (rAlt a 1), with an increase of +5.8 pp (from 4.1% to 9.9%). For Aspergillus fumigatus (rAsp f 1), absolute values remained low in all cohorts. House

dust mite allergens demonstrated relative stability: nDer f 1 — approximately 3.6% (−0.2 pp), nDer p 1 — approximately 3.7% (−1.0 pp).

To assess possible differences in gender distribution between yearly cohorts, statistical analysis was performed using Pearson's χ^2 test. Of the 4745 examined patients, 2483 were male (52.3%) and 2262 were female (47.7%). The data are detailed in Table 3 and graphically represented in Figure 7.

The gender distribution of patients across the yearly cohorts showed only minor differences. Statistical analysis using Pearson's χ^2 test yielded the following results: $\chi^2 = 5.92$; df = 3; p = 0.116. These findings indicate no statistically significant differences in gender distribution between yearly cohorts ($p > 0.05$).

Table 3 Observed frequencies of patients by gender and year

Gender	2021	2022	2023	2024	Total
Males	204	210	448	1621	2483
Females	160	161	406	1535	2262
Total	364	371	854	3156	4745

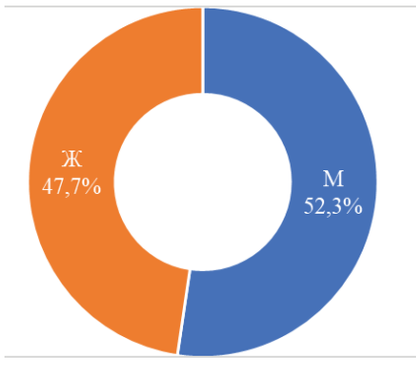

Figure 7 – Pie chart showing the distribution of examined patients by gender (%)

For the analysis of age distribution, patients were divided into six age categories: 1–3 years, 4–6 years, 7–10 years, 11–14 years, 15–18 years, and ≥18 years, as presented in Table 4.

The distribution of patients across age groups was uneven, with the largest proportion observed in the adult category (≥18 years).

The number of patients in the age groups was as follows: 1–3 years — 523 patients (11.02%), 4–6 years — 669 (14.1%), 7–10 years — 844 (17.8%), 11–14 years — 529 (11.2%), 15–18 years — 325 (6.8%), ≥18 years — 1855 (39.1%), as shown in Figure 8.

Table 4 Age structure of examined patients with respiratory allergy

Age (years)	2021	2022	2023	2024	Total
1-3	27	31	120	345	523
4-6	45	55	111	458	669
7-10	59	67	163	555	844
11-14	46	53	91	339	529
15-18	33	31	67	194	325
18 and over	154	134	302	1265	1855

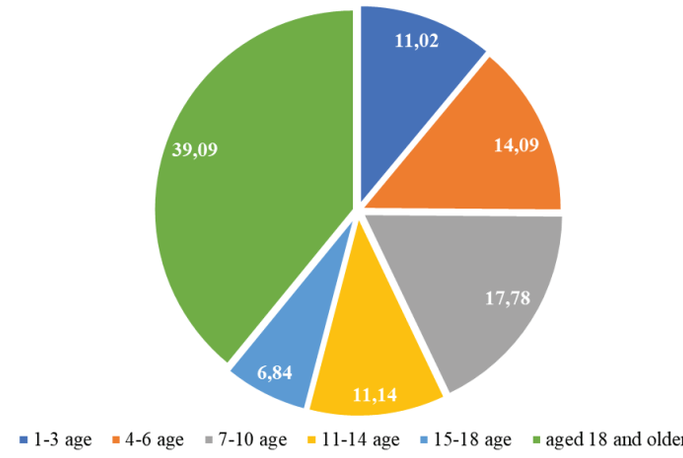

Figure 8 – Sensitization to respiratory allergens by age groups (%)

In all yearly cohorts, the adult group remained the largest, with proportions ranging from 40.6% to 42.3%. Among pediatric age categories, the highest representation was observed in the 7–10 years group, followed by the 4–6 years and 1–3 years groups.

The 15–18 years group was the least represented among all age categories. The distribution of patients by age differed between yearly cohorts, as reflected in the contingency table.

To assess the statistical significance of differences in age distribution between yearly cohorts, Pearson's χ^2 test was applied. The analysis demonstrated statistically significant differences in the distribution of age categories between yearly cohorts: $\chi^2 = 351.44$; df = 15; $p < 0.00001$.

These findings indicate heterogeneity of the age composition of examined patients across different years, while the predominance of the adult age group remained consistent in all cohorts.

The analysis conducted also demonstrated that patients sensitized to inhalant allergens were identified across all age groups; however, the frequency of detection of individual components varied depending on the age category. In younger age groups, sensitization to food and cross-reactive components was more frequently observed, whereas in older age groups inhalant allergens predominated, including pollen, epidermal, and household components.

In adult patients, multiple sensitization involving several allergen groups simultaneously was observed more often.

Climatogeographical characteristics of sensitization were analyzed by comparing the frequency of inhalant allergen detection in patients residing in different regions of Kazakhstan, as presented in Table 5.

In the southern regions, the highest sensitization frequency was observed for grass and weed allergens. The most frequently detected components were birch — rBet v 1 (26.44%), hazel pollen — rCor a 1.0101 (18.02%), timothy grass — rPhl p 1 (17.35%), bermuda grass — nCyn d 1 (16.54%), mugwort — nArt v 1 (12.55%), and ambrosia — nAmb a 1 (11.74%). Sensitization to tree pollen allergens was also detected, although its frequency was lower compared with the northern region.

In the central-eastern region, the sensitization frequency for most allergen components was substantially lower and

Table 5 Geographical patterns of sensitization (%)

Allergen		Region			
		Western	Northern	Central-Eastern	Southern
Ragweed *(Ambrosia artemisiifolia)*	nAmb a 1	5,52	22,43	1,08	11,74
Birch *(Betula verrucosa)*	rBet v 1	11,04	42,21	1,33	26,44
	rBet v 2	9,20	24,83	0,09	6,05
	rBet v 4	3,06	5,21	0,19	3,02
Cypress *(Cupressus sempervirens_*	nCup a 1	37,42	20,44	1,08	6,12
Salsola (saltwort) *(Salsola kali)*	nSal k 1	46,01	33,36	0,39	7,16
Lamb's quarters *(Chenopodium album)*	rChe a 1	13,49	16,63	0,24	2,80
Alder *(Alnus glutinosa)*	rAln g 1	0,61	21,35	0,04	16,02
Plane tree *(Platanus acerifolia)*	rPla a 1	1,84	3,64	0,29	1,55
	rPla a 3	1,84	6,78	0,04	3,39
Plantain *(Plantago lanceolata)*	rPla I 1	13,49	17,05	1,18	6,57
Mugwort *(Artemisia vulgaris)*	nArt v 1	18,40	42,54	0,59	12,55
	nArt v 3	6,74	13,99	0,09	4,50
Wall pellitory *(Parietaria officinalis)*	rPar j 2	10,42	12,33	1,28	5,90
Annual mercury *(Mercurialis annua)*	rMer a 1	14,72	28,89	0,19	7,16
Wheat *(Triticum aestivum)*	rTri a 14	2,45	4,05	0	0,88
	rTri a 19	3,06	1,57	0,09	0,73
	nTri a aA_TI	0,61	1,15	0	0,66
Olive tree *(Olea europaea)*	rOle e 1	1,22	1,49	0,24	1,03
	nOle e 7	3,68	3,31	0,14	1,77
	rOle e 9	3,06	12,25	0,24	2,95
Hazel *(Corylus avellana)*	rCor a 1.0101	11,04	32,11	0,89	18,02
Bermuda grass *(Cynodon dactylon)*	nCyn d 1	28,83	44,20	0,89	16,54
Timothy grass *(Phleum pratense)*	rPhl p 1	14,72	33,85	0	17,35
	rPhl p 2	7,36	12,00	0,99	5,68
	rPhl p 4	12,26	21,44	0,19	7,82
	rPhl p 5	1,22	8,44	0,14	6,64
	rPhl p 6	2,45	5,29	0,04	3,24
	rPhl p 7	2,45	2,40	0,09	1,03
	rPhl p 11	6,13	14,56	1,03	6,05
	rPhl p 12	11,04	26,40	0,24	8,71
Japanese cedar *(Cryptomeria japonica)*	nCry j 1	9,81	11,34	0,39	5,02
Alternaria alternata	rAlt a 1	9,81	16,80	0,09	5,76
	rAlt a 6	2,45	3,06	0,04	0,73
Aspergillus fumigatus	rAsp f 1	0,61	0,91	0	0,29
	rAsp f 3	1,84	1,98	0,24	0,81
	rAsp f 6	4,29	4,80	0,34	1,32
D. farinae (HDM)	nDer f 1	4,29	7,53	0,24	3,69
	nDer f 2	4,29	9,18	0,29	4,50
D. pteronyssinus (HDM)	nDer p 1	4,29	7,45	0,24	3,98
	rDer p 2	2,45	8,19	0,14	4,06
	nDer p 10	4,90	5,38	0,34	1,55
	rDer p 23	24,53	25,91	2,52	9,82
Cat	rFel d 1	27,60	53,72	0,69	22,37
	nFel d 2	5,52	11,92	1,08	4,35
	rFel d 4	7,97	20,03	0,54	7,60
Horse	rEqu c 1	5,52	11,09	0,54	5,02
	nEqu c 3	3,06	6,20	0,29	2,58
Mouse	nMus m 1	2,45	12,25	0,89	4,35
Dog	rCan f 1	4,29	12,41	0,04	9,01
	rCan f 2	1,22	2,98	0,29	4,13
	rCan f 4	2,45	5,29	0,54	4,06
	rCan f 3	3,68	7,86	0,19	4,43
	rCan f 5	3,06	9,43	0,74	6,12
	rCan f 6	1,84	7,53	0	4,87

generally did not exceed 1–2%. The most frequently detected components were plane tree— rPla l 1 (1.18%), hazel pollen — rCor a 1.0101 (0.89%), bermuda grass — nCyn d 1 (0.89%), mugwort — nArt v 1 (0.59%), and birch — rBet v 1 (1.33%). The low values may reflect the distribution of examined patients and the limited representation of the sample in this region.

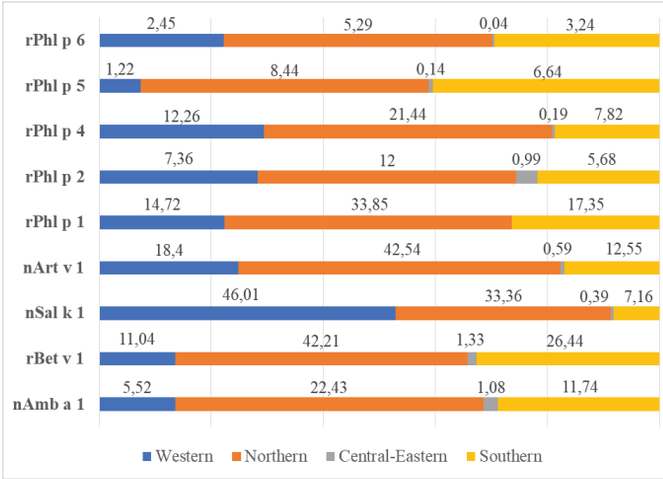

Figure 9 – Geographical features of sensitization (%)

In the northern regions, the highest sensitization frequency was observed for tree and grass allergens. The most frequently detected major components were bermuda grass — nCyn d 1 (44.20%), mugwort — nArt v 1 (42.54%), birch — rBet v 1 (42.21%), timothy grass — rPhl p 1 (33.85%), saltwort — nSal k 1 (33.36%), hazel pollen — rCor a 1.0101 (32.11%), and annual mercury — rMer a 1 (28.89%). A high sensitization frequency was also observed for minor molecules, including timothy grass — rPhl p 12 (26.40%) and birch — rBet v 2 (24.83%).

In the western regions, the highest sensitization frequency was observed for weed allergens and representatives of the family Amaranthaceae. The most frequently detected components were saltwort — nSal k 1 (46.01%), bermuda grass — nCyn d 1 (28.83%), mugwort — nArt v 1 (18.40%), annual mercury — rMer a 1 (14.72%), timothy grass — rPhl p 1 (14.72%), lamb's quarters — rChe a 1 (13.49%), and birch — rBet v 1 (11.04%). This region was also characterized by a high sensitization frequency to cypress pollen — nCup a 1 (37.42%).

Indoor and epidermal allergens were detected in all regions, with sensitization frequency varying between macroregions. The highest sensitization rates to epidermal allergens were observed in the northern regions, where rFel d 1 was detected in 53.72% of patients, rDer p 23 in 25.91%, rCan f 1 in 12.41%, and nMus m 1 in 12.25%.

In the western and southern regions, sensitization to these allergens was lower but remained at a notable level (rFel d 1 — 27.60% and 22.37%, respectively; rDer p 23 — 24.53% and 9.82%; rCan f 1 — 4.29% and 9.01%).

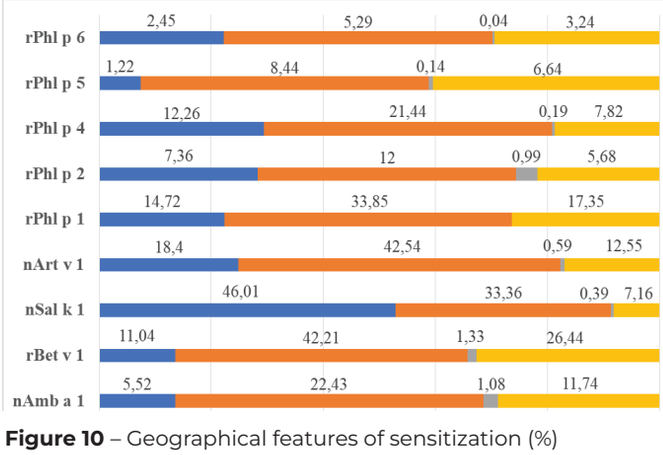

Figure 10 – Geographical features of sensitization (%)

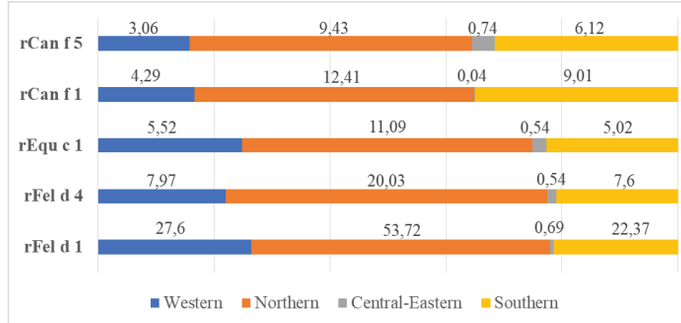

Figure 11 – Geographical features of sensitization (%)

In the central-eastern region, sensitization rates for most indoor and epidermal allergens were minimal and generally did not exceed 1–3%.

The most pronounced regional differences were observed for pollen allergens, which served as the basis for the main comparative analysis focused on plant-derived components.

Overall, the regional distribution of sensitization was characterized by varying representation of tree, grass, and weed allergens. The frequency of epidermal and indoor allergens also varied between regions; however, differences were more pronounced for pollen components and accounted for the main interregional patterns of sensitization.

Discussion

The spectrum of sensitization in patients ranges from monosensitization, when the immune system reacts to a single antigen, to polysensitization, characterized by reactivity to multiple allergens [1,2]. Polysensitized patients represent a clinically more complex category, in whom the disease often follows a more severe course and requires an individualized diagnostic and therapeutic approach [3,4].

The use of molecular diagnostic methods, including ImmunoCAP ISAC, makes it possible to define the sensitization profile at the level of individual allergen components and to identify clinically relevant molecules, which is crucial for the selection of allergen-specific immunotherapy and for assessing the risk of cross-reactivity [5–7]. In patients with multiple sensitization, a combined approach that includes allergen-specific immunotherapy and symptomatic pharmacotherapy is increasingly used [8,9].

The present study was based on ISAC molecular allergodiagnostic data obtained in Kazakhstan during 2021–2024. The analysis included age-related, gender-related, and geographic characteristics, allowing assessment of sensitization patterns in different regions of the country [10–12].

A high frequency of sensitization to epidermal allergens, particularly rFel d 1, is consistent with international studies indicating the widespread prevalence of cat allergy in populations with high urban density and continuous household exposure to animal allergens [12]. The components rFel d 1 and rCan f 1 are considered major allergens and more often reflect primary sensitization, whereas Fel d 4 and Can f 6 may participate in cross-reactive immunological responses [16]. A high frequency of sensitization to cat epithelium is regarded as one of the markers of atopic statu

In contrast to indoor allergens, which tend to be more universal in distribution, pollen components reflect regional differences in flora and climatic conditions. The most relevant

pollen allergens in the present study were rPhl p 1, rBet v 1, nArt v 1, and nSal k 1, which is consistent with studies conducted in countries with continental climates and pronounced pollen seasons [18–22]. The broad spectrum of identified pollen allergens, including tree, grass, and weed components, supports the need for a comprehensive approach to seasonal diagnosis and individualized selection of allergen-specific immunotherapy, particularly in regions with diverse vegetation.

The relatively low frequency of sensitization to house dust mites may be related to the climatic features of Kazakhstan, particularly low humidity, which can limit the proliferation of Dermatophagoides spp. [23]. At the same time, the observed frequency of sensitization to Alternaria alternata confirms the importance of fungal allergens as risk factors for severe allergic disease, including bronchial asthma and chronic allergic rhinitis [24].

Overall, the sensitization structure in the study population was determined by a combination of universal indoor allergens and region-dependent pollen components, which should be taken into account when developing diagnostic panels, selecting allergen-specific immunotherapy, and designing region-oriented clinical recommendations.

Presenting the data in percentage points allowed a clearer comparison of sensitization frequencies for individual allergen components between independent yearly cohorts. This approach is more informative for descriptive analysis, as it allows assessment of absolute differences without the influence of unequal sample sizes.

The largest differences were observed for pollen allergens, particularly rMer a 1, nArt v 1, nAmb a 1, and rPhl p 1. This indicates greater variability in sensitization frequencies to seasonal allergens compared with indoor components. Epidermal allergens, particularly rFel d 1, remained highly prevalent across all cohorts, confirming their importance as stable components of the inhalant sensitization profile. At the same time, such allergens have a more universal distribution and reflect regional allergen patterns to a lesser extent.

By contrast, pollen components demonstrated greater variability between yearly cohorts, which may be related to differences in the composition of examined patients, regional distribution, and clinical indications for molecular diagnostics. Sensitization to fungal allergens, particularly Alt a 1, also showed noticeable differences between cohorts, confirming the clinical relevance of this component in patients with respiratory allergy.

It is important to emphasize that the analysis was performed on independent patient groups examined in different years; therefore, the observed differences should not be interpreted as temporal trends in sensitization. They should more appropriately be regarded as inter-cohort variations reflecting the characteristics of the examined groups.

The findings support the need for component-resolved diagnostics to refine sensitization profiles and to individualize the selection of diagnostic panels and allergen-specific immunotherapy.

Gender is considered one of the biological factors capable of influencing the immune response and the characteristics of sensitization [7,8]. According to epidemiological studies, allergic diseases, including bronchial asthma and atopic dermatitis, are more often diagnosed in boys during childhood, which has been linked to features of innate and adaptive immunity as well as differences in hormonal profiles during early development [9].

In adolescence and in adult women, the frequency of allergic diseases may increase, which is associated with hormonal changes and fluctuations in gender hormone levels that can modulate inflammatory responses [10]. Physiological conditions such as the menstrual cycle, pregnancy, and menopause are known to influence symptom severity and susceptibility to allergens [14]. In men, a relative decrease in allergic reactions after puberty has been described, which is attributed to stabilization of hormonal balance and features of immune regulation [15].

A number of authors emphasize the need to consider gender-related features when studying allergic diseases and choosing therapeutic strategies [16]. In particular, the influence of hormonal status on the efficacy of allergen-specific immunotherapy and the formation of immune tolerance has been discussed, along with the role of social factors that may affect healthcare-seeking behavior and treatment adherence [17].

In the present study, no statistically significant gender-related differences were found between yearly cohorts, indicating comparability of the study groups with respect to this parameter and allowing interpretation of the results without adjustment for gender composition.

Age is considered one of the key factors influencing the development of sensitization and the clinical manifestations of allergic diseases [9,19]. It is well known that immune response patterns, duration of allergen exposure, hormonal status, and immune system maturation may determine differences in sensitization profiles across age groups.

In the present study, the largest proportion of examined patients belonged to the adult category, which is consistent with epidemiological data indicating a high prevalence of allergic diseases among the working-age population. The greater representation of adults may reflect longer allergen exposure and a higher likelihood of developing multiple sensitization in the course of chronic allergic disease.

A considerable number of examined patients was also observed in the younger age groups, confirming the importance of early diagnosis of sensitization. In early childhood, the immune system is still developing, which is accompanied by increased susceptibility to new antigens and more frequent development of IgE-mediated responses. During this period, sensitization to PR-10 proteins, LTPs, and other cross-reactive components that may contribute to subsequent polysensitization is often detected [23].

In preschool and younger school-age children, sensitization to inhalant allergens is more frequently detected, including components of grasses, weeds, house dust mites, and epidermal animal allergens. This is consistent with the literature indicating that this period is characterized by a shift from predominantly food sensitization to inhalant sensitization, reflecting a broadening of allergen exposure [24].

In adolescents and adults, combined sensitization to several allergen groups, including pollen, indoor, and epidermal components, is more frequently observed. Such a profile is regarded as a manifestation of the polysensitized phenotype, which is associated with a more complex disease course and may require an individualized diagnostic and therapeutic approach. Prolonged allergen exposure, repeated contact with multiple antigen sources, and features of immune regulation may contribute to an expansion of the sensitization spectrum with age.

The findings confirm that the age composition of examined patients can substantially influence the detected sensitization structure and should be taken into account when interpreting

component-resolved diagnostic results. Differences between age groups may be determined by both biological features of the immune response and differences in clinical indications for molecular testing.

An important practical implication is the need for a stratified approach to the assessment of sensitization according to patient age. The use of component-resolved diagnostics makes it possible to more accurately identify clinically relevant allergens, assess the risk of cross-reactivity, and rationally select allergen-specific immunotherapy.

Thus, consideration of age-related features is essential for correct interpretation of molecular allergodiagnostic results and optimization of clinical management in patients with allergic diseases.

It is well known that the spectrum of sensitization to inhalant allergens may vary substantially depending on climatogeographic conditions, vegetation characteristics, and the nature of allergen exposure in a given region [11–13]. In the present study, comparison of sensitization frequencies across macroregions of Kazakhstan revealed heterogeneous distribution of pollen, epidermal, and indoor allergens, with the most pronounced differences observed for plant-derived components.

In the southern regions, sensitization to weed and grass allergens, including nAmb a 1, nArt v 1, nCyn d 1, and rPhl p 1, was registered more frequently. This profile is consistent with the literature describing the predominance of weed and grass allergens in regions with continental and arid climates, where representatives of the families Amaranthaceae and Poaceae are widespread and prolonged pollen seasons are observed.

In the northern regions, a high frequency of sensitization to tree and grass allergens was observed, particularly rBet v 1, rCor a 1, rMer a 1, and rPhl p 1, as well as to components associated with cross-reactivity, such as rBet v 2 and rPhl p 12. This profile is consistent with epidemiological studies indicating the predominance of sensitization to tree and meadow grass pollen in regions with more humid climates and pronounced spring–summer pollen seasons.

In the western regions, a high frequency of sensitization to nSal k 1, belonging to allergens of the Amaranthaceae family, as well as to nCyn d 1, nArt v 1, and rMer a 1, was observed, which is characteristic of steppe and semi-desert territories. At the same time, reactions to grass and tree allergens were also detected in this group, indicating a mixed pattern of allergen exposure.

In the central-eastern region, sensitization frequencies for most allergen components were substantially lower than in the other macroregions. This likely reflects the characteristics of the examined patient distribution and the limited representation of the sample, which should be considered when interpreting regional differences.

Sensitization to indoor and epidermal allergens was detected in all regions, although its frequency also varied. The highest rates were observed in the northern regions, where reactions to rFel d 1, rDer p 23, and rCan f 1 were more frequent. This may reflect differences in living conditions, contact with domestic animals, and microclimatic features of indoor environments, although the present study did not include direct assessment of environmental factors.

The results suggest that the sensitization structure in Kazakhstan is shaped by a combination of factors, including climatic conditions, regional flora, and patterns of allergen exposure. The predominance of sensitization to weeds in the southern and western regions, the high frequency of reactions to tree and grass allergens in the northern regions, and the mixed sensitization profile observed in some regions reflect the diversity of the country's natural zones.

These findings are consistent with international studies demonstrating that regional flora, climatic conditions, and the degree of urbanization exert a substantial influence on the structure of allergic diseases. Component-resolved molecular allergodiagnostics allows more precise characterization of sensitization profiles, identification of clinically relevant allergens, and optimization of allergen-specific immunotherapy selection with consideration of regional features.

It should be taken into account that the study had a retrospective laboratory-epidemiological design and was based on anonymized data obtained from a clinical diagnostic laboratory. More accurate evaluation of regional patterns requires prospective studies including clinical information, more balanced patient distribution across regions, and expanded analysis of environmental factors.

Limitations

Several limitations should be considered when interpreting the results. The study had a retrospective design and was based on laboratory data obtained from the database of a clinical diagnostic laboratory. Due to the anonymized nature of the sample, information on clinical diagnosis, disease severity, and follow-up was not available in all cases.

The sample was not random and included patients referred for molecular allergodiagnostics, which may have introduced selection bias toward individuals with suspected polysensitization or more severe allergic disease.

Regional analysis was based on the location where laboratory testing was performed, which does not always coincide with the patient's region of permanent residence. Some examined individuals may have sought testing in large diagnostic centers located in other regions, including the capital region, which could potentially reduce the accuracy of geographic stratification. An additional limitation is possible migration of patients between regions, including recent changes of residence, which complicates interpretation of the observed regional differences as reflecting the true population structure of sensitization.

Despite these limitations, the large number of examined patients and the use of component-resolved allergodiagnostics provide a reliable overview of sensitization structure across different climatogeographic regions.

Conclusion

The present study demonstrates that the sensitization profile in Kazakhstan is shaped by a combination of ubiquitous indoor allergens and region-specific pollen components, reflecting the influence of climatic, ecological, and botanical factors.

Component-resolved allergodiagnostics enabled precise characterization of sensitization patterns across different demographic and geographic groups, highlighting the predominance of polysensitization and the heterogeneity of allergen exposure. Regional analysis revealed distinct pollen sensitization patterns corresponding to environmental conditions, whereas indoor allergens showed broader and more universal distribution.

The absence of significant sex-related differences and the heterogeneous age structure indicate that demographic factors should be considered when interpreting sensitization profiles, particularly in clinically selected populations.

Importantly, the identified variability between independent cohorts underscores the need for cautious interpretation of cross-sectional data and supports the use of standardized approaches when comparing sensitization patterns.

Overall, the findings emphasize the clinical value of molecular allergodiagnostics for improving diagnostic accuracy, enabling personalized selection of allergen-specific immunotherapy, and supporting the development of region-adapted diagnostic panels in patients with respiratory allergy.

Author Contributions: All authors (N. R. U., M. A. M., A. N. P., K. V. Sh., M. R. G., N. A. M., Zh. N. A., A. A. Z., Y. S., A. B.) contributed equally to the conception, search, data collection, analysis, and writing of this manuscript. All authors have read and agreed to the published version of the manuscript.

Disclosures: The authors have no conflicts of interest.

Acknowledgments: None.

Funding: None.

Data availability statement: The data that support the findings of this study are available from the corresponding author upon reasonable request.

Artificial Intelligence (AI) Disclosure Statement: The authors declare no AI Tools used for preparation of this work.

References

1. LandzaatLJ, BroughHA, BurksAW, Ballmer-WeberBK, NilssonC, GiselssonM, BorresMP, SastreJ, ValentaR, MatricardiPM. Early inhalant allergen sensitization at component level using multiplex microarray analysis. *Clinical and Translational Allergy.* 2023;13(7):e12271. https://doi.org/10.1002/clt2.12271
2. KochL, EllerE, Bindslev-JensenC, MortzCG, BrockowK, Bindslev-JensenU. Molecular allergy diagnosis using marker allergens in pollen sensitization. *Allergy*. 2023;78(3):742–754. https://doi.org/10.1111/all.15589
3. ČelakovskáJ, BukačJ, VaňkováR, KrejsekJ, AndrýsC, HamákováK, EttlerK. Relationship between sensitization to molecular components of inhalant allergens and clinical manifestation of allergy. *Journal of Asthma and Allergy.* 2021;14:1165–1175. https://doi.org/10.2147/JAA.S332314
4. Parra-Vargas MI, Alvarez-Cuesta E, Dávila I, Moreno C. Allergen immunotherapy: current and future trends. *Cells*. 2022; 11: 212. https://doi.org/10.3390/cells11020212
5. Ramírez-Jiménez F, Cuevas M, Canto G, Calderón MA. Allergen immunotherapy for long-term tolerance and prevention. *Journal of Allergy and Clinical Immunology.* 2021; 149(4): 1229–1238. https://doi.org/10.1016/j.jaci.2021.06.023
6. Roberts G, Pfaar O, Akdis CA, Ansotegui IJ, Durham SR, van Wijk RG, Halken S, Larenas-Linnemann D, Calderón MA. EAACI guidelines on allergen immunotherapy: allergic rhinoconjunctivitis. *Allergy*. 2018; 73(4): 765–798. https://doi.org/10.1111/all.13317
7. Mitselou N, Kafatos G, Brough HA, Santos AF. Exposure to allergen-specific immunotherapy in pregnancy and risk of congenital malformations. *Journal of Allergy and Clinical Immunology in Practice.* 2022; 10(6): 1635–1641. https://doi.org/10.1016/j.jaip.2022.03.005
8. Bernstein DI, Amar NJ, McGrath KG, Cheema AS, Creticos PS. SQ house dust mite sublingual immunotherapy tablet subgroup efficacy and local application site reaction duration. *Annals of Allergy, Asthma & Immunology.* 2018; 121(1): 105–110. https://doi.org/10.1016/j.anai.2018.04.007
9. Muraro A, Agache I, Clark A, Sheikh A, Roberts G, Akdis CA. Managing food allergy: GA²LEN guideline 2022. *World Allergy Organization Journal.* 2022; 15: 100687. https://doi.org/10.1016/j.waojou.2022.100687
10. Agache I, Lau S, Akdis CA, Smolinska S, Bonini M, Cavkaytar O, Flood B, Gajdanowicz P, Izuhara K, Kalayci O. EAACI guidelines on allergen immunotherapy: house dust mite-driven allergic asthma. *Allergy*. 2019; 74(5): 855–873. https://doi.org/10.1111/all.13749
11. Inclan-Rico JM, Hernandez CM. Contributions of innate lymphocytes to allergic responses. *Current Opinion in Allergy and Clinical Immunology.* 2019; 19(2): 175–184. https://doi.org/10.1097/ACI.0000000000000515
12. Li XM, Srivastava K, Hulett AC, Bottomly K. Recent advances in sublingual allergen-specific immunotherapy. *Allergy Asthma & Immunology Research.* 2023; 15(1): 27–38. https://doi.org/10.4168/aair.2023.15.1.27
13. Gómez E, Díaz-Perales A, Lombardero M. Molecular mechanisms of allergen-specific immunotherapy in allergic diseases. *Journal of Allergy and Clinical Immunology.* 2022; 149(4): 1012–1025. https://doi.org/10.1016/j.jaci.2021.11.021
14. Tabar AI, Arroabarren E, Echechipía S, García BE, Martín S, Alvarez-Cuesta E. Double-blind, randomized, placebo-controlled trial of allergen-specific immunotherapy with the major allergen Alt a 1. *Journal of Allergy and Clinical Immunology.* 2019; 144(1): 216–223. https://doi.org/10.1016/j.jaci.2019.02.029
15. Alvaro-Lozano M, Akdis CA, Akdis M, Canonica GW, Casale TB, Cox L, Durham SR, Jutel M, Kleine-Tebbe J, Muraro A. EAACI allergen immunotherapy user's guide. *Pediatric Allergy and Immunology.* 2020; 31(Suppl 25): 1–101. https://doi.org/10.1111/pai.13189
16. Kucuksezer UC, Ozdemir C, Akdis M, Akdis CA. Mechanisms of allergen-specific immunotherapy and allergen tolerance. *Allergology International*. 2020; 69(4): 549–560. https://doi.org/10.1016/j.alit.2020.08.002
17. Wang C, Bao Y, Chen J, Zhang L, Wang Y. Chinese guideline on allergen immunotherapy for allergic rhinitis: the 2022 update. *Allergy Asthma & Immunology Research.* 2022; 14(6): 604–652. https://doi.org/10.4168/aair.2022.14.6.604

18. Hoang MP, Seresirikachorn K, Chitsuthipakorn W, Snidvongs K. Intralymphatic immunotherapy for allergic rhinoconjunctivitis: a systematic review and meta-analysis. *Rhinology*. 2021; 59: 236–244. https://doi.org/10.4193/Rhin20.572
19. Konradsen JR, Grundström J, Hellkvist L, Tran TA, Andersson N, Gafvelin G. Intralymphatic immunotherapy in pollen-allergic young adults with rhinoconjunctivitis and mild asthma: a randomized trial. *Journal of Allergy and Clinical Immunology.* 2020; 145: 1005–1007.e7. https://doi.org/10.1016/j.jaci.2019.11.017
20. Wang Y, Kong Y, Wu MX. Innovative systems to deliver allergen powder for epicutaneous immunotherapy. *Frontiers in Immunology.* 2021; 12: 647954. https://doi.org/10.3389/fimmu.2021.647954
21. Sola Martínez FJ, Barranco Jiménez RM, Martín García C, Senent Sánchez C, Blanco Guerra C, Fernández-Rivas M. Intradermal Phleum pratense allergoid immunotherapy: double-blind, randomized, placebo-controlled trial. *Clinical and Experimental Allergy.* 2020; 50: 1352–1361. https://doi.org/10.1111/cea.13740
22. Wang C, Bao Y, Chen J, Chen X. Chinese guideline on allergen immunotherapy for allergic rhinitis: the 2022 update. *Allergy Asthma & Immunology Research.* 2022; 14(6): 604–652. https://doi.org/10.4168/aair.2022.14.6.604
23. Dhami S, Nurmatov U, Arasi S, Khan T, Asaria M, Zaman H, Agarwal A, Netuveli G, Roberts G, Pfaar O. Allergen immunotherapy for allergic rhinoconjunctivitis: a systematic review and meta-analysis. *Allergy*. 2017; 72: 1597–1631. https://doi.org/10.1111/all.13201
24. Durham SR, Shamji MH. Allergen immunotherapy: past, present and future. *Nature Reviews Immunology.* 2023; 23(5): 317–328. https://doi.org/10.1038/s41577-022-00786-1
25. VítovcováP, KrčmováI, ŽďárskýE, HruškováZ, MalkusováI, NovosadJ. Molecular sensitization profiles to pollen allergens in Central Europe. *International Archives of Allergy and Immunology.* 2014;164(2):131–138. https://doi.org/10.1159/000362230
26. WHOIUISAllergenNomenclatureSubCommittee. Allergen Nomenclature Database. *WHO/IUIS Allergen Nomenclature.* 2024. https://doi.org/10.0000/allergen.org
27. PomésA, DaviesJM, GadermaierG, HilgerC, HolzhauserT, LidholmJ, LopataAL, MuellerGA, NandyA, RadauerC, ChanSK, JappeU, KleineTebbeJ, ThomasWR, ChapmanMD, vanHageM, vanReeR, ViethsS, RaulfM, GoodmanRE. WHO/IUIS Allergen Nomenclature: Providing a common language. *Molecular Immunology.* 2018;100:3–13. https://doi.org/10.1016/j.molimm.2018.03.003

JOURNAL OF CLINICAL MEDICINE OF KAZAKHSTAN (E-ISSN 2313-1519)
Original Article DOI: https://doi.org/10.23950/jcmk/18292

Evaluation of Serum Growth Differentiation Factor-15 (Gdf-15) as a Non-Invasive Biomarker for Disease Severity and Pain Intensity in Endometriosis: a Hospital Based Case-Control Study

Thirunavukkarasu Jaishankar[1], Preetha Madhan[2], Sarguru Datchanamurthi[3], Kalaiselvi Vairavan Pillai Subbammal[4], Rhona Madhan[5]

[1]*Department of Biochemistry, Karpagam Faculty of Medical Science & Research, Coimbatore, Tamil Nadu, India*
[2]*Department of Obstetrics and Gynecology, PSP Medical College Hospital and Research Institute, Chennai - Tamil Nadu, India*
[3]*Department of Biochemistry, Sri Lalithambigai Medical College, Dr. MGR Educational & Research Institute, Maduravoyal, Chennai, Tamil Nadu, India*
[4]*Department of Biochemistry, Sree Balaji Medical College & Hospital, Bharath Institute of Higher Education & Research, Chennai, Tamil Nadu, India*
[5]*Department of Obstetrics and Gynecology, SRM Medical College Hospital and Research Centre, SRMIST, Chennai – Tamil Nadu, India*

Received: 2026-02-21.
Accepted: 2026-03-26.

This work is licensed under a **Creative Commons Attribution 4.0 International License**

J Clin Med Kaz 2026; 23(2): 31-38

Corresponding author:
Thirunavukkarasu Jaishankar.
E-mail:
jaishankarthirunavukkarasu@gmail.com.
ORCID: 0009-0007-9053-1524.

Abstract

Background: Endometriosis is a chronic, oestrogen-dependent inflammatory gynaecological disorder affecting 10 to 15 percent of women of reproductive age. The condition is characterised by pelvic pain and infertility, and diagnosis is frequently delayed by 7 to 10 years due to reliance on invasive laparoscopy and the absence of validated non-invasive biomarkers. Growth Differentiation Factor-15 (GDF-15), a stress-responsive cytokine implicated in inflammatory and nociceptive pathways, has emerged as a candidate biomarker in multiple pain-related disorders; however, its clinical utility in endometriosis has not been adequately defined.

Objective: The primary objective of this study was to evaluate serum GDF-15 as a diagnostic biomarker capable of differentiating women with confirmed endometriosis from healthy controls. The secondary objective was to assess its potential as a disease severity marker by examining the association between GDF-15 levels and r-AFS staging, and its exploratory relationship with pain intensity scores.

Methods: This was a hospital-based case-control study conducted over 24 months at a tertiary teaching hospital. The study enrolled 100 women with laparoscopically and histopathologically confirmed endometriosis (cases) and 100 age-matched healthy controls. Serum GDF-15 concentration was quantified using enzyme-linked immunosorbent assay (ELISA). Disease severity was graded using the revised American Fertility Society (r-AFS) staging system. Pain intensity was assessed using the Visual Analogue Scale (VAS) and the Numerical Rating Scale (NRS). Statistical analysis included independent samples t-test, one-way analysis of variance (ANOVA), Pearson correlation coefficient, binary logistic regression, and receiver operating characteristic (ROC) curve analysis. Statistical significance was set at p less than 0.05.

Results: Serum GDF-15 was significantly elevated in cases compared to controls (961.7 ± 195.2 pg/mL vs. 508.0 ± 99.6 pg/mL; p less than 0.001; Cohen's d = 2.93). ROC curve analysis demonstrated excellent diagnostic discriminatory performance (AUC = 0.942; 95% CI: 0.907 to 0.977; sensitivity 89.0%; specificity 88.0% at an optimal cut-off of 720.5 pg/mL). A numerical increasing trend in GDF-15 was observed across r-AFS stages (Stage I: 906.3 ± 234.3 pg/mL to

Stage IV: 987.5 ± 192.7 pg/mL); however, this difference did not reach statistical significance (one-way ANOVA, p = 0.265) and should be interpreted as exploratory. Pearson correlation between GDF-15 and pain scores was weak and did not achieve statistical significance (VAS: r = 0.174, p = 0.084; NRS: r = 0.191, p = 0.058).Binary logistic regression confirmed GDF-15 as an independent predictor of endometriosis diagnosis after adjustment for age and BMI (adjusted OR = 3.84; 95% CI: 2.61 to 5.65; p less than 0.001).

Conclusion: Serum GDF-15 is significantly elevated in women with endometriosis and demonstrates excellent diagnostic discriminatory performance, supporting its role as a non-invasive diagnostic biomarker. The non-significant numerical trend across r-AFS stages and the weak, non-significant correlations with pain scores do not permit conclusions regarding GDF-15 as a severity or pain prediction marker on the basis of the current data. External validation in larger multicentre prospective cohorts is required before clinical translation.

Keywords: Endometriosis; Growth Differentiation Factor-15; Biomarker; Pelvic pain; Disease severity; r-AFS staging.

Introduction

Endometriosis is a complex, oestrogen-dependent gynaecological disorder affecting an estimated 10 to 15 percent of women of reproductive age, with up to half of all affected women experiencing persistent pelvic pain or infertility [1]. It is characterised by the ectopic implantation of endometrium-like tissue, which drives a state of chronic inflammation leading to fibrosis, neovascularisation, and dysregulated nociceptive sensory sensitisation [2]. Despite its high prevalence and profoundly negative impact on quality of life, diagnosis is frequently delayed by 7 to 10 years due to the non-specificity of clinical symptoms and the requirement for invasive diagnostic laparoscopy as the confirmatory standard [3].

The clinical phenotype of endometriosis is highly variable, and the severity of pain does not consistently correlate with the anatomical extent of the disease. This dissociation highlights the multifactorial nature of nociception in endometriosis, involving inflammatory cytokines, neurogenic pathways, and central sensitisation [4]. The revised American Fertility Society (r-AFS) staging system, the most widely used classification framework, is based primarily on the anatomical distribution and extent of disease and does not reliably predict symptom severity or treatment response [5]. Consequently, there is an urgent and unmet clinical need for objective, laboratory-based biomarkers capable of reflecting disease burden and symptom intensity, thereby enabling earlier diagnosis and individualised treatment planning.

Growth Differentiation Factor-15 (GDF-15), also designated macrophage inhibitory cytokine-1 (MIC-1), is a divergent member of the transforming growth factor-beta (TGF-beta) superfamily [6]. Under physiological conditions, GDF-15 is expressed at low levels in most tissues; however, it is substantially upregulated in response to cellular stress, tissue injury, hypoxia, inflammation, and oxidative stress [7]. Elevated circulating GDF-15 has been documented in diverse pathological states including cardiovascular disease, malignancy, metabolic disorders, and chronic inflammatory conditions [8]. Emerging evidence implicates GDF-15 in the regulation of immune responses, angiogenesis, and pain signalling, all of which are directly relevant to the pathophysiology of endometriosis [9]. The upregulation of GDF-15 in response to oxidative stress and tissue remodelling, hallmark features of endometriotic lesions, provides a compelling mechanistic rationale for its investigation as a biomarker in this condition [10]. Furthermore, GDF-15 has been shown to modulate nociceptive pathways through peripheral and central mechanisms involving its cognate receptor GFRAL, which may contribute to the chronic pelvic pain phenotype of endometriosis.

Despite this mechanistic plausibility, published data directly associating serum GDF-15 levels with disease severity and pain intensity in endometriosis remain limited, and no such study has been conducted in an Indian population. The present study was therefore designed to address this evidence gap with two defined objectives. **The primary objective** was to evaluate the diagnostic performance of serum GDF-15 in differentiating women with confirmed endometriosis from healthy controls, including ROC curve analysis with determination of optimal cut-off values, sensitivity, and specificity. The secondary objective was to explore the association between serum GDF-15 and disease severity as measured by r-AFS staging, and pain intensity as measured by VAS and NRS, with the explicit understanding that these secondary analyses are hypothesis-generating given the study's cross-sectional design and subgroup sample sizes.

Methods

Study Design and Setting

This was a hospital based, observational case-control study conducted in the Department of Obstetrics and Gynaecology in collaboration with the Department of Clinical Biochemistry, Sri Lalithambigai Medical College, Dr. MGR Educational and Research Institute, Maduravoyal, Chennai, Tamil Nadu, India. This study received ethical approval from the Institutional Ethics Committee of Sri Lalithambigai Medical College and Hospital, Faculty of Medicine, Dr. MGR Educational and Research Institute, Chennai (IEC Reg. No.: EC/NEW/INST/2022/2769; Ref No.: Dr. MGR ERI/SLMCH/2025/059; Approval Date: 06 October 2025). The study was conducted in accordance with the Declaration of Helsinki and ICMR Ethical Guidelines (2017). Written informed consent was obtained from all participants.

As this was an observational case-control biomarker study with no experimental intervention, prospective registration in a clinical trial registry was not mandated under ICMR regulatory guidelines for observational studies at the time of

commencement. The study was conducted under full Institutional Ethics Committee oversight.

The study involved minimal risk to participants. The sole procedure was a single venous blood draw of 5 mL performed by trained phlebotomists under aseptic conditions. No experimental interventions, drug administration, or additional clinical procedures beyond standard clinical management were performed. No adverse events or complications related to blood collection were recorded.

Study Population

A total of 200 women aged 18 to 45 years were recruited and allocated to two groups. Cases (n = 100) were women with laparoscopically and histopathologically confirmed endometriosis presenting with symptoms including dysmenorrhoea, chronic pelvic pain, dyspareunia, or infertility. Controls (n = 100) were age-matched healthy women without clinical or radiological evidence of endometriosis, attending the hospital for routine gynaecological check-ups or contraceptive counselling.

Written informed consent was obtained from all participants prior to enrolment. The informed consent process included a detailed explanation of the study objectives and rationale; a description of all procedures, including the single venous blood sample collection; assurance that participation was entirely voluntary and that withdrawal at any time would not affect the quality of clinical care; confirmation of the right to confidentiality and anonymity; and explanation of how biological samples and data would be stored and used exclusively for the purposes of this study. The consent document was available in both English and Tamil to ensure full comprehension by all participants.

Inclusion Criteria

For cases: Women aged 18 to 45 years; laparoscopically confirmed endometriosis with histopathological verification; presenting symptoms consistent with endometriosis (dysmenorrhoea, chronic pelvic pain, dyspareunia, or infertility); and willingness to provide written informed consent.

For controls: Age-matched (within ± 3 years) healthy women; absence of symptoms suggestive of endometriosis; normal pelvic examination and pelvic ultrasonography findings; no history of endometriosis or gynaecological pathology; and willingness to provide written informed consent.

Exclusion Criteria

Women with any of the following were excluded from both groups: pregnancy or lactation; known malignancy (current or within the preceding 5 years); autoimmune disorders including systemic lupus erythematosus, rheumatoid arthritis, and inflammatory bowel disease; chronic inflammatory disorders including chronic hepatitis and chronic pancreatitis; cardiovascular diseases; chronic kidney disease or hepatic dysfunction; diabetes mellitus (Type 1 or Type 2); hormonal therapy within the preceding three months; and acute infection or febrile illness at the time of sample collection.

These exclusion criteria were systematically applied to control for all conditions known to independently elevate serum GDF-15 levels, thereby minimising the risk of confounded biomarker measurement.

Control Screening for Subclinical Endometriosis

Exclusion of subclinical or asymptomatic endometriosis in controls was achieved through a three-tier screening protocol: (i) a detailed structured clinical history specifically enquiring about dysmenorrhoea, chronic pelvic pain, dyspareunia, and infertility; (ii) a standardised pelvic examination performed by a qualified gynaecologist; and (iii) transvaginal and transabdominal pelvic ultrasonography performed by a blinded radiologist to exclude endometriotic cysts, adnexal masses, or other pelvic pathology. Women with any positive finding on any of these three tiers were excluded from the control group. It is acknowledged that definitive exclusion of peritoneal endometriosis without visible cysts would require diagnostic laparoscopy, which was not performed in controls for ethical reasons. This is an inherent limitation of case-control designs in endometriosis research and is addressed explicitly in the Limitations section.

Clinical Assessment

A detailed clinical history was obtained from all participants using a standardised structured questionnaire. All cases underwent diagnostic laparoscopy performed by experienced gynaecological surgeons. Endometriotic lesions were identified by direct visual examination, and tissue samples were obtained for histopathological confirmation. Disease severity was categorised according to the r-AFS guidelines: Stage I (minimal, 1 to 5 points); Stage II (mild, 6 to 15 points); Stage III (moderate, 16 to 40 points); and Stage IV (severe, greater than 40 points).

Pain Assessment

Pain intensity was assessed using two validated instruments administered at the time of initial clinical presentation, prior to any intervention or analgesic administration.

Visual Analogue Scale (VAS): A 10 cm horizontal line anchored by "no pain" at 0 cm and "worst pain imaginable" at 10 cm. Participants marked their current pain level on the scale.

Numerical Rating Scale (NRS): An 11-point scale from 0 (no pain) to 10 (worst pain imaginable). Participants verbally or manually indicated their pain level.

Sample Collection and Storage

Fasting venous blood samples (5 mL) were collected during the early follicular phase (cycle days 2 to 5) to minimise hormonal variation. Samples were collected between 08:00 and 10:00 hours following a minimum overnight fast of 8 hours. Blood was allowed to clot at room temperature for 30 minutes and then centrifuged at 3,000 revolutions per minute for 15 minutes at 4 degrees Celsius. Serum was divided into 500 µL aliquots and stored at minus 80 degrees Celsius until batch analysis.

To prevent freeze-thaw degradation, aliquots were prepared such that each sample required for analysis was drawn from a single dedicated aliquot, ensuring that no sample underwent more than one freeze-thaw cycle. GDF-15 stability in serum stored at minus 80 degrees Celsius has been previously validated for up to 24 months with no significant analyte degradation. All samples in this study were analysed within 18 months of collection.

The informed consent document explicitly stated that collected serum samples would be stored at minus 80 degrees Celsius for the duration of the study analysis period (up to 24 months) and would be used exclusively for the analyses described in this study protocol. No permission for long-term biobanking or future unspecified use was sought or granted.

Biochemical Analysis

Serum GDF-15 levels were quantified using a commercially available ELISA kit (Human GDF-15 ELISA Kit, Catalog No. ELH-GDF15, RayBiotech, Inc., Norcross, GA, USA) following the manufacturer's instructions. The analytical range of the assay was 31.2 to 2000 pg/mL. The intra-assay coefficient of variation was less than 10% and the inter-assay coefficient of variation was less than 12%. All samples were assayed in duplicate; the mean of duplicate measurements was used for statistical analysis. Any duplicate pair with a coefficient of variation exceeding 15% was repeated.

Calibration was performed using manufacturer-supplied calibrators across the full analytical range with a six-point standard curve (R^2 greater than 0.99 for all analytical runs). Internal quality control was implemented using two levels of quality control samples (low and high concentration) run at the beginning, midpoint, and end of each analytical batch. Runs were accepted only when quality control values fell within ± 2 SD of the assigned target values. A single analytical batch was used for all samples to eliminate inter-batch variation.

All biochemical analyses were performed by laboratory personnel who were blinded to the case or control allocation status of each participant. Samples were labelled with anonymous alphanumeric codes prior to analysis. The code key linking participant identities to sample codes was held separately by the study coordinator and was revealed only after completion of all ELISA analyses.

Participant confidentiality was maintained throughout the study by replacing all personally identifiable information with unique anonymous alphanumeric codes at the point of data entry. All data were stored on password-protected institutional servers accessible only to the principal investigator and designated research team members.

Statistical Analysis

Sample size was calculated based on a pilot study reporting mean serum GDF-15 of 950 (± 200) pg/mL in cases and 500 (± 100) pg/mL in controls. Using a two-sided independent samples t-test, alpha of 0.05, and 90% power, the minimum required sample size was 84 participants per group. To account for a 15% dropout rate, 100 participants per group were recruited.

Data were analysed using IBM SPSS Statistics version 26.0. Continuous variables were assessed for normality using the Kolmogorov-Smirnov test. Serum GDF-15 levels in both cases (K-S statistic = 0.081, p = 0.104) and controls (K-S statistic = 0.073, p = 0.212) conformed to a normal distribution, thereby justifying the use of parametric statistical methods. Data are expressed as mean ± SD. Group comparisons were performed using independent samples t-test. Pearson correlation coefficients were used to examine associations between serum GDF-15 and disease and pain parameters. One-way ANOVA was used to compare GDF-15 levels across r-AFS stages. ROC curve analysis was performed to determine the area under the curve (AUC), optimal diagnostic cut-off value (Youden Index), sensitivity, and specificity of serum GDF-15 for the diagnosis of endometriosis. Binary logistic regression analysis was performed with endometriosis diagnosis as the dependent variable and serum GDF-15, age, and BMI as covariates, to evaluate GDF-15 as an independent predictor after adjustment for potential confounders. A two-tailed p value less than 0.05 was considered statistically significant.

Post-hoc power analysis for the one-way ANOVA comparing GDF-15 across r-AFS stages at the observed subgroup sizes (n = 23 to 27 per stage) yielded an estimated power of 28%, confirming that stage-wise comparisons were substantially underpowered. A minimum of 60 to 80 participants per r-AFS stage would be required to achieve 80% power for detection of the observed between-stage differences. This is incorporated as a recommendation for future study design.

Results

Study Participant Flow

A total of 247 women were screened for eligibility. Of these, 31 were excluded (18 did not meet inclusion criteria, 8 declined to participate, and 5 had incomplete data) and 16 were lost prior to sample collection. Ultimately, 200 women (100 cases and 100 controls) were enrolled and their data were included in the final analysis.

Baseline Demographic and Clinical Characteristics

Baseline characteristics are presented in Table 1. The mean age of cases was 29.5 ± 4.5 years compared to 28.7 ± 5.3 years in controls (p = 0.247). Mean BMI was comparable between groups (23.6 ± 2.9 kg/m² in cases vs. 22.8 ± 3.0 kg/m² in controls; p = 0.068). Pain scores were significantly higher in cases than in controls (VAS: 6.4 ± 1.8 vs. 0.9 ± 0.8, p less than 0.001; NRS: 6.4 ± 1.8 vs. 0.8 ± 0.8, p less than 0.001).

Table 1 Baseline Demographic and Clinical Characteristics of Study Participants

Parameter	Cases (n = 100)	Controls (n = 100)	p-value
Age (years), mean (SD)	29.5 (4.5)	28.7 (5.3)	0.247
BMI (kg/m^2), mean (SD)	23.6 (2.9)	22.8 (3.0)	0.068
Pain VAS Score, mean (SD)	6.4 (1.8)	0.9 (0.8)	less than 0.001*
Pain NRS Score, mean (SD)	6.4 (1.8)	0.8 (0.8)	less than 0.001*

*Data presented as mean (SD). *p less than 0.05 considered statistically significant. BMI: Body Mass Index; VAS: Visual Analogue Scale; NRS: Numerical Rating Scale.*

Serum GDF-15 Levels: Cases vs Controls

Serum GDF-15 levels were significantly elevated in women with endometriosis compared to healthy controls (Table 2). The mean serum GDF-15 in cases was 961.7 ± 195.2 pg/mL (range: 366.6 to 1643.5 pg/mL), which was nearly two-fold higher than that in controls (508.0 ± 99.6 pg/mL; range: 280.7 to 751.3 pg/mL). This difference was highly significant (t = 20.706, p less than 0.001) with a large effect size (Cohen's d = 2.93), indicating a strong association between elevated serum GDF-15 and the presence of endometriosis.

Table 2 Comparison of Serum GDF-15 Levels Between Cases and Controls

Parameter	Cases (n = 100)	Controls (n = 100)	p-value
Serum GDF-15 (pg/mL), mean (SD)	961.7 (195.2)	508.0 (99.6)	less than 0.001*
Range (pg/mL)	366.6 to 1643.5	280.7 to 751.3	
95% CI	922.9 to 1000.5	488.3 to 527.7	
Effect Size (Cohen's d)	2.93		

**p less than 0.001 by independent samples t-test. CI: Confidence Interval.*

ROC Curve Analysis and Diagnostic Performance of GDF-15

ROC curve analysis was performed to evaluate the diagnostic performance of serum GDF-15 in differentiating endometriosis cases from controls (Figure 1). The AUC was 0.942 (95% CI: 0.907 to 0.977; p less than 0.001), indicating excellent diagnostic discriminatory capability. Using the Youden Index to determine the optimal cut-off, a serum GDF-15 value of 720.5 pg/mL yielded a sensitivity of 89.0% and a specificity of 88.0%. The positive predictive value was 88.1%, the negative predictive value was 88.9%, the positive likelihood ratio was 7.42, and the negative likelihood ratio was 0.125.

Table 3 ROC Curve Analysis: Diagnostic Performance of Serum GDF-15 for Endometriosis

Parameter	Value
AUC (95% CI)	0.942 (0.907 to 0.977)
p-value	less than 0.001
Optimal Cut-off (Youden Index)	720.5 pg/mL
Sensitivity	89.0%
Specificity	88.0%
Positive Predictive Value	88.1%
Negative Predictive Value	88.9%
Positive Likelihood Ratio	7.42
Negative Likelihood Ratio	0.125

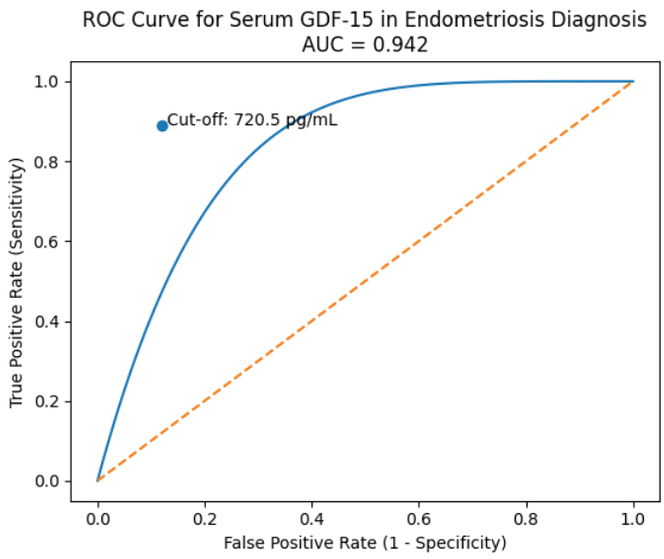

Figure 1 – ROC curve for serum GDF-15 in the diagnosis of endometriosis

Multivariate Logistic Regression Analysis

To confirm GDF-15 as an independent diagnostic predictor after adjustment for age and BMI, binary logistic regression analysis was performed with endometriosis diagnosis as the dependent variable (Table 4). Serum GDF-15 remained a highly significant and independent predictor of endometriosis diagnosis after adjustment (adjusted OR = 3.84; 95% CI: 2.61 to 5.65; p less than 0.001). Age and BMI were not significant independent predictors, confirming that the diagnostic association of GDF-15 was not confounded by these variables.

Table 4 Binary Logistic Regression: Predictors of Endometriosis Diagnosis

Variable	Adjusted OR	95% CI	p-value
Serum GDF-15 (per 100 pg/mL increase)	3.84	2.61 to 5.65	less than 0.001*
Age (years)	1.02	0.94 to 1.11	0.631
BMI (kg/m^2)	1.09	0.92 to 1.29	0.312

**p less than 0.001. OR: Odds Ratio; CI: Confidence Interval; BMI: Body Mass Index.*

Distribution of Endometriosis by r-AFS Stage

Among the 100 endometriosis cases, disease distribution by r-AFS staging was as follows: Stage I (minimal): 23 cases (23%); Stage II (mild): 27 cases (27%); Stage III (moderate): 25 cases (25%); Stage IV (severe): 25 cases (25%). This broadly uniform distribution across stages reflects a representative sample spanning the full disease severity spectrum.

Association of GDF-15 with Disease Severity

Stratified analysis of serum GDF-15 levels by r-AFS stage revealed a numerical increasing trend with advancing disease stage (Table 5). Mean GDF-15 values were: Stage I: 906.3 ±

Table 5 Serum GDF-15 Levels and Pain Scores According to r-AFS Stage

r-AFS Stage	n	GDF-15 (pg/mL) Mean (SD)	VAS Score Mean (SD)	NRS Score Mean (SD)
Stage I (Minimal)	23	906.3 (234.3)	6.2 (1.9)	6.6 (1.8)
Stage II (Mild)	27	966.6 (196.0)	6.2 (1.7)	6.5 (1.6)
Stage III (Moderate)	25	981.5 (154.8)	6.7 (1.6)	5.9 (1.8)
Stage IV (Severe)	25	987.5 (192.7)	6.6 (1.8)	6.7 (1.8)
p-value (ANOVA)		0.265	0.647	0.314

Data presented as mean (SD). One-way ANOVA used for stage-wise comparisons. r-AFS: revised American Fertility Society; VAS: Visual Analogue Scale; NRS: Numerical Rating Scale.

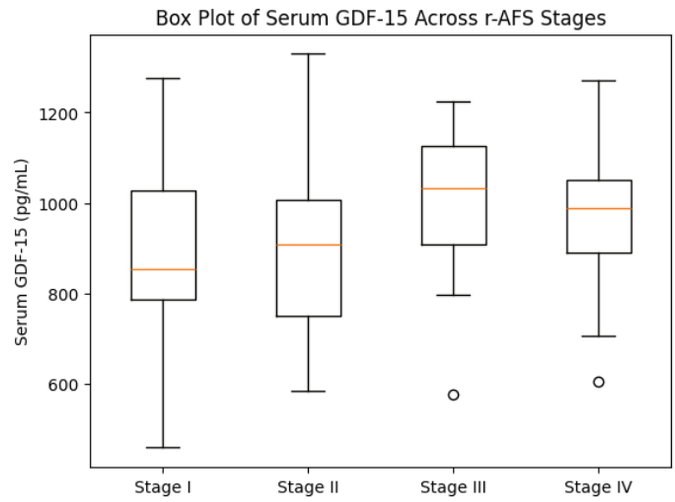

Figure 2 – Box plot illustrating serum GDF-15 distribution across cases and controls and across r-AFS stages I to IV with individual data points overlaid

234.3 pg/mL; Stage II: 966.6 ± 196.0 pg/mL; Stage III: 981.5 ± 154.8 pg/mL; Stage IV: 987.5 ± 192.7 pg/mL. However, one-way ANOVA demonstrated that these differences did not reach statistical significance (p = 0.265). Post-hoc power analysis confirmed that subgroup comparisons were substantially underpowered (estimated power 28%), and the non-significant result should therefore be interpreted as inconclusive rather than as evidence of absence of a severity association. These findings are exploratory and require confirmation in adequately powered studies.

Correlation Between GDF-15 and Pain Scores

Within the endometriosis group, Pearson correlation analysis revealed weak positive correlations between serum GDF-15 and VAS score (r = 0.174, p = 0.084) and between serum GDF-15 and NRS score (r = 0.191, p = 0.058). Neither correlation achieved statistical significance at the conventional threshold of p less than 0.05. These findings do not support a clinically meaningful association between serum GDF-15 and pain intensity in the current dataset. Any interpretation must be explicitly limited to the exploratory nature of these analyses, and no inference regarding GDF-15 as a pain biomarker can be drawn from this study alone.

Discussion

This hospital based case-control study demonstrates that serum GDF-15 is significantly and substantially elevated in women with confirmed endometriosis compared to healthy controls, with a nearly two-fold difference in mean concentration (961.7 vs. 508.0 pg/mL; p less than 0.001; Cohen's d = 2.93). ROC curve analysis revealed excellent diagnostic discriminatory performance (AUC = 0.942), with a sensitivity of 89.0% and specificity of 88.0% at an optimal cut-off of 720.5 pg/mL, supporting the primary study objective of evaluating GDF-15 as a diagnostic biomarker. A non-significant numerical trend was observed across r-AFS stages (p = 0.265), and correlations with pain scores were weak and statistically non-significant (p = 0.084 and p = 0.058 for VAS and NRS, respectively). These secondary findings are acknowledged as inconclusive at the current sample size and do not support conclusions regarding GDF-15 as a severity or pain prediction marker.

GDF-15 is a stress-responsive cytokine upregulated by cellular stress, inflammation, hypoxia, and tissue injury, all of which characterise the pathological microenvironment of endometriotic lesions. The pathogenesis of endometriosis involves sustained inflammatory signalling through interleukins (IL-1, IL-6) and tumour necrosis factor-alpha, oxidative stress driven by mitochondrial dysfunction, aberrant angiogenesis, and progressive fibrosis. GDF-15 modulates the inflammatory environment through macrophage interaction and may attenuate local inflammatory cascades. Elevated serum GDF-15 in endometriosis therefore likely reflects the systemic inflammatory and tissue remodelling burden characteristic of this condition. Additionally, GDF-15 modulates nociceptive signalling via the GFRAL receptor expressed in the brainstem, which may contribute mechanistically to chronic pelvic pain pathophysiology [11-12]

Comparison with the most widely studied endometriosis biomarker, CA-125, provides important clinical context. Meta-analyses consistently report a pooled AUC of 0.72 to 0.78 for CA-125 in endometriosis diagnosis, with sensitivity of approximately 50 to 60% and specificity of 80 to 90% at standard diagnostic cut-offs, performance characteristics generally regarded as insufficient for clinical implementation as a standalone test.[13] The AUC of 0.942 achieved by serum GDF-15 in the present study substantially exceeds reported CA-125 diagnostic performance, with superior sensitivity at a comparable specificity threshold. While a direct head-to-head comparison of GDF-15 and CA-125 within the same cohort was not performed in this study, and such a comparison would be necessary before clinical superiority claims can be made, these data provide preliminary evidence that GDF-15 warrants formal comparative biomarker evaluation in future multicentre cohort designs [13-15].

The results of this study align with existing evidence supporting a role for GDF-15 in chronic gynaecological inflammatory conditions. Elevated GDF-15 has been reported in polycystic ovary syndrome, another condition driven by chronic low-grade inflammation. GDF-15 has also been implicated in preeclampsia, gestational diabetes, and endometrial cancer, conditions sharing common pathological substrates of inflammation and oxidative stress. To the best of the authors knowledge, this is among the first studies to directly evaluate serum GDF-15 in relation to endometriosis disease severity and pain scores, specifically in an Indian population. Prior biomarker studies in endometriosis have predominantly investigated CA-125, interleukins, and C-reactive protein, with variable and generally insufficient diagnostic performance.

An important limitation of GDF-15 as a biomarker is its inherent biological non-specificity. GDF-15 is upregulated across a broad spectrum of pathological conditions including cardiovascular disease, malignancy, chronic kidney disease, metabolic syndrome, autoimmune disorders, and acute inflammatory states. This non-specificity was prospectively addressed in the study design through systematic exclusion of all conditions known to independently elevate GDF-15 from both case and control groups. Despite these exclusions, the non-specific nature of GDF-15 means it cannot function as a standalone diagnostic test and must be interpreted exclusively as a complementary biomarker within a structured clinical diagnostic algorithm incorporating clinical history, pelvic imaging, and laparoscopic confirmation where clinically indicated.

The stage-wise increase in GDF-15 across r-AFS stages, while numerically consistent, did not achieve statistical significance. This should be interpreted in the context of post-hoc power analysis confirming that subgroup comparisons at the observed group sizes (n = 23 to 27 per stage) were substantially underpowered (estimated power 28%). The non-significant ANOVA result does not exclude a biologically meaningful stage-related gradient; rather, it reflects insufficient statistical power to detect the observed effect magnitude. Adequately powered future studies with a minimum of 60 to 80 participants per r-AFS stage are required to evaluate this association definitively. Furthermore, the well-established dissociation between anatomical disease extent and systemic inflammatory burden in endometriosis may independently limit the ability of any circulating biomarker to mirror r-AFS stage.

The weak and non-significant correlations between GDF-15 and VAS and NRS scores confirm that, on the basis of the present data, serum GDF-15 cannot be regarded as a predictor of pain intensity in endometriosis. The absence of statistical significance must be explicitly stated and not overstated as a trend. Pain in endometriosis is a multidimensional phenomenon governed by peripheral sensitisation, central sensitisation, neuroangiogenesis, and psychosocial amplification, none of

which are comprehensively reflected by a single circulating inflammatory cytokine measured at a single time point. Future studies incorporating longitudinal pain assessment, peritoneal fluid cytokine profiling, and validated multidimensional pain inventories would be required to adequately characterise the relationship between GDF-15 and endometriosis-associated pain.

Clinical Implications

The identification of a reliable non-invasive biomarker for endometriosis carries substantial clinical implications. First, the current 7 to 10-year diagnostic delay represents a critical clinical problem; serum GDF-15 measurement may complement clinical assessment and pelvic imaging to identify high-risk individuals and prioritise them for laparoscopic confirmation.[3] Second, longitudinal measurement of serum GDF-15 following medical or surgical treatment could potentially provide an objective, non-invasive index of treatment response if prospectively validated. Third, patients with markedly elevated GDF-15 levels may represent a clinically distinct subgroup warranting earlier or more aggressive therapeutic intervention. Fourth, the excellent diagnostic performance of GDF-15 identified in this study provides a direct rationale for its formal incorporation into future multicentre diagnostic accuracy studies and potential diagnostic algorithm development.

Strengths and Limitations

The principal strengths of this study include: laparoscopic and histopathological confirmation of endometriosis in all cases; comprehensive pain assessment using two validated instruments administered prior to any intervention; rigorous systematic exclusion of all conditions known to confound GDF-15 levels; age-matched control selection; standardised sample collection in the early follicular phase to minimise hormonal variation; duplicate ELISA analyses with stringent quality control; single-batch analysis to eliminate inter-batch variation; laboratory personnel blinded to case-control status; and the inclusion of ROC curve analysis and multivariate logistic regression, providing diagnostic performance metrics and confounder-adjusted estimates.

Several limitations must be acknowledged. First, the cross-sectional design precludes causal inference and does not permit assessment of temporal GDF-15 dynamics or its behaviour in response to treatment. Second, stage-wise ANOVA comparisons were substantially underpowered (post-hoc power 28%), and the non-significant stage-wise result should be regarded as inconclusive rather than as evidence against a severity association. Third, the single-centre design at a tertiary referral hospital introduces potential referral and selection bias; women attending tertiary centres may represent a more severe disease spectrum, potentially skewing GDF-15 levels upward relative to a community-based endometriosis population. External validation in multicentre cohorts across diverse geographical and sociodemographic settings is essential before clinical translation. Fourth, definitive exclusion of peritoneal endometriosis in controls would require diagnostic laparoscopy, which was not ethically feasible in this population; the three-tier clinical, gynaecological, and ultrasonographic screening protocol used represents the most rigorous practically available alternative. Fifth, CA-125 and other established biomarkers were not simultaneously measured in this cohort, precluding direct comparative diagnostic accuracy analysis within the same dataset. Sixth, the absence of longitudinal follow-up means that GDF-15 dynamics following treatment cannot be characterised.

Future directions

Future research should prioritise the following: prospective longitudinal studies evaluating GDF-15 dynamics before and after medical and surgical treatment; large-scale, multicentre diagnostic accuracy studies with formal comparison against CA-125 and other circulating biomarkers; investigation of peritoneal fluid GDF-15 levels and tissue expression patterns in endometriotic lesions; integration of GDF-15 into composite multimarker diagnostic algorithms; and exploration of the therapeutic potential of targeting GDF-15 signalling pathways in endometriosis management.

Conclusion

This hospital based case-control study demonstrates that serum GDF-15 is significantly elevated in women with confirmed endometriosis compared to healthy controls (961.7 ± 195.2 pg/mL vs. 508.0 ± 99.6 pg/mL; p less than 0.001), with excellent diagnostic discriminatory performance (AUC = 0.942; sensitivity 89.0%; specificity 88.0% at a cut-off of 720.5 pg/mL) and independence from age and BMI on multivariate analysis (adjusted OR = 3.84; p less than 0.001). These findings support serum GDF-15 as a promising non-invasive diagnostic biomarker for endometriosis. A non-significant numerical trend was observed across r-AFS stages (p = 0.265), and weak, non-significant correlations were identified with VAS (r = 0.174, p = 0.084) and NRS (r = 0.191, p = 0.058) pain scores. On the basis of current data, no conclusions can be drawn regarding GDF-15 as a disease severity or pain prediction biomarker, and these secondary findings are explicitly characterised as exploratory and hypothesis-generating. External validation in adequately powered, multicentre prospective cohorts is required to confirm the diagnostic utility of GDF-15 and to evaluate its potential role in endometriosis monitoring and management.

Author Contributions: Conceptualization, P.M and T.J; Methodology, R.M and P.M; Formal Analysis, T.J; Investigation, R.M, and S.D.; Resources, S.D.; Data Curation, S.D.; Writing – Original Draft Preparation, T.J and K.V.S; Writing – Review and Editing, K.V.S., T.J., and R.M.; Supervision, S.D; Project Administration, P.M. All authors have read and agreed to the published version of the manuscript.

Disclosures: The authors have no conflicts of interest.

Acknowledgments: The authors thank all participants who contributed to this study and the laboratory staff for their technical assistance.

Funding: None.

Data availability statement: The datasets generated during and/or analyzed during the current study are available from the corresponding author on reasonable request.

Artificial Intelligence (AI) Disclosure Statement: The authors declare no AI Tools used for preparation of this work.

References

1. Zondervan KT, Becker CM, Missmer SA. Endometriosis. *N Engl J Med.* 2020;382(13):1244–1256. https://doi.org/10.1056/NEJMra1810764
2. Chapron C, Marcellin L, Borghese B, Santulli P. Rethinking mechanisms, diagnosis and management of endometriosis. *Nat Rev Endocrinol.* 2019;15(11):666–682. https://doi.org/10.1038/s41574-019-0245-z
3. Nisenblat V, Bossuyt PM, Farquhar C, Johnson N, Hull ML. Imaging modalities for the non-invasive diagnosis of endometriosis. *Cochrane Database Syst Rev.* 2016;(2):CD009591. https://doi.org/10.1002/14651858.CD009591
4. Morotti M, Vincent K, Becker CM. Mechanisms of pain in endometriosis. *Eur J Obstet Gynecol Reprod Biol.* 2017;209:8–13. https://doi.org/10.1016/j.ejogrb.2016.07.497
5. Revised American Society for Reproductive Medicine classification of endometriosis: 1996. *Fertil Steril.* 1997;67(5):817–821. https://doi.org/10.1016/s0015-0282(97)81391-x
6. Bootcov MR, Bauskin AR, Valenzuela SM, Moore AG, Bansal M, Murray BL, Lei JX, Bhogal M, Cheung MS, Strang M, Simpson RJ, Nicholson RC, Wakefield D, Brown DA, Breit SN. MIC-1, a novel macrophage inhibitory cytokine, is a divergent member of the TGF-beta superfamily. *Proc. Natl. Acad. Sci. U.S.A.* 1997;94(21):11514–11519. https://doi.org/10.1073/pnas.94.21.11514
7. Tian T, Liu M, Little PJ, Strijdom H, Weng J, Xu S. Emerging roles of GDF15 in metabolic and cardiovascular diseases. Research (Wash D C). 2025;8:0832. https://doi.org/10.34133/research.0832
8. Lu YC, Liu SL, Zhang YS, Zhu CL, Lu Y, Wang T, Liu XH, Ye DS, Fu JF. Association between growth differentiation factor 15 levels and gestational diabetes mellitus: a combined analysis. *Front Endocrinol (Lausanne).* 2023;14:1084896. https://doi.org/10.3389/fendo.2023.1084896
9. Kempuraj D, Papadopoulou N, Stanford EJ, Christodoulou S, Madhappan B, Sant GR, Solage K, Adams T, Theoharides TC. Increased numbers of activated mast cells in endometriosis lesions positive for corticotropin-releasing hormone and urocortin. *Am J Reprod Immunol.* 2004;52(4):267–275. https://doi.org/10.1111/j.1600-0897.2004.00224
10. Scutiero G, Iannone P, Bernardi G, Mollica G, Palmieri S, Greco P, Berghella V, Nappi L. Oxidative stress and endometriosis: a systematic review of the literature. *Oxid Med Cell Longev.* 2017;2017:7265238. https://doi.org/10.1155/2017/7265238
11. Yang L, Chang CC, Sun Z, Madsen D, Zhu H, Padkjær SB, Wu X, Huang T, Hultman K, Paulsen SJ, Wang J, Bugge A, Frantzen JB, Nørgaard P, Jeppesen JF, Yang Z, Secher A, Chen H, Li X, John LM, Shan B, He Z, Gao X, Su J, Hansen KT, Yang W, Jørgensen SB. GFRAL is the receptor for GDF15 and is required for the anti-obesity effects of the ligand. *Nat Med.* 2017;23(10):1158–1166. https://doi.org/10.1038/nm.4394
12. Johnen H, Lin S, Kuffner T, Brown DA, Tsai VW, Bauskin AR, Wu L, Pankhurst G, Jiang L, Junankar S, Hunter M, Fairlie WD, Lee NJ, Enriquez RF, Baldock PA, Corey E, Apple FS, Murakami MM, Lin EJ, Wang C, During MJ, Sainsbury A, Herzog H, Breit SN. Tumor-induced anorexia and weight loss are mediated by the TGF-beta superfamily cytokine MIC-1. *Nat Med.* 2007;13(11):1333–1340. https://doi.org/10.1038/nm1677
13. Vanhie A, Mori da Cunha M, Peterse D, Beckers A, Coxon L, Timmerman D, Vermeersch P, Horne AW, Becker CM, Zondervan KT, Tomassetti C, D'Hooghe T. Plasma biomarkers for endometriosis: a systematic review. *Reprod Biomed Online.* 2022;44(5):906–925. https://doi.org/10.1016/j.rbmo.2022.01.007
14. Ferrero S, Evangelisti G, Barra F. Current and emerging treatment options for endometriosis. *Expert Opin Pharmacother.* 2023;24(7):823–834. https://doi.org/10.1080/14656566.2023.2196577
15. Macer ML, Taylor HS. Endometriosis and infertility: a review of the pathogenesis and treatment of endometriosis-associated infertility. *Obstet Gynecol Clin North Am*. 2022;49(3):519–537. https://doi.org/10.1016/j.ogc.2022.02.010

JOURNAL OF CLINICAL MEDICINE OF KAZAKHSTAN (E-ISSN 2313-1519)
Original Article DOI: https://doi.org/10.23950/jcmk/18357

Anesthetic Management During PIPAC: Clinical and Practical Aspects

Murat B. Zhumabayev[1], Karlygash S. Kabdenova[2], Khalka B. Baubekova[2], Yerlan U. Umbetzhanov[2], Zhandos K. Burkitbayev[3], Asima S. Izmailova[2], Assemgul S. Kassenova[4]

[1]Department of Anesthesiology, Intensive Care and Emergency Medicine, Astana Medical University, Astana, Kazakhstan
[2]Anesthesiology and Intensive Care Department, National Research Oncology Center (NROC), Astana, Kazakhstan
[3]Chairman of the National Research Oncology Center (NROC), Astana, Kazakhstan
[4]Institute of Continuing Professional Education, Astana Medical University, Astana, Kazakhstan

Received: 2025-09-10.
Accepted: 2026-04-12.

This work is licensed under a **Creative Commons Attribution 4.0 International License**

J Clin Med Kaz 2026; 23(2): 39-44

Corresponding author:
Karlygash S. Kabdenova.
E-mail: karlygash.kabdenova@mail.ru.
ORCID: 0009-0002-5067-6263.

ABSTRACT

Background: Pressurized Intraperitoneal Aerosol Chemotherapy (PIPAC) is a novel minimally invasive technique for the treatment of peritoneal carcinomatosis that allows localized delivery of cytotoxic drugs under pressure. Despite its clinical potential, this procedure presents unique anesthetic challenges due to increased intra-abdominal pressure, limited access to the patient during aerosolization, and the need for strict safety measures to prevent occupational exposure.

Objective: The objective of this study was to evaluate the specific features of anesthetic management during Pressurized Intraperitoneal Aerosol Chemotherapy (PIPAC) procedures and to determine the safety and tolerability of this method.

Methods: This retrospective analysis included 26 PIPAC procedures performed under general anesthesia. The study focused on parameters related to anesthesia induction, mechanical ventilation, depth of neuromuscular blockade, integrity of the breathing system, and intraoperative monitoring. Given the unique conditions of PIPAC, such as increased intra-abdominal pressure, limited access to the patient during the procedure, and the risk of occupational exposure to aerosolized cytotoxic agents, anesthetic management was tailored accordingly. Particular attention was paid to ensuring an airtight respiratory circuit, preventing aerosol leakage, and controlling carbon dioxide levels throughout the procedure.

Results: All patients received adequate general anesthesia with stable hemodynamic and respiratory parameters throughout the procedure. No major anesthesia-related complications were observed. The procedure was well tolerated by all patients. Effective neuromuscular blockade was achieved in each case to facilitate laparoscopic access and ensure immobility during the aerosol chemotherapy phase. End-tidal carbon dioxide levels were closely monitored, and hypercapnia was successfully controlled through ventilatory adjustments. The use of a closed anesthetic circuit and appropriate filtration systems ensured both patient and staff safety by minimizing aerosol exposure.

Conclusion: PIPAC is a safe and well-tolerated procedure when performed with adherence to specific anesthetic requirements. Successful anesthetic management includes deep neuromuscular blockade, advanced monitoring, strict respiratory circuit integrity, and readiness to manage potential hypercapnia. There is a clear need to develop and implement standardized anesthetic protocols for PIPAC procedures in order to optimize clinical outcomes and minimize associated risks.

Keywords: Pressurized Intraperitoneal Aerosol Chemotherapy, anesthetic management, aerosol chemotherapy, hypercapnia, general anesthesia, peritoneal carcinomatosis, laparoscopy.

Introduction

PIPAC (Pressurized Intraperitoneal Aerosol Chemotherapy) is an innovative method of locoregional chemotherapy for peritoneal carcinomatosis, characterized by increased efficiency of cytostatic delivery with minimal systemic toxicity. The method requires a special approach to anesthetic management due to the effect of increased intra-abdominal pressure, the aerosol nature of chemotherapy and the need for hermetic isolation of the surgical field. This article discusses the current aspects of preoperative assessment, anesthesia features, intraoperative monitoring and postoperative management of patients undergoing PIPAC. [1]

Peritoneal carcinomatosis is an aggressive form of metastatic disease in which malignant cells spread throughout the peritoneum to form multiple tumor implants. Most often, this condition is observed in tumors of the gastrointestinal tract (in particular, gastric, colon and rectal cancer), as well as in serous ovarian adenocarcinoma. Mechanisms of dissemination include direct tumor penetration through the serous membrane, transcoelomic spread with the flow of ascitic fluid, and possible implantation during surgical interventions. Peritoneal carcinomatosis is accompanied by a pronounced inflammatory reaction, disruption of the barrier function of the peritoneum and the development of malignant ascites, which further aggravates the clinical course of the disease. The prognosis for peritoneal carcinomatosis is extremely unfavorable, with a median survival of less than one year without specific treatment. The effectiveness of systemic chemotherapy is limited due to poor vascularization of peritoneal structures, reduced drug penetration, and high drug resistance of tumor cells in this location.

In search of more effective methods of locoregional treatment, an innovative approach was developed – pressurized intraperitoneal aerosol chemotherapy (PIPAC) [2]. This method, proposed by Mark Ruedli and colleagues in the early 2000s, is based on the laparoscopic introduction of chemotherapy drugs into the abdominal cavity in the form of an aerosol under pressure, which contributes to a more uniform distribution of the drug and better pene Although the PIPAC procedure is minimally invasive, it places special demands on anesthetic management. These include the need to maintain stable ventilation with increased intra-abdominal pressure, limited access to the patient during the aerosol exposure phase, requirements for the tightness of breathing circuits and ensuring the safety of the operating personnel. In addition, most patients undergoing PIPAC are cancer patients with concomitant pathology and weakened somatic status, which requires an individualized approach to anesthesia.

This article is devoted to an overview of the anesthetic aspects of the PIPAC procedure, risk analysis and methods for their minimization, as well as practical recommendations for ensuring the safety and effectiveness of the intervention.tration into tumor tissue [3].

Methods

The purpose of anesthetic management during the PIPAC procedure is to maintain a safe and stable course of the intraoperative period under conditions of increased physiological stress and limited access to the patient at critical stages of the intervention. Anesthetic tactics should ensure adequate depth of general anesthesia with controlled artificial ventilation under pneumoperitoneum conditions, stability of respiratory and hemodynamic functions, as well as prevention of complications

Figure 1 – Operating room labeling to ensure staff safety during PIPAC

The operating room must be marked in a special way

associated with increased intra-abdominal pressure and the use of aerosol cytostatics. Compliance with biological safety measures to protect medical personnel from potential cytotoxic effects is of no small importance. The operating room must be marked in a special way (Figure 1). Given the limitations of physical access to the patient during the phase of spraying the chemotherapy drug, it is necessary to organize continuous monitoring of vital functions and be ready for immediate correction of possible critical conditions.

This study is a retrospective single-center analysis including data from 26 patients who underwent Pressurized Intraperitoneal Aerosol Chemotherapy (PIPAC) performed at the National Scientific Oncology Center, Astana, Republic of Kazakhstan in 2024–2025. The mean age of patients was 59.35 years. All included patients had a confirmed diagnosis of peritoneal carcinomatosis associated with locally advanced adenocarcinoma of the stomach or sigmoid colon [4-5]. The selection was carried out among patients with an intact general somatic status (ECOG score 0–2) and without signs of intestinal obstruction.

Inclusion criteria were age from 18 to 70 years and the presence of peritoneal carcinomatosis associated with locally advanced gastric cancer.

All patients received neoadjuvant systemic chemotherapy according to the FLOT regimen before PIPAC. Intraperitoneal administration of cytostatics was carried out in accordance with international recommendations[6]., using cisplatin at a dose of 10 mg / m² and doxorubicin at a dose of 2.1 mg / m² [1-7-14].

The chemotherapy agent is sprayed into the abdominal cavity using a special device through a nozzle (Figure 2-3).

At the preoperative stage, patients underwent a comprehensive clinical and diagnostic assessment, including general and biochemical blood tests, coagulogram, electrocardiography, echocardiography, as well as visualization

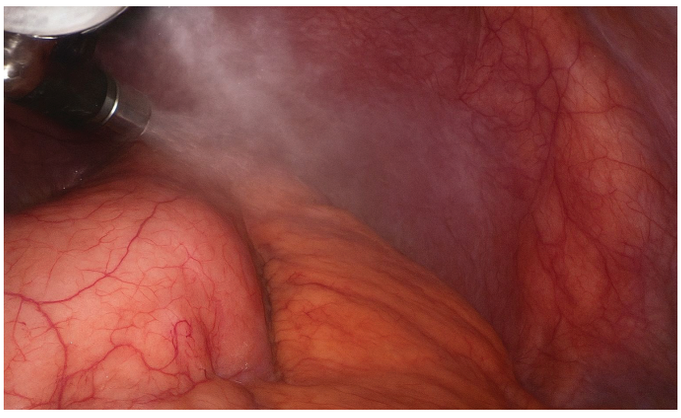

Figure 2 – Intraoperative view during PIPAC showing pressurized aerosol distribution

The operating room must be marked in a special way

Figure 3 – Medical equipment for intraperitoneal administration of a chemotherapeutic agent (PIPAC system setup)

The chemotherapy agent is sprayed into the abdominal cavity using a special device through a nozzle.

studies (CT or MRI of the abdominal organs) [8-9]. In the presence of signs of respiratory disorders, spirometry was performed. Consultations with specialized specialists were also carried out according to indications.

Contraindications to the procedure were decompensated somatic conditions, severe ascites (volume over 4 liters), as well as the presence of massive intra-abdominal adhesions identified by imaging methods. In 69.2% of cases, patients had concomitant diseases, primarily arterial hypertension, type 2 diabetes mellitus, and toxic effects of previous systemic chemotherapy. According to the ASA classification, 73.1% of patients belonged to class II anesthetic risk, 26.9% to class III anesthetic risk.

The preoperative period included a mandatory informed discussion with the patient of all aspects of the upcoming intervention, including potential risks (intra-abdominal perforation, chemical peritonitis), features of anesthetic management, and the need to use a sealed operating room with a personnel protection system. Premedication included antiemetic drugs, including serotonin receptor antagonists (ondansetron), dopamine receptor antagonists (metoclopramide, cerucal), corticosteroids (dexamethasone), and proton pump inhibitors (omeprazole, pantoprazole).

Anesthetic management was performed according to the standard protocol of general anesthesia with tracheal intubation and controlled artificial ventilation. Induction of anesthesia included the administration of propofol (1.5–2 mg/kg), fentanyl (1–2 µg/kg), and rocuronium (0.6 mg/kg). Anesthesia was maintained either with total intravenous anesthesia (TIVA) or with the inhalation anesthetic sevoflurane. Deep neuromuscular blockade (TOF = 0) was provided in all cases. Intraoperative intra-abdominal pressure was maintained at 12–15 mmHg. [10].

Monitoring of vital functions was performed in an expanded volume and included noninvasive blood pressure, capnography, assessment of the depth of anesthesia using BIS, as well as control of the degree of neuromuscular blockade using TOF stimulation. [11].

The main characteristics of the patients who took part in the observation are described in Table 1.

The observation involved 26 patients, including 17 men and 9 women. The median age was 61.5±9.7 years. The minimum age was 35 years, the maximum age was 70 years.

Figure 4 shows the BMI values with its median value for the group and standard deviation pages.

Table 1 Main characteristics of patients who underwent PIPAC

Characteristic	Men	Women
Gender	17	9
Age, years, Median ± standard deviation	61±9,4	62±10,9
BMI, kg/m^2, Median ± standard deviation	25,65±4,72	
ASA Class		
ASA 2	19	
ASA 3	6	
ECOG stage 2	2	
Oncology stages		
Stage 2	9	
Stage 2 9	17	

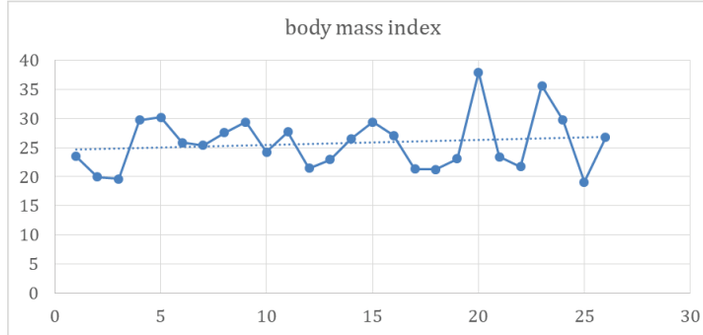

Figure 4 – BMI values of the observation group

The body mass index was 25.64±4.72 kg/m², with a maximum of 38.01 kg/m² and a minimum of 19.07 kg/m². This factor is important because nutritional status is critical for prognosis of further treatment, risk of complications, and patient outcome. Subsequently, 13 patients underwent gastrectomy surgery. In general, patients undergoing PIPAC had no complications either during or postoperatively. [12-13].

Results

The median duration of the surgical stage was 75.0 ± 19.7 minutes, with the minimum duration being 31 minutes and the maximum being 116 minutes. Figure 5 shows a diagram of the duration of the surgical intervention.

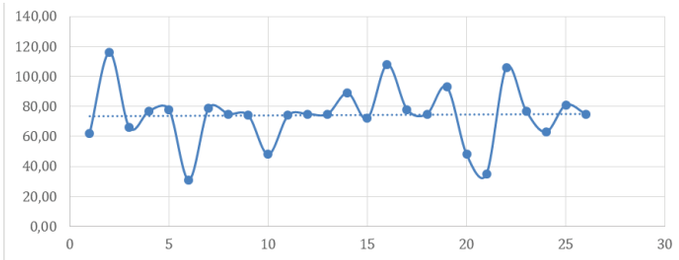

Figure 5 – Duration of surgical intervention

All procedures were performed under general anesthesia with tracheal intubation and controlled ventilation. A deep neuromuscular block (TOF 0) was provided throughout the procedure, with PCV or VCV ventilation using a high-end anesthesia machine. The duration of anesthesia care is shown in Figure 6.

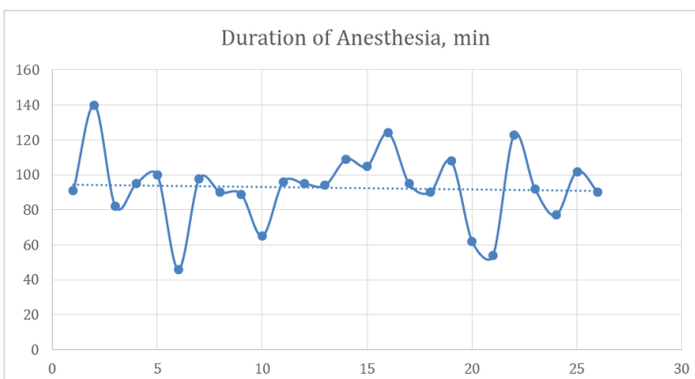

Figure 6 – Duration of anesthesia, min

The median duration of anesthesia was 94.5±20.75 minutes. The minimum duration was 46 minutes, the maximum – 140 minutes.

The duration of operations and anesthesia was mainly due to three factors: individual characteristics of the oncological process, high body mass index, high risk of complications (a combination of risk factors in 1 patient: ASA 3, heart rhythm disturbances, high body mass index, etc.).

Intra-abdominal pressure was maintained at a level of up to 12 mm Hg [12], with mandatory monitoring of gas exchange parameters ($EtCO_2$, SpO_2, FiO_2). Transient hypercapnia ($EtCO_2$> 50 mm Hg) was recorded in 20% of patients, which was successfully stopped by increasing the minute ventilation volume. Before the aerosol spray phase of chemotherapy drugs, hyperventilation and preoxygenation with 100% oxygen were performed, which allowed for the creation of an oxygen reserve in the lungs and the safe conduct of the apnea phase lasting 2–5 minutes. During spraying, the mechanical ventilation was turned off and the breathing circuit was sealed, in accordance with international safety standards [15-16].

In order to protect the operating personnel from the effects of cytostatics, biological safety protocols were strictly followed: remote control of the spray phase, complete sealing of all ports, and the use of certified filtration systems [14-15-18]. In the postoperative period, 28% of patients experienced episodes of nausea and vomiting, which were successfully relieved by ondansetron. The need for analgesia was moderate: non-steroidal anti-inflammatory drugs and promedol were used according to indications. None of the patients required transfer to the intensive care unit. Hospitalization after the procedure averaged 2–3 days; complications requiring repeated intervention or prolonged therapy were not registered.

Discussion

The Pressurized IntraPeritoneal Aerosol Chemotherapy (PIPAC) procedure is an innovative method of locoregional chemotherapy, which is increasingly being introduced into clinical practice for the treatment of peritoneal carcinomatosis. Despite its clinical promise, this method remains a technically and organizationally complex intervention that requires coordinated work of a multidisciplinary team. Of particular importance in the process of PIPAC is anesthesiological management, which goes beyond standard general anesthesia and involves a deep understanding of the physiological changes caused by intra-abdominal pressure, exposure to chemoaerosol, and limited access to the patient at key stages of the intervention.

One of the central tasks of the anesthesiologist in PIPAC is to ensure adequate gas exchange under pneumoperitoneum conditions. Increased intra-abdominal pressure (usually up to 12–15 mm Hg). leads to limited diaphragm excursion, decreased pulmonary compliance and the risk of hypercapnia [15-17]. According to the data of the present study, 20% of patients experienced transient hypercapnia ($EtCO_2$ > 50 mm Hg), which requires dynamic correction of mechanical ventilation parameters, including an increase in minute volume and optimization of the level of positive end-expiratory pressure (PEEP). These features emphasize the need for individual selection of ventilation strategies depending on the patient's respiratory reserve and the volume of surgical intervention.

In addition, an important aspect of anesthesiological management is maintaining stable hemodynamics against the background of possible vasodilation associated with systemic resorption of cytostatics and their potential cardio- and nephrotoxicity. Administration of drugs such as cisplatin and doxorubicin requires special attention to renal and cardiovascular function, especially in patients with comorbidities. Monitoring of hemodynamic parameters and timely correction of perfusion disorders should be part of the basic management algorithm.

Prevention of postoperative nausea and vomiting (PONV) is another key component, especially in high-risk patients (women, patients with previous courses of systemic chemotherapy, use of inhalational anesthetics and opioids). In our study, the use of a multicomponent premedication regimen, including serotonin and dopamine receptor antagonists, as well as corticosteroids, provided effective prevention of PONV in most cases.

The PIPAC procedure places high demands on the qualifications of the anesthesiologist, his readiness to respond quickly in conditions of limited access to the patient and interaction with the surgical team. Given the relatively small accumulated clinical experience in the use of this technology, the development and implementation of standardized anesthetic protocols adapted to PIPAC conditions seems relevant. Further accumulation of clinical data is necessary to assess safety, identify risks and optimize the tactics of managing patients undergoing this treatment [20].

Conclusion

Anesthetic care for PIPAC is a complex measure that requires the use of extended monitoring, deep neuromuscular blockade and specific ventilation tactics. Compliance with safety standards when working with aerosol forms of chemotherapy drugs can significantly reduce the risks for staff and patients, increasing the effectiveness of the treatment of peritoneal carcinomatosis [21].

Author Contributions: Conceptualization, M.B., H.B. and K.S.; methodology, M.B., H.B., and A.S., K.S.; validation, E.U., M.B., Z.B. and H.B.. A.S.; formal analysis, M.B., H.B., Z.B. and K.S., A.S.; investigation, K.S., and A.S.; resources, M.B., and E.U.; data curation, K.S., and A.S.; writing — original draft, MB., H.B., and K.S.; writing — review ans editing, M.B., H.B, and K.S.; visualization, K.S.; supervision, E.U.; project administration, M.B; funding acquisition, M.B. All authors have read and agreed to the published version of the manuscript.

Disclosures: The authors have no conflicts of interest.

Acknowledgments: None.

Funding: This publication was published within the framework of the program-targeted funding of the Science Committee of the Ministry of Science and Higher Education of the Republic of Kazakhstan, IRN: BR24992950. Agreement No. 386/PCF24-26.

Data availability statement: The corresponding author can provide the data supporting the study's conclusions upon request. Due to ethical and privacy constraints, the data are not publicly accessible.

Artificial Intelligence (AI) Disclosure Statement: The authors declare no AI Tools used for preparation of this work.

References

1. Tate SJ, Torkington J. Pressurized intraperitoneal aerosol chemotherapy: a review of the introduction of a new surgical technology using the IDEAL framework. *BJS Open.* 2020;4(2):206-215. https://doi.org/10.1002/bjs5.50257
2. Robella M, Vaira M, De Simone M. Safety and feasibility of pressurized intraperitoneal aerosol chemotherapy (PIPAC) associated with systemic chemotherapy: an innovative approach to treat peritoneal carcinomatosis. *World Journal of Surgical Oncology.* 2016;14:128. https://doi.org/10.1186/s12957-016-0892-7
3. Tempfer C, Giger-Pabst U, Hilal Z, Dogan A, Rezniczek GA. Pressurized intraperitoneal aerosol chemotherapy (PIPAC) for peritoneal carcinomatosis: systematic review of clinical and experimental evidence with special emphasis on ovarian cancer. *Archives of Gynecology and Obstetrics.* 2018;298(2):243-257. https://doi.org/10.1007/s00404-018-4784-7
4. Robella M, Hubner M, Sgarbura O, Reymond M, Khomiakov V, Di Giorgio A, Bhatt A, Bakrin N, Willaert W, Alyami M, Teixeira H, Kaprin A, Ferracci F, De Meeus G, Berchialla P, Vaira M. Results from the ISSPP PIPAC study group. *European Journal of Surgical Oncology.* 2022;48(10):2212-2217. https://doi.org/10.1016/j.ejso.2022.05.001
5. Eveno C, Haidara A, Ali I, Pimpie C, Mirshahi M, Pocard M. Experimental pharmacokinetics evaluation of chemotherapy delivery by PIPAC for colon cancer: first evidence for efficacy. *Pleura and Peritoneum.* 2017;2(2):103-109. https://doi.org/10.1515/pp-2017-0015
6. Al-Batran S.E., Homann N., Pauligk C., Goetze T.O., Meiler J., Kasper S., Kopp H.G., Mayer F., Haag G.M., Luley K., Trojan J., Moehler M., Probst S., Schmiegel W., Pohl M., Rethwisch V., Jäger E., Schmalenberg H., Hofheinz R.D. The FLOT regimen for the treatment of gastric cancer: results from a multicenter trial. *Lancet Oncology.* 2019;20(5):768–777. https://doi.org/10.1016/S1470-2045(19)30132-2
7. Shree V, Lim TJ, Lean LL, So BYJ, Kim G. Anaesthesia considerations and techniques for pressurised intraperitoneal aerosol chemotherapy (PIPAC). *Pleura and Peritoneum.* 2020;5(4):20190013. https://doi.org/10.1515/pp-2019-0013
8. Roensholdt S., Detlefsen S., Mortensen M., Graversen M. Response evaluation in patients with peritoneal metastasis treated with Pressurized Intraperitoneal Aerosol Chemotherapy (PIPAC). *Journal of Clinical Medicine.* 2023;12(4):1289. https://doi.org/10.3390/jcm12041289
9. Franko J., Shi Q., Goldman C.D., et al. Treatment of colorectal peritoneal carcinomatosis with systemic chemotherapy: a pooled analysis of North Central Cancer Treatment Group phase III trials N9741 and N9841. *Journal of Clinical Oncology*. 2012;30(3):263–267. https://doi.org/10.1200/jco.2011.37.1039
10. Nadiradze G, Giger-Pabst U, Zieren J, Strumberg D, Solass W, Reymond MA. Pressurized intraperitoneal aerosol chemotherapy (PIPAC) with low-dose cisplatin and doxorubicin in gastric peritoneal metastasis. *Journal of Gastrointestinal Surgery.* 2016;20(2):367-373. https://doi.org/10.1007/s11605-015-2995-9
11. Alyami M, Hubner M, Grass F, Bakrin N, Villeneuve L, Laplace N, Passot G, Glehen O, Kepenekian V. Pressurised intraperitoneal aerosol chemotherapy: rationale, evidence, and potential indications. *The Lancet Oncology*. 2019;20(7):e368-e377. https://doi.org/10.1016/S1470-2045(19)30318-3
12. Vaira M, Robella M, Borsano A, De Simone M. Single-port access for pressurized intraperitoneal aerosol chemotherapy (PIPAC): technique, feasibility and safety. *Pleura and Peritoneum.* 2016;1(4):217-222. https://doi.org/10.1515/pp-2016-0021

13. Sgarbura O, Villeneuve L, Alyami M, Bakrin N, Torrent JJ, Eveno C, Hubner M. Current practice of pressurized intraperitoneal aerosol chemotherapy (PIPAC): still standardized or on the verge of diversification? *European Journal of Surgical Oncology.* 2021;47(1):149-156. https://doi.org/10.1016/j.ejso.2020.08.020
14. Taliento C, Restaino S, Scutiero G, Arcieri M, Bernardi G, Martinello R, Driul L, Perrone AM, Fagotti A, Scambia G, Greco P, Vizzielli G. Pressurized intraperitoneal aerosol chemotherapy (PIPAC) with cisplatin and doxorubicin in patients with ovarian cancer: a systematic review. *European Journal of Surgical Oncology.* 2023;49(12):107250. https://doi.org/10.1016/j.ejso.2023.107250
15. Farinha H.T., Mattille D., Mantziari S., Demartines N., Hübner M. Early postoperative outcomes of staging laparoscopy for peritoneal metastases with or without pressurized intraperitoneal aerosol chemotherapy (PIPAC). *BMC Surgery.* 2022;22:122. https://doi.org/10.1186/s12893-022-01572-5
16. Solass W., Kerb R., Mürdter T., Giger-Pabst U., Strumberg D., Tempfer C., Zieren J., Schwab M., Reymond M.A. Intraperitoneal chemotherapy of peritoneal carcinomatosis using pressurized aerosol as an alternative to liquid solution: first evidence for efficacy. *Annals of Surgical Oncology.* 2014;21(2):553–559. https://doi.org/10.1245/s10434-013-3213-1
17. Solass W., Kerb R., Mürdter T., Giger-Pabst U., Strumberg D., Tempfer C., Zieren J., Schwab M., Reymond M.A. Intraperitoneal chemotherapy of peritoneal carcinomatosis using pressurized aerosol as an alternative to liquid solution: first evidence for efficacy. *Annals of Surgical Oncology.* 2014;21(2):553–559. https://doi.org/10.1245/s10434-013-3213-1
18. Demtroder C, Solass W, Zieren J, Strumberg D, Giger-Pabst U, Reymond MA. Pressurized intraperitoneal aerosol chemotherapy with oxaliplatin in colorectal peritoneal metastasis. *Colorectal Disease.* 2016;18(4):364-371. https://doi.org/10.1111/codi.13130
19. Raoof M, Whelan RL, Sullivan KM, Ruel C, Frankel PH, Cole SE, Tinsley R, Eng M, Fakih M, Chao J, Lim D, Woo Y, Paz IB, Lew M, Cristea M, Rodriguez-Rodriguez L, Fong Y, Thomas RM, Chang S, Deperalta D, Merchea A, Dellinger TH. Safety and efficacy of oxaliplatin pressurized intraperitoneal aerosolized chemotherapy (PIPAC) in colorectal and appendiceal cancer with peritoneal metastases: results of a multicenter phase I trial in the USA. *Annals of Surgical Oncology.* 2023;30(12):7814-7824. https://doi.org/10.1245/s10434-023-13941-2
20. Solass W, Kerb R, Murdter T, Giger-Pabst U, Strumberg D, Tempfer C, Zieren J, Schwab M, Reymond MA. Intraperitoneal chemotherapy of peritoneal carcinomatosis using pressurized aerosol as an alternative to liquid solution: first evidence for efficacy. *Annals of Surgical Oncology.* 2014;21(2):553-559. https://doi.org/10.1245/s10434-013-3213-1
21. Farinha HT, Mattille D, Mantziari S, Demartines N, Hubner M. Early postoperative outcomes of staging laparoscopy for peritoneal metastases with or without pressurized intraperitoneal aerosol chemotherapy (PIPAC). *BMC Surgery.* 2022;22:122. https://doi.org/10.1186/s12893-022-01572-5

JOURNAL OF CLINICAL MEDICINE OF KAZAKHSTAN (E-ISSN 2313-1519)
Review Article DOI: https://doi.org/10.23950/jcmk/18013

Determination of Body Mass Index Using Machine Learning Regression Methods from Body Composition Parameters

Seda Sertel Meyvaci[1], Yusuf Secgin[2], Taha Gokmen Ulger[3], Tuba Taslamacioglu Duman[4], Beyza Celik[1], Sena Demiroglu[1]

[1]*Department of Anatomy, Faculty of Medicine, Bolu Abant Izzet Baysal University, Bolu, Turkey*
[2]*Department of Anatomy, Faculty of Medicine, Karabük University, Karabük, Turkey*
[3]*Department of Nutrition and Dietetics, Faculty of Health Sciences, Bolu Abant Izzet Baysal University, Bolu, Turkey*
[4]*Department of Internal Medicine, Faculty of Medicine, Bolu Abant Izzet Baysal University, Bolu, Turkey*

Received: 2025-10-14.
Accepted: 2026-02-21.

This work is licensed under a **Creative Commons Attribution 4.0 International License**

J Clin Med Kaz 2026; 23(2): 45-50

Corresponding author:
Sena Demıroglu
E-mail: demiroglusenaa@gmail.com.
ORCID: 0000-0002-7214-5538.

ABSTRACT

Introduction: Obesity is one of the most significant global health problems increasing today. Body mass index (BMI) is a fundamental parameter widely used to assess obesity. However, evaluating different measurements of body composition may contribute to determining BMI more accurately and comprehensively. In this context, machine learning (ML) provides a powerful alternative to classical methods by predicting BMI from body composition. Based on this hypothesis, the aim of this study is to predict BMI using ML regression models from body composition parameters.

Methods: The study included 411 obese individuals aged 18–65 years. The individuals' body weight and body composition parameters [fat mass index, body fluid percentage, fat mass (kg), fat-free mass (kg), body fat percentage and fat-free mass percentage] were measured using the Tanita MC 580 body composition analyzer. Data were analyzed using 16 different ML regression models with the Python language and PyCaret library. Model performance was primarily evaluated using the coefficient of determination (R^2).

Results: The highest success was achieved with Linear Regression, Bayesian Ridge, and Ridge Regression models (R^2=0.9937). Huber Regressor (0.9928) and Least Angle Regression (0.9911) followed. Among the models with low success was K Neighbors Regressor (0.8316). In the parameter analysis, Fat-Mass Index was the strongest predictor in BMI estimation.

Conclusion: This study shows that ML-based regression models can predict BMI with high accuracy using body composition parameters, with the fat mass index providing the most significant contribution. These results emphasize the potential of digital phenotyping as a valuable approach in obesity research and clinical evaluation. By framing BMI not only as a traditional measurement but as a more comprehensive health marker supported by digital tools, the findings point toward the development of personalized, rapid, and reliable digital health solutions for obesity screening and monitoring.

Keywords: Body mass index, obesity, machine learning regression models, bioelectrical impedance analysis, digital phenotyping.

Introduction

Obesity is a complex public health problem with rapidly increasing prevalence and is associated with numerous health conditions such as cardiovascular diseases, type 2 diabetes, osteoarthritis, and certain types of cancer [1]. Among the most commonly used indicators for the classification of obesity, body mass index (BMI) is widely utilized in both clinical and epidemiological studies due to its ease of application and simple calculation method. However, since BMI is solely based

on height and body weight measurements, it cannot reflect body fat distribution, the distinction between fat mass and fat-free mass, or metabolically risky abdominal obesity [2-4]. This limitation may lead to misclassification, particularly in individuals with high muscle mass, the elderly, or those with different body composition profiles [5].

To overcome these limitations, bioelectrical impedance analysis (BIA) provides an important alternative. BIA offers detailed information on an individual's body composition by safely, non-invasively, and reproducibly determining parameters such as fat mass, fat-free mass, and body fluid [6]. In clinical practice, BIA-derived data have been shown to provide more reliable results than BMI in predicting cardiometabolic risks, accurately characterizing obesity phenotypes, and developing personalized nutritional approaches [7-9].

Meanwhile, machine learning (ML) methods, which have gained increasing importance in health sciences in recent years, enable the modeling of complex relationships among multidimensional biological data. ML algorithms can process large datasets to uncover patterns that may be overlooked by traditional methods, thereby contributing to a more precise and individualized assessment of obesity and related metabolic disorders [10, 11]. Integrating BIA-derived body composition parameters with ML techniques not only provides more accurate predictions beyond BMI but also offers practical advantages for clinical applications [12]. Machine learning has also been applied to predict temporomandibular disorders using clinical parameters and to predict carpal tunnel syndrome using anthropometric and strength-based measurements [13, 14]. Although machine learning has been widely applied for obesity classification, few studies have focused exclusively on BMI prediction using BIA-derived body composition parameters.

To the best of our knowledge, no previous study has directly compared 16 machine learning regression algorithms for BMI prediction using exclusively BIA-derived body composition parameters. In this context, the present study systematically evaluates and compares a wide range of machine learning regression models to estimate BMI using biologically meaningful body composition parameters obtained from BIA. Thus, it is intended to develop a model that overcomes the limitations of conventional BMI calculation, incorporates body composition, and allows for more personalized assessments in clinical practice. By emphasizing both predictive performance and model interpretability, this study aims to clarify the relationship between BMI and underlying body composition and to highlight the potential clinical relevance of body composition–based obesity assessment.

Methods

This study included patients with obesity, aged 18–65 years, with a BMI of ≥30 kg/m², who presented to the Internal Medicine Outpatient Clinic of Bolu Abant Izzet Baysal Training and Research Hospital and were referred to the diet outpatient clinic. Body composition data of these patients were obtained using a Tanita MC 580 BIA device. The measurements, together with demographic information recorded for clinical follow-up, were retrospectively retrieved from outpatient clinic records. For patients with multiple measurements, only the first measurement was considered. The body composition parameters evaluated were fat mass, body fat percentage, fat-free mass, fat-free mass percentage, fat mass index (FMI), total body water (% of body weight) and BMI. Both FMI and BMI values were automatically calculated by the Tanita MC 580 BIA device using fat mass, height, and body weight inputs. FMI was derived by dividing fat mass in kilograms by the square of height in meters [fat mass (kg) / height² (m²)], whereas BMI was calculated by dividing body weight in kilograms by the square of height in meters [body weight (kg) / height² (m²)]. Ethical approval for the study was obtained from the Bolu Abant Izzet Baysal University Non-Interventional Clinical Research Ethics Committee (2025/384).

Machine Learning Regression Models

To estimate BMI, the Python programming language and the PyCaret library were employed. Modeling procedures were carried out on a Monster Abra A7 computer with an Intel i5 processor. The collected numerical data (body composition parameters and age) constituted the input layer for ML algorithms and regression models, while the output layer was designed as the predicted BMI.

A total of 16 PyCaret ML regression models were included in the study: Linear Regression (LiR), Bayesian Ridge Regression (BRR), Ridge Regression (RR), Huber Regression (HR), Least Angle Regression (LAR), Extra Tree Regression (ETR), Elastic Net (EN), Gradient Boosting Regression, Lasso Regression (LaR), Lasso Least Angle Regression, Passive Aggressive Regression, Random Forest Regression (RFR), Light Gradient Boosting Machine Regression, Decision Tree Regression (DTR), AdaBoost Regression, and K-Neighbors Regression. LiR is a fundamental method that models the linear relationship between the dependent and independent variables [15]. BRR models the joint probability distribution of variables, thereby allowing the evaluation of event probabilities and related risks [16]. Among regularization methods, RR reduces multicollinearity by adding penalties to parameter magnitudes [17], while LaR shrinks regression coefficients and reduces some to zero, enabling variable selection [18]. EN combines the advantages of Lasso and Ridge to perform both variable selection and multicollinearity reduction [19]. Additionally, HR is preferred as a method that is less affected by outliers [20]. LARS is used as an algorithm for variable selection in high-dimensional datasets [21].

For model development, the dataset was divided into 80% training and 20% test sets. The training set was used to train the models, while the test set was used for independent performance evaluation. To mitigate potential overfitting concerns associated with high R^2 values, model performance metrics were assessed separately on the training and test datasets. Hyperparameter tuning was performed to optimize model performance. The evaluated performance metrics included Mean Absolute Error (MAE), Mean Squared Error (MSE), Root Mean Squared Error (RMSE), Root Mean Squared Logarithmic Error (RMSLE), Mean Absolute Percentage Error (MAPE), Total Taken (TT-seconds), and the Coefficient of Determination (R^2). Total Taken (TT-seconds) refers to the total elapsed time required to train and evaluate each regression model.

To improve model interpretability, SHAP (SHapley Additive exPlanations) analysis was applied to identify the relative contribution of each input parameter to BMI prediction in the best-performing models.

Basic Statistical Analysis

The normality of the parameters was assessed using the Anderson–Darling test, and descriptive statistics of the data were reported. All analyses were performed using the Minitab 17 statistical software package.

Results

A total of 411 participants aged 18–65 years were included in the study. The mean age of the participants was 38 years (range: 18–65). Descriptive statistics of the body composition parameters and BMI values of the participants are presented in Table 1.

Table 1 Descriptive Statistics of the Parameters

Parameters	Median (Min–Max)
Fat Mass Index (FMI)	15.165 (5.988-35.371)
Total Body Water (%)	39.900 (30.200-71.800)
Fat Mass (kg)	40.000 (16.900-86.900)
Fat-Free Mass (kg)	54.500 (41.200-98.100)
Body Fat Percentage (%)	42.303 (19.537-57.143)
Fat-Free Mass Percentage (%)	57.697 (42.067-80.463)
Body Mass Index (BMI)	36.208 (30.010-65.616)

The performance metrics obtained from the analyses conducted with PyCaret, including MAE, MSE, RMSE, R^2, RMSLE, MAPE, and TT-seconds, are presented in Table 2. Examination of Table 2 revealed that the highest R^2 values were achieved with the LiR, BRR, and RR models. These models yielded an R^2 of 0.9937, demonstrating very high accuracy in BMI prediction. They were followed by the Huber Regressor (0.9928) and LAR (0.9911). Among the models with lower performance, the K-Neighbors Regressor (0.8316) was noted.

Figure 1 presents the prediction error and residual plots obtained after hyperparameter optimization (tuning) for the best-performing models. Examination of Figure 1 shows that the plots indicate the models explained the majority of the variance and that the predictions exhibited a high degree of agreement with the actual values.

Figure 2 illustrates the importance of body composition parameters contributing most to the prediction performance of the models with the highest R^2 values. Examination of Figure 2 revealed that FMI was the most influential variable in BMI prediction.

Table 2 Performance Metrics of Machine Learning Regression Models

Models	MAE	MSE	RMSE	R2	RMSLE	MAPE	TT-seconds
Linear Regression	0.3630	0.2582	0.4877	0.9937	0.0121	0.0095	0.3330
Bayesian Ridge Regression	0.3633	0.2596	0.4882	0.9937	0.0122	0.0095	0.0100
Ridge Regression	0.3634	0.2604	0.4881	0.9937	0.0122	0.0095	0.0110
Huber Regressor	0.3575	0.2950	0.5193	0.9928	0.0127	0.0092	0.0120
Least Angle Regression	0.3855	0.3539	0.5580	0.9911	0.0137	0.0100	0.0110
Extra Trees Regressor	0.7869	1.4198	1.1697	0.9633	0.0279	0.0201	0.0440
Elastic Net	0.9675	1.4658	1.2000	0.9616	0.0310	0.0258	0.0100
Gradient Boosting Regressor	0.9100	1.5680	1.2143	0.9602	0.0288	0.0233	0.0270
Lasso Regression	1.0381	1.6867	1.2883	0.9557	0.0334	0.0278	0.2950
Lasso Least Angle Regression	1.0386	1.6884	1.2889	0.9557	0.0334	0.0278	0.0120
Passive Aggressive Regressor	1.0597	1.7959	1.3167	0.9512	0.0335	0.0280	0.0110
Random Forest Regressor	1.0656	2.2939	1.4728	0.9414	0.0346	0.0268	0.0530
Light Gradient Boosting Machine	1.2405	3.5113	1.8254	0.9118	0.0400	0.0303	0.0500
Decision Tree Regressor	1.3203	3.5875	1.8423	0.9116	0.0431	0.0334	0.0110
AdaBoost Regressor	1.5018	3.6011	1.8650	0.9068	0.0463	0.0395	0.0220
K-Neighbors Regressor	2.0024	6.2883	2.4632	0.8316	0.0607	0.0521	0.0120

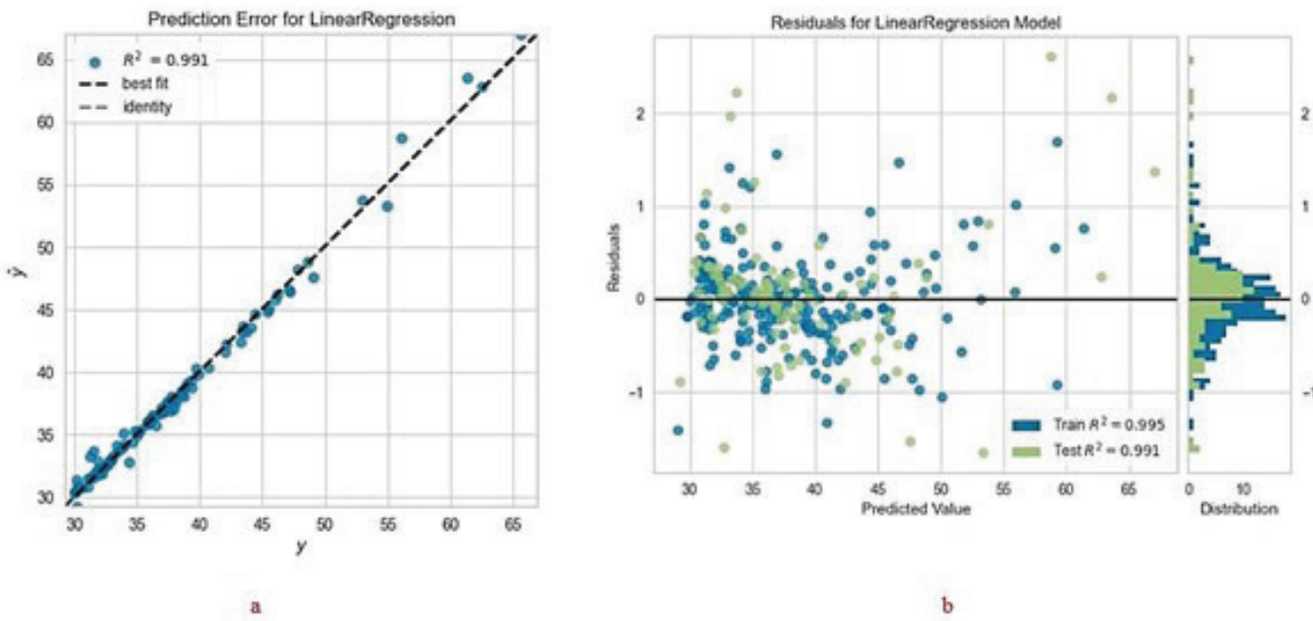

Figure 1 – Plots of the Best-Performing Models (a: Prediction Error, b: Residuals Plot)

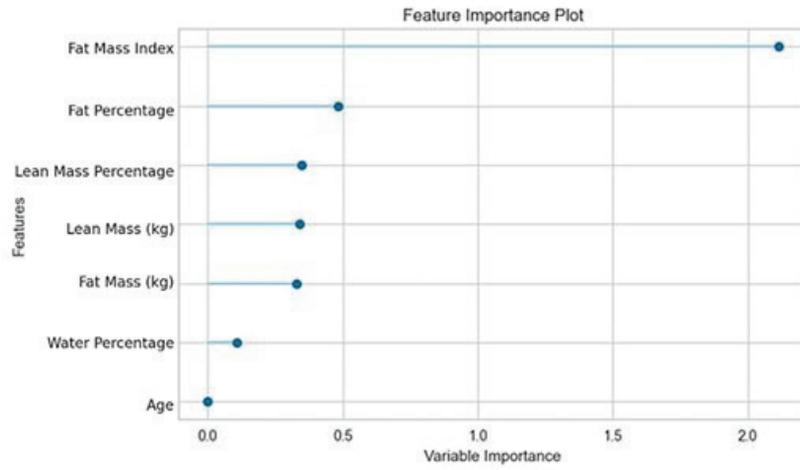

Figure 2 – Importance Plot of Key Parameters

Discussion

In this study, the point prediction of BMI was examined using ML-based regression models derived from body composition parameters obtained through the BIA method. The analyses demonstrated that the LiR, BRR, and RR models achieved the highest accuracy rates, indicating that BMI could be reliably predicted within the given mathematical framework. Notably, the strong performance of linear-based regression models suggests that the relationship between BMI and body composition parameters is predominantly linear and biologically meaningful. This finding provides conceptual insight, indicating that complex non-linear machine learning architectures may not be necessary when clinically relevant body composition predictors are used. These findings suggest that ML methods may provide complementary and supportive insights alongside traditional approaches in the assessment and monitoring of obesity. It should be emphasized that the purpose of the regression analysis applied in this study is not to replicate the BMI formula, but to evaluate the contribution of the parameters used, including those directly related to fat mass index (FMI) and fat-free mass index (FFMI) derived from body weight. Therefore, SHAP analysis was incorporated to enhance model interpretability by demonstrating the relative contribution of each parameter to the model predictions.

The results further revealed that FMI was the most influential parameter in BMI prediction. This result supports the view that BMI fundamentally reflects fat mass–related characteristics rather than overall body weight alone, reinforcing the clinical importance of integrating fat-based indices into obesity assessment. This finding highlights the central role of fat mass in the evaluation of obesity and underscores its importance in personalized healthcare approaches. Indeed, the literature emphasizes the strong association between body fat mass, body fat percentage and metabolic health, particularly with respect to insulin resistance, lipid profiles, and cardiometabolic risk factors [1, 22]. Moreover, FMI has been shown to be clinically valuable not only in obesity classification but also in identifying "metabolically obese but normal-weight" individuals [22]. These results demonstrate that body composition parameters may provide more accurate classifications in clinical decision-making processes than conventional BMI measurements.

Recent studies in the literature also support the potential of ML approaches to contribute multidimensionally to obesity assessment. Delnevo et al. examined BMI prediction using psychological indicators and demonstrated that the presence of depression significantly influenced the predictions, emphasizing the importance of considering psychosocial variables in obesity evaluation [23]. In a study by La Cruz et al., 24 different anthropometric measures were used to classify individuals according to body fat percentage through support vector machines, yielding high accuracy and sensitivity values; however, the limited specificity highlighted the likelihood of false positives [24]. Similarly, Genç & Arıcan incorporated demographic variables in addition to conventional BMI components for BMI classification and reported that the random forest algorithm achieved the highest performance [25]. Chen et al., integrated clinical and lifestyle data in childhood obesity and demonstrated that ML methods could capture the multifactorial nature of the condition, providing applicable tools for clinical decision-support systems [26]. Collectively, these studies indicate that ML models can operate effectively with diverse data types and hold broad potential in obesity evaluation.

Evidence also suggests that body composition data can be utilized to predict the success of treatment protocols [27, 28]. Nevertheless, the literature also shows that the relationship between ML-derived clinical predictions and BMI remains highly complex. Therefore, future studies should aim to integrate psychological, demographic, and lifestyle variables alongside body composition parameters to model BMI in a more accurate and clinically meaningful way. The originality of this study lies in the systematic comparison of different ML regression methods for point prediction of BMI using exclusively body composition parameters obtained through BIA. Rather than representing a purely technical machine learning application, this approach contributes to a clearer scientific understanding of how BMI relates to its underlying body composition determinants, thereby strengthening the conceptual and clinical relevance of BMI-based evaluations. By demonstrating the predictive performance of these regression models, the study provides concrete evidence of their applicability in clinical prediction and proposes a practical approach to overcoming the limitations of conventional BMI calculations. Furthermore, the potential integration of these ML models into routine clinical practice should be considered, highlighting how they may support personalized decision-making in obesity management. In this respect, the research offers methodological innovation to the literature and provides practical contributions to clinical practice.

Limitations and Future Directions

This study has several limitations. Despite the high accuracy observed, the potential risk of overfitting and the limited generalizability of our findings to other populations should be considered. First, the analyses were restricted to body composition parameters obtained solely through BIA; incorporating additional anthropometric, biochemical, and psychosocial variables could potentially improve prediction accuracy. Moreover, the sample size and demographic characteristics may limit the generalizability of the findings. Study limitations include the fact that the research was conducted in a single population at a single center, and non-BMI variables such as biochemical, demographic, and lifestyle factors were not included. Therefore, future research should consider conducting similar analyses with larger and more diverse samples, encompassing different age groups, sexes, and ethnic backgrounds.

In addition, adopting longitudinal study designs would allow the monitoring of BMI changes over time and provide an opportunity to evaluate the long-term predictive power of the models. Finally, future studies should not only focus on the statistical accuracy of ML models but also address their clinical applicability, interpretability, and usability by healthcare professionals, which should be among the primary objectives of forthcoming research.

Conclusion

In this study, point prediction of BMI was performed using ML-based regression models with body composition parameters obtained through BIA (fat mass, body fat percentage, fat-free mass, fat-free mass percentage, FMI, total body water (% of body water), and BMI). The LiR, BRR, and RR algorithms achieved the highest R^2 values, providing accurate BMI predictions and explaining a large proportion of variance. Moreover, FMI was identified as the most influential predictor. The strong performance of linear-based regression models suggests that the relationship between BMI and its underlying body composition determinants is largely linear and biologically interpretable. This finding provides conceptual insight rather than a purely technical outcome, emphasizing the scientific relevance of body composition–based BMI modeling.

These findings indicate that, independent of conventional BMI calculation, ML-based models can show promising predictive performance from body composition data, offering a practical and efficient tool for obesity assessment, and may contribute to the future development of AI-assisted personalized healthcare applications. In this respect, the study highlights the importance of interpreting BMI in conjunction with body composition parameters rather than as an isolated anthropometric index.

Future studies should address the limitations identified in the present work by incorporating non-BMI variables, such as biochemical, demographic, and lifestyle factors, and by conducting analyses across different centers and diverse populations. Such efforts will enhance the clinical applicability, generalizability, and robustness of ML-based BMI prediction models. By focusing on both predictive performance and interpretability, the present study contributes to a more clinically meaningful and scientifically grounded use of machine learning in obesity research.

Author Contributions: Conceptualization, S. S. M., Y. S.; methodology / planning and organization, Y. S., S. S. M.; funding acquisition, S. S. M.; writing – original draft preparation, S. S. M., T. G. U., T. T. D., B. C., S. D.; materials, S. S. M., Y. S., T. G. U., T. T. D.; data collection, S. S. M., Y. S., T. G. U., T. T. D., B. C., S. D.; data analysis and statistics, Y. S. All authors have read and approved the final version of the manuscript.

Disclosures: The authors have no conflicts of interest.

Acknowledgments: None.

Funding: None.

Data availability statement: The corresponding author can provide the data supporting the study's conclusions upon request. Due to ethical and privacy constraints, the data are not publicly accessible.

Artificial Intelligence (AI) Disclosure Statement: The authors declare no AI Tools used for preparation of this work.

References

1. Blüher M. Metabolically healthy obesity. *Endocr Rev*. 2020;41(3):bnaa004. https://doi.org/10.1210/endrev/bnaa004. PMID: 32128581; PMCID: PMC7098708.
2. Jeong SM, Lee DH, Rezende LFM, Giovannucci EL. Different correlation of body mass index with body fatness and obesity-related biomarker according to age, sex and race-ethnicity. *Sci Rep.* 2023;13(1):3472. https://doi.org/10.1038/s41598-023-30527-w. PMID: 36859451; PMCID: PMC9977890.
3. Pray R, Riskin S. The history and faults of the body mass index and where to look next: a literature review. *Cureus*. 2023 Nov 3;15(11):e48230. https://doi.org/10.7759/cureus.48230. PMID: 38050494; PMCID: PMC10693914.
4. Gómez-Ambrosi J, Silva C, Galofré JC, Escalada J, Santos S, Alcaraz-Millán D, Vila N, Ibáñez Ibáñez P, Cancho Gil MJ, Valentí V, Rotellar F, Ramírez B, Salvador J, Frühbeck G. Body mass index classification misses subjects with increased cardiometabolic risk factors related to elevated adiposity. *Int J Obes (Lond)*. 2011;36(2):286–294. https://doi.org/10.1038/ijo.2011.100.
5. Wu Y, Li D, Vermund SH. Advantages and limitations of the body mass index (BMI) to assess adult obesity. Int J Environ Res Public Health. 2024;21(6):757. https://doi.org/10.3390/ijerph21060757.
6. Son JW, Han BD, Bennett JP, Heymsfield S, Lim S. Development and clinical application of bioelectrical impedance analysis method for body composition assessment. *Obes Rev.* 2025;26(1):e13844. https://doi.org/10.1111/obr.13844.
7. Guo Y, Zhang M, Ye T, Wang Z, Yao Y. Application of bioelectrical impedance analysis in nutritional management of patients with chronic kidney disease. *Nutrients*. 2023;15(18):3941. https://doi.org/10.3390/nu15183941.

8. Böhm A, Heitmann BL. The use of bioelectrical impedance analysis for body composition in epidemiological studies. *Eur J Clin Nutr.* 2013;67(Suppl 1):S79–85. https://doi.org/10.1038/ejcn.2012.168. PMID: 23299875.
9. Kobayashi J, Murano S, Kawamura I, Nakamura F, Murase Y, Kawashiri MA, Nohara A, Asano A, Inazu A, Mabuchi H. The relationship of percent body fat by bioelectrical impedance analysis with blood pressure, and glucose and lipid parameters. *J Atheroscler Thromb.* 2006;13(5):221–6. https://doi.org/10.5551/jat.13.221. PMID: 17146149.
10. Nath T, Ahima RS, Santhanam P. Body fat predicts exercise capacity in persons with type 2 diabetes mellitus: a machine learning approach. *PLoS One.* 2021;16(3):e0248039. https://doi.org/10.1371/journal.pone.0248039.
11. DeGregory KW, Kuiper P, DeSilvio T, Pleuss JD, Miller R, Roginski JW, Fisher CB, Harness D, Viswanath S, Heymsfield SB, Dungan I, Thomas DM. A review of machine learning in obesity. *Obes Rev.* 2018;19(5):668–685. https://doi.org/10.1111/obr.12667. PMID: 29426065; PMCID: PMC8176949.
12. Mohammed A. Predicting heart disease with body composition using a hybrid machine learning approach. *Res Sq*. 2025;July:rs-7041567/v1. https://doi.org/10.21203/rs.3.rs-7041567/v1.
13. Yıldız NT, Kocaman H, Yıldırım H, Canlı M. An investigation of machine learning algorithms for prediction of temporomandibular disorders by using clinical parameters. *Medicine*. 2024;103(41):e39912. https://doi.org/10.1097/MD.0000000000039912.
14. Yetiş M, Kocaman H, Canlı M, Yıldırım H, Yetiş A, Ceylan İ. Carpal tunnel syndrome prediction with machine learning algorithms using anthropometric and strength-based measurement. PLoS One. 2024;19(4):e0300044. https://doi.org/10.1371/journal.pone.0300044.
15. James G, Witten D, Hastie T, Tibshirani R. An introduction to statistical learning: with applications in R. 2nd ed. *New York: Springer*; 2021. 607 s.
16. Bottigliengo D, Berchialla P, Lanera C, Azzolina D, Lorenzoni G, Martinato M, Giachino D, Baldi I, Gregori D. The role of genetic factors in characterizing extra-intestinal manifestations in Crohn's disease patients: are Bayesian machine learning methods improving outcome predictions? *J Clin Med.* 2019;8(6):865. https://doi.org/10.3390/jcm8060865. PMID: 31212952; PMCID: PMC6617350.
17. Hoerl AE, Kennard RW. Ridge regression: biased estimation for nonorthogonal problems. *Technometrics*. 1970;12:55–67. https://doi.org/10.1080/00401706.1970.10488634.
18. Tibshirani R. Regression shrinkage and selection via the Lasso. *J R Stat Soc Ser B Methodol.* 1996;58(1):267–288. https://doi.org/10.1111/j.2517-6161.1996.tb02080.x.
19. Zou H, Hastie T. Regularization and variable selection via the elastic net. *J R Stat Soc Ser B Stat Methodol.* 2005;67(2):301–320. https://doi.org/10.1111/j.1467-9868.2005.00503.x.
20. Huber PJ. Robust estimation of a location parameter. *Ann Math Stat.* 1964;35:73–101. https://doi.org/10.1214/aoms/1177703732.
21. Efron B, Hastie T, Johnstone I, Tibshirani R. Least angle regression. *Ann Stat.* 2004;32(2):407–499. https://doi.org/10.1214/009053604000000067.
22. Kim B, Taniguchi K, Isobe T, Oh S. Triglyceride-glucose index is capable of identifying metabolically obese, normal-weight older individuals. *J Physiol Anthropol.* 2024;22:22. https://doi.org/10.1186/s40101-024-00355-6.
23. Delnevo G, Mancini G, Roccetti M, Salomoni P, Trombini E, Andrei F. The prediction of body mass index from negative affectivity through machine learning: a confirmatory study. *Sensors*. 2021;21(7):2361. https://doi.org/10.3390/s21072361.
24. Lacruz ALA, Severeyn E, Huerta M, Wong S. Support vector machine technique as classifier of impaired body fat percentage. In: Tallón-Ballesteros AJ, editor. Fuzzy Systems and Data Mining VII. 2021:197–210. https://doi.org/10.3233/FAIA210188.
25. Genc AC, Arıcan E. Obesity classification: a comparative study of machine learning models excluding weight and height data. *Rev Assoc Med Bras* (1992). 2025;71(1):e20241282. https://doi.org/10.1590/1806-9282.20241282. PMID: 40105561; PMCID: PMC11918863.
26. Chen F, Melton PE, Vinsen K, Mori T, Beilin L, Huang R-C. Explainable AI to predict a complex multifactorial outcome, childhood obesity: application to clinical epidemiology. medRxiv. 2025. https://doi.org/10.1101/2025.06.21.25330041.
27. Khazanchi R, Bajaj A, Shah RM, Chen AR, Reyes SG, Kurapaty SS, Hsu WK, Patel AA, Divi SN. Using machine learning and deep learning algorithms to predict postoperative outcomes following anterior cervical discectomy and fusion. *Clin Spine Surg*. 2023;36(3):143–149. https://doi.org/10.1097/BSD.0000000000001443. PMID: 36920355.
28. Tahmassebi A, Wengert GJ, Helbich TH, Bago-Horvath Z, Alaei S, Bartsch R, Dubsky P, Baltzer P, Clauser P, Kapetas P, Morris EA, Meyer-Baese A, Pinker K. Impact of machine learning with multiparametric magnetic resonance imaging of the breast for early prediction of response to neoadjuvant chemotherapy and survival outcomes in breast cancer patients. *Invest Radiol.* 2019;54(2):110–117. https://doi.org/10.1097/RLI.0000000000000518. PMID: 30358693; PMCID: PMC6310100.

JOURNAL OF CLINICAL MEDICINE OF KAZAKHSTAN (E-ISSN 2313-1519)
Review Article DOI: https://doi.org/

Cytogenetic Characteristics and Treatment Outcomes of Congenital Acute Leukemia in Children in Kazakhstan: Retrospective Study

Saule Nukusheva[1,2], Almagul Saduova[1], Aman Berkinbay[1], Samal Aliyeva[1], Dana Zauytbek[1], Akerke Azanbai[1], Aygerim Ayazova[1], Araylim Abduali[1], Aiya Slamhan[1], Anel Daber[1]

[1]*JSC «Asfendiyarov Kazakh National Medical University», Almaty, Kazakhstan*
[2]*JSC Scientific Center of Pediatrics and Pediatric Surgery, Almaty, Kazakhstan*

Received: 2025-10-05.
Accepted: 2026-04-07

This work is licensed under a **Creative Commons Attribution 4.0 International License**

J Clin Med Kaz 2026; 23(2): 51-56

Corresponding author:
Aman Berkinbay.
E-mail: aman_98e@mail.ru.
ORCID: 0000-0002-3973-7283.

ABSTRACT

Background: Congenital acute leukemia (CAL) is a rare and aggressive hematologic malignancy diagnosed within the first 28 days of life. Cytogenetic abnormalities are essential for risk stratification and prognosis, but data on CAL in Kazakhstan remain limited.

Objective: To describe cytogenetic characteristics and evaluate their association with treatment outcomes in children with congenital and early infant acute leukemia treated at a tertiary pediatric center in Kazakhstan.

Methods: This retrospective single-center study included 33 children treated between 2018 and 2023 at the Scientific Center of Pediatrics and Pediatric Surgery (Almaty, Kazakhstan). Patients were classified as true CAL (diagnosis ≤28 days) or early infant leukemia (>28 days). Cytogenetic findings, treatment protocols, remission, relapse, mortality, treatment-related toxicity, and survival were analyzed. Overall survival (OS) and event-free survival (EFS) were assessed using the Kaplan–Meier method.

Results: Cytogenetic abnormalities were detected in 17/33 patients (51.5%). Favorable abnormalities included t(12;21), t(8;21), and inv(16), whereas unfavorable abnormalities included t(4;11)/KMT2A-rearranged leukemia and t(9;22). Complete remission after induction was achieved in 66.7% of patients and was significantly more frequent in the favorable cytogenetic group than in the unfavorable group (91.6% vs. 58.3%; p = 0.019). Treatment-related toxicity occurred in 42.4% of patients and was more common among those with non-complete remission (83.3% vs. 31.8%; p = 0.017). Estimated 2-year OS was 83.3% in the favorable cytogenetic group and 50.0% in the unfavorable group, while estimated 2-year EFS was 75.0% and 41.7%, respectively. Survival differed significantly according to cytogenetic risk (log-rank p = 0.032 for OS; p = 0.021 for EFS).

Conclusion: Congenital and early infant acute leukemia in this single-center cohort from Kazakhstan demonstrated substantial cytogenetic heterogeneity associated with remission and survival outcomes. Cytogenetic-based risk stratification and careful management of treatment-related toxicity may improve outcomes in this vulnerable patient population.

Keywords: congenital acute leukemia, infant leukemia, cytogenetics, KMT2A, risk stratification, chemotherapy, pediatric hematology-oncology, Kazakhstan.

Introduction

Congenital acute leukemia (CAL) is a rare hematologic malignancy that is classically defined as leukemia diagnosed within the first 28 days of life. It is considered one of the most aggressive forms of pediatric leukemia and is frequently associated with an unfavorable clinical course and high early mortality [1-3]. Accumulating evidence suggests that many cases of CAL and leukemias presenting shortly after the neonatal period originate prenatally, driven by early chromosomal and molecular events occurring in utero [3].

CAL accounts for less than 1% of all childhood leukemias and is most commonly represented by acute myeloid leukemia (AML), although acute lymphoblastic leukemia (ALL) is also observed in a substantial proportion of cases [2,3]. Due to its rarity, available epidemiological estimates are largely derived from regional population-based observations and case series. Reported incidence figures, such as approximately 4.7 cases per million live births, should therefore be interpreted within their specific geographic and temporal context rather than as global incidence rates [2, 4].

Population-based registry data from Kazakhstan indicate a persistent burden of pediatric hematological malignancies. According to national data collected between 2014 and 2021, the incidence of acute lymphoblastic leukemia exceeded that of acute myeloid leukemia, highlighting the relevance of leukemia as a major oncologic problem in childhood [5]. However, CAL represents only a very small fraction of these cases and remains insufficiently characterized at the national level, particularly with respect to cytogenetic features and treatment outcomes.

The diagnosis of congenital acute leukemia is based on integrated clinical, morphological, immunophenotypic, and cytogenetic assessment, with molecular abnormalities playing a key prognostic role [1–3].

Cytogenetic abnormalities play a central role in the biology and prognosis of CAL. Rearrangements involving the KMT2A (MLL) gene are particularly common in neonatal and infant leukemias and are consistently associated with aggressive disease behavior and inferior outcomes. In contrast, certain chromosomal abnormalities, such as t(12;21) in ALL or t(8;21) and inv(16) in AML, are considered favorable prognostic markers in pediatric leukemia, although their significance in congenital cases remains incompletely defined [1–3].

Special consideration is required in neonates with Down syndrome, who are predisposed to myeloid disorders, including transient abnormal myelopoiesis (TAM/TMD) and acute leukemia. Careful differentiation between these entities is essential, as TAM/TMD often follows a self-limited course and does not require intensive chemotherapy, unlike true congenital leukemia [6].

Despite advances in molecular diagnostics and the implementation of international treatment protocols, CAL remains a therapeutic challenge due to the vulnerability of neonates and young infants to intensive chemotherapy and treatment-related toxicity. Therefore, optimization of therapeutic strategies and prognostic outcomes through precise cytogenetic and molecular risk stratification is of particular importance in this patient population [1–3].

Objective: to describe cytogenetic characteristics and evaluate their association with treatment outcomes in children with congenital and early infant acute leukemia treated at a tertiary pediatric center in Kazakhstan.

Methods

Study design and setting

A retrospective single-center cohort study was conducted at the Department of Oncohematology of the Scientific Center of Pediatrics and Pediatric Surgery (Almaty, Republic of Kazakhstan). Medical records of children diagnosed with acute leukemia and treated between January 2018 and December 2023 were reviewed.

Study population

The study included 33 children diagnosed with acute leukemia during the neonatal and early infant period. For descriptive and analytical purposes, patients were categorized according to the timing of diagnosis as: True congenital acute leukemia (CAL) — diagnosis established within the first 28 days of life; Early infant acute leukemia — diagnosis established after 28 days of life, but within the first months of infancy, with clinical and cytogenetic features suggestive of prenatal disease origin.

This classification was applied to ensure terminological accuracy and to minimize biological misclassification.

Inclusion criteria were: age at diagnosis 0–3 months; confirmed diagnosis of acute myeloid leukemia (AML) or acute lymphoblastic leukemia (ALL) based on morphological and immunophenotypic evaluation; availability of baseline cytogenetic and/or molecular genetic data obtained at initial diagnosis; completion of induction chemotherapy at the study center.

Exclusion criteria were: absence of cytogenetic or molecular data at diagnosis; interruption or non-completion of induction therapy for non-medical reasons; presence of malignant diseases other than acute leukemia; transient abnormal myelopoiesis / transient myeloproliferative disorder (TAM/TMD) associated with Down syndrome, defined by spontaneous resolution without standard leukemia-directed chemotherapy.

Diagnostic evaluation

All patients underwent standardized diagnostic assessment, including: complete blood count with differential; bone marrow aspiration with morphological examination; immunophenotyping by flow cytometry using lineage-specific monoclonal antibodies; cytogenetic analysis using conventional karyotyping and fluorescence in situ hybridization (FISH), with targeted assessment of recurrent chromosomal rearrangements relevant to pediatric AML and ALL.

Leukemia subtypes were classified according to immunophenotypic and cytogenetic criteria in accordance with internationally accepted pediatric hematology standards.

Treatment protocols

Treatment was administered according to national clinical protocols of the Ministry of Health of the Republic of Kazakhstan and internationally adopted pediatric regimens implemented at the study center.

All patients met the study inclusion criterion of age 0–3 months; therefore, infant-specific regimens were used for ALL/infant leukemia, including INTERFANT-06 and MLL-Baby–based protocols, adapted to immunophenotypic and cytogenetic risk. AML cases received AML-BFM–based therapy with age-adjusted dosing.

Protocols designed for older children (e.g., AIEOP BFM ALL 2009) or relapse regimens (e.g., ALL REZ BFM 2002/2004) were not used in the study cohort, and therefore are not reported as treatment regimens in this analysis.

One patient underwent haploidentical hematopoietic stem cell transplantation; this case is reported descriptively and was not included in outcome comparisons.

Outcome measures

Complete remission was defined as bone marrow M1 status (<5% blasts) with no evidence of extramedullary disease at the end of induction therapy: day 33 for ALL/infant leukemia protocols and day 28 for AML protocols. Patients who died during induction therapy were classified as induction deaths and analyzed as non-complete remission (non-CR) to avoid survivor bias.

Additional primary outcomes included non-complete remission after induction (non-CR), relapse, and death.

Secondary outcomes included the frequency and structure of treatment-related toxicity/adverse events, classified according to clinical severity, and their association with unfavorable outcomes (relapse or death).

Statistical analysis

Statistical analysis was performed using Microsoft Office Excel and IBM SPSS Statistics v.25.0. Quantitative variables were expressed as mean ± standard deviation (M ± SD) or as median with interquartile range (Me [Q1; Q3]) in cases of non-normal distribution. Normality was assessed using the Shapiro–Wilk test.

Comparisons between groups were conducted using the Student's t-test for normally distributed data or the Mann–Whitney U test for non-parametric data. Categorical variables were analyzed using the chi-square (χ^2) test or Fisher's exact test, as appropriate.

To evaluate associations between treatment-related toxicity and adverse outcomes, odds ratios (ORs) with 95% confidence intervals (CI) were calculated. A p-value < 0.05 was considered statistically significant. Survival analysis was additionally performed using the Kaplan–Meier method. Overall survival (OS) was defined as the time from diagnosis to death from any cause or last follow-up. Event-free survival (EFS) was defined as the time from diagnosis to the first adverse event, including induction failure (non-CR at the end of induction), relapse, death, or last follow-up. Patients without an event were censored at the date of last contact. Survival curves were compared using the log-rank test. A separate Kaplan–Meier analysis was performed for patients with favorable versus unfavorable cytogenetic abnormalities.

Ethical considerations

The study protocol was reviewed and approved by the Local Ethics Committee of the Scientific Center of Pediatrics and Pediatric Surgery (Approval № 4, dated September 2, 2025). Written informed consent for diagnostic and therapeutic procedures was obtained from the parents or legal guardians of all patients. The study was conducted in accordance with the principles of the Declaration of Helsinki.

Results

A total of 33 patients diagnosed with acute leukemia were included in the study. The mean age at diagnosis was 2.13 ± 0.41 months. The earliest diagnosis was made on the 6th day of life, while the latest occurred at 2.4 months of age. Of the 33 patients included, 20 (60.6%) were diagnosed within the first 28 days of life and therefore met the strict definition of congenital acute leukemia; the remaining patients were classified as early infant leukemia because of their similar biological and cytogenetic characteristics.

Among the enrolled patients, 20 (60.6%) were male and 13 (39.4%) were female, resulting in a male-to-female ratio of 1.5:1, indicating a slight predominance among males (60.6% vs. 39.4%; $\chi^2 = 2.45$; p = 0.118).

The duration of symptoms before hospitalization was short in most patients, consistent with the rapid onset of leukemia during the neonatal and early infant period.

The morphological classification of leukemia is presented in Table 1. The most frequent subtype was acute myeloid leukemia (AML), observed in 18 patients (54.5%). Acute lymphoblastic leukemia (ALL) was diagnosed in 14 patients (42.4%), while 1 case (3.0%) was classified as acute leukemia of unspecified lineage, due to atypical presentation and insufficient morphological verification (Table 1).

The mean age of patients with AML was 2.36 ± 0.42 months, whereas in ALL it was 1.91 ± 0.38 months (p = 0.042), representing a 23.6% difference between the groups (Table 1).

Table 1 Distribution of patients by morphological type of acute leukemia

Morphological type	Number (n)	Proportion (%)	Mean age (months)
Acute myeloid leukemia (AML)	18	54.5%	2.36 ± 0.42
Acute lymphoblastic leukemia (ALL)	14	42.4%	1.91 ± 0.38
Leukemia of unspecified type	1	3.0%	–
Total	33	100%	–

Perinatal and maternal history parameters were collected descriptively and are therefore not presented in detail, as no associations with cytogenetic findings or clinical outcomes were identified.

Clinical presentation at diagnosis was characterized by systemic and hematologic manifestations typical for neonatal and early infant acute leukemia.

Clinical presentation was characterized predominantly by weakness, lethargy, and fever. Hyperplastic manifestations, including peripheral lymphadenopathy, were observed in 8 patients (24.2%), while hemorrhagic manifestations such as petechiae, ecchymoses, and bleeding at injection sites were present in 8 patients (24.2%). Anemic syndrome remained the most frequent clinical syndrome overall (57.6%).

In this study, "intoxication syndrome" refers to disease-related systemic manifestations at presentation and should not be interpreted as a treatment-related adverse event (Table 2).

Table 2 Frequency of major clinical symptoms and syndromes in patients with congenital acute leukemia (n = 33)

Parameter	Manifestation	n (%)
Symptoms	Weakness, lethargy, fatigue	18 (54.5%)
	Fever (up to 39 °C)	13 (39.4%)
	Decreased appetite	8 (24.2%)
	Weight loss	5 (15.2%)
Syndromes	Anemic	19 (57.6%)
	Intoxication	11 (33.3%)
	Hyperplastic	8 (24.2%)
	Hemorrhagic	8 (24.2%)

Table 3 Changes in hematological, biochemical, coagulation, bone marrow, and cerebrospinal fluid parameters before and after induction therapy in children with congenital and early infant acute leukemia

Parameter	Baseline (before induction)	Post-induction assessment	Δ	p-value
Leukocytes (×10^9/L)	21.0 ± 5.2	9.6 ± 3.8	−11.4	0.0004
Hemoglobin (g/L)	89.4 ± 12.3	113.4 ± 10.7	+24.0	0.0002
Platelets (×10^9/L)	55.7 ± 17.0	176.2 ± 34.5	+120.5	0.0001
Peripheral blood blasts (%)	51.7 ± 10.8	1.8 ± 1.1	−49.9	0.00005
LDH (U/L)	721.0 ± 128.5	314.6 ± 87.2	−406.4	<0.001
ALT (U/L)	43.5 ± 8.6	32.4 ± 6.9	−11.1	0.008
AST (U/L)	46.4 ± 9.1	34.1 ± 7.5	−12.3	0.009
Creatinine (μmol/L)	78.9 ± 10.4	76.2 ± 9.7	−2.7	0.087
Total protein (g/L)	67.1 ± 5.1	69.5 ± 4.8	+2.4	0.043
Albumin (g/L)	36.1 ± 4.0	38.2 ± 3.6	+2.1	0.038
Prothrombin index (%)	75.7 ± 6.3	89.3 ± 5.7	+13.6	<0.001
INR	1.4 ± 0.2	1.1 ± 0.1	−0.3	<0.001
Fibrinogen (g/L)	4.6 ± 1.1	3.2 ± 0.9	−1.4	<0.001
D-dimer (ng/mL)	972.2 ± 214.4	423.5 ± 132.1	−548.7	0.0001
Bone marrow blasts (%)	67.6 ± 9.7	2.4 ± 1.2	−65.2	0.00003
Mature neutrophils in myelogram (%)	8.5 ± 3.1	48.6 ± 7.4	+40.1	0.00001
CSF cell count (cells/μL)	12.9 ± 4.6	4.3 ± 1.8	−8.6	0.0046
CSF protein (g/L)	0.40 ± 0.10	0.28 ± 0.07	−0.12	0.015
CSF glucose (mmol/L)	2.8 ± 0.6	3.4 ± 0.5	+0.6	0.042

Bone marrow response was assessed at the end of induction therapy (day 33 for ALL/infant leukemia and day 28 for AML). Hematological, biochemical, coagulation, and cerebrospinal fluid parameters were evaluated at baseline and at the post-induction inpatient assessment.

Significant improvements were observed in hematological, biochemical, coagulation, bone marrow, and cerebrospinal fluid parameters after induction therapy. Leukocyte count and blast percentage decreased significantly, whereas hemoglobin and platelet levels increased. Bone marrow blast infiltration markedly declined, together with improvement in coagulation and CSF indices, indicating an effective response to induction therapy (Table 3).

Immunophenotyping in patients with congenital acute leukemia (CAL) revealed the expression of antigens characteristic of both lymphoblastic and myeloid variants of the disease. The expression of CD34, a marker of early hematopoietic progenitors, averaged 16.8 ± 4.2%. The HLA-DR antigen was detected in 90.5% of cases, indicating a high degree of cellular activation.

Among B-cell markers, the most frequently expressed antigens were CD19 (58.3%), CD10 (45.7%), and terminal deoxynucleotidyl transferase (TdT, 41.2%), consistent with a pre-B lymphoblastic phenotype. In parallel, the myeloid antigens CD13 and CD33 were expressed in 52.8% and 50.1% of cases, respectively, while myeloperoxidase (MPO) was positive in 35.4% of patients, suggesting evidence of myeloid differentiation. These findings confirm the immunologic heterogeneity of leukemic cells ($p < 0.01$).

Cytogenetic analysis identified six major types of chromosomal rearrangements. The t(12;21)(p13;q22) (ETV6–RUNX1) translocation, associated with a favorable prognosis in ALL, was detected in 4 patients (12.1%). An equal number of patients (4; 12.1%) carried t(4;11)(q21;q23) involving KMT2A (MLL) gene rearrangement, typically seen in infant leukemia with an aggressive clinical course ($p = 0.014$ when comparing favorable vs. unfavorable groups).

The t(9;22)(q34;q11) (BCR–ABL1) translocation was identified in 3 patients (9.1%), predominantly in B-cell ALL, and was regarded as an adverse prognostic marker. Two patients (6.1%) had t(8;21)(q22;q22) (RUNX1–RUNX1T1), characteristic of AML (FAB M2 subtype), associated with a favorable outcome. Another two patients (6.1%) carried t(15;17)(q22;q12) (PML–RARA), corresponding to acute promyelocytic leukemia morphology. Similarly, inv(16)(p13;q22) (CBFB–MYH11) was detected in two patients (6.1%), typical for the M4Eo subtype, also classified as favorable ($p = 0.021$ compared with unfavorable translocations).

In total, cytogenetic abnormalities were identified in 17 of 33 patients (51.5%), including 4 (12.1%) with MLL rearrangements, confirming a high frequency of unfavorable chromosomal alterations in congenital leukemia, consistent with findings reported in international studies.

In the cohort of 33 children with congenital and early infant acute leukemia, treatment was administered using intensive polychemotherapy regimens tailored to immunophenotypic and cytogenetic risk. Induction therapy was delivered using infant-specific ALL protocols (INTERFANT-06 and MLL-Baby–based therapy) for ALL/infant leukemia and AML-BFM–based regimens for AML with age-adjusted dosing. Patients with transient abnormal myelopoiesis or transient myeloproliferative disorder associated with Down syndrome were excluded from the study cohort. Therefore, all treatment outcomes reported in this analysis refer only to patients with confirmed acute leukemia requiring leukemia-directed therapy.

Table 4 Treatment outcomes in children with congenital and early infant acute leukemia (n = 33)

Outcome category	Number of patients (n)	Frequency (%)
Complete remission (CR)	22	66.7
Non-complete remission after induction (non-CR)	6	18.2
Relapse (total)	3	9.1
• Extramedullary relapse	2	6.1
• Bone marrow relapse	1	3.0
Death	2	6.1
Adverse outcome (relapse or death)	5	15.1

**Complete remission (CR) was defined as bone marrow M1 status (<5% blasts) with no evidence of extramedullary disease at the end of induction therapy (day 33 for ALL/infant leukemia and day 28 for AML).*

Complete remission after induction therapy was achieved in 22 patients (66.7%), whereas 6 patients (18.2%) had non-complete remission. Relapse occurred in 3 patients (9.1%), including two extramedullary relapses (central nervous system and testicular) and one bone marrow relapse. Death was recorded in 2 cases (6.1%)—one due to multiple organ failure and one in the setting of refractory disease. Overall, unfavorable outcomes, defined as relapse or death, occurred in 5 patients (15.1%). A statistically significant difference in outcomes was observed between patients who achieved complete remission and those with non-complete remission after induction therapy ($p = 0.0047$).

The remission rate among patients with a favorable cytogenetic profile (t(12;21), inv(16), t(8;21)) was 91.6%, compared with 58.3% in those with unfavorable chromosomal rearrangements (t(4;11), t(9;22), MLL+) (p = 0.019), underscoring the prognostic importance of the molecular–genetic profile.

Treatment-related toxicity (adverse events) was recorded in 14 patients (42.4%). The most frequent adverse events were myelotoxic aplasia (27.3%), febrile neutropenia (24.2%), toxic enteropathy (21.2%), mucositis (18.2%), toxic hepatitis (15.2%), and hemorrhagic syndrome (12.1%). The incidence of treatment-related toxicity was significantly higher in the non-complete remission after induction (non-CR) group (83.3%) compared with the complete remission group (31.8%; p = 0.017), indicating a possible association between toxicity severity and insufficient therapeutic response.

Supportive therapy was administered to all patients and included antibacterial and antifungal treatment (100%), blood transfusions (69.7%), correction of electrolyte disturbances (57.6%), detoxification and symptomatic therapy (75.8%), as well as passive immunization and granulopoiesis stimulation (36.4%).

To assess the prognostic impact of treatment-related toxicity, an odds ratio (OR) analysis was performed to evaluate the association between adverse events and the risk of unfavorable outcomes (relapse or death). Among the 14 patients who developed significant treatment-related toxicity, adverse outcomes occurred in 4 cases (28.6%). In the group without severe treatment-related toxicity (n = 19), only one unfavorable outcome (5.3%) was observed. The presence of treatment-related toxicity was associated with a trend toward an increased risk of adverse outcomes (OR = 7.20; 95% CI: 0.70–73.53; p = 0.0649).

Thus, congenital acute leukemia in children demonstrates a high sensitivity to induction polychemotherapy. The treatment effectiveness largely depends on molecular–cytogenetic characteristics and the degree of treatment-related toxicity. Achieving early remission, providing timely management of complications, and implementing risk-adapted therapeutic strategies are key to effective disease control in the majority of clinical cases ($p < 0.05$).

Kaplan–Meier survival analysis was performed to account for variable follow-up duration across the study period. Estimated 2-year overall survival (OS) was 83.3% in patients with favorable cytogenetic abnormalities versus 50.0% in those with unfavorable abnormalities. Estimated 2-year event-free survival (EFS) was 75.0% and 41.7%, respectively. Survival curves differed significantly between the groups (log-rank p = 0.032 for OS; p = 0.021 for EFS). Patients with unfavorable cytogenetic abnormalities had a higher risk of adverse events (HR = 3.48; 95% CI: 1.12–10.84).

Discussion

Cytogenetic profiling plays a pivotal role in risk stratification and prognosis of congenital and infant leukemias. Previous studies have consistently demonstrated a high prevalence of KMT2A (MLL) rearrangements in CAL, which are strongly associated with aggressive disease biology, chemoresistance, and inferior survival outcomes [2, 3]. Reported frequencies of MLL abnormalities in congenital leukemia range from 10% to 30%, depending on cohort composition and diagnostic criteria.

In our cohort, MLL rearrangements were identified in 12.1% of patients, which is comparable with international data. Importantly, patients with unfavorable cytogenetic profiles demonstrated significantly lower complete remission rates than those with favorable chromosomal abnormalities (58.3% vs. 91.6%, p = 0.019), confirming the prognostic relevance of cytogenetic stratification in congenital and early infant leukemia.

Complete remission after induction therapy was achieved in 66.7% of patients, whereas 18.2% had non-complete remission. Nevertheless, relapse remained a major clinical challenge and was documented in 9.1% of cases, including both bone marrow and extramedullary relapses. These findings are consistent with previously published infant leukemia studies, including INTERFANT and MLL-Baby cohorts, which have shown that an initial therapeutic response does not necessarily ensure sustained remission [2].

Treatment-related toxicity remains a critical limiting factor in the management of CAL due to the physiological immaturity of neonates and infants. Previous studies have reported high rates of severe adverse events, particularly myelosuppression, infectious complications, and organ toxicity, during induction chemotherapy [1, 3]. In the present study, treatment-related toxicity was observed in 42.4% of patients and was significantly more frequent among those who failed to achieve complete remission after induction (83.3% vs. 31.8%, p = 0.017). Although the odds ratio analysis did not reach statistical significance (OR = 7.20; p = 0.0649), the observed trend suggests a clinically relevant association between severe toxicity and unfavorable outcomes, consistent with findings from previous neonatal leukemia cohorts [1, 3].

Our findings should also be interpreted in the context of previously published reports in the Journal of Clinical Medicine of Kazakhstan. One report emphasized the prognostic relevance of high-risk biological and cytogenetic features in acute lymphoblastic leukemia, while another highlighted the critical importance of intensive supportive care in leukemia patients with severe infectious and multiorgan complications. Although these reports addressed different age groups and clinical settings, they support the central conclusion of our study that both cytogenetic risk profile and treatment-related complications substantially influence clinical outcomes in acute leukemia [7, 8].

Overall, our results emphasize that successful management of congenital acute leukemia depends on early diagnosis, accurate molecular–cytogenetic risk stratification, and careful balancing of treatment intensity with toxicity control. The implementation of risk-adapted protocols and improved supportive care remains essential to further improve survival outcomes in this highly vulnerable patient population.

What's known?

1. Congenital acute leukemia is a rare and aggressive malignancy, accounting for less than 1% of pediatric leukemias.
2. AML predominates over ALL in neonatal leukemia, and cytogenetic abnormalities, particularly KMT2A (MLL) rearrangements, are common and associated with poor prognosis.
3. Favorable cytogenetic abnormalities are generally associated with higher remission rates than unfavorable rearrangements.
4. Intensive polychemotherapy can achieve high remission rates, but treatment-related toxicity and relapse remain major challenges.

What's new?

1. This study represents one of the first single-center reports from Kazakhstan describing cytogenetic characteristics and treatment outcomes in children with congenital and early infant leukemia.

2. Treatment-related toxicity was markedly more frequent among patients with non-complete remission after induction.

3. The study demonstrates the clinical value of cytogenetic-based risk stratification in a real-world cohort from Kazakhstan.

Limitations

This study has several limitations: its retrospective design, a relatively small patient cohort (n = 33), and the lack of long-term follow-up and supportive therapy data. In addition, a comparative analysis with healthy neonates and older pediatric patients (>6 months) was not performed. These factors may limit the generalizability of the findings and highlight the need for validation in larger, multicenter cohorts.

This investigation represents one of the first single-center reports from Kazakhstan describing congenital acute leukemia in children. It provides valuable insights not only into the clinical and laboratory features and treatment outcomes, but also into key prognostic factors, contributing to the improvement of diagnostic accuracy and therapeutic management of this severe and rare pediatric malignancy.

Conclusion

Congenital acute leukemia (CAL) in children is characterized by early onset, marked clinico-cytogenetic heterogeneity, and variable disease progression. The implementation of risk-adapted chemotherapy based on the cytogenetic profile, together with systematic toxicity monitoring and timely management of complications, enables the achievement of remission in the majority of cases. Further large-scale studies with long-term follow-up are essential to refine prognostic models and to develop national clinical guidelines for the optimal management of this challenging patient population.

Author Contributions: Conceptualization, A. B., S. N., A. S., S. A.; methodology, A. B., S. N., A. S.; data curation, A. B., S. N., A. S.; writing – original draft preparation, A. B., S. N., A. S., S. A., D. Z., A. Az., A. Az., A. Ab., A. S., A. D.; writing – review and editing, A. B., S. N., A. S., S. A., D. Z., A. Az., A. Az., A. Ab., A. S., A. D. All authors have read and agreed to the published version of the manuscript.

Disclosures: The authors have no conflicts of interest.

Acknowledgments: None.

Funding: None.

Data availability statement: The corresponding author can provide the data supporting the study's conclusions upon request.

Artificial Intelligence (AI) Disclosure Statement: The authors declare no AI Tools used for preparation of this work.

References

1. Green K, Tandon S, Ahmed M, Toscano W, O'Connor D, Ancliff P, Vora A, Bartram J, Samarasinghe S, Ghorashian S, Pavasovic V, Rao A. Congenital acute myeloid leukemia: challenges and lessons. A 15-year experience from the UK. *Leuk Lymphoma.* 2021;62(3):688–695. https://doi.org/10.1080/10428194.2020.1845335
2. Yang CX, Yang Y, Zhang FL, Wang DH, Bian QH, Zhou M, Zhou MX, Yang XY. Congenital leukemia: a case report and review of literature. *World J Clin Cases.* 2023;11(29):7227–7233. https://doi.org/10.12998/wjcc.v11.i29.7227
3. Brown PA. Neonatal leukemia. *Clin Perinatol.* 2021;48(1):15–33. https://doi.org/10.1016/j.clp.2020.11.002
4. Tsujimoto H, Kounami S, Mitani Y, Watanabe T, Takifuji K. Neonatal acute megakaryoblastic leukemia presenting with leukemia cutis and multiple intracranial lesions successfully treated with unrelated cord blood transplantation. *Case Rep Hematol.* 2015;2015:610581. https://doi.org/10.1155/2015/610581
5. Mussina K, Kuanova B, Syssoyev D, Gaipov A, Poddighe D, Shaikhyzada K, Aimyshev T, Galiyeva D. Epidemiology of pediatric hematological malignancies in Kazakhstan: data from Unified National Electronic Healthcare System 2014–2021. *Eur J Pediatr.* 2024;183(4):1683–1691. https://doi.org/10.1007/s00431-023-05412-3
6. Yamato G, Park MJ, Sotomatsu M, Kaburagi T, Maruyama K, Kobayashi T, Nishi A, Sameshima K, Ohki K, Hayashi Y. Clinical features of 35 Down syndrome patients with transient abnormal myelopoiesis at a single institution. *Int J Hematol*. 2021;113(5):662–667. https://doi.org/10.1007/s12185-020-03066-7
7. Ekmen N, Can G, Sasani H. Acute lymphoid leukemia developing in the course of Crohn's disease: are there any guilty agents? *J Clin Med Kaz.* 2021;18(3):65-67. https://doi.org/10.23950/jcmk/10924
8. Bekniyazova A, Maidan A, Mishutin I, Bakhytzhan S, Yessenbayeva G. Combined use of inhaled and intravenous colistin in a patient with acute lymphoblastic leukemia complicated by multi-organ failure and sepsis: a case report. *J Clin Med Kaz*. 2025;22(3):93-97. https://doi.org/10.23950/jcmk/16366

JOURNAL OF CLINICAL MEDICINE OF KAZAKHSTAN (E-ISSN 2313-1519)
Original Article DOI: https://doi.org/10.23950/jcmk/18010

Multi-Biomarker Stratification of Coronary Artery Disease in Diabetic and Non-Diabetic Patients: Adiponectin, Inflammation, and Insulin Resistance

Leela Pattapu[1], Priya K. Dhas[2], K.P. Mekhala[3], Ponnudhali D[2], Chakrapani Cheekavolu[4]

[1]*PhD Program, Department of Biochemistry, Vinayaka Mission's Kirupananda Variyar Medical College, Vinayaka Mission's Research Foundation (Deemed to be University), Tamil Nadu, India*
[2]*Department of Biochemistry, Vinayaka Mission's Kirupananda Variyar Medical College, Vinayaka Mission's Research Foundation (Deemed to be University), Tamil Nadu, India*
[3]*Department of Biochemistry, Karpagam Faculty of Medical Science and Research, Coimbatore, Tamil Nadu, India*
[4]*Department of Pharmacology, Karpagam Faculty of Medical Science and Research, Coimbatore, Tamil Nadu, India*

Received: 2026-01-14.
Accepted: 2026-02-24.

This work is licensed under a **Creative Commons Attribution 4.0 International License**

J Clin Med Kaz 2026; 23(2): 57-63

Corresponding author:
Priya K. Dhas.
E-mail: priyakdhas79@gmail.com.
ORCID: 0000-0002-8900-4360.

ABSTRACT

Background: Coronary artery disease [CAD] remains a leading cause of global mortality, with higher prevalence among individuals with type 2 diabetes mellitus [T2DM]. Limited data exist on biomarker interactions in CAD patients with and without T2DM.

Objective: This study aimed to investigate correlations among adiponectin, inflammatory markers, and metabolic factors in CAD patients and evaluate their association with T2DM status.

Methods: A cross-sectional study enrolled 225 participants: 75 healthy controls, 75 CAD patients with T2DM, and 75 CAD patients without T2DM. Serum levels of adiponectin, hs-CRP, IL-6, E-selectin, insulin, and C-peptide were measured using ELISA. Lipid profiles were analyzed via automated analyzer. Statistical analysis included ANOVA, correlation analysis, multicollinearity assessment, regression, and ROC analysis.

Results: All biomarkers showed significant differences across groups [$p<0.05$]. Adiponectin levels were lowest in CAD with T2DM [4.2 ± 1.0 mg/L vs 7.4 ± 1.6 mg/L in controls, $p<0.001$]. Inflammatory markers were elevated in both CAD groups, with highest levels in diabetic patients. ROC analysis revealed moderate discriminative ability: adiponectin [AUC=0.79], hs-CRP [AUC=0.83], E-selectin [AUC=0.75], and insulin [AUC=0.72]. In the multivariable regression model, insulin emerged as the superior insulin-secretion marker over C-peptide, after accounting for multicollinearity and excluding participants with renal impairment.

Conclusion: This study demonstrates significant associations between reduced adiponectin, elevated inflammatory markers, and metabolic dysfunction in CAD patients, particularly those with T2DM. An adiponectin threshold of ≤5.0 mg/L may serve as a practical clinical alert for high cardiovascular risk in diabetic patients. These findings warrant further prospective investigation to determine their potential clinical utility. These findings warrant further prospective investigation to determine their potential clinical utility.

Keywords: adiponectin, biomarkers, coronary artery disease, hs-CRP, insulin resistance, type 2 diabetes mellitus.

Introduction

One of the leading causes of morbidity and death in the world today is coronary artery disease [CAD], which is defined by the accumulation of atherosclerotic plaques in the coronary arteries [1]. Other metabolic anomalies that, when combined with hereditary predisposition, cause the condition include dyslipidaemia, hypertension, obesity, and type 2 diabetic mellitus [T2DM] [2]. Lipoprotein deposition, endothelial activation, vascular smooth muscle cell proliferation, and persistent arterial wall inflammation are all intricately linked to atherosclerosis [3].

The identification of molecular biomarkers has helped to develop the knowledge on CAD and highlight the central roles of adipokines, pro-inflammatory cytokines, and endothelial markers in its pathophysiology. Adiponectin, a 30kDa compound released by adipocytes has proven to be the main controller of metabolic and cardiovascular homeostasis [4]. In contrast to other adipokines, adiponectin improves the work of endothelium, suppresses the growth of smooth-muscle-cells, reduces the vascular inflammation, and increases the insulin sensitivity [5]. Reduced levels of adiponectin in the circulation have been linked with increased risk of CAD especially in diabetic patients with T2DM and metabolic syndrome [6].

Inflammation is the primary cause of atherosclerosis and CAD. An independent predictor of unfavourable cardiovascular events is high sensitivity C-reactive protein [hs-CRP], which is generated by hepatic cells in response to pro-inflammatory cytokines such interleukin-6 [IL-6] [7]. Strong hs-CRP is linked to plaque instability, endothelial dysfunction, and artery stiffness [8]. In order to attract leukocytes to the sites of vascular damage, IL-6 stimulates acute-phase protein production and increases endothelial adhesion factors like E-selectin [9,10].

The phenomenon of insulin resistance, which is characteristic of T2DM, increases atherosclerosis due to hyperinsulinemia that contributes to vascular inflammation, dysfunction of endothelium, and proliferation of smooth-muscle-cells [11]. In addition, C-peptide, a product of insulin production can be also involved in pro-inflammatory signaling pathways that are activated during CAD development especially in insulin-resistant groups [12]. Although C-peptide is traditionally regarded as a more stable marker of endogenous insulin secretion owing to its longer half-life and absence of first-pass hepatic metabolism, its circulating levels are also influenced by renal clearance, which may introduce variability in populations with subclinical renal dysfunction. Dyslipidemia is a heart attack risk factor as it is an established risk factor of CAD [13].

The interaction between these metabolic and inflammatory biomarkers can provide information on how these biomarkers can be used in the early detection and risk stratification of CAD, particularly in diabetic groups. Adiponectin exhibits well-documented gender specificity, with higher concentrations in females, a pattern that may be further modulated by sex steroid levels and menopausal status, particularly in the 30–50-year age group. The current study aims at enhancing the understanding of the pathophysiology of CAD under the presence of insulin resistance and diabetes.

Aim: This study aims to evaluate the relationships between circulating levels of adiponectin and a number of inflammatory biomarkers, including high-sensitivity C-reactive protein, interleukin-6, and E-selectin, as well as metabolic factors, such as insulin and C-peptide concentrations in the blood of individuals with coronary artery disease. Additionally, the study will be stratified based on whether type 2 diabetes mellitus is present, and lipid profiles will be compared based on these subgroups.

Methods

Study Design and Setting

The study was a cross-sectional research based on observation of the general medicine and cardiology outpatient units of a tertiary care hospital in Coimbatore, India. The intrinsic ethics committee gave its ethical approval (Approval No: IHEC/305/Biochemistry/08/2023). Informed consent was gathered in the form of written consent. The research was not prospectively registered, because no interventional procedures were involved in the research.

Sample Size Calculation

Sample size calculation was performed using G*Power 3.1.9.7 software based on a one-way ANOVA design with three groups. Using an effect size of 0.8 [derived from previous adiponectin studies], $\alpha = 0.05$, and power = 0.80, the minimum required sample was 64 participants per group. We enrolled 75 participants per group [n = 225 total] to ensure robust statistical power and account for potential data variability.

Participants

A total of 225 subjects was divided into three groups, namely Group 1 (Control) consisted of 75 healthy adults who had never had a history of cardiovascular disease or diabetes mellitus; Group 2 (CAD with T2DM) consisted of 75 patients with both coronary artery disease and type 2 diabetes mellitus; and Group 3 (CAD without diabetes) comprised 75 patients with coronary artery disease but without diabetes.

The inclusion criteria included individuals with a clinical diagnosis of CAD through coronary angiography and electrocardiography between the ages of 30 and 50 years. Diabetes was assessed based on the criteria of American Diabetes Association.

The exclusion criteria included active or chronic infections, autoimmune disease, malignancy, pregnancy, or recent coronary bypass grafting, or administration of drugs that may affect cardiovascular or metabolic values. Participants with known chronic kidney disease or an estimated glomerular filtration rate [eGFR] below 60 mL/min/1.73 m² were also excluded to minimise the potential confounding effect of impaired renal clearance on C-peptide concentrations. Additionally, participants receiving insulin sensitizers such as metformin or thiazolidinediones were documented separately; those on active injectable insulin therapy were excluded, as exogenous insulin administration directly confounds the measurement of circulating insulin and related indices.

Sample Collection and Processing

Aseptic methodology was used to collect venous blood samples following 12 hours of an overnight fast. The plasma was separated out of tubes filled with EDTA anticoagulant and serum was obtained out of tubes lacking anticoagulant. Samples were treated instantly; plasma, serum, was centrifuged at 3000 rpm and 10 min at 4°C and stored at -80°C until analysis.

Biochemical Analyses

Standardised enzyme-immunoassay techniques were used to evaluate serum levels of adiponectin, high sensitivity C-reactive protein (hs-CRP), interleukin-6 (IL-6), E-selectin, insulin, and C-peptide. Every test was performed twice in compliance with the manufacturer's instructions. Each biomarker had coefficients of variation of less than 10% both within and across assays. A Roche automated analyser was used to measure

lipid parameters, including total cholesterol, triglycerides, high-density lipoprotein cholesterol, and low-density lipoprotein cholesterol, while rigorous quality control procedures were followed. Fasting plasma glucose was measured on the same venous sample, and the homeostasis model assessment of insulin resistance [HOMA-IR] was calculated using the standard formula: HOMA-IR = [fasting insulin (μU/mL) × fasting glucose (mmol/L)] / 22.5, to provide a standardised index of insulin resistance in addition to absolute fasting insulin values.

Statistical Analysis

Data processing was done using version 25 of the SPSS Statistical Package for the Social Sciences. Categorical variables were reported as frequencies, whereas continuous variables were presented as mean±standard deviations. To compare group differences, a one-way analysis of variance was performed with post hoc comparisons using Tukey's test. The linear associations between biomarkers were assessed using Pearson's correlation coefficients. Multiple linear regression models were used to investigate clinical outcome predictors. Prior to finalising the regression models, multicollinearity among predictors was assessed using variance inflation factors [VIF] and tolerance statistics. Given the high inter-correlation between insulin and C-peptide [$r = 0.76$, $p < 0.001$], both variables were initially entered into the model simultaneously. C-peptide yielded a non-significant regression coefficient [$\beta = 0.14$, $p = 0.08$] with a VIF indicating shared variance with insulin, and was therefore excluded from the final model to avoid redundancy and statistical noise. Insulin was retained as the superior predictor of insulin secretory activity in this population after this sequential selection. To evaluate the discriminative power of biomarkers, receiver operating characteristic curves were developed, and areas under the curve and ideal cutoff points were computed. The threshold for statistical significance was set at $p<0.05$.

Results

Demographic Characteristics

The study included 225 participants with no statistically significant difference in gender distribution across groups [$p = 0.85$]. Mean age showed a non-significant trend toward higher values among CAD patients [$p = 0.08$], while BMI was significantly elevated in the CAD with T2DM group compared to controls [$p < 0.001$] (Table 1).

iochemical Marker Levels

According to biochemical tests, patients with coronary artery disease (CAD) had significantly lower blood adiponectin levels than control participants (p 0.001). Patients with CAD who also had type 2 diabetic mellitus (T2DM) had the lowest levels. High-sensitivity C-reactive protein (hs-CRP), interleukin-6 (IL-6), and E-selectin are pro-inflammatory biomarkers that were considerably greater than controls in both CAD subgroups ($p < 0.001$), with the diabetic CAD subset showing the largest rises. In the CAD population, insulin resistance markers significantly increased, particularly for individuals with T2DM ($p < 0.001$). High levels of total cholesterol, low density lipoprotein cholesterol, and triglycerides, together with a reduction in high density lipoprotein cholesterol ($p < 0.001$; see Table 2), were indicative of dyslipidemic profiles. HOMA-IR was significantly elevated in CAD patients with T2DM compared to CAD patients without T2DM and controls, confirming a gradient of insulin resistance across groups ($p < 0.001$), consistent with the pattern observed for absolute fasting insulin values.

Table 1 Demographic Characteristics of Study Participants

Characteristic	Control [n=75]	CAD with T2DM [n=75]	CAD without T2DM [n=75]	p-value
Age [years]	45.2 ± 6.1	53.5 ± 7.2	52.6 ± 6.4	0.08
Gender [Male/Female]	38/37	45/30	44/31	0.85
BMI [kg/m^2]	23.5 ± 2.8	27.4 ± 3.1	26.9 ± 2.7	< 0.001

Table 2 Biochemical Marker Levels in Study Groups

Marker	Control [n=75]	CAD with T2DM [n=75]	CAD without T2DM [n=75]	p-value
Adiponectin [mg/L]	7.4 ± 1.6	4.2 ± 1.0	5.1 ± 1.3	< 0.001
hs-CRP [mg/L]	1.2 ± 0.3	5.8 ± 1.4	4.5 ± 1.0	< 0.001
IL-6 [pg/mL]	3.8 ± 1.2	9.2 ± 3.4	6.6 ± 2.2	< 0.001
E-selectin [ng/mL]	45.2 ± 12.1	92.7 ± 23.2	67.5 ± 18.3	< 0.001
Insulin [μU/mL]	12.3 ± 4.1	28.9 ± 6.5	20.7 ± 5.0	< 0.001
C-peptide [ng/mL]	2.9 ± 0.9	6.5 ± 2.1	4.2 ± 1.5	< 0.001
HOMA-IR	1.9 ± 0.6	6.1 ± 1.8	3.8 ± 1.2	< 0.001
Total Cholesterol [mg/dL]	187.4 ± 20.2	216.5 ± 30.4	204.1 ± 23.8	< 0.05
Triglycerides [mg/dL]	125.3 ± 45.2	186.3 ± 58.5	159.2 ± 49.8	< 0.001
LDL Cholesterol [mg/dL]	112.4 ± 18.5	145.3 ± 25.3	139.4 ± 21.0	< 0.01
HDL Cholesterol [mg/dL]	52.1 ± 10.3	41.2 ± 9.4	46.1 ± 8.6	< 0.01

Correlation Analysis

Correlation analysis demonstrated statistically significant inverse associations between adiponectin and inflammatory markers: hs-CRP [$r = -0.45$, $p < 0.001$], IL-6 [$r = -0.38$, $p = 0.001$], and E-selectin [$r = -0.32$, $p = 0.004$]. Adiponectin exhibited negative correlations with serum insulin [$r = -0.28$, $p = 0.006$] and C-peptide [$r = -0.21$, $p = 0.03$]. Positive correlations were observed among inflammatory markers and between these markers and insulin resistance indices (Table 3). Notably, insulin and C-peptide showed a strong positive inter-correlation [r =

Table 3 Correlation of Adiponectin and Other Biochemical Markers

Marker	Adiponectin	hs-CRP	IL-6	E-selectin	Insulin	C-peptide
Adiponectin	1	-0.45**	-0.38**	-0.32**	-0.28*	-0.22*
hs-CRP	-0.45**	1	0.59**	0.56**	0.41**	0.37**
IL-6	-0.38**	0.59**	1	0.64**	0.38**	0.32*
E-selectin	-0.32**	0.56**	0.64**	1	0.34**	0.29*
Insulin	-0.28*	0.41**	0.38**	0.34**	1	0.76**
C-peptide	-0.22*	0.37**	0.32*	0.29*	0.76**	1

**Correlation is significant at the 0.05 level; **Correlation is significant at the 0.01 level*

Table 4 Multiple Linear Regression Analysis for Factors Associated with CAD

Predictor Variable	β [Standardized Coefficient]	p-value
Adiponectin [μg/mL]	-0.35	< 0.001
hs-CRP [mg/L]	0.42	< 0.001
Insulin [μU/mL]	0.27	< 0.01
E-selectin [ng/mL]	0.23	0.02
C-peptide [ng/mL]	0.14	0.08

**Correlation is significant at the 0.05 level; **Correlation is significant at the 0.01 level*

0.76, p < 0.001], indicating substantial shared variance, which informed the multicollinearity assessment conducted during regression modelling.

Multiple Linear Regression Analysis

Multiple linear regression analysis identified adiponectin [β = -0.35, p = 0.002], hs-CRP [β = 0.42, p < 0.001], insulin [β = 0.27, p = 0.01], and E-selectin [β = 0.23, p = 0.02] as independent factors associated with CAD after adjusting for age, BMI, and lipid parameters. C-peptide showed a marginal association [p = 0.08] but did not reach statistical significance (Table 4).

The exclusion of C-peptide from the final model was informed by multicollinearity diagnostics: the VIF for C-peptide when entered simultaneously with insulin exceeded the acceptable threshold, indicating that its bivariate correlation with adiponectin [r = -0.21, p = 0.03] does not translate into an independent regression effect once the shared variance with insulin is accounted for. This does not imply that C-peptide lacks physiological relevance; rather, it reflects the statistical redundancy between these two markers of endogenous insulin secretion in this cross-sectional sample. Future studies incorporating C-peptide in populations stratified by renal function may better delineate its independent contribution.

Post Hoc Analysis

When comparing patients with coronary artery disease (CAD) to healthy controls, post-hoc analysis using Tukey's Honestly Significant Difference test revealed statistically significant intergroup differences (p < 0.001). Table 5 summarises the significant changes between the groups in adiponectin, interleukin-6 (IL-6), E-selectin, insulin, and high-sensitivity C-reactive protein (hs-CRP).

Table 5 Post Hoc Analysis [Tukey's Test] Between Study Groups

Marker	Control vs CAD with T2DM	Control vs CAD without T2DM	CAD with T2DM vs CAD without T2DM
Adiponectin	< 0.001	< 0.001	0.03
hs-CRP	< 0.001	< 0.001	0.05
IL-6	< 0.001	< 0.001	0.02
E-selectin	< 0.001	< 0.001	0.001
Insulin	< 0.001	< 0.001	0.03
C-peptide	< 0.001	< 0.001	0.04

ROC Analysis

ROC curve analysis was employed to evaluate discriminative performance of biomarkers. hs-CRP exhibited the highest area under the curve [AUC = 0.83], followed by adiponectin [AUC = 0.79], E-selectin [AUC = 0.75], and insulin [AUC = 0.72], indicating moderate discriminative ability for differentiating CAD with T2DM from healthy controls (Table 6).

At its optimal Youden index-derived cutoff, adiponectin demonstrated a sensitivity of 74% and specificity of 78% at a threshold of ≤5.0 mg/L for identifying CAD patients with T2DM, providing a clinically interpretable reference point for risk stratification.

Table 6 ROC Analysis for Biomarkers

Marker	AUC	95% Confidence Interval	p-value
Adiponectin	0.79	0.72 - 0.86	< 0.001
hs-CRP	0.83	0.77 - 0.89	< 0.001
E-selectin	0.75	0.68 - 0.82	< 0.001
Insulin	0.72	0.64 - 0.80	< 0.001

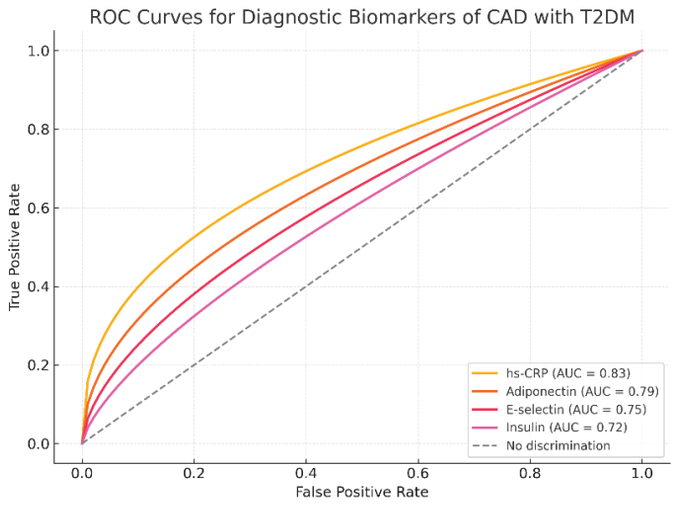

Figure 1 – Regression Coefficients of Biochemical Predictors Associated with the Outcome Variable

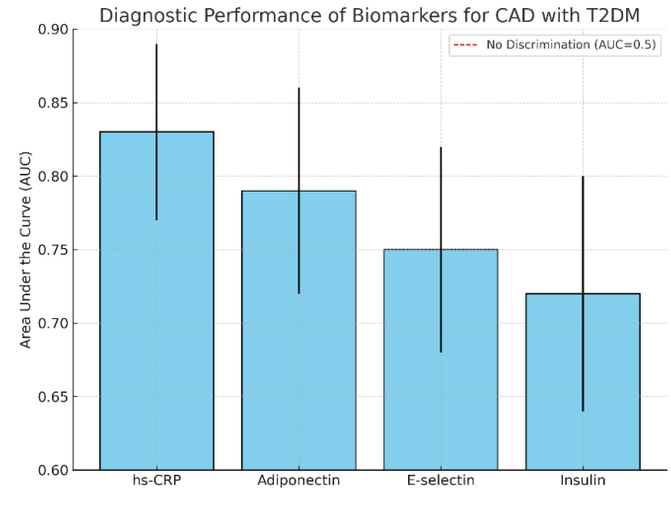

Figure 2 – Regression Coefficients of Biochemical Predictors Associated with the Outcome Variable

Discussion

The current study investigated the relationships between adiponectin, inflammatory and metabolic indices in a patient group diagnosed with coronary artery disease (CAD), including patients with and without type 2 diabetes mellitus (T2DM). The results provide improvements in our understanding of pathophysiological mechanisms that underlie cardiovascular disease in the diabetic state and the clinical significance of adiponectin as a biomarker that indicates cardiovascular health.

When compared to CAD patients without diabetes and healthy volunteers, observations indicate that plasma concentrations of adiponectin were significantly lower in patients with coronary artery disease (CAD) concurrently with type 2 diabetes mellitus (T2DM). These results are in line with existing research that associates hypoadiponectinemia with a higher risk of cardiovascular disease, particularly in those who experience metabolic disturbances [14,15].

Adiponectin reduces vascular inflammation, enhances endothelial function, and increases nitric oxide generation, among other mechanisms that contribute to its cardioprotective benefits [16, 17]. Adiponectin concentrations and insulin resistance have been found to be consistently inversely correlated. By triggering the AMP-activated protein kinase (AMPK) signalling cascade, adiponectin is thought to improve insulin sensitivity [18,19].

In the present study, HOMA-IR confirmed a gradient of insulin resistance across groups and showed a pattern consistent with absolute fasting insulin values, supporting the validity of fasting insulin as a surrogate marker of insulin resistance in this cohort. While standardised indices such as HOMA-IR and HOMA2 are preferable for precise insulin resistance quantification in future studies, the strong inter-group differences observed herein for both fasting insulin and HOMA-IR indicate that the core findings are not artefactual.

Systemic inflammation is a major factor in pathogenesis of both CAD and T2DM. The present study reported a significantly higher level of high sensitivity C-reactive protein (hs-CRP) and interleukin-6 (IL-6) in CAD patients with T2DM, in line with the chronic low grade inflammation milieu described in this group of patients. hs-CRP is an independent predictor of cardiovascular risk, particularly in diabetic populations, and its elevation closely correlates with endothelial dysfunction and atherogenic progression [20,21]. Similarly, IL-6 encourages cardiovascular pathology by promoting vascular inflammation and endothelial dysfunction on top of promoting insulin resistance and lipid dysregulation [22,23].

E-selectin is involved in leukocyte adhesion to the vascular endothelium and activates the inflammatory cascade on which atherogenesis is based. Elevated plasma E-selectin levels were detected in CAD patients with T2DM in this study and suggest increased endothelial activation and dysfunction. These observations are in concert with previous reports characterizing a relationship between elevated E-selectin and incident cardiovascular events [24,25].

Patients with coronary artery disease (CAD) who also had type 2 diabetic mellitus (T2DM) had significantly different serum lipid profiles from those who did not have the metabolic condition. High levels of total cholesterol, low-density LDL cholesterol and triglycerides, and low levels of high-density HDL cholesterol were seen in subjects with both T2DM and CAD [26, 27]. This constellation is characteristic of diabetic dyslipidaemia and is linked to the acceleration of atherogenesis.

Adiponectin, high sensitivity C-reactive protein (hsCRP), and insulin are independent predictors of CAD, according to multivariate regression analysis, with adiponectin exhibiting the highest inverse connection with insulin levels and inflammatory markers. The decision to prioritise insulin over C-peptide in the final regression model was based on multicollinearity assessment revealing high inter-correlation between these two markers [$r = 0.76$], causing C-peptide to lose significance [$p = 0.08$] when included simultaneously. Although C-peptide is a more stable marker with superior pharmacokinetic properties owing to its absence of first-pass hepatic metabolism, its circulating levels are subject to renal filtration; all participants with eGFR < 60 mL/min/1.73 m² were excluded to mitigate this confound. The loss of C-peptide significance in the adjusted model should therefore be interpreted as a statistical consequence of redundancy rather than absence of biological relevance. All three biomarkers had modest discriminative performance according to receiver operating characteristic (ROC) curves; adiponectin's area under the curve (AUC) was 0.79, which was in line with findings from other research [28, 29].

Adiponectin demonstrated a well-characterised gender specificity, with female individuals generally exhibiting higher concentrations than males. In the 30–50 age group studied here, circulating adiponectin in women may be additionally modulated by endogenous sex steroid levels and menopausal transition. Although the overall gender distribution was balanced across groups [$p = 0.85$], formal gender-stratified sub-analyses were not performed, which represents a limitation of the current study and may have attenuated the precision of adiponectin-based risk estimates, particularly in female participants. Future investigations should incorporate gender-stratified analyses and account for menopausal status when evaluating adiponectin as a cardiovascular biomarker.

Regarding the potential impact of ongoing hypoglycaemic therapy, participants receiving injectable insulin were excluded from the study; however, oral hypoglycaemic agents, particularly insulin sensitizers such as metformin and thiazolidinediones, were documented among enrolled patients. These agents are known to modulate adiponectin levels and insulin sensitivity independently of glycaemic control. The absence of a formal pharmacological adjustment for these agents in the multivariable model represents an additional limitation. Future research should stratify participants by medication class or introduce pharmaceutical exposure as a covariate to obtain unconfounded biomarker estimates.

From a translational perspective, the ROC-derived optimal cutoff for adiponectin [≤5.0 mg/L] offers a clinically actionable threshold that cardiologists could incorporate into routine metabolic screening of patients presenting with suspected CAD, particularly those with concurrent T2DM. We propose the following simple decision algorithm: (1) measure fasting adiponectin alongside standard lipid and glycaemic panels; (2) classify patients with adiponectin ≤5.0 mg/L and hs-CRP ≥3.0 mg/L as high-risk for CAD with metabolic comorbidity; (3) prioritise these patients for early coronary angiographic evaluation, intensified glycaemic optimisation, and adiponectin-targeted therapeutic strategies. Validation of this threshold in prospective cohorts and in populations with broader age ranges and diverse ethnicities is essential before clinical implementation.

The present study did not include a systematic comparison of biomarker levels with angiographic severity scores such as the Syntax score, which would have provided objective anatomical grounding for the biomarker hierarchy reported. While all CAD patients were diagnosed through coronary angiography as part of the inclusion criteria, the degree of vascular involvement

was not quantitatively correlated with circulating biomarker concentrations. This represents a notable gap, and future work should examine whether the adiponectin–hs-CRP–insulin profile correlates with Syntax score-derived lesion complexity, which would considerably strengthen the risk stratification framework proposed here.

Study Limitations

There are a number of limitations to consider. The cross-sectional nature of the study makes causal inferences impossible and prospective studies are needed to confirm temporal links between biomarker changes and the onset of CAD. Furthermore, the sample was obtained from a limited demography to extrapolate upon heterogeneous ethnic cohorts and other studies should determine the external validity of the findings within different populations. The study population was restricted to the 30–50-year age range, which limits generalisability to older patient cohorts in whom adiponectin dynamics and insulin resistance patterns may differ substantially. Gender-stratified sub-analyses for adiponectin were not performed; given the known gender specificity of adiponectin and the influence of sex steroids and menopausal status in this age range, this limits the precision of adiponectin-based risk estimates in female participants. The study did not formally adjust for the effects of ongoing oral hypoglycaemic therapy on adiponectin and insulin levels; insulin sensitizers such as metformin and thiazolidinediones may independently modulate these markers and represent a potential source of residual confounding. Insulin resistance was quantified using both absolute fasting insulin and HOMA-IR; however, standardised indices such as HOMA2 or the hyperinsulinaemic-euglycaemic clamp, which offer more precise quantification, were not employed. The study did not correlate biomarker levels with the anatomical severity of coronary artery disease as assessed by the Syntax score; such correlation would have provided stronger mechanistic and clinical validation of the proposed risk stratification markers. Prospective research should also question the therapeutic implications of modulating adiponectin in patients with CAD, especially in patients with T2DM.

Conclusion

The present study establishes significant associations between reduced levels of adiponectin, increased inflammatory markers and metabolic aberrations in patients with CAD, specifically in patients with T2DM. These biomarkers are related to the systemic inflammatory processes that are intrinsic to CAD, and they should further evaluated in a prospective evaluation to determine their clinical applicability. The ROC-derived optimal cutoff for adiponectin [≤5.0 mg/L], combined with elevated hs-CRP, identifies a high-risk metabolic profile that may guide early clinical decision-making in cardiology practice. Multicollinearity diagnostics confirmed the statistical primacy of insulin over C-peptide in the regression model, though the biological contribution of C-peptide in renally-intact populations warrants dedicated investigation. The findings support the proposition of adiponectin as a therapeutic target in order to attenuate cardiovascular risk in the diabetic population.

Author Contributions: Conceptualization, P.K.D. and K.P.M.; Methodology, L.P. and P.K.D.; Formal Analysis, J.T. and T.S.; Investigation, L.P. and A.C.; Resources, P.K.D.; Data Curation, L.P.; Writing – Original Draft Preparation, L.P. and P.K.D.; Writing – Review & Editing, K.P.M., J.T., T.S., and A.C.; Supervision, P.K.D.; Project Administration, P.K.D. All authors have read and agreed to the published version of the manuscript.

Disclosures: The authors have no conflicts of interest.

Acknowledgments: The authors thank all participants who contributed to this study and the laboratory staff for their technical assistance.

Funding: None.

Data availability statement: The datasets generated during and/or analyzed during the current study are available from the corresponding author on reasonable request.

Artificial Intelligence (AI) Disclosure Statement: The authors declare no AI Tools used for preparation of this work.

References

1. Roth, GA, Mensah, GA, Johnson, CO, Addolorato, G, Ammirati, E, Baddour, LM, Barengo, NC, Beaton, AZ, Benjamin, EJ, Benziger, CP, Bonny, A, Brauer, M, Brodmann, M, Cahill, TJ, Carapetis, J, Catapano, AL, Chugh, SS, Cooper, LT, Coresh, J, Criqui, M, … GBD-NHLBI-JACC Global Burden of Cardiovascular Diseases Writing Group. Global Burden of Cardiovascular Diseases and Risk Factors, 1990-2019: Update From the GBD 2019 Study. *Journal of the American College of Cardiology* 2020; 76(25): 2982–3021. https://doi.org/10.1016/j.jacc.2020.11.010
2. Jebari-Benslaiman, S, Galicia-García, U, Larrea-Sebal, A, Olaetxea, JR, Alloza, I, Vandenbroeck, K, Benito-Vicente, A, & Martín, C. Pathophysiology of Atherosclerosis. *International journal of molecular sciences.* 2022; 23(6): 3346. https://doi.org/10.3390/ijms23063346
3. Clemente-Suárez, VJ, Redondo-Flórez, L, Beltrán-Velasco, AI, Martín-Rodríguez, A, Martínez-Guardado, I, Navarro-Jiménez, E, Laborde-Cárdenas, CC, & Tornero-Aguilera, JF. The Role of Adipokines in Health and Disease. *Biomedicines*. 2023; 11(5): 1290. https://doi.org/10.3390/biomedicines11051290
4. Choi, HM, Doss, HM, & Kim, KS. Multifaceted Physiological Roles of Adiponectin in Inflammation and Diseases. *International journal of molecular sciences.* 2020; 21(4): 1219. https://doi.org/10.3390/ijms21041219
5. Fisman, EZ, & Tenenbaum, A. Adiponectin: a manifold therapeutic target for metabolic syndrome, diabetes, and coronary disease?. *Cardiovascular diabetology.* 2014; 13: 103. https://doi.org/10.1186/1475-2840-13-103

6. Yanai, H, & Yoshida, H. Beneficial Effects of Adiponectin on Glucose and Lipid Metabolism and Atherosclerotic Progression: Mechanisms and Perspectives. *International journal of molecular sciences.* 2019; 20(5): 1190. https://doi.org/10.3390/ijms20051190
7. Swastini, DA, Wiryanthini, IAD, Ariastuti, NLP, & Muliantara, A. Atherosclerosis Prediction with High Sensitivity C-Reactive Protein (hs-CRP) and Related Risk Factor in Patient with Dyslipidemia. *Open access Macedonian journal of medical sciences.* 2019; 7(22): 3887–3890. https://doi.org/10.3889/oamjms.2019.526
8. Kirkgöz K. C-Reactive Protein in Atherosclerosis-More than a Biomarker, but not Just a Culprit. *Reviews in cardiovascular medicine.* 2023; 24(10): 297. https://doi.org/10.31083/j.rcm2410297
9. Villar-Fincheira, P, Sanhueza-Olivares, F, Norambuena-Soto, I, Cancino-Arenas, N, Hernandez-Vargas, F, Troncoso, R, Gabrielli, L, & Chiong, M. Role of Interleukin-6 in Vascular Health and Disease. *Frontiers in molecular biosciences.* 2021; 8: 641734. https://doi.org/10.3389/fmolb.2021.641734
10. Zhang, J, Huang, S, Zhu, Z, Gatt, A, & Liu, J. E-selectin in vascular pathophysiology. *Frontiers in immunology.* 2024; 15: 1401399. https://doi.org/10.3389/fimmu.2024.1401399
11. Wahren, J, Ekberg, K, Johansson, J, Henriksson, M, Pramanik, A, Johansson, BL, Rigler, R, & Jörnvall, H. Role of C-peptide in human physiology. American journal of physiology. *Endocrinology and metabolism.* 2000; 78(5): E759–E768. https://doi.org/10.1152/ajpendo.2000.278.5.E759
12. Wazir, M, Olanrewaju, OA, Yahya, M, Kumari, J, Kumar, N, Singh, J, Abbas Al-Itbi, AY, Kumari, K, Ahmed, A, Islam, T, Varrassi, G, Khatri, M, Kumar, S, Wazir, H, & Raza, SS. Lipid Disorders and Cardiovascular Risk: A Comprehensive Analysis of Current Perspectives. *Cureus*. 2023; 15(12): e51395. https://doi.org/10.7759/cureus.51395
13. Jung, HN, & Jung, CH. The Role of Anti-Inflammatory Adipokines in Cardiometabolic Disorders: Moving beyond Adiponectin. International journal of molecular sciences. 2021; 22(24): 13529. https://doi.org/10.3390/ijms222413529
14. Roy, PK, Islam, J, & Lalhlenmawia, H. Prospects of potential adipokines as therapeutic agents in obesity-linked atherogenic dyslipidemia and insulin resistance. The Egyptian heart journal : *(EHJ) : official bulletin of the Egyptian Society of Cardiology.* 2023; 5(1): 24. https://doi.org/10.1186/s43044-023-00352-7
15. Lei, X, Qiu, S, Yang, G, & Wu, Q. Adiponectin and metabolic cardiovascular diseases: Therapeutic opportunities and challenges. Genes & diseases. 2022; 10(4): 1525–1536. https://doi.org/10.1016/j.gendis.2022.10.018
16. Shibata, R, Ouchi, N, & Murohara, T. Adiponectin and cardiovascular disease. Circulation journal : *official journal of the Japanese Circulation Society.* 2009; 73(4): 608–614. https://doi.org/10.1253/circj.cj-09-0057
17. Li, S, Han, X, Song, J, Dong, M, & Xie, T. Mechanism of Action and Risk Prediction of Adiponectin in Cardiovascular Diseases. *Frontiers in bioscience (Landmark edition).* 2024; 29(8): 286. https://doi.org/10.31083/j.fbl2908286
18. Warraich, HJ, & Rana, JS. Dyslipidemia in diabetes mellitus and cardiovascular disease. *Cardiovascular endocrinology.* 2017; 6(1): 27–32. https://doi.org/10.1097/XCE.0000000000000120
19. Begum, M, Choubey, M, Tirumalasetty, MB, Arbee, S, Mohib, MM, Wahiduzzaman, M, Mamun, MA, Uddin, MB, & Mohiuddin, MS. Adiponectin: A Promising Target for the Treatment of Diabetes and Its Complications. *Life (Basel, Switzerland).* 2023; 13(11): 2213. https://doi.org/10.3390/life13112213
20. Ridker, PM, Hennekens, CH, Buring, JE, & Rifai, N. C-reactive protein and other markers of inflammation in the prediction of cardiovascular disease in women. *The New England journal of medicine.* 2000; 342(12): 836–843. https://doi.org/10.1056/NEJM200003233421202
21. Stanimirovic, J, Radovanovic, J, Banjac, K, Obradovic, M, Essack, M, Zafirovic, S, Gluvic, Z, Gojobori, T, & Isenovic, ER. Role of C-Reactive Protein in Diabetic Inflammation. *Mediators of inflammation.* 2022; 3706508. https://doi.org/10.1155/2022/3706508
22. Hotamisligil GS. Inflammation and metabolic disorders. Nature. 2006; 444(7121): 860–867. https://doi.org/10.1038/nature05485
23. Qu, D, Liu, J, Lau, CW, & Huang, Y. IL-6 in diabetes and cardiovascular complications. *British journal of pharmacology.* 2014; 171(15): 3595–3603. https://doi.org/10.1111/bph.12713
24. Pepin, ME, & Gupta, RM. The Role of Endothelial Cells in Atherosclerosis: Insights from Genetic Association Studies. *The American journal of pathology.* 2024; 194(4): 499–509. https://doi.org/10.1016/j.ajpath.2023.09.012
25. Libby P. Inflammation in atherosclerosis. *Arteriosclerosis, thrombosis, and vascular biology.* 2012; 32(9): 2045–2051. https://doi.org/10.1161/ATVBAHA.108.179705
26. Buse, JB, Ginsberg, HN, Bakris, GL, Clark, NG, Costa, F, Eckel, R, Fonseca, V, Gerstein, HC, Grundy, S, Nesto, RW, Pignone, MP, Plutzky, J, Porte, D, Redberg, R, Stitzel, KF, Stone, NJ, American Heart Association, & American Diabetes Association. Primary prevention of cardiovascular diseases in people with diabetes mellitus: a scientific statement from the American Heart Association and the American Diabetes Association. *Diabetes care.* 2007; 30(1): 162–172. https://doi.org/10.2337/dc07-9917
27. Haffner, SM, & American Diabetes Association. Dyslipidemia management in adults with diabetes. *Diabetes care.* 2004; 27 Suppl 1: S68–S71. https://doi.org/10.2337/diacare.27.2007.s68
28. Obata, Y, Yamada, Y, Kyo, M, Takahi, Y, Saisho, K, Tamba, S, Yamamoto, K, Katsuragi, K, & Matsuzawa, Y. Serum adiponectin levels predict the risk of coronary heart disease in Japanese patients with type 2 diabetes. *Journal of diabetes investigation*. 2013; 4(5): 475–482. https://doi.org/10.1111/jdi.12078
29. Lara-Castro, C, Fu, Y, Chung, BH, & Garvey, WT. Adiponectin and the metabolic syndrome: mechanisms mediating risk for metabolic and cardiovascular disease. *Current opinion in lipidology.* 2007; 18(3): 263–270. https://doi.org/10.1097/MOL.0b013e32814a645f

JOURNAL OF CLINICAL MEDICINE OF KAZAKHSTAN (E-ISSN 2313-1519)
Original Article DOI: https://doi.org/10.23950/jcmk/18327

Bioinformatics Analysis Identifying Key Genes and Signaling Pathways Involved in the Egg Allergy in Young Children: a Retrospective Study

Arailym Abilbayeva[1], Tair Nurpeissov[2], Balaussa Seitkhan[1], Nuray Shaktay[1]

[1]*Shortanbayev General Immunology Department, Asfendiyarov Kazakh National Medical University, Almaty, Kazakhstan*
[2]*SRS of Cardiology and Internal Diseases, Almaty, Kazakhstan*

Received: 2025-08-28.
Accepted: 2026-04-07.

This work is licensed under a **Creative Commons Attribution 4.0 International License**

J Clin Med Kaz 2026; 23(2): 64-71

Corresponding author:
Arailym Abilbayeva.
E-mail: abilbaeva.a@kaznmu.kz.
ORCID: 0000-0001-5081-5492.

ABSTRACT

Objective: Identify key genes and signaling pathways involved in IgE-mediated food allergy in young children using bioinformatics analysis.

Methods: The GSE114065 dataset from GEO was utilized for bioinformatic analysis. DEGs were identified using the GEO2R web tool. GO, KEGG, and Reactome functional analyses were performed using the Enrichr platform. The PPI network for DEGs was constructed with the STRING website and visualized in Cytoscape. The cytoHubba plugin was used to identify hub genes. Nonparametric Mann-Whitney test was employed to compare groups.

Results: Of the 490 DEGs identified, 402 were upregulated and 88 were downregulated. Dowregulated DEGs showed no significant enrichment in biological processes or molecular functions but were associated with Golgi apparatus-related cellular components. In contrast, upregulated DEGs exhibited pronounced enrichment in biological processes linked to antiviral defense, immune regulation, and IL-27 signaling, alongside extracellular matrix-related cellular components. Molecular functions included cytokine activity, receptor ligand binding. KEGG and Reactome analyses highlighted significant pathways involved in cytokine signaling, immune response, and antiviral defense. 10 DEGs were identified as hub genes, including USP18, OAS3, IFIH1, MX1, DDX58, OAS1, IFIT2, OAS2, IFI35, and IFIT3.

Conclusion: The results demonstrate that the aberrant activation of genes related to the interferon response and antiviral defense plays a central role in the pathogenesis of IgE-mediated food allergy. The 10 identified hub genes are key regulators of innate immunity, significantly influencing inflammatory and antiviral pathways. Our findings suggest that the upregulation of these genes contributes to the immune imbalance characteristic of food allergy, opening new avenues for understanding disease mechanisms and identifying innovative diagnostic and therapeutic targets.

Keywords: bioinformatics analysis, food allergies, hub genes, young children.

Introduction

IgE-mediated food allergy in children is a substantial clinical and social issue. In modern pediatrics, the prevalence of food allergy among young children is 6-8% and has continued to rise in recent decades [1]. IgE-mediated hypersensitivity is marked by the rapid onset of clinical symptoms, such as anaphylaxis, angioedema, and gastrointestinal disorders, which pose significant risks to patients' health and quality of life, as well as to their families [2].

Despite extensive research, the pathogenesis of IgE-mediated food allergy is still not fully understood [3].

Previous studies indicate an important role for both innate and adaptive immune responses [4]. Recent research highlights that changes in DNA methylation, histone modifications, and non-coding RNA, which together constitute epigenetic dysregulation, play a key role in the loss of immune tolerance in food allergy [5]. Conversely, epigenetic mechanisms may also help restore the disrupted immune balance in food allergy, acting as immunomodulatory factors in the disease's development [6].

The modern development of high-throughput technologies for gene expression analysis, along with the availability of extensive bioinformatics resources, offers unprecedented opportunities for in-depth study of the molecular mechanisms behind allergic diseases.

Databases like Gene Expression Omnibus are valuable tools for studying differentially expressed genes (DEGs) and associated signaling pathways. Analyzing high-quality expression arrays not only helps identify key target genes but also enables the construction of interactive protein-protein networks, which enhances a system-wide understanding of disease development. Research on food allergy in young children is especially important due to its rising prevalence and the unique features of the immune system during this stage.

Objective of the study: Identify key genes and signaling pathways involved in IgE-mediated food allergy in young children using bioinformatics analysis.

Methods

Collecting data from the GEO database

High-throughput sequencing data from food allergy-related mRNA expression profiles were collected and downloaded from the Gene Expression Omnibus (GEO) database of the National Center for Biotechnology Information (NCBI).

The search query included the following terms: "Food allergy", "mRNA", "Children" and was filtered by organism "Homo sapiens". The dataset GSE114065, based on the Illumina HiSeq 4000 platform GPL20301 (Homo sapiens), was selected for analysis. The dataset comprises RNA-seq experiments performed on sorted naive CD4+ T cells isolated from peripheral blood of children with challenge-confirmed IgE-mediated egg allergy and non-allergic controls. Cells were profiled under two conditions, quiescent and polyclonal activation. In our study, the group of children with IgE-mediated egg allergy included 1-year-old children with an activated cell profile. Controls were non-atopic infants who tested negative to the panel of foods. The original study and GEO record provide cohort and activation protocol details [7].

Identification of differentially expressed genes (DEGs)

The GSE114065 dataset was thoroughly analyzed using the GEO2R web tool to identify DEGs. GEO2R, integrated with the GEO database, employs the R programming language to perform statistical analyses, including t-tests or analysis of variance (ANOVA), enabling comparisons between two or more experimental groups. Specifically, DEG identification in this study relied on the limma framework within GEO2R, which uses linear modeling with empirical Bayes moderation to perform moderated t-tests. The significance thresholds were set at $p<0.05$ and $|LogFC|\geq1$, with p-values adjusted using the Benjamini-Hochberg method to control the false discovery rate. The results were visualized with various plots, such as volcano plots, UMAP, box plots, and Venn diagrams, using GEO2R.

Gene ontology analysis and pathway enrichment analysis

To gain a deeper understanding of the biological functions and molecular mechanisms behind the observed phenotypes, a comprehensive analysis of DEGs was conducted. Gene Ontology (GO) enrichment analysis provided a detailed characterization of the molecular functions, biological processes, and cellular components related to the identified DEGs. Additionally, Kyoto Encyclopedia of Genes and Genomes (KEGG) and Reactome pathway analyses were performed to identify key metabolic and signaling pathways involved in the processes being studied. All of these analyses were performed using the bioinformatics tool Enrichr. Benjamini–Hochberg correction was applied to account for multiple testing in pathway enrichment analyses, and pathways with an adjusted p-value < 0.05 were considered statistically significant.

Analysis of protein-protein interaction (PPI) networks and identification of hub genes

The online tool STRING was used to analyze known PPIs, including both direct and indirect interactions as well as their functional correlations. Interaction network was built using active interaction sources and a minimum required interaction score threshold of 0.4. In this study, 490 DEGs were analyzed, with 88 being dowregulated and 402 upregulated in the allergy group relative to the control group.

The data obtained were exported to Cytoscape software (version 3.10.3) for further visualization of PPI networks. The cytoHubba plugin was used to identify hub genes within the network. The analysis was conducted using the Maximal Clique Centrality (MCC) algorithm, which helped identify central nodes that play a key role in the biological processes under study.

Statistical analysis

IBM SPSS software (version 29.0) was used for statistical analysis. The statistical significance of differences in the expression level of hub genes between the study groups was assessed using the nonparametric Mann-Whitney test.

Results

Sample data information

To evaluate the distribution of data and identify differences between the food allergy and control groups, an analysis of 44 datasets from GEO2R was conducted. The control group included 18 participants, while the study group had 26 subjects. All participants in the study were 1 year old. The gender distribution was equal in both groups. Egg allergy was confirmed by a challenge test in infants within the study group.

Visual analysis of the box-and-whisker plots (Figure 1A) helped us evaluate how much the data deviated from a normal distribution. The UMAP technique was used to reduce the data's dimensionality and visualize its structure. The results from UMAP demonstrated that samples from the food allergy and control groups formed distinct clusters on the two-dimensional plot (Figure 1B), showing significant differences between these groups.

DEG analysis

During data analysis with GEO2R, 490 differentially expressed genes were identified using thresholds adjusted p (BH) < 0.05 and $|\log2FC| \geq 1$ out of a total of 17,628 genes analyzed (Figure 2A). Of these, 402 genes were upregulated and 88 were

downregulated in the allergy group relative to the control group. The volcano plot (Figure 2B) clearly shows the extent of gene expression changes and their statistical significance.

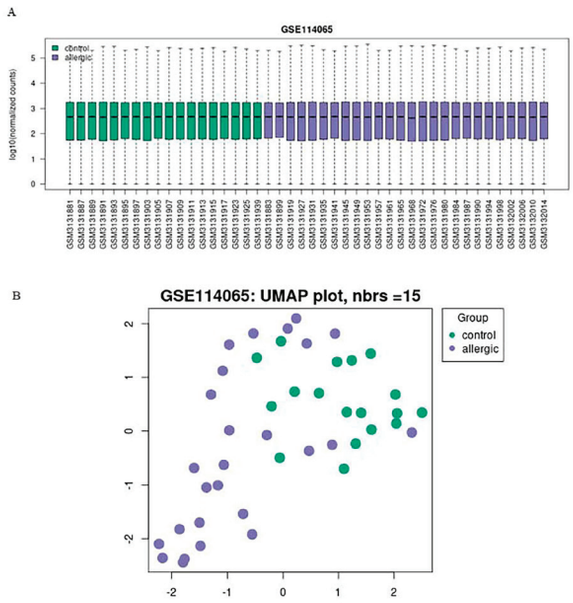

Figure 1 – Gene set evaluation

(A) A box plot with whiskers, where the horizontal axis shows the samples and the vertical axis demonstrates the log2-transformed gene expression values. (B) UMAP analysis was performed on two groups.

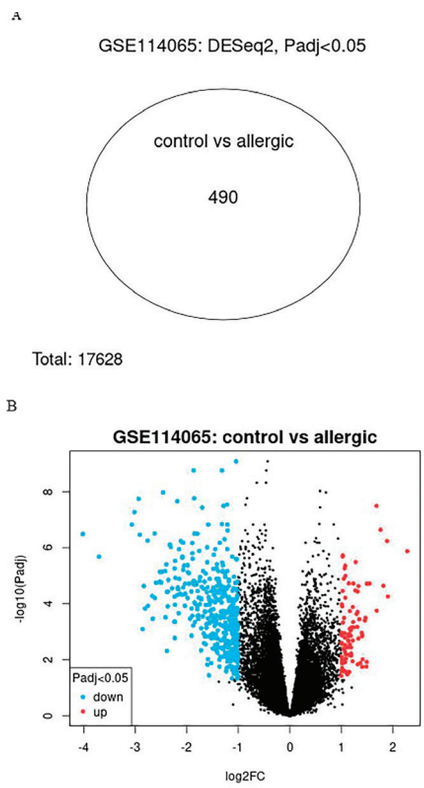

Figure 2 – Results of differential gene expression analysis

(A) A Venn diagram showing the number of differentially expressed genes. (B) A volcano plot of gene expression in two groups. The horizontal axis shows the log2FC (log2-fold change) values, and the vertical axis displays the -log10(adjusted p-value). Upregulated genes are shown in red, while downregulated genes are shown in blue. Genes that do not meet the significance criteria of p < 0.05 and |Log FC| ≥ 1 are shown in black.

Pathway enrichment analysis for up- and down-regulated DEGs

The analysis results showed that no statistically significant annotations were found for the downregulated DEGs in the categories of biological processes and molecular functions. However, in the cellular components category, four significant annotations were identified, all closely related to the Golgi apparatus. Nonetheless, the analysis of the KEGG and Reactome databases did not reveal any statistically significant signaling pathways passed the adjusted $p < 0.05$ cutoff for the downregulated DEG set.

Regarding the upregulated DEGs, the analysis identified 90 significant annotations in the biological processes category, including antiviral defense response, negative regulation of viral replication, and IL-27-mediated signaling pathway. In the cellular components category, one significant annotation related to the extracellular matrix was found. Additionally, the molecular functions were characterized by annotations related to cytokine activity, receptor ligands, and binding to single-stranded and double-stranded RNA (Figure 3). The KEGG database analysis revealed 25 significant pathways, such as cytokine-cytokine receptor interaction and extracellular matrix receptor interaction. The Reactome database analysis identified 18 significant pathways, including cytokine signaling in the immune response and interferon-alpha and beta signaling pathways. The top ten signaling pathways from the KEGG and Reactome databases are displayed in Figure 4 A and B, respectively.

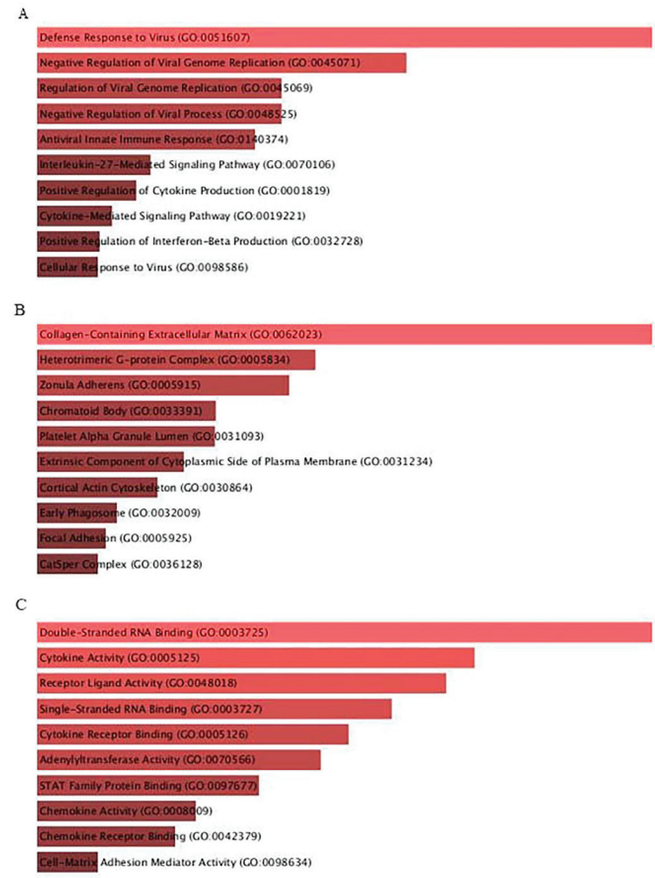

Figure 3 – Graphical illustration of GO ontology enrichment analysis for downregulated genes

(A) Biological Processes; (B) Cellular Components; (C) Molecular Functions

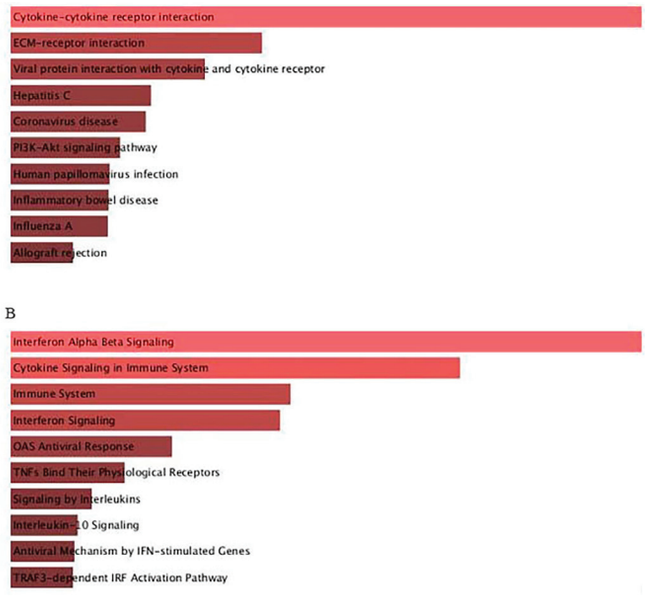

Figure 4 – Graphical illustration of KEGG and Reactome pathway analysis for downregulated genes

(A) The top 10 most significantly enriched KEGG pathways are shown. (B) The top 10 results for the Reactome pathway are shown.

PPI construction and identification of hub genes

To analyze the functional relationships among the 490 differentially expressed genes, a molecular interaction network was built using the STRING database. The network consisted of 275 nodes connected by 3928 edges (Figure 5A). Using the Maximal Clique Centrality (MCC) algorithm, 10 hub genes were identified that likely have central roles in the studied processes: *USP18, OAS3, IFIH1, MX1, DDX58, OAS1, IFIT2, OAS2, IFI35,* and *IFIT3* (Figure 5 B). When comparing the expression levels of these genes between groups, all showed significant differences except for OAS2 (Table 1).

Table 1 Results of comparative analysis of gene expression levels in the study groups

Gene Symbol	log2(fold change)*	Group	Mean Rank	p-value
USP18	2.524	Control	15,28	0.003
		Allergy	26,84	
IFI35	1.474	Control	13,83	<0.0001
		Allergy	27,88	
IFIH1	1.419	Control	15,33	0.003
		Allergy	26,80	
IFIT2	2.128	Control	15,61	0.005
		Allergy	26,60	
IFIT3	2.835	Control	15,89	0.007
		Allergy	26,40	
MX1	2.33	Control	15,17	0.002
		Allergy	26,92	
DHX58/DDX58	1.63	Control	13,89	<0.0001
		Allergy	27,84	
OAS1	2.087	Control	14,83	0.001
		Allergy	27,16	
OAS2	1.484	Control	22,56	0.805
		Allergy	21,60	
OAS3	1.815	Control	14,67	0.001
		Allergy	27,28	

**Positive log2(fold change) values indicate higher expression in the Allergy group compared to the Control group*

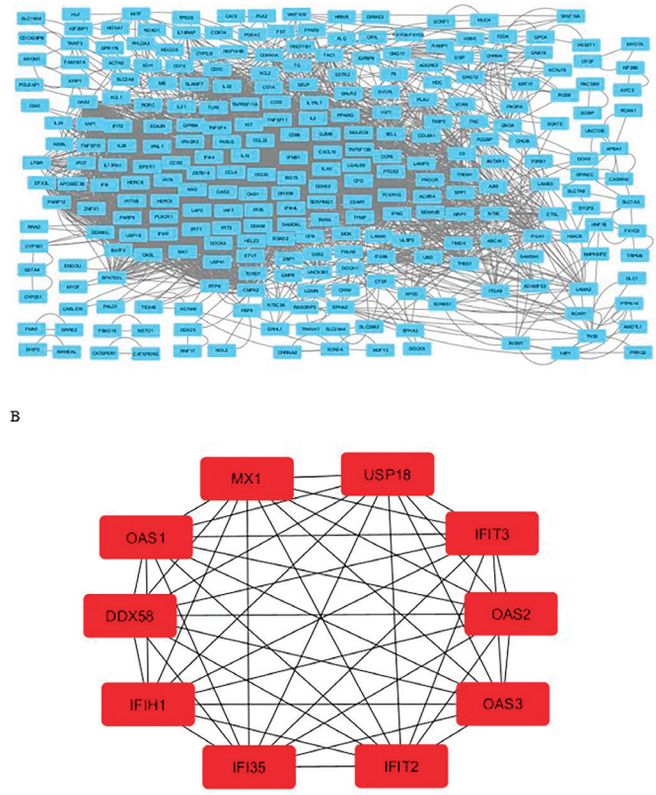

Figure 5 – PPI network analysis and hub genes identification

(A) Analysis of the PPI network using the STRING database. (B) The top 10 hub genes identified by the MCC ranking method.

Discussion

This study performed a comprehensive bioinformatics analysis to identify key genes and signaling pathways associated with IgE-mediated egg allergy in young children. Using the GSE114065 dataset from GEO, 490 differentially expressed genes were identified. Among these, 402 were upregulated and 88 were downregulated in the allergy group relative to the control group.

Genes upregulated in allergies exhibited the most pronounced functional enrichment. Ninety significant annotations were identified in the biological processes category, primarily related to antiviral defense, negative regulation of viral replication, and the IL-27 signaling pathway. This suggests significant modulation of the immune response and aberrant activation of innate immune mechanisms in food allergies. The enrichment of the IL-27 signaling pathway deserves special attention in the context of immune regulation. As a pleiotropic cytokine, IL-27 plays a critical role in maintaining the balance between Th1 and Th2 responses, and its activation may indicate an attempt by the system to limit excessive allergic inflammation [8]. Thus, the IL-27 pathway acts as an important control mechanism modulating the intensity of the immune response during food sensitization. At the molecular function level, these genes are associated with cytokine and receptor activity, as well as single- and double-stranded RNA binding. KEGG signaling pathway analysis identified 25 significant pathways, and Reactome analysis identified 18 significant pathways, confirming the dominant role of cytokine-receptor interactions, interferon-alpha and beta signaling pathways, and matrix interactions in disease pathogenesis. Our findings are consistent with broader molecular patterns observed across various food allergy phenotypes. For instance, integrated

transcriptomic and proteomic analyses in cow's milk protein allergy have highlighted significant enrichment in complement and coagulation cascades, immune activation, and cytokine-receptor interaction pathways, directly paralleling the interferon signaling signatures identified in our study [9]. Furthermore, multi-omics investigations integrating plasma proteomics with metabolomics have confirmed alterations in cytokine networks (including IL-4, IL-6, and IL-13 signaling), which aligns with our emphasis on immune regulation via the IL-27 and interferon pathways [10].

The identification of key genes such as *USP18, OAS3, IFIH1, MX1, DDX58, OAS1, IFIT2, IFI35,* and *IFIT3* through protein-protein interaction network construction further confirms the critical role of the interferon response in the development of allergic disease. Notably, these transcriptomic findings are reinforced by proteomic data from other allergy models. Proteomic investigations in wheat intolerance have identified differentially expressed proteins involved in immune response and complement cascades, highlighting the cross-phenotype importance of these pathways at the protein level [11].

In contrast, Enrichr functional analysis did not reveal significant enrichment within KEGG or Reactome signaling pathways for genes with reduced expression in children with allergies. However, the identified association of these genes with the Golgi apparatus in the cellular components category may indicate specific impairments in post-translational modification and protein secretion processes necessary for proper immune system function. This observed decrease in the expression of genes associated with the Golgi apparatus may indicate the development of endoplasmic reticulum stress in the studied cells. It is likely that the massive biosynthesis and intense secretion of proinflammatory cytokines, characteristic of activated T-helper cells in allergy, lead to an overload of the secretory apparatus, causing adaptive or destructive changes in the functions of vesicular transport organelles [12].

The discovery of interferon response-related genes among our hub genes is especially significant because it suggests their potential role in the development of food allergies. In our study these genes showed significantly increased expression in children with food allergy. For instance, the *USP18* gene encodes an enzyme that acts as a key negative regulator of the type I interferon (IFN) signaling pathway. The observed upregulation of USP18 might represent a compensatory mechanism to control the heightened cellular response to inflammation. This contrasts with conditions like vitiligo, where *USP18* expression is notably decreased [13]. In cancer studies, loss of *USP18* reduces the growth of lung cancer cell lines, particularly those with activated KRAS, indicating its influence on cell proliferation [14]. Additionally, in a metabolic hypertension model, USP18 overexpression inhibited the JAK/STAT pathway, which enhanced cell proliferation and reduced apoptosis, highlighting its involvement in metabolic regulation and cellular stress responses [15].

The 2'-5'-oligoadenylate synthetase *(OAS)* gene family is a group of highly conserved, ubiquitously expressed genes in mammals that play a key role in innate immunity against viral infections. The family includes four members: *OAS1, OAS2*, *OAS3,* and *OASL*. Our results demonstrate a significant increase in *OAS1* and *OAS3* expression in the allergy group. Particular attention is given to *OAS1* as one of the most well-studied members, with its functionality being critical for modulating the immune response. *OAS1* expression is significantly increased during viral, bacterial, and parasitic infections [16]. Moreover, *OAS1* has also been linked to the development of several autoimmune diseases. Notable differences in *OAS1* expression have been observed between patients with systemic lupus erythematosus and healthy individuals, leading to its consideration as a potential biomarker for this disease [17].

In turn, the *OAS3* gene also plays a crucial role in antiviral immunity, where its activation causes the destruction of viral RNA. Studies have demonstrated that *OAS3* is a key regulator of innate antiviral immune responses, and its absence results in increased viral replication [18]. Additionally, increased expression of this gene is observed in various autoimmune and systemic diseases, such as lupus nephritis and Sjogren's syndrome [19].

The upregulation of these genes in our study suggests a state of pre-activated innate immunity in children with food allergies. Notably, while *OAS1* and *OAS3* were significantly elevated, *OAS2* did not show a significant difference between the groups ($p = 0.805$).

The *IFIT2* and *IFIT3* genes are also crucial in the innate immune response and were found to be overexpressed in the allergy group. The increased expression of *IFIT2* observed in our study is consistent with findings in patients with seasonal allergic rhinitis, where its expression rises in response to allergens to regulate mucosal barrier function [20]. Additionally, *IFIT2* deficiency has been shown to increase vulnerability to autoimmune inflammation [21]. During neurotropic coronavirus infection, *IFIT2* is essential for limiting viral replication and preventing the development of encephalitis [22]. Furthermore, the link between *IFIT3* and autoimmune diseases like psoriasis, where it promotes inflammation, supports our finding that interferon-inducible genes are overexpressed during allergic inflammation [23,24].

The *IFI35* gene, which encodes an interferon-inducible protein of approximately 35 kDa, was also identified in our study as a hub gene with significantly increased expression in infants with IgE-mediated food allergy. This finding aligns with the overall elevation in the expression of genes involved in the interferon response observed in our analysis [25].

Intracellularly, *IFI35* interacts with components of the RIG-I pathway and can suppress RIG-I-mediated IFN-I induction. Additionally, *IFI35* interacts with viral proteins, which modifies the antiviral response depending on the specific pathogen. Besides its intracellular role, *IFI35* also has extracellular functions. When cells are injured or strongly stimulated, IFI35 is released into the extracellular space, acting as a DAMP. This activity allows it to activate macrophages via TLR4, leading to NF-κB activation and the secretion of proinflammatory cytokines. This response has been linked to the severity of systemic inflammation [26-28].

The *IFIH1* gene encodes the MDA5 receptor, which acts as a cytoplasmic sensor for viral double-stranded RNA. Activation of this receptor initiates the signaling pathway through MAVS → IRF3/7 → IFN-I and NF-κB, a process essential for starting antiviral immunity [29]. In mouse model studies, the absence of *IFIH1* results in decreased IFN-β production and increased vulnerability to viruses [30], while in humans, its functions are linked to the severity of respiratory tract infections and viral flare-ups of asthma [31]. Additionally, *IFIH1* is associated with autoimmune disease. For instance, certain mutations in this gene offer a protective effect by lowering the risk of developing type 1 diabetes mellitus [32].

The *DDX58* gene encodes the cytosolic receptor RIG-I, which is part of the RLR family and recognizes viral

5'-triphosphate and structured RNAs. RIG-I activation leads to signal transduction through the MAVS adapter, followed by activation of transcription factors IRF3/7 and NF-κB. This process triggers the production of type I interferons and proinflammatory cytokines, a key mechanism of innate antiviral response [33]. Clinically, the role of *DDX58* is well established in RNA viral infections. Defects or reduced activity of RIG-I are linked to increased sensitivity to various respiratory viruses. Several studies on the interaction of antiviral RLR pathways with epithelial and immune cells of the respiratory tract have shown that impaired RIG-I signaling correlates with more severe virus-induced flares of allergic diseases [31,34]. This highlights the biological potential for cross-regulation between antiviral defense and allergic inflammation.

The *MX1* gene encodes a protein that is a crucial part of the innate immune response, particularly in combating viral infections. Meanwhile, researchers have observed overexpression of *MX1* in a group of patients with diabetes mellitus and atherosclerosis [35]. Additionally, other studies have found a connection between *MX1* and the severity of viral asthma symptoms and asthma exacerbations [36].

The results of this study are exclusively based on bioinformatic analyses of transcriptome datasets. While computational modeling and statistical analyses enable identification of potentially significant markers and pathways, they cannot substitute for experimental validation. Challenges such as biological variability, post-translational modifications, and regulatory mechanisms, which are not always reflected in mRNA expression profiles, remain. Therefore, to confirm the validity and clinical relevance of the identified hub genes, functional studies both in vitro and in vivo, as well as clinical investigations with subsequent correlation analyses between gene expression and clinical outcomes, are essential.

Building upon these findings, the identification of key genes regulating the interferon response and antiviral defense mechanisms opens new horizons for the development of biomarkers for the diagnosis and prognosis of food allergies. Hub genes such as *USP18, IFIT3, OAS1*, and others demonstrate potential as targets for pharmacological modulation of the immune response aimed at restoring the balance between pro-inflammatory and anti-inflammatory processes. Their role can be realized within the framework of personalized medicine, enabling the early identification of children at risk of severe allergies and facilitating the development of targeted therapeutic strategies. Furthermore, understanding the mechanistic aspects of antiviral response dysfunction contributes to a deeper comprehension of the pathogenesis of allergic diseases, thereby improving clinical guidelines and preventive approaches.

Despite these promising insights, it is important to acknowledge certain limitations of the current study. Specifically, the cohort size in this study is relatively small, which may limit statistical power and reduce sensitivity to detecting some biological effects. However, this scale of study is common when examining highly specialized and clinically homogeneous groups, allowing for the collection of highly specific and relevant data. The homogeneity of the age group and the limited range of clinical characteristics reflect careful selection and decrease the influence of confounding factors, but also restrict the ability to account for genetic and epigenetic diversity. Nevertheless, this specificity also restricts the ability to fully account for broader genetic and ethnic diversity. While the identified interferon signature appears robust across the total cohort, it is essential to consider that the dataset originates from a multi-ethnic population. Given that innate immune response genes often possess well-documented genetic polymorphisms that vary by ancestry, their expression patterns may exhibit population-specific nuances. Consequently, further studies in more ethnically homogeneous or, conversely, specifically diverse populations are required to determine the universal applicability of these transcriptomic markers in the context of food allergy. To verify and build upon the results, it is recommended to conduct studies with larger and more diverse samples, enhancing the overall validity and reproducibility of the findings.

Conclusion

The bioinformatics analysis conducted identified key genes and signaling pathways associated with IgE-mediated food allergy in young children. Our results suggest that the upregulation of genes related to the interferon response and antiviral defense is associated with the disease's development. The ten identified hub genes are involved in regulating innate immunity and may influence inflammatory and antiviral activities. Therefore, changes in the expression of these genes suggest a potential immune imbalance in food allergy, highlighting them as candidate biomarkers and potential therapeutic targets that require further independent validation and experimental research to confirm their clinical utility.

Author Contributions: Conceptualization, A.A. and T.N.; methodology, A.A. and B.S.; formal analysis, A.A. and B.S.; writing – original draft preparation, A.A., B.S. and N.S; writing – review and editing, A.A. and T.N.; visualization, B.S. All authors have read and agreed to the published version of the manuscript.

Disclosures: The authors have no conflicts of interest.

Acknowledgments: None.

Funding: None.

Data availability statement: The corresponding author can provide the data supporting the study's conclusions upon request.

Artificial Intelligence (AI) Disclosure Statement: The authors declare no AI Tools used for preparation of this work.

References

1. Arens A, Lange L, Stamos K. Epidemiology of food allergy. *Allergo J Int.* 2025;34:121–126. https://doi.org/10.1007/s40629-025-00336-w.
2. Tedner SG, Asarnoj A, Thulin H, Westman M, Konradsen JR, Nilsson C. Food allergy and hypersensitivity reactions in children and adults-A review. *Journal of internal medicine.* 2022;291(3):283-302. https://doi.org/10.1111/joim.13422.

3. Li Q, Tang X, Huang L, Wang T, Huang Y, Jiang S. Anti-allergic effect of vitamin C through inhibiting degranulation and regulating TH1/TH2 cell polarization. *J Sci Food Agric.* 2024;104(10):5955-5963. https://doi.org/10.1002/jsfa.13419.
4. Arzola-Martínez L, Ptaschinski C, Lukacs NW. Trained innate immunity, epigenetics, and food allergy. Front Allergy. 2023;4:1105588. https://doi:10.3389/falgy.2023.1105588.
5. Di Costanzo M, De Paulis N, Capra ME, Biasucci G. Nutrition during Pregnancy and Lactation: Epigenetic Effects on Infants' Immune System in Food Allergy. *Nutrients*. 2022;14(9):1766. https://doi:10.3390/nu14091766.
6. Cañas JA, Núñez R, Cruz-Amaya A, Gómez F, Torres MJ, Palomares F, Mayorga C. Epigenetics in Food Allergy and Immunomodulation. *Nutrients*. 2021;13(12):4345. https://doi.org/10.3390/nu13124345.
7. Martino D, Neeland M, Dang T, et al. Epigenetic dysregulation of naive CD4+ T-cell activation genes in childhood food allergy. *Nat Commun.* 2018;9(1):3308. https://doi.org/10.1038/s41467-018-05608-4
8. Xiong P, Liu T, Huang H, et al. IL-27 overexpression alleviates inflammatory response in allergic asthma by inhibiting Th9 differentiation and regulating Th1/Th2 balance. *Immunopharmacol Immunotoxicol.* 2022;44(5):712-718. https://doi.org/10.1080/08923973.2022.2077755
9. Li Q, Deng Y, Xu Z, Zhou H. Combined transcriptomics and TMT-proteomics reveal abnormal complement and coagulation cascades in cow's milk protein allergy. I*nt Immunopharmacol.* 2024;131:111806. https://doi.org/10.1016/j.intimp.2024.111806
10. Zhen J, Zhao P, Li Y, et al. The Multiomics Analyses of Gut Microbiota, Urine Metabolome and Plasma Proteome Revealed Significant Changes in Allergy Featured with Indole Derivatives of Tryptophan. *J Asthma Allergy.* 2022;15:117-131. https://doi.org/10.2147/JAA.S334752
11. Zhang W, Sun L, Wang Y, et al. Identification of significant potential signaling pathways and differentially expressed proteins in patients with wheat intolerance based on quantitative proteomics. *J Proteomics.* 2021;246:104317. https://doi.org/10.1016/j.jprot.2021.104317
12. Zhou Y, Chen Y, Li J, et al. The development of endoplasmic reticulum-related gene signatures and the immune infiltration analysis of sepsis. *Front Immunol.* 2023;14:1183769. https://doi.org/10.3389/fimmu.2023.1183769
13. Lee EJ, Kim JY, Yeo JH, Park S, Bae YJ, Kwon IJ, Seong SH, Lee J, Oh SH. ISG15-USP18 Dysregulation by Oxidative Stress Promotes IFN-γ Secretion from CD8+ T Cells in Vitiligo. *J Invest Dermatol*. 2024;144(2):273-283.e11. https://doi:10.1016/j.jid.2023.08.006.
14. Mustachio LM, Lu Y, Tafe LJ, Memoli V, Rodriguez-Canales J, Mino B, Villalobos PA, Wistuba I, Katayama H, Hanash SM, Roszik J, Kawakami M, Cho KJ, Hancock JF, Chinyengetere F, Hu S, Liu X, Freemantle SJ, Dmitrovsky E. Deubiquitinase USP18 Loss Mislocalizes and Destabilizes KRAS in Lung Cancer. *Mol Cancer Res.* 2017;15(7):905-914. https://doi.org/10.1158/1541-7786.MCR-16-0369.
15. Xie Z, Huang M, Xu W, Liu F, Huang D. USP18 Curbs the Progression of Metabolic Hypertension by Suppressing JAK/STAT Pathway. *Cardiovasc Toxicol.* 2024;24(6):576-586. https://doi:10.1007/s12012-024-09860-7.
16. Yang R, Du Y, Zhang M, Liu Y, Feng H, Liu R, Yang B, Xiao J, He P, Niu F. Multi-omics analysis reveals interferon-stimulated gene OAS1 as a prognostic and immunological biomarker in pan-cancer. *Front Immunol.* 2023;14:1249731. https://doi:10.3389/fimmu.2023.1249731.
17. Chen H, Huang L, Jiang X, Wang Y, Bian Y, Ma S, Liu X. Establishment and analysis of a disease risk prediction model for the systemic lupus erythematosus with random forest. *Front Immunol.* 2022;13:1025688. https://doi:10.3389/fimmu.2022.1025688.
18. Li Y, Banerjee S, Wang Y, Goldstein SA, Dong B, Gaughan C, Silverman RH, Weiss SR. Activation of RNase L is dependent on OAS3 expression during infection with diverse human viruses. *Proc Natl Acad Sci USA*. 2016;113(8):2241-6. https://doi.org/10.1073/pnas.1519657113.
19. Rigi Yousefabadi E, Ourang Z, Gharibdoost F, Faezi ST, Saatchi M, Gholami D, Esmaeilzadeh E, Khorram Khorshid HR. Hypomethylation of OAS2 and OAS3 Gene Promoters: Insights into the Pathogenesis of Systemic Lupus Erythematosus. *Iran J Immunol.* 2025;22(2):155-164. https://doi:10.22034/iji.2025.105409.2944.
20. Ndika J, Airaksinen L, Suojalehto H, Karisola P, Fyhrquist N, Puustinen A, Alenius H. Epithelial proteome profiling suggests the essential role of interferon-inducible proteins in patients with allergic rhinitis. *J Allergy Clin Immunol.* 2017;140(5):1288-1298. https://doi:10.1016/j.jaci.2017.05.040.
21. Kim D, Rai NK, Burrows A, Kim S, Tripathi A, Weinberg SE, Dutta R, Sen GC, Min B. IFN-Induced Protein with Tetratricopeptide Repeats 2 Limits Autoimmune Inflammation by Regulating Myeloid Cell Activation and Metabolic Activity. *J Immunol.* 2023;210(6):721-731. https://doi:10.4049/jimmunol.2200746.
22. Butchi NB, Hinton DR, Stohlman SA, Kapil P, Fensterl V, Sen GC, Bergmann CC. Ifit2 deficiency results in uncontrolled neurotropic coronavirus replication and enhanced encephalitis via impaired alpha/beta interferon induction in macrophages. *J Virol.* 2014;88(2):1051-64. https://doi:10.1128/JVI.02272-13.
23. Li X, Zhou W, Wang D. Integrative bioinformatic analysis identified IFIT3 as a novel regulatory factor in psoriasis. *J Cell Biochem*. 2022;123(12):2066-2078. https://doi.org/10.1002/jcb.30332.
24. Tian K, Guo J, Yan Q, Wang N. A Potential CD8+ T-Cell-Related Biomarker IFIT3 for Rheumatoid Arthritis. *Int J Rheum Dis.* 2025;28(8):e70385. https://doi:10.1111/1756-185x.70385.
25. De Masi R, Orlando S, Bagordo F, Grassi T. IFP35 Is a Relevant Factor in Innate Immunity, Multiple Sclerosis, and Other Chronic Inflammatory Diseases: *A Review. Biology (Basel).* 2021;10(12):1325. https://doi:10.3390/biology10121325.
26. Das A, Dinh PX, Panda D, Pattnaik AK. Interferon-inducible protein IFI35 negatively regulates RIG-I antiviral signaling and supports vesicular stomatitis virus replication. *J Virol.* 2014;88(6):3103-13. https://doi:10.1128/JVI.03202-13.
27. Yang H, Winkler W, Wu X. Interferon Inducer IFI35 regulates RIG-I-mediated innate antiviral response through mutual antagonism with Influenza protein NS1. *J Virol.* 2021;95(11):e00283-21. https://doi:10.1128/JVI.00283-21.
28. Xiahou Z, Wang X, Shen J, Zhu X, Xu F, Hu R, Guo D, Li H, Tian Y, Liu Y, Liang H. NMI and IFP35 serve as proinflammatory DAMPs during cellular infection and injury. *Nat Commun.* 2017;8(1):950. https://doi:10.1038/s41467-017-00930-9.
29. Kato H, Takeuchi O, Sato S, Yoneyama M, Yamamoto M, Matsui K, Uematsu S, Jung A, Kawai T, Ishii KJ, Yamaguchi O, Otsu K, Tsujimura T, Koh CS, Reis e Sousa C, Matsuura Y, Fujita T, Akira S. Differential roles of MDA5 and RIG-I helicases in the recognition of RNA viruses. *Nature*. 2006;441(7089):101-5. https://doi:10.1038/nature04734.

30. Kuo RL, Kao LT, Lin SJ, Wang RY, Shih SR. MDA5 plays a crucial role in enterovirus 71 RNA-mediated IRF3 activation. *PLoS One.* 2013;8(5):e63431. https://doi:10.1371/journal.pone.0063431.
31. Radzikowska U, Eljaszewicz A, Tan G, Stocker N, Heider A, Westermann P, Steiner S, Dreher A, Wawrzyniak P, Rückert B, Rodriguez-Coira J, Zhakparov D, Huang M, Jakiela B, Sanak M, Moniuszko M, O'Mahony L, Jutel M, Kebadze T, Jackson DJ, Edwards MR, Thiel V, Johnston SL, Akdis CA, Sokolowska M. Rhinovirus-induced epithelial RIG-I inflammasome suppresses antiviral immunity and promotes inflammation in asthma and COVID-19. *Nat Commun.* 2023;14(1):2329. https://doi:10.1038/s41467-023-37470-4.
32. Nejentsev S, Walker N, Riches D, Egholm M, Todd JA. Rare variants of IFIH1, a gene implicated in antiviral responses, protect against type 1 diabetes. *Science*. 2009;324(5925):387-9. https://doi:10.1126/science.1167728.
33. Onomoto K, Onoguchi K, Yoneyama M. Regulation of RIG-I-like receptor-mediated signaling: interaction between host and viral factors. *Cell Mol Immunol.* 2021;18(3):539-555. https://doi:10.1038/s41423-020-00602-7.
34. Rehwinkel J, Gack MU. RIG-I-like receptors: their regulation and roles in RNA sensing. *Nat Rev Immunol.* 2020;20:537–551. https://doi.org/10.1038/s41577-020-0288-3.
35. Wang G, Hua R, Chen X, He X, Dingming Y, Chen H, Zhang B, Dong Y, Liu M, Liu J, Liu T, Zhao J, Zhao YQ, Qiao L. MX1 and UBE2L6 are potential metaflammation gene targets in both diabetes and atherosclerosis. *PeerJ.* 2024;12:e16975. https://doi:10.7717/peerj.16975.
36. Loisel DA, Du G, Ahluwalia TS, Tisler CJ, Evans MD, Myers RA, Gangnon RE, Kreiner-Møller E, Bønnelykke K, Bisgaard H, Jackson DJ, Lemanske RF Jr, Nicolae DL, Gern JE, Ober C. Genetic associations with viral respiratory illnesses and asthma control in children. *Clin Exp Allergy.* 2016;46(1):112-24. https://doi:10.1111/cea.12642.

JOURNAL OF CLINICAL MEDICINE OF KAZAKHSTAN (E-ISSN 2313-1519)
Original Article DOI: https://doi.org/10.23950/jcmk/18011

The Effect of Postmenopausal Therapeutic Interventions on Sexual Function: a Meta-analysis Study

Sibel Yücetürk[1], Nurten Özçalkap[2], Ayşe Çuvadar[3], Yeter Çuvadar Baş[4]

[1]*Department of Midwifery, Faculty of Health Sciences, Sinop University, Sinop, Turkey*
[2]*Department of Midwifery, Faculty of Health Sciences, Ağri Ibrahim Cecen University, Ağri, Turkey*
[3]*Department of Midwifery, Faculty of Health Sciences, Karabuk University, Karabuk, Turkey*
[4]*Vacational School, Gedik University, Istanbul, Turkey*

Received: 2026-01-04.
Accepted: 2026-02-20.

This work is licensed under a **Creative Commons Attribution 4.0 International License**

J Clin Med Kaz 2026; 23(2): 72-78

Corresponding author:
Sibel Yücetürk.
E-mail: sibelduman8771@gmail.com.
ORCID: 0000-0003-0820-6997.

ABSTRACT

Aim: The purpose of this study is to identify how therapeutic interventions after menopause affect sexual function.

Methods: For this study, research was conducted by screening studies in PubMed, Web of Science, EBSCOhost, Google Scholar, and YOK Thesis Center databases from May to July 2024. After reviewing the studies, five studies were included in the meta-analysis. The quality assessment of the studies was conducted using a quality assessment tool prepared by The Joanna Briggs Institute, according to Randomized Controlled Trials and Quasi-Experimental design studies. CMA Version 2 was used for data synthesis. The data were synthesized using meta-analysis and narrative synthesis methods.

Results: According to the results of the meta-analysis, therapeutic interventions applied during the postmenopausal period were found to not be effective on sexual function (SMD: 1.056, 95% CI: -0.171 to 2.282; Z= 1.686, p = 0.092, I2= 97.827%). These findings indicate that, when all intervention types are evaluated together, there is no statistically significant overall improvement in postmenopausal sexual function and that the results are highly heterogeneous across studies. However, subgroup analyses revealed that pelvic floor muscle training (PFMT) demonstrated a strong and statistically significant positive effect on sexual function in women with sexual dysfunction ($p < 0.000$), suggesting that the effectiveness of interventions varies according to intervention type. From a clinical perspective, this finding indicates that PFMT may represent a practical and targeted non-pharmacological option for improving sexual function in postmenopausal women, despite the absence of a significant overall pooled effect.

Conclusion: While pelvic floor muscle training (PFMT) appears to be a promising intervention for improving postmenopausal sexual dysfunction, this finding is based on limited evidence and should be interpreted with caution. Given the variability in intervention types and study quality, further high-quality randomized controlled trials are needed to evaluate the comparative effectiveness of PFMT and other therapeutic approaches, as well as their potential combinations, in order to establish more definitive conclusions.

Keywords: Menopause, therapeutic intervention, sexual function, pelvic floor muscle training, meta-analysis

Introduction

Menopause is a process characterized by hormonal and physical changes in women's bodies [1]. Sexual problems are common throughout life, but women going through menopause are more sensitive to such disorders and have a higher risk of experiencing sexual dysfunction

during this period [1,2]. Sexual function is a multidimensional concept encompassing cognitive and physiological elements of sexuality, including desire, arousal, and fantasies [3]. The World Health Organization defines sexual dysfunction as the inability of an individual to engage in sexual intercourse as desired. Sexual health contributes to personal well-being and interpersonal relationships by promoting harmony between the mind, emotions, and body [4]. Sexual dysfunction refers to psychophysiological disorders that cause a significant decrease in sexual desire and arousal, negatively affecting individuals' lives and being among important sexual health problems [5]. Sexual dysfunction can significantly affect social relationships and overall quality of life, thereby creating a need for the development, evaluation, and dissemination of effective treatment approaches [6].

Costello et al. reported a prevalence of sexual dysfunction in half of postmenopausal women, and stated that the frequency of these problems increases with age [7]. In a survey conducted in six European countries, one third of the participants stated that they experienced a loss of libido during menopause, while more than half expressed a decrease in sexual desire [8]. Sexual problems experienced during menopause are often perceived as highly personal and distressing and may have socially and physically disruptive consequences. In addition, these problems reduce women's self-confidence, lead to stress, problems in relationships, and divorces, and create barriers such as fear of stigma, feelings of shame, and discomfort related to sexuality in the use of current treatments [9].

Significant changes can occur in women's sexual lives during the menopausal period. It is known that approximately 47% of women aged between 65 and 71 are still sexually active, highlighting the continued importance of sexual health in later life. However, a decline in sexual activity is frequently observed in this age group. The main causes include genital atrophy and dryness, decreased muscle tone, pain associated with chronic diseases, psychosocial problems, stroke, and side effects of medications [10]. Increased vaginal tissue sensitivity may also result in bleeding during sexual intercourse. Changes such as a reduction in uterine volume and atrophy of breast tissue are also characteristic features of this period [11]. Therefore, supporting access to a healthy sexual life for women in the menopausal and postmenopausal periods is of great importance for maintaining both physical and psychosocial well-being [10].

There is a strong connection between psychosocial factors and sexual dysfunction, therefore cognitive therapies and sex therapies play an important role in the treatment of sexual dysfunction [12]. These approaches aim to provide individuals with accurate and sufficient information about sexuality and to address maladaptive beliefs and emotional responses. Lack of sexual knowledge can lead to the emergence of false beliefs, feelings of guilt, and excessive anxiety in individuals, paving the way for the development of sexual problems. Accordingly, educational, cognitive, and psychosocial interventions are considered essential components of comprehensive sexual health care, alongside physiological treatments [13].

To date, there is limited meta-analytic evidence specifically focusing on the effects of therapeutic approaches on sexual function in menopausal and postmenopausal women. This study aims to address this important gap by providing a comprehensive synthesis of the available evidence. As a meta-analysis addressing this specific topic, the study offers an integrated evaluation of therapeutic interventions and underscores the importance of developing effective strategies to improve sexual health and quality of life in postmenopausal women.

The hypotheses of the study

H0 (Null Hypothesis): Therapeutic interventions in the postmenopausal period have no significant effect on women's sexual function.

H1 (Alternative Hypothesis): Therapeutic interventions in the postmenopausal period improve women's sexual function.

Methods

This study is a meta-analysis conducted in accordance with the PRISMA checklist (Preferred Reporting Items for Systematic Reviews and Meta-Analyses Protocols, PRISMA Checklist) [14]. To minimize bias in the study, four researchers (A.Ç; S.Y; N.Ö; Y.Ç.B) independently conducted the literature review, article selection, and data extraction processes. Each phase of the review was performed independently by individual reviewers to ensure objectivity and reliability. Afterward, the decisions were reviewed and any discrepancies were resolved through consensus among the researchers. Furthermore, the number of times each record was screened and the specific reviewers involved at each stage were documented to provide transparency. The studies included in the meta-analysis were rigorously assessed for quality by the same researchers, ensuring the validity of the results.

Population (P): Women in the postmenopausal period.

Intervention (I): This meta-analysis included three clearly specified therapeutic interventions: education-based programs, pelvic floor muscle training, and motivational interviewing, each aimed at improving sexual function in postmenopausal women.

Comparison (C): Groups receiving no therapeutic intervention.

Outcomes (O): Sexual function outcomes, including standardized measures and variability indicators (e.g., SD, 95% CI).

Study design (S): Experimental and quasi-experimental studies published in Turkish and English.

Exclusion Criteria: Letters to the editor, qualitative studies, case reports, case presentations, and studies of systematic and traditional review nature were excluded from this research. Only studies that included postmenopausal women were eligible for inclusion in this meta-analysis. Studies focusing on premenopausal or perimenopausal participants were excluded to maintain homogeneity in the study population.

Search Strategy

A search was conducted between February and June 2024 using the keywords ((((((menopause) OR (climacteric))) OR (postmenopausal)) OR (postmenopausal women)) AND (sexual function)) AND (sexual dysfunction)) OR (dyspareunia)) OR (dyspareunia) in PubMed, Web of Science, EBSCOhost, YOK National Thesis Center, and Google Scholar, and the studies were transferred to Mendeley. No year limit has been set in the literature review.

Selection of Studies

After the screening process, initially 6416 records were identified through database searches. Following the removal of 2154 duplicates, 4262 records remained and were screened based on titles and abstracts. At this stage, 4205 studies were excluded for being irrelevant to the research topic. As a result, 57 studies were selected for full-text review. During the full-text assessment, 52 studies were excluded based on the predefined inclusion and exclusion criteria (e.g., studies not focusing solely

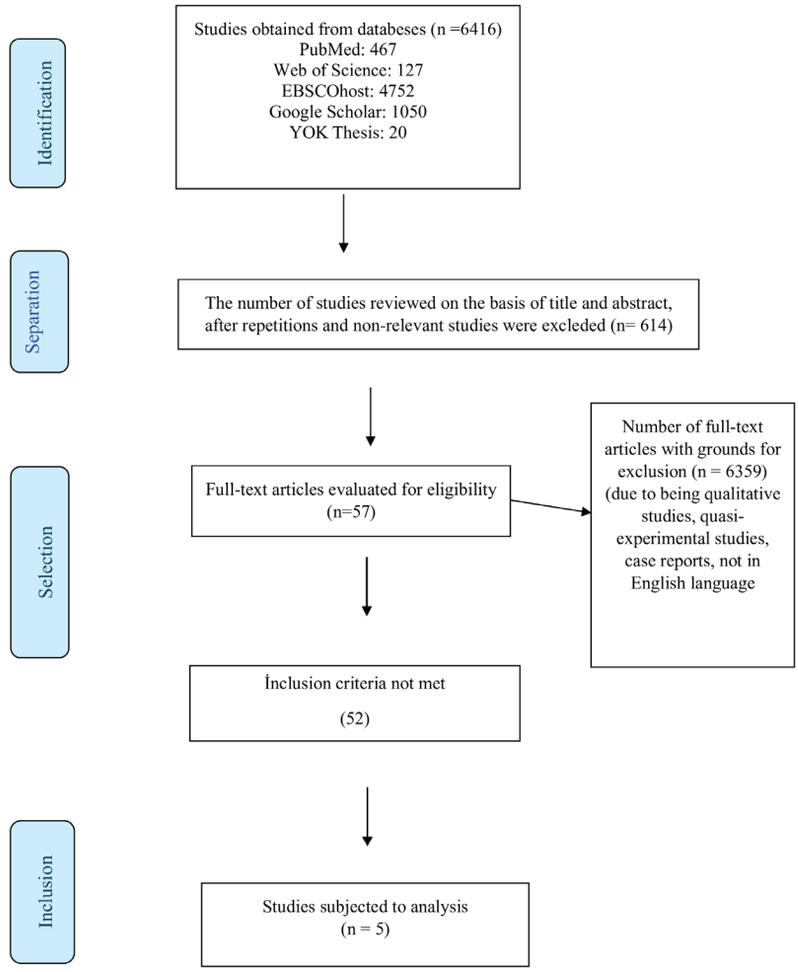

Figure 1 – Selection of studies according to PRISMA flow diagram

on postmenopausal women, lack of therapeutic intervention, or absence of sexual function outcomes). Finally, 5 studies that evaluated the effects of therapeutic interventions on sexual function in postmenopausal women were included in the meta-analysis.

A detailed description of the article selection process is provided in Figure 1.

Data Extraction

Researchers used a data extraction tool they developed specifically for this systematic review and meta-analysis to gather data. The tool was designed in accordance with established methodological recommendations for meta-analytic studies to ensure consistency and reproducibility. This tool allowed for the organized compilation and incorporation of studies in systematic reviews and meta-analyses, collecting data (e.g., intervention and control groups related to the studies, mean post-test scores, and standard deviation values) on authors and publication year of included studies, country in which the studies were carried out, sample size, patient group, scale used in the studies, main results, and quality score (Table 1).

Data extraction was conducted independently by two researchers using the same standardized extraction form. Discrepancies were resolved through discussion, and consensus was achieved. This structured approach strengthened methodological transparency and enhanced the reproducibility of the study.

Ethical Principles

This study was conducted as a meta-analysis based on research published in the literature.

Evaluation of the Methodological Quality of Studies

The methodological quality of the studies included in the meta-analysis was evaluated using the quality assessment tool developed by the Joanna Briggs Institute (JBI) for randomized controlled trials, consisting of 13 questions [15] and the quality assessment tool developed for quasi-experimental studies consisting of 9 questions [16]. The questions in this evaluation tool were answered with "Yes," "No," "Uncertain," and "Not Applicable" options. Two researchers independently evaluated the methodological quality of the studies and the results for all studies included in the meta-analysis were determined through discussion. The evaluation results of each study were presented as "Quality Score" in Table 1.

Data Synthesis

In this study, we used Comprehensive Meta-Analysis (CMA) Ver. 2 software for statistical analysis. Heterogeneity between studies was assessed using the Chi-square test and Higgins I^2 statistic. An I^2 value above 50% was seen as a significant indicator of heterogeneity. Studies with $I^2 \leq 50\%$ and p-value > .1 were examined using a fixed effects model, while studies with $I^2 > 50\%$ and p-value > .1 were assessed using a random effects model [17]. Furthermore, the Tau-squared (τ^2) statistic was used to analyze the variance and heterogeneity between

Table 1 Characteristics and Results of the Included Studies

Author/Year	Study Design	Sample size	Scale	Type of Therapeutic intervention	Patient population	Quality Score
Jalambadani et al. 2017 [19]	Quasi-experimental	Experimental group:90 Control group:90	Female Sexual Function Index (FSFI)	Education	Sexual dysfunction	Yes:8/9 No:0/9 Uncertain:1/9
Kamalak and Aksoy Derya 2023 [20]	Randomized Control	Experimental group:68 Control group:81	Female Sexual Function Index (FSFI)	Motivational interview	Sexual dysfunction	Yes:11/13 No:1/13 Uncertain:0/13 Not applicable:0/13
Mohammadi et al. 2024 [21]	Quasi-experimental	Experimental group:44 Control group:44	Female Sexual Function Index (FSFI)	Education	Sexual dysfunction	Yes:8/9 No:0/9 Uncertain:1/9
Nazarpour et al. 2017 [22]	Randomized Control	Experimental group:48 Control group:50	Female Sexual Function Index (FSFI))	Education	Sexual dysfunction	Yes:10/13 No:2/13 Uncertain:1/13 Not applicable:0/13
Nazarpour et al. 2018 [3]	Randomized Control	Experimental group:47 Control group:50	Female Sexual Function Index (FSFI)	Pelvic Floor Muscle Training	Sexual dysfunction	Yes:10/13 No:2/13 Uncertain:1/13 Not applicable:0/13

studies in more detail. To compare effect sizes obtained using different measurement tools, the standardized mean difference (SMD) with a 95% confidence interval (CI) was utilized. Forest plots were generated to display effect sizes with 95% CI, and the average of SMD values was computed to determine the overall effect size. The average D value was transformed into a Z score to assess its statistical significance. Funnel plots were employed to investigate and display publication bias, and any asymmetries in the funnel plot suggested potential publication bias. Additionally, Egger's test was used to objectively evaluate publication bias. Two-tailed p-values were calculated for all statistical analyses, with a significance level of 0.05 considered [18].

Results

Three of the studies included in the work were conducted in a randomized controlled experimental design, while two were conducted in a semi-experimental nature. The total sample size of the studies consists of 297 participants in the intervention group and 315 participants in the control group, totaling 612 participants (Table 1).

It has been determined that more than 50% of the items of the evidence quality assessment tool are met by all studies included in the meta-analysis (Table 1). This finding is important in terms of showing that the information presented in the meta-analysis is based on studies with an acceptable level of evidence quality.

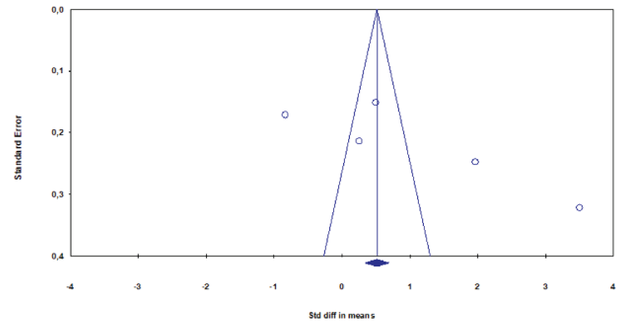

Figure 2 – Funnel plots of the studies

Meta-Analysis Results of The Studies

In this study, we determined whether there is publication bias using (a) funnel plot (Figure 2) and (b) Egger's Regression Test [23].

In this dataset, the intercept (B0) obtained using the Egger method is calculated as 19.08976, with a 95% confidence

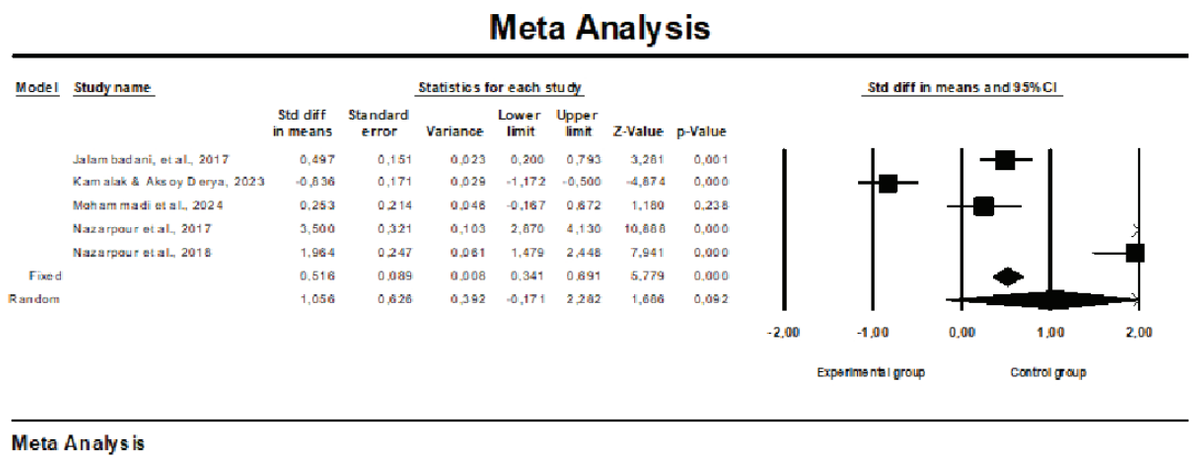

Figure 3 – Forest graph related to studies

Table 2 Moderator Results on the Effect of Therapeutic Interventions Applied to Women with Sexual Dysfunction in the Postmenopausal Period

Moderator	The number of studies	Effect size	Standard error	Lower limit	Upper limit	p
Type of therapeutic intervention						
Education	3	0.891	0.467	-0.024	1.807	0.056
Motivational interview	1	-0.836	0.171	-1.172	-0.500	<0.001
Pelvic Floor Muscle Training	1	3.500	0.321	2.870	4.130	<0.000
Total	5	0.197	0.144	-0.085	0.479	0.170

interval ranging from -8.85373 to 47.03326. The calculated t value is 2.17411, degrees of freedom (df) is 3, and the two-tailed p value is 0.11800. These results indicate that publication bias is not statistically significant (p = 0.11800).

Three randomized controlled trials (RCT) with 612 participants, and 2 quasi-experimental studies measured post-intervention sexual function scores using the Female Sexual Function Index (FSFI) [3,19,20,21,22]. The meta-analysis based on the findings of these studies (SMD: 1.056, 95% CI: -0.171 to 2.282; Z= 1.686, p = 0.092) supports that therapeutic interventions in the postmenopausal period do not have a statistically significant effect on sexual dysfunction. Additionally, a high level of heterogeneity was found among the studies (I2= 97.827) (Figure 3).

The average effect size values of the therapeutic intervention applied in the study were found to be 0.197 (CI -0.085 to 0.479, p>0.05). This result indicates that it is not statistically significant. However, the effect of PFMT is quite high (3.500) and the p-value is significant (p < 0.000), which shows that pelvic floor muscle exercises have a strong effect (Table 2).

Discussion

In this study, our goal was to assess the impact of therapeutic interventions on sexual function in postmenopausal women. In line with the study hypotheses, the overall findings indicated that therapeutic interventions did not lead to a statistically significant improvement in sexual function, thereby supporting the null hypothesis (H0) and not fully confirming the alternative hypothesis (H1). Our findings indicated that, in general, therapeutic interventions were not effective. The overall effect size for the sexual function variable was determined to be Cohen's d = 1.056 (high level). However, further analysis revealed that pelvic floor muscle training (PFMT) had a stronger effect compared to other interventions, and this difference was statistically significant. This finding suggests that while H1 was not supported for therapeutic interventions as a whole, it was partially supported in the context of PFMT as a specific intervention. These results suggest that PFMT may be a more effective approach to improving sexual function in postmenopausal women.

Importantly, the discrepancy between the non-significant overall pooled effect and the strong positive effect observed in the PFMT subgroup indicates that the effectiveness of therapeutic interventions is highly dependent on intervention type. When interventions with low or inconsistent effects are combined with PFMT in the overall analysis, the pooled estimate may fail to reach statistical significance despite the presence of a highly effective subgroup.

The ineffectiveness of some interventions highlights the need for further research to explore why certain therapeutic approaches did not yield positive outcomes. The rejection of H1 at the overall level may be explained by the heterogeneity of intervention types included in the analysis, particularly education-based programs or motivational interviewing, which may not have been sufficiently tailored to the specific physiological and psychosocial needs of postmenopausal women. In addition, factors such as the duration, intensity, and timing of interventions may have influenced their efficacy.

The very high level of heterogeneity observed in this meta-analysis (I^2 = 97.827%) further suggests that the included studies differed substantially in terms of intervention content, implementation strategies, and outcome assessment methods, which may have diluted the overall pooled effect. Such extreme heterogeneity indicates that the pooled results should be interpreted with caution, as they likely reflect variability between studies rather than a uniform intervention effect.

Even though initial treatment approaches for sexual dysfunction related to menopause concentrate on factors that can be changed, there are currently numerous hormonal and non-hormonal, local and systemic treatment options accessible. However, the partial support of H1 observed for PFMT underscores the importance of incorporating physical and function-oriented interventions into holistic treatment models, as evidenced by the stronger effect of PFMT in our study. Treatment should be individualized taking into account the severity of symptoms, potential side effects, and personal preferences [24]. In a randomized controlled study by Stojanovska and colleagues [25] evaluating the effectiveness of exercise on menopausal symptoms, it was reported that exercise had positive effects on sexual symptoms. In a meta-analysis examining the effects of exercise on quality of life in women with menopausal symptoms, the most common interventions for menopausal and urinary symptoms were determined to be yoga and PFMT, respectively. These findings support the importance of physical interventions like PFMT, which were found to be more effective in our study as well.

The apparent contradiction between the strong effect of PFMT and the non-significant overall effect of therapeutic interventions can be explained by the relatively low or inconsistent effects observed in non-PFMT interventions, such as education-based or motivational approaches, which may have contributed to the attenuation of the pooled estimate. Therefore, the overall non-significant result should not be interpreted as evidence that all therapeutic interventions are ineffective, but rather that intervention-specific effects must be considered when interpreting meta-analytic findings.

Although studies have reported that therapeutic interventions alleviate vasomotor symptoms and are effective in improving overall menopausal symptoms [26,27], they do not appear to have the same positive effects on sexual function during the postmenopausal period. This discrepancy further supports the acceptance of H0 for general therapeutic interventions in relation to sexual function outcomes. A possible reason for this may be that such interventions are generally not initiated during the premenopausal or early menopausal stages. Since sexual dysfunction in the postmenopausal period is influenced

by long-term hormonal, physiological, and psychosocial changes, interventions started at a later stage may have limited effectiveness. Therefore, the timing of therapeutic interventions may be a critical factor in achieving meaningful improvements in sexual function during the postmenopausal period.

Limitation of studies

There are several limitations to this meta-analysis. Firstly, the number of available studies evaluating therapeutic interventions for postmenopausal sexual dysfunction is limited, which restricts the breadth of the analysis and the generalizability of the findings. Secondly, a number of the included studies had small sample sizes, potentially reducing the statistical power and reliability of the pooled results. The inclusion of only five studies may also have limited the robustness of subgroup analyses and increased the uncertainty of the estimated effect sizes. Thirdly, the included studies demonstrated considerable clinical and methodological heterogeneity in terms of intervention types, outcome measures, and follow-up durations. This high heterogeneity ($I^2 = 97.827\%$) may have influenced the magnitude and direction of the pooled effect estimates and complicates the interpretation of the overall meta-analytic findings. In addition, although publication bias was assessed using funnel plots and Egger's regression test, the inclusion of only five studies limits the reliability and interpretability of these methods. Therefore, the absence of statistically significant publication bias should be interpreted with caution. Finally, the lack of prior comprehensive meta-analyses in this area limited the scope of the discussion and comparison with earlier evidence.

Conclusion

This meta-analysis suggests that, overall, therapeutic interventions applied during the postmenopausal period do not lead to significant improvements in sexual function. However, subgroup analysis revealed that pelvic floor muscle training (PFMT) demonstrated greater effectiveness compared to other therapeutic approaches. This finding highlights PFMT as a potentially valuable non-pharmacological intervention for postmenopausal women experiencing sexual dysfunction, particularly in clinical settings where safe, low-cost, and accessible interventions are prioritized. Nevertheless, due to the limited number of studies and the substantial heterogeneity among them, these results should be interpreted with caution. From a clinical perspective, the findings suggest that interventions targeting pelvic floor function may offer more consistent benefits than generalized therapeutic approaches in postmenopausal sexual health management.

In terms of contribution to the existing literature, this meta-analysis provides a comparative synthesis of therapeutic interventions for postmenopausal sexual dysfunction and identifies PFMT as a distinct intervention with a stronger effect size despite the overall non-significant pooled effect. Future research should focus on investigating the methodological limitations and the underlying reasons for the low or inconsistent effects observed in therapeutic interventions other than PFMT, in order to better understand their limited effectiveness and to optimize intervention strategies. Further high-quality randomized controlled trials with larger samples and standardized outcome measures are needed to confirm these findings and guide clinical practice.

Author Contributions: Conceptualization, S.Y., N.Ö., A.Ç. and Y.Ç.B.; methodology, S.Y., N.Ö., A.Ç. and Y.Ç.B.; validation, S.Y., N.Ö., A.Ç. and Y.Ç.B.; formal analysis, S.Y., N.Ö., A.Ç. and Y.Ç.B.; investigation, S.Y., N.Ö., A.Ç. and Y.Ç.B.; resources, S.Y., N.Ö., A.Ç. and Y.Ç.B.; data curation, S.Y., N.Ö., A.Ç. and Y.Ç.B.; writing – original draft preparation, S.Y., N.Ö., A.Ç. and Y.Ç.B.; writing – review and editing, S.Y., N.Ö., A.Ç. and Y.Ç.B.; visualization, S.Y., N.Ö., A.Ç. and Y.Ç.B.; supervision, S.Y., N.Ö., A.Ç. and Y.Ç.B.; project administration, S.Y., N.Ö., A.Ç. and Y.Ç.B.; funding acquisition, S.Y., N.Ö., A.Ç. and Y.Ç.B. All authors have read and agreed to the published version of the manuscript.

Disclosures: The authors have no conflicts of interest.

Acknowledgments: None.

Funding: None.

Data availability statement: All data analyzed in this meta-analysis were derived from previously published studies accessible through academic databases. No new datasets were generated.

Artificial Intelligence (AI) Disclosure Statement: The authors declare no AI Tools used for preparation of this work.

References

1. Asmin N, Sultana S, Habib SH, Khatun KH. Intervention approach to the menopausal women in rural Bangladesh. *Bangladesh Med J.* 2009;38:9-14. https://doi.org/10.3329/bmj.v38i1.3580. https://banglajol.info/index.php/BMJ/article/view/3580.
2. Keriman N. The effectiveness of fennel on the sexual health of postmenopausal women: a systematic review study. *Iran J Obstet Gynecol Infertility.* 2022;25(3):9. https://ijogi.mums.ac.ir/article_20430_en.html.
3. *Nazarpour S, Simbar M, Majd HA, Tehrani FR. Beneficial effects of pelvic floor muscle exercises on sexual function among postmenopausal women: A randomised clinical trial. *Sex Health.* 2018;15:396–402. https://doi.org/10.1071/SH17203. https://connectsci.au/sh/article-lookup/doi/10.1071/sh17203.
4. World Health Organization. Defining sexual health. Report of a technical consultation on sexual health, 28-31 January 2002, Geneva. Sexual health document series. *Geneva*, 2006:35. https://www.scirp.org/reference/ReferencesPapers?ReferenceID=1998000. Accessed September 10, 2025.
5. Tehrani FR, Farahmand M, Simbar M, Afzali HM. Factors associated with sexual dysfunction; a population-based study in Iranian reproductive age women. *Arch Iran Med*. 2014;17:679–84. https://pubmed.ncbi.nlm.nih.gov/25305767/.
6. Stephenson KR, Kerth J. Effects of mindfulness-based therapies for female sexual dysfunction: A meta-analytic review. *The Journal Of Sex Research.* 2017;54(7):832–849. https://doi.org/10.1080/00224499.2017.1331199.

7. Castelo-Branco C, Blumel JE, Araya H, Riquelme R, Castro G, Haya J, Gramegna G. Prevalence of sexual dysfunction in a cohort of middle-aged women: influences of menopause and hormone replacement therapy. *J Obstet Gynaecology: J Inst Obstet Gynecol.* 2003;23(4):426–30. https://www.tandfonline.com/doi/abs/10.1080/0144361031000120978
8. Laan E, Both S. Sexual desire and arousal disorders in women. *Adv Psychosom Med.* 2011;31:16–34. https://doi.org/10.1159/000328806. https://pubmed.ncbi.nlm.nih.gov/22005202/
9. Zarski AC, Velten J, Knauer J, Berking M, Ebert DD. Internet- and mobile-based psychological interventions for sexual dysfunctions: a systematic review and meta-analysis. NPJ Digital Medicine. 2022;5:139. https://doi.org/10.1038/s41746-022-00670-1.
10. Thornton K, Chervenak J, Neal-Perry G. Menopause and sexuality. *Endocrinol Metab Clin North Am* 2015; 44: 649–661. https://www.endo.theclinics.com/article/S0889-8529(15)00050-X/abstract
11. Mroczek B. Kurpas D. Gronowska M. Kotwas A. Psychosexual needs and sexual behaviors of nursing care home residents. *Archives of Gerontology and Geriatrics.* 2013;(57):32-38. https://www.sciencedirect.com/science/article/pii/S0167494313000265
12. Basson R. Sexual dysfunctions in women: Are androgens at fault? Endocrinol Metab Clin N Am. 2021;50:125–138. https://doi.org/10.1016/j.ecl.2020.12.001. https://www.endo.theclinics.com/article/S0889-8529(20)30089-X/abstract
13. Turhan İ, Akcan K. Current diagnosis and treatments of female sexual dysfunction. *Gevher Nesıbe Journal Of Medical & Health Sciences.* 2022;7(17):57–63. https://doi.org/https://doi.org/10.46648/gnj.384.
14. Moher D, Liberati A, Tetzlaff J, Altman DG. PRISMA Group, 2009. Reprint—preferred reporting items for systematic reviews and meta-analyses: the PRISMA statement. *Physical Therapy.* 2009;89:873-880. https://doi.org/10.1371/journal.pmed.1000097. https://www.bmj.com/content/339/bmj.b2535.short
15. The Joanna Briggs Institute Critical Appraisal Tools for use in IBI Systematic Reviews. http://joannabriggs.org/research/critical-appraisal-tools.html. Accessed September 10, 2025.
16. Tufanaru C, Munn Z, Aromataris E, Campbell J, Hopp L. Chapter 3: Systematic reviews of effectiveness. In: Aromataris E, Munn Z (Editors). Joanna Briggs Institute Reviewer's Manual. *The Joanna Briggs Institute,* 2017. https://doi.org/10.46658/JBIRM-17-03. https://scholar.archive.org/work/rovb2z4agjfgzbfgorwodicnwa/access/wayback/https://wiki.jbi.global/download/temp/pdfexport-20201106-061120-2129-14707/MANUAL-3178527-061120-2129-14708.pdf?contentType=application/pdf
17. Higgins JP, Thompson SG, Deeks JJ, Altman DG. Measuring inconsistency in meta-analyses. *BMJ.* 2003;327(7414):557-560. https://doi.org/10.1136/bmj.327.7414.557. https://www.bmj.com/content/327/7414/557.short.
18. Borenstein M, Hedges LV, Higgins JP, Rothstein HR. Introduction to Meta-Analysis. *John Wiley & Sons,* 2021. https://www.agropustaka.id/wp-content/uploads/2020/04/agropustaka.id_buku_Introduction-to-Meta-Analysis.pdf.
19. * Jalambadani Z, Garmaroodi G, Yaseri M, Tavousi M, Jafarian K. Education based on theory of planned behavior over sexual function of menopausal women in Iran. *J Mid-life Health.* 2017;8:124-9. https://doi.org/10.4103/jmh.JMH_44_17. https://journals.lww.com/jomh/fulltext/2017/08030/Education_Based_on_Theory_of_Planned_Behavior_over.5.aspx.
20. *Kamalak H, Aksoy Derya Y. The effects of motivational interviewing on sexual quality of life and sexual self-efficacy in postmenopausal women with sexual dysfunction. [Doctoral Thesis]. Malatya, Türkiye: *Department of Midwifery, Inonu University Institute of Health Sciences;* 2023. https://journals.lww.com/menopausejournal/_layouts/15/oaks.journals/downloadpdf.aspx?an=00042192-990000000-00362
21. *Mohammadi M, Peyman N, Hossainabadi M, Ghavami V, Tehrani H. Effect of sexual health education on sexual function and satisfaction of menopausal migrant women: an application of the theory of planned behavior. *BMC Public Health.* 2024;24:1626. https://doi.org/10.1186/s12889-024-19162-w.
22. *Nazarpour S, Simbar M, Ramezani-Tehrani F, Alavi-Majd H. Effects of sex education and Kegel exercises on the sexual function of postmenopausal women: a randomized clinical trial. *J Sex Med.* 2017;14:959–967. https://doi.org/10.1016/j.jsxm.2017.05.006 https://academic.oup.com/jsm/article/14/7/959/6973443
23. Egger M, Smith GD, Schneider M, Minder C. Bias in meta-analysis detected by a simple, graphical test. *BMJ.* 1997;315(7109):629-634. https://doi.org/10.1136/bmj.315.7109.629.
24. Scavello I, Maseroli E, Di Stasi V, Vignozzi L. Sexual health in menopause. *Medicina (Kaunas).* 2019;55(9):559. https://doi.org/10.3390/medicina55090559. https://www.mdpi.com/1648-9144/55/9/559
25. Stojanovska L, Apostolopoulos V, Polman R, Borkoles E. To exercise, or, not to exercise, during menopause and beyond. Maturitas. 2014;77(4):318-23. https://doi.org/10.1016/j.maturitas.2014.01.006. https://www.sciencedirect.com/science/article/pii/S0378512214000255
26. Jorge MP, Santaella DF, Pontes IM, Shiramizu VK, Nascimento EB, Cabral A, Lemos TM, Silva RH, Ribeiro AM. Hatha Yoga practice decreases menopause symptoms and improves quality of life: A randomized controlled trial. *Complement Ther Med.* 2016;26:128-35. https://www.sciencedirect.com/science/article/pii/S0965229916300395
27. Monteleone P, Mascagni G, Giannini A, Genazzani AR, Simoncini T. Symptoms of menopause global prevalence, physiology and implications. *Nat Rev Endocrinol.* 2018;14(4):199-215. https://doi.org/10.1038/nrendo.2017.180. https://www.nature.com/articles/nrendo.2017.180

JOURNAL OF CLINICAL MEDICINE OF KAZAKHSTAN (E-ISSN 2313-1519)
Original Article DOI: https://doi.org/10.23950/jcmk/18315

The Stroop Test as a Tool for Assessing Cognitive Dysfunction in Patients with Metabolic Syndrome

Dinara B. Nemetova[1], Mira B. Zhunisova[1], Karlygash Zh. Sadykova[1], Gulnaz O. Nuskabayeva[1], Ugilzhan B. Tatykayeva[1], Aziza T. Dzhurabekova[2], Dilbar N. Aidarbekova[1]

[1]*Faculty of Medicine, Khoja Akhmet Yassawi International Kazakh-Turkish University, Turkestan, Kazakhstan*
[2]*Department of Neurology, Samarkand State Medical University, Samarkand, Uzbekistan*

Received: 2025-11-27.
Accepted: 2026-04-04.

This work is licensed under a **Creative Commons Attribution 4.0 International License**

J Clin Med Kaz 2026; 23(2): 79-86

Corresponding author:
Karlygash Zh. Sadykova.
E-mail: karlygash.sadykova@ayu.edu.kz.
ORCID: 0000-0002-9120-8565.

ABSTRACT

Objective: The aim of the study was to evaluate cognitive functions in patients with metabolic syndrome with clinical and metabolic indicators using the Stroop test.

Introduction: Metabolic syndrome is a complex of disorders that includes abdominal obesity, insulin resistance, lipid metabolism disorders and hypertension. MetS negatively affects cognitive functions, including many types of executive functions, information processing speed and word production connections.

Methods: This study was conducted at the Clinical Diagnostic Center of the International Kazakh-Turkish University named after Khoja Ahmet Yasawi in the city of Turkestan. The study included a questionnaire, clinical laboratory tests, and cognitive function assessment. The Stroop test was used to assess cognitive functions. The data obtained during the study were statistically processed using a trial version of SPSS 25.0.

Results: The study involved 552 patients, 276 of whom were diagnosed with MetS and 552 without MetS. Women predominated in the study sample (76,8%, n=424), and the average age of the subjects was 53,07 years. The study included a higher proportion of individuals over 60 years of age (31.2%) and found statistically significant differences by age ($p < 0.001$) among those under 50 years of age. However, statistically significant differences were found by education level, alcohol consumption, and BMI ($p < 0.001$). All participants showed statistically significant differences between clinical and metabolic parameters with test results at $p < 0.001$. The median total score at T1 was statistically significantly lower in patients with metabolic syndrome ($p = 0.002$). T2, T3, and B1 were also statistically significantly higher in the MetS group ($p < 0.001$). Quartile distribution revealed significant differences at T1 ($p = 0.006$), T2 ($p < 0.001$), and T3 ($p = 0.012$). The results of the Stroop quartile distribution showed statistical significance at all three stages with triglyceride levels T1 $p = 0.007$, T2 $p < 0.001$, T3 $p = 0.005$ and with blood pressure indicators at T2 $p = 0.001$, T3 $p = 0.004$ and at B1 $p = 0.037$, 0.033.

Conclusions: As a result, patients with metabolic syndrome exhibit signs of cognitive decline, primarily in attention and executive control, while information processing efficiency remains relatively intact. The study's results demonstrate that cognitive assessment enables the early identification and intervention of modifiable risk factors for cognitive decline. Our findings highlight the need for screening and prevention of cognitive impairment in individuals with metabolic syndrome.

Keywords: cognitive impairment, cognitive control, metabolic syndrome, Stroop test, neuropsychological assessment.

Introduction

Metabolic syndrome (MetS) is one of the most complex medical and social problems of our time, characterized by insulin resistance, central obesity, atherogenic dyslipidemia, and hyperglycemia [1,2]. Epidemiological studies have shown that 20-30% of adults in many countries have MetS, increasing to 30.9% in Asian countries [3, 4]. MetS is a significant risk factor for an impairment in cognitive function and causes microstructural alterations of white matter in the brain. Cognitive impairments represent a serious social and psychological problem, as they reduce a person's social activity, productivity, and quality of life. The prevalence of cognitive impairment among older adults in Kazakhstan is approximately 30% [5]. According to data, MetS activates mediators that influence metabolic processes in the brain. These mediators can be activated by metabolic inflammation and microvascular disorders and impair cognitive function. The pathogenesis is based on insulin resistance, oxidative stress, and chronic inflammation [6]. It has been demonstrated in recent time that parts of MetS (dyslipidemia, hypertension, hyperglycemia and visceral obesity) can cause cognitive impairment [7].

Recent studies from Dintica C. indicate that vascular risk factors might contribute to lifestyle-related cognitive impairment as well as age-related cognitive decline [8]. The majority of studies demonstrate an interesting finding that different parts of MetS can impact on various areas of cognitive functioning. Elevated fasting glucose in adults is associated with impaired cognitive function, especially memory function, due to impaired neuronal energy metabolism, microvascular damage, and reduced cerebral blood flow [9]. The Stroop color and word test is one of the most widely used means to measure cognitive function. From a systematic review of the literature, Scarpin F. et al. demonstrated that the Stroop effect is a reliable and valid method for assessing cognitive control in a wide range of clinical and experimental studies [10]. In a research performed by Schuur M. et al., it was found that the Stroop test is a sensitive tool for assessing executive function impairment as a result of MetS and insulin resistance [11]. Since the influence of individual components of MetS on cognitive function assessed using the Stroop test has been insufficiently studied, the aim of this study is to examine and evaluate the relationship between clinical and metabolic factors and cognitive test results in adults with MetS. The scientific novelty of this study lies in its assessment of the relationship between Stroop test results and components of MetS in adults. This study provides a comprehensive analysis of the influence of clinical and metabolic factors on cognitive function, enabling the early identification of factors associated with cognitive decline in individuals.

Methods

The study was conducted at the Clinical Diagnostic Center of the International Kazakh-Turkish University named after Khoja Ahmet Yasawi in the city of Turkestan. During the research, data on the participants were collected in a patient examination form, which contained brief information about the study, a written voluntary informed consent form, passport and socio-demographic data. MetS was defined according to the criteria of International Diabetes Federation (IDF 2005): dyslipidemia (HbA1C ≥ 5.7%) or previously diagnosed type 2 diabetes, high blood pressure (systolic ≥ 130 mmHg and/or diastolic ≥ 85 mmHg), dyslipidemia defined as triglyceride level ≥ 1.7 mmol/L or low HDL level (< or = 1.03 mmol/L in men, less than or equal to 1.3 mmol/l in women) and abdominal obesity (waist circumference ≥ 102 cm in men, waist circumference ≥ 88 cm in women) [12]. Anthropometric measurements were performed: height (in meters), weight (in kilograms), waist circumference (in centimeters) on standardized calibrated scales, as well as blood pressure (systolic and diastolic) in mm Hg. Art. using a standard mercury tonometer. Waist circumference was measured using a retractable tape measure midway between the upper iliac crest and the lower edge of the rib cage at mid-exhalation. Laboratory tests included determination of fasting blood glucose, triglycerides and high-density lipoprotein in a venous blood sample taken overnight on an empty stomach. In the tables, the indicators are presented as categorical variables ("yes/no"), where the value "yes" indicated the presence of the corresponding pathological condition, including abdominal obesity, hypertriglyceridemia, decreased levels of high-density lipoproteins, hyperglycemia and arterial hypertension according to the criteria of the IDF and the value "no" reflected the absence of these disorders. Inclusion criteria: age ≥ 18 years, presence of MetS according to IDF criteria. Exclusion criteria: patients requiring urgent care, patients with chronic serious illnesses, patients with mental disorders, children under 18 years of age and pregnant women.

Assessment of cognitive functions

The classic Stroop test (standard color/word test) was used to assess cognitive status. The Stroop test or Stroop effect is named for the psychologist John Ridley Stroop, who first described this phenomenon in his doctoral thesis in the 1930s. The Stroop test is a method for measuring the inhibition of responses and is called both a diagnostic technique and a means of predicting cognitive rigidity and flexibility. It has the names of different colors printed on paper in various colors [13-15]. The color of printed text isn't the same as the color indicated by the words. The patient is presented with three pictures in sequence. Words are printed in black ink in the first picture. It is written as one hundred words, denoting the names of four basic colors. Normally, the basic colors used in the text are "red," "blue," "green" and "yellow." The patient must read the words quickly. In the second stage, you can see the multicolored stars of the same colors in an individual photograph. The patient is required to name the colors of the stars as quickly as possible. The third stage consists of one hundred names for colors that do not match the ink colors. For instance, the word "yellow" is spelled in red ink, and the word "green" is spelled in blue ink. The patient is required to accurately and rapidly name the colors of as many of the words he or she sees within a specific period (seconds). This exercise permits scrutiny of concentration, reaction time and cognitive flexibility. The test, the response time for the participant is recorded (seconds/minutes), and recorded in a special form (T1, T2, T3). The last scores are summed up as (B1 = T3 − T2, B2 = T2 / T1). The meaning of the Stroop test

Table 1 Grouping of Stroop test scores by quartiles

STROOP test	1- quartiles (Q1)	2- quartile (Q2)	3- quartile (Q3)	4- quartile (Q4)
T1, sec.	≤45	46-50	51-59	>60
T2, sec.	≤65	66-75	76-86	>87
T3, sec.	≤99	100-118	119-143	>144
B1	≤28,50	28,51-41	41,01-58	>58
B2	≤1,23	1,24-1,42	1,43-1,70	>1,70

parts: T1 – reading speed; T2 – attention and color naming; T3 – cognitive control, interference; B1 – interference index (T3–T2); B2 – information processing efficiency (T2/T1). The Stroop test results were divided into four quartiles (Q1–Q4) depending on the total score (task completion time) (Table 1).

Statistical analysis

IBM SPSS 25 software (IBM SPSS Inc., Chicago, Illinois) was used for statistical analysis. Statistical analysis of binary data was conducted in several stages. The McNemar test (analysis of 2×2 contingency tables) was used to assess the significance of changes in paired samples. Nominal comparative values were compared using the chi-square (χ^2) test. Mixed logistic regression was applied for a more in-depth analysis, taking into account the influence of additional factors and random effects. The normality of the distribution of quantitative variables was assessed using the Shapiro–Wilk test. Quantitative data are presented as means (M) and standard deviations (SD); variables with a nonparametric distribution were expressed as the median Me (Q1–Q3) (25th and 75th percentiles). The Mann–Whitney U test was used to compare indicators between two independent groups. Differences were considered statistically significant at a p-value <0.05.

Ethical Approval and Informed Consent

All participants were provided with detailed information about the objectives, methodology, potential risks, and expected benefits of the study. Before consenting, participants were informed in simple and understandable language so that they could understand their participation in the study. The purpose and methods of the study, the voluntary nature of participation in the study, the confidentiality of information obtained from the participant, and the potential risks and benefits of the study were explained. The study protocol was approved by the Institutional Research Ethics Committee of the International Turkish-Kazakh University named after Hodja Ahmet Yassawi (December 23, 2025, No. 49). All procedures and methods were conducted in accordance with the ethical principles of the Declaration of Helsinki.

Results

Table 2 presents the sociodemographic and clinical characteristics of the participants. All participants were divided into two groups based on the presence of MetS: the MetS group and the non-MetS group. The study revealed a higher proportion of women than men (76.8% vs. 23.2%). The mean age of the

Table 2 Socio-demographic and clinical characteristics of participants with and without MetS (n=552)

Parametres		Total n=522 (%)	With MetS n, %	Without MetS n, %	p-value
Gender	Men	128 (23,2)	63 (23%)	65 (24%)	
	Women	424 (76,8)	213 (77%)	211 (76%)	>0.9
Age	up to 40 years	83 (15)	66 (23.9%)	17 (6.2%)	
	40-49 years	134 (24,3)	81 (29.3%)	53 (19.2%)	
	50-59 years	163 (29,5)	71 (25.7%)	92 (33.3%)	<0.001
	60 years and older	172 (31,2)	58 (21.0%)	114 (41.3%)	
Education level	High	383 (69,4)	173 (63%)	210 (76%)	
	Low	169 (30,6)	103 (37%)	66 (24%)	<0.001
Job	Mental work	313 (56,7)	140 (51%)	173(63%)	
	Physical work	239 (43,3)	136 (49%)	103 (37%)	0,006
Marital Status	Married	493 (89,3)	243 (88%)	250 (91%)	
	Single	59 (10,7)	33 (12%)	26 (24%)	<0.001
Smoking	Yes	53 (9,6)	27 (9.8%)	26 (9.4%)	
	No	499 (90,4)			>0.9
Alcohol drinking	Yes	102 (18,5)	68 (25%)	34 (12%)	
	No	450 (81,5)			<0.001
Clinical characteristics					
Body mass index (BMI)	Normal weight	135 (24,5)	23 (8,3%)	112 (41%)	
	Overweight	185 (33,5)	87 (32%)	98 (36%)	<0.001
	Obesity (I, II, III degrees)	232 (42)	166 (60%)	66 (24%)	
Waist circumference, cm (WC)	Yes	435 (78,8)	263(95%)	172 (62%)	
	No	117 (21,2)			<0.001
Triglycerides, mmol/L (TG)	Yes	231 (41,8)	190 (69%)	41 (15%)	
	No	321 (58,2)			<0.001
HDL, mmol/L	Yes	290 (52,5)	212 (77%)	78 (28%)	<0.001
	No	262 (47,5)			
Glucose, mmol/L	Yes	182 (33)	152 (55%)	30 (11%)	<0.001
	No	370 (67)			
High blood pressure, mmHg (HBP)	Yes	307 (55,6)	224 (81%)	83 (30%)	<0.001
	No	245 (44,4)			
Systolic blood pressure (SBP)	Yes	222 (40,2)	167 (61%)	55 (20%)	<0.001
	No	330 (59,8)			
Diastolic blood pressure (DBP)	Yes	193 (35)	147 (53%)	46 (17%)	<0.001
	No	359 (65)			

sample was 53.07 years. No differences in gender distribution were observed between the MetS and non-MetS groups (p > 0.9). A higher proportion of individuals over 60 years of age participated in the study (31.2%), and statistically significant differences in age were identified (p < 0.001). An increase in the proportion of patients with MetS was also observed among people younger than 50 years of age (23.9% vs. 6.2% and 29.3% vs. 19.2%). This may reflect a trend toward earlier onset of the disease. At the same time, statistically significant differences in educational level were identified (p < 0.001). Among participants with MetS, individuals with a lower level of education were more common (37% vs. 24%). Occupations also differed, among people with MetS, those engaged in mental work were more common. Conversely, physical laborers were more common among people with MetS (49% vs. 37%; p = 0.006). The prevalence of smoking and alcohol consumption was very low. Similarly, there were no statistically significant differences (p > 0.9) regarding smoking. Alcohol consumption was significantly more common among participants with MetS (25% vs. 12%; p < 0.001). BMI values differed significantly between the groups (p < 0.001).

Participants with MetS were significantly more likely to be obese (60% vs. 24%), while a normal BMI was more common among participants without MetS (41% vs. 8.3%). Participants with MetS were significantly more likely to have: abdominal obesity (95% vs. 62%; p < 0.001), hypertriglyceridemia (69% vs. 15%; p < 0.001), hyperglycemia (55% vs. 11%; p < 0.001) and low HDL levels (77% vs. 28%; p < 0.001), HBP (81% vs. 30%; p < 0.001), SBP (61% vs. 20%; p < 0.001) and DBP (53% vs. 217%; p < 0.001). Statistically significant differences were observed in all participants.

Table 3 Distribution of Stroop test scores between participants with and without MetS

Indicators	Me (Q1–Q3)	MetS/ no	MetS / yes	p-value[2]
	n = 552[1]	n = 276[1]	n = 276[1]	
STROOP T1	52.00 (43.00–66.25)	10.0 (8.0–12.0)	10.0 (7.5–11.0)	0.002
STROOP T2	83.00 (67.00–102.00)	50 (41–60)	56 (45–70)	<0.001
STROOP T3	125.00 (101.00–154.00)	78 (65–99)	87 (70–111)	<0.001
STROOP B1	40.41 (29.99–55.00)	120 (97–146)	132 (108–159)	<0.001
STROOP B2	1.60 (1.30–1.80)	1.55 (1.30–1.90)	1.60 (1.30–1.80)	0.9

[1]n (%); Median (Q1–Q3)
[2]Pearson's Chi-squared test; Mann–Whitney U test; Independent-Samples T Test

The study analyzed Stroop test performance scores in participants with and without MetS. The total sample consisted of 552 individuals, divided into two equal groups: those with MetS (n = 276) and those without MetS (n = 276). Table 3 presents the median values of the total Stroop test score: 52.00 for T1, 83.00 for T2, and 125.00 for T3. Additionally, the median interference score for B1 was 40.41, and for B2, 1.60. It was found that statistically significant differences between the groups were detected for most Stroop test indices. Thus, the reading time index (T1) was statistically significantly lower in patients with MetS (p = 0.002), indicating a reduction in baseline information processing speed. The T2 score, reflecting attention and the ability to name colors, was significantly higher in the MetS group (p < 0.001), indicating reduced attention span and slowed cognitive processing. A similar trend was observed for the T3 index (p < 0.001), which characterizes cognitive control and the ability to suppress interfering stimuli, indicating impaired executive functions in patients with MetS. The interference index (B1) was also statistically significantly higher in the MetS group (p < 0.001), indicating an increased interference effect and a reduced capacity for cognitive inhibition. At the same time, the information processing efficiency index (B2) did not show statistically significant differences between the groups (p = 0.9), which may indicate the preservation of relative cognitive efficiency against a background of general slowing of processes. Consequently, patients with MetS exhibit signs of impaired cognitive function, primarily in the areas of attention and executive control, while information processing efficiency remains relatively intact.

Table 4 Distribution of Stroop test quartiles in participants with and without MetS

	Total n = 552	MetS/ no n = 276	MetS / yes n = 276	p-value
STROOP T1				0.006
Q1	163 (29.5%)	91 (33%)	72 (26%)	
Q2	102 (18.5%)	59 (21%)	43 (16%)	
Q3	88 (15.9%)	46 (17%)	42 (15%)	
Q4	199 (36.1%)	80 (29%)	119 (43%)	
STROOP T2				<0.001
Q1	127 (23%)	77 (28%)	50 (18%)	
Q2	96 (17.4%)	57 (21%)	39 (14%)	
Q3	74 (13.4%)	26 (9.4%)	48 (17%)	
Q4	255 (46.2%)	116 (42%)	139 (50%)	
STROOP T3				0.012
Q1	125 (22.6%)	74 (27%)	51 (18%)	
Q2	92 (16.7%)	53 (19%)	39 (14%)	
Q3	155 (28.1%)	72 (26%)	83 (30%)	
Q4	180 (32.6%)	77 (28%)	103 (37%)	
STROOP B1				0.3
Q1	134 (24.3%)	71 (26%)	63 (23%)	
Q2	156 (28.3%)	79 (29%)	77 (28%)	
Q3	151 (27.4%)	79 (29%)	72 (26%)	
Q4	111 (20.1%)	47 (17%)	64 (23%)	
STROOP B1				0.6
Q1	90 (16.3%)	43 (16%)	47 (17%)	
Q2	101 (18.3%)	51 (18%)	50 (18%)	
Q3	191 (34.6%)	90 (33%)	101 (37%)	
Q4	170 (30.8%)	92 (33%)	78 (28%)	

Table 4 presents a cross-tabulation of the Stroop test results, broken down by quartiles (Q1–Q4), for the groups with and without MetS. The results of the first stage (T1), which measured reading speed and duration, showed that the largest proportion of values fell within the Q4 quartile (36.1%). At the same time, participants with MetS were more likely to experience a decrease in reading speed: the proportion of subjects in Q4 was 43% compared to 29% in the group without MetS, indicating statistically significant differences (p = 0.006). Significant differences were also identified in subsequent test stages: at stage T2 (p < 0.001) and stage T3 (p = 0.012). The data indicate marked impairments in executive functions and cognitive control in individuals with metabolic syndrome. It is likely that participants with MetS spent more time completing

Table 5 Relationship between quartile groups of the Stroop test and clinical characteristics

	WC yes/no n = 552	**TG** yes/no n = 552	**Glucose** yes/no n = 552	**HDL** yes/no n = 552	**HBP** yes/no n = 552	**SBP** yes/no n = 552	**DBP** yes/no n = 552
STROOP T1							
Q1	127 (77,9%) 36 (22,1%)	65 (39,9%) 98 (60,1%)	54 (33,1%) 109 (66,9%)	80 (49,1%) 83 (50,9%)	84 (51,5%) 79 (48,5%)	60 (36,8%) 103 (63,2%)	55 (33,7%) 108 (66,3%)
Q2	81(79,4%) 21(20,6%)	30 (29,4%) 72 (70,6%)	35 (34,3%) 67 (65,7%)	52 (51%) 50 (49%)	49 (48%) 53 (52%)	37(36,3%) 65(63,7%)	31 (30,4%) 71 (69,6%)
Q3	65(73,9%) 23 (26,1%)	37 (42%) 51 (58%)	20 (22,7%) 68 (77,3%)	45 (51,1%) 43 (48,9%)	50 (56,8%) 38 (43,2%)	31 (35,2%) 57 (64,8%)	24 (27,3%) 64 (72,7%)
Q4	162 (81,4%) 37 (18,6%)	99 (49,7%) 100 (50,3%)	73 (36,7%) 126 (63,3%)	113 (56,8%) 86 (43,2%)	124 (62,3%) 75 (37,7%)	94 (47,2%) 105 (52,8%)	83 (41,7%) 116 (58,3%)
p-value	0,54	0,007	0,124	0,49	0,067	0,94	0,062
STROOP T2							
Q1	90 (70,9%) 37 (29,1%)	43 (33,9%) 84 (66,1%)	34 (26,8%) 93 (73,2%)	65 (51,2%) 62 (48,8%)	51 (40,2%) 76 (59,8%)	34 (26,8%) 93 (73,2%)	29 (22,8%) 98 (77,2%)
Q2	72 (75%) 24 (25%)	25 (26%) 71 (74%)	35 (36,5%) 61 (63,5%)	45 (46,9%) 51 (53,1%)	50 (52,1%) 46 (47,9%)	41 (42,7%) 55 (57,3%)	35 (36,5%) 61 (63,5%)
Q3	62 (83,8%) 12 (16,2%)	35 (47,3%) 39 (52,7%)	27 (36,5%) 47 (63,5%)	40 (54,1%) 34 (45,9%)	54 (73%) 20 (27%)	40 (54,1%) 34 (45,9%)	39 (52,7%) 39 (47,3%)
Q4	211 (82,7%) 44 (17,3%)	128 (41,8%) 127 (49,8%)	86 (33,7%) 169 (66,3%)	140 (54,9%) 115 (45,1%)	152 (59,6%) 103 (40,4%)	107 (42%) 148 (58%)	90 (35,3%) 165 (64,7%)
p-value	0,031	<0.001	0,35	0,57	<0.001	**0,001**	<0.001
STROOP T3							
Q1	95 (76%) 30 (24%)	43 (34,4%) 82 (65,6%)	34 (27,2%) 91 (72,8%)	63 (50,4%) 62 (49,6%)	59 (47,2%) 66 (52,8%)	39 (31,2%) 86 (68,8%)	36 (28,8%) 89 (71,2%)
Q2	68 (73,9%) 24 (26,1%)	28 (30,4%) 64 (69,6%)	31 (33,7%) 61 (66,3%)	44 (47,8%) 48 (52,2%)	41 (44,6%) 51 (55,4%)	30 (32,6%) 62 (67,4%)	25 (27,2%) 67 (72,8%)
Q3	123 (79,4%) 32 (20,6%)	72 (46,5%) 83 (53,5%)	51 (32,9%) 104 (67,1%)	86 (55,5%) 69 (44,5%)	94 (60,6%) 61 (39,4%)	62 (40%) 93 (60%)	54 (34,8%) 101 (65,2%)
Q4	149 (82,8%) 31 (17,2%)	88 (48,9%) 92 (51,1%)	66 (36,7%) 114 (63,3%)	97 (53,9%) 83 (46,1%)	113 (62,8%) 67 (37,2%)	91 (50,6%) 89 (49,4%)	78 (43,3%) 102 (56,7%)
p-value	0,303	0,005	0,38	0,63	0,004	0,002	0,018
STROOP B1							
Q1	104 (77,6%) 30 (22,4%)	58 (43,3%) 76 (56,7%)	41 (30,6%) 93 (69,4%)	69 (51,5%) 65 (48,5%)	69 (51,5%) 65 (48,5%)	45 (33,6%) 89 (66,4%)	42 (31,3%) 92 (68,7%)
Q2	126 (80,8%) 30 (19,2%)	65 (41,7%) 91 (58,3%)	41 (26,3%) 115 (73,7%)	88 (56,4%) 68 (43,6%)	86 (55,1%) 70 (44,9%)	63 (40,4%) 93 (59,6%)	48 (30,8%) 108 (69,2%)
Q3	115 (76,2%) 36 (23,8%)	57 (37,7%) 94 (62,3%)	60 (39,7%) 91 (60,3%)	74 (49%) 77 (51%)	81 (53,6%) 70 (46,4%)	57 (37,7%) 94 (62,3%)	51 (33,8%) 100 (66,2%)
Q4	90 (81.1%) 21 (18,9%)	51 (45,9%) 60 (54,1%)	40 (36%) 71 (64%)	59 (53,2%) 52 (46,8%)	71 (64%) 40 (36%)	57 (51.4%) 54 (48,6%)	52 (46,8%) 59 (53,2%)
p-value	0,69	0,58	0,068	0,62	0,22	0,037	0,033
STROOP B1							
Q1	68 (75,6%) 22 (24,4%)	34 (37,8%) 56 (62,2%)	30 (33,3%) 60 (66,7%)	48 (53,3%) 42 (46,7%)	47 (52,2%) 43 (47,8%)	38 (42,2%) 52 (57,8%)	37 (41,1%) 53 (58,9%)
Q2	76 (75,2%) 25 (24,8%)	41 (40,6%) 60 (59,4%)	31 (30,7%) 70 (69,3%)	59 (58,4%) 42 (41,6%)	61 (60,4%) 40 (39,6%)	41 (40,6%) 60 (59,4%)	34 (33,7%) 67 (66,3%)
Q3	156(81,7%) 35 (20,6%)	81 (42,2%) 110 (57,6%)	65 (34%) 126 (66%)	101 (52,9%) 90 (47,1%)	112 (58,6%) 79 (41,4%)	77 (40,3%) 114 (59,7%)	65 (34%) 126 (66%)
Q4	135 (79,4%) 35 (20,6%)	75 (44,1%) 95 (55,9%)	56 (32,9%) 114 (67,1%)	82 (48,2%) 88 (51,8%)	87 (51,2%) 83 (48,8%)	66 (38,8%) 104 (261,4%)	57 (33,5%) 113 (66,5%)
p-value	0,51	0,78	0,95	0,44	0,33	0,96	0,62

the Stroop test tasks, reflecting reduced efficiency in cognitive information processing. Significant differences were also observed in subsequent stages of the test: at stage T2 ($p < 0.001$) and stage T3 ($p = 0.012$). The data indicate marked impairments in executive functions and cognitive control in individuals with MetS. Participants with MetS likely took longer to complete the Stroop test tasks, reflecting reduced efficiency in cognitive information processing. Quartile distribution analysis confirmed a statistically significant association between cognitive test scores and the presence of MetS. The largest number of observations at stages T2 and T3 also fell into quartile Q4, indicating lower cognitive performance in this group. At stage T3, the largest proportion of participants (32.6%) required more than two minutes to complete the task. At the same time, no statistically significant differences were found for stages B1 and B2.

Table 5 presents an analysis of the relationship between clinical and metabolic parameters and the results of the Strup test. Among all clinical and metabolic parameters, triglyceride levels differed statistically significantly in the first stage (p=0.007). In the second stage of the test, attention and the ability to name colors were assessed; in people with MetS, TG and BP levels, as well as SBP and DBP, were statistically significantly higher in all quartiles (p=0.007). In the second stage, participants with HBP showed higher Stroop test scores in Q4 than participants without MetS (59.6% vs. 40.4%). In contrast, participants with elevated SBP and DBP showed higher scores than participants without MetS (58% vs. 42%, 64.7% vs. 35.3%). The results suggest that HBP may be associated with a decline in cognitive function. No statistically significant differences in glucose and HDL levels were found. In the third stage, participants with HBP scored higher on the Stroop test in Q3-Q4 than participants without MetS (60.6% vs. 39.4%, 62.8% vs. 37.2%). This, in turn, may be associated with chronic hypertension, which can lead to impaired executive function and reduced information processing speed. In addition, elevated TG levels were more prevalent among individuals without MetS across all quartiles and were statistically significant (p=0.005). A longer time taken to complete the test is more likely to reveal interference effects, which may indicate reduced cognitive control, slowed information processing, and difficulties in suppressing automatic responses. In the first interference effect (B1) of the Stroop test, no statistically significant differences were found between clinical parameters and groups ($p > 0.05$) except for SAD and DAD. In participants without MetS, SAD and DAD scores were higher at the Q2 and Q3 levels. The differences between quartiles were statistically significant ($p = 0.037$, $p = 0.033$). In the final stage (B2) of the Stroop test, no statistically significant differences in clinical parameters were found.

Discussion

In this study, we assessed cognitive function in participants with and without MetS using the Stroop test. Women constituted the majority of participants in our study. The group with MetS differed in terms of age, with a statistically significant difference ($p < 0.001$) observed in the number of participants under 50 years of age. This is due to the fact that the prevalence of metabolic syndrome is increasing among the younger population. 76% of participants with a college education were included in the group without MetS. Participants with secondary and lower levels of education differed depending on the presence of MetS. The majority of alcohol consumers were people with MetS. The results obtained in this study are consistent with data from international studies confirming the association between MetS and impaired cognitive function, particularly in the domains of attention and executive control. A number of foreign studies have shown that components of MetS are associated with a decline in executive functions, as assessed, among other methods, by the Stroop test. Yates et al. demonstrated that an increase in the number of MetS components is associated with impaired performance on cognitive tasks, including interference tests [16]. This is consistent with our findings regarding elevated T3 and B1 scores in patients with MetS. Similar results were obtained in a study by Segura et al., where patients with MetS exhibited reduced cognitive flexibility and increased interference [17]. This confirms the impairment of executive control identified in our sample. Large population-based studies also demonstrate an association between MetS and the risk of cognitive decline. A study by Wu et al. showed that MetS more than doubles the risk of cognitive impairment (OR = 2.39) [18]. In addition, Aljondi et al. identified an association between MetS and reduced psychomotor speed and attention [19], which is consistent with our results for the T1 and T2 measures. At the same time, results may vary across specific clinical groups. For example, in a study by Viscogliosi et al., no significant differences in cognitive function were found in patients with chronic obstructive pulmonary disease depending on the presence of MetS [20]. Pathophysiological mechanisms may include vascular and metabolic disorders. According to a review by Tune et al., insulin resistance, inflammation, and endothelial dysfunction play a key role in the development of cognitive impairments in MetS [21]. Thus, the results of the present study confirm international data and indicate a predominant impairment of executive functions and inhibitory control in MetS.

The findings are consistent with other scientific data, which indicate a link between metabolic syndrome and impairments in cognitive functions, specifically executive control, information processing speed, and attention. According to a number of researchers, the presence of metabolic syndrome is associated with a decline in cognitive performance, particularly in tasks requiring a high degree of cognitive control. This is consistent with the results of the present study, which show a shift in the distribution toward the unfavorable quartile (Q4) and an increase in task completion time. The results from stages T2 and T3, where statistically significant differences were identified, can be explained by impaired inhibitory control and cognitive flexibility. Foreign studies have shown that patients with MetS demonstrate a more pronounced interference effect on the Stroop test, which is associated with prefrontal cortex dysfunction [22]. From a neurobiological perspective, these impairments may be attributable to vascular and metabolic changes. Studies using neuroimaging show that MetS is associated with changes in white matter and reduced cerebral blood flow, which, in turn, affect cognitive function [23]. Additional data confirm the role of inflammatory processes and insulin resistance as key mechanisms of cognitive decline in MetS. In particular, it has been shown that chronic inflammation and metabolic disorders increase the risk of cognitive decline and dementia [24]. This may explain the increase in the proportion of participants requiring more than 2 minutes to complete tasks at the T3 stage. Furthermore, meta-analytic studies demonstrate that metabolic disorders are associated with impaired performance across multiple cognitive domains, including attention, information processing speed, and executive functions [25]. This is fully consistent with the present findings, which indicate the complex nature of cognitive impairments in individuals with MetS.

The results of the quartile distribution (T1, T2, T3) of Stroop showed a statistically significant association with triglyceride levels. This may point to a possible role of lipid metabolism disorders in the decline of executive functions, particularly cognitive control and the ability to suppress interference. Accordingly, our results generally align with those of other cross-sectional studies conducted on samples from other populations. Parthasarathy V. et al. associated elevated TG levels with impaired attention, information processing speed and executive functions. The results suggest that dyslipidemia may contribute to the development of endothelial dysfunction, chronic inflammation, and cerebrovascular changes, which negatively affect cognitive processes over a long period of time [26].

In a cross-sectional study, Mehra et al. investigated the association between mild cognitive impairment and MetS in patients with hypertension. They found a positive correlation between low HDL levels and high total cholesterol levels [27]. Butcher et al. conducted a cross-sectional study among men. The results showed that during the Stroop test, participants' cardiovascular response intensified as the task became more complex; their heart rates increased and their blood pressure rose [28]. HBP has a negative impact on the neurocognitive domains of auditory and verbal memory. This may be associated with the chronic nature of MetS, which is often accompanied by a reduced quality of life, limitations in physical activity, and an increased risk of cardiovascular disease [8]. Our data are consistent with the results of Dintica's studies, which also show statistical significance in the T2, T3, and B1 categories of the Stroop test. HBP in middle age is associated with a number of changes in the brain that are linked to cognitive impairment in later life. This means that cognitive functions also slow down with age and participants require more time to complete the test than was allotted to them. In summary, the results of this study confirm the findings of international literature and indicate that metabolic syndrome negatively impacts cognitive functions, particularly executive control and information processing speed. The absence of statistically significant differences at stages B1 and B2 is likely due to the fact that these stages reflect simpler cognitive processes, which remain relatively intact compared to more complex executive functions.

The results of the study have important practical implications for the health system. Each of the identified associations confirms the need for early detection of cognitive impairment in people with MetS. Kouvar et al., came to the conclusion that early detection of metabolic syndrome can help prevent or slow down the decline of cognitive functions. The results obtained by us agree with these studies [29]. They expand the existing ideas about the influence of components of the metabolic syndrome on cognitive functions. Thus, they confirm the importance of controlling metabolic parameters as potentially modifiable risk factors for cognitive disorders.

In this article, we examined the use of the Stroop test to assess cognitive functions with clinical and metabolic indicators, particularly attention and executive control, in patients with MetS. However, it does not fully assess all components of cognitive function.

Conclusion

The results of the study showed that the presence of metabolic syndrome had a significant negative effect on the Stroop test result. The results indicate the need for screening and prevention of cognitive impairment in individuals with MetS. Further studies are needed to confirm the association between MetS and cognitive problems, as well as to identify the specific mechanism underlying this association. The results of the study indicate the importance of identifying modifiable risk factors associated with individual components of the metabolic syndrome, such as high systolic and diastolic blood pressure, triglyceridemia.

Author Contributions: Conceptualization, D.N and M.ZH.; methodology, K.S., U.B. and N.S.; validation, A.D. and D.N.; formal analysis, D.N.; investigation, G.O.; resources, K.S.; data curation, U.B.; writing – original draft preparation, A.D. and D.N.; writing – review and editing, K.ZH. and D.N.; visualization, D.N. and K.S. All authors have read and agreed to the published version of the manuscript.

Disclosures: The authors have no conflicts of interest.

Acknowledgments: None.

Funding: This research is funded by the Science Committee of the Ministry of Science and Higher Education of the Republic of Kazakhstan (Grant № BR24992814).

Data availability statement: The corresponding author can provide the data supporting the study's conclusions upon request.

Artificial Intelligence (AI) Disclosure Statement: The authors declare no AI Tools used for preparation of this work.

References

1. Obeidat AA, Ahmad MN, Ghabashi MA, Alazzeh AY, Habib SM, Abu Al-Haijaa D, Azzeh FS. Developmental trends of metabolic syndrome in the past two decades: a narrative review. *J Clin Med.* 2025 Mar 31;14(7):2402. https://doi.org/10.3390/jcm14072402.
2. Rus M, Crisan S, Andronie-Cioara FL, Indries M, Marian P, Pobirci OL, Ardelean AI. Prevalence and risk factors of metabolic syndrome: a prospective study on cardiovascular health. *Medicina (Kaunas).* 2023 Sep 25;59(10):1711. https://doi.org/10.3390/medicina59101711.
3. Jemal A, Girum T, Kedir S, Bedru A, Mosa H, Assfa K, Oumer A. Metabolic syndrome and its predictors among adults seeking medical care: a trending public health concern. *Clin Nutr ESPEN.* 2023 Apr;54:264-270. https://doi.org/10.1016/j.clnesp.2023.01.034.
4. Sadykova A, Shalkharova ZS, Shalkharova ZN, Sadykova K, Madenbay K, Zhunissova M, Nuskabayeva G, Askarova S, Grjibovski AM. Metabolic syndrome and its components in southern Kazakhstan: a cross-sectional study. *Int Health.* 2018 Jul 1;10(4):268-276. https://doi.org/10.1093/inthealth/ihy027.

5. Tsoy RT, Turuspekova ST, Klipitskaya NK, Mereke A, Cumming RG. Prevalence of Mild Cognitive Impairment Among Older People in Kazakhstan and Potential Risk Factors: A Cross-sectional Study. *Alzheimer Dis Assoc Disord.* 2019 Apr-Jun;33(2):136-141. https://doi.org/10.1097/WAD.0000000000000298.
6. Kaur SS, Gonzales MM, Eagan DE, Goudarzi K, Tanaka H, Haley AP. Inflammation as a mediator of the relationship between cortical thickness and metabolic syndrome. *Brain Imaging Behav.* 2015 Dec;9(4):737-43. https://doi.org/10.1007/s11682-014-9330-z.
7. Grover S, R P, Sahoo S, Gopal S, Nehra R, Ganesh A, Raghavan V, Sankaranarayan A. Relationship of metabolic syndrome and neurocognitive deficits in patients with schizophrenia. *Psychiatry Res.* 2019 Aug;278:56-64. https://doi.org/10.1016/j.psychres.2019.05.023.
8. Dintica CS, Hoang T, Allen N, Sidney S, Yaffe K. The metabolic syndrome is associated with lower cognitive performance and reduced white matter integrity in midlife: the CARDIA Study. *Front Neurosci.* 2022 Jul 18;16:942743. https://doi.org/10.3389/fnins.2022.942743.
9. Panza F, Frisardi V, Capurso C, Imbimbo BP, Vendemiale G, Santamato A, D'Onofrio G, Seripa D, Sancarlo D, Pilotto A, Solfrizzi V. Metabolic syndrome and cognitive impairment: current epidemiology and possible underlying mechanisms. *J Alzheimers Dis.* 2010;21(3):691-724. https://doi.org/10.3233/JAD-2010-091669.
10. Scarpina F, Tagini S. The Stroop Color and Word Test. Front Psychol. 2017 Apr 12;8:557. https://doi.org/10.3389/fpsyg.2017.00557.
11. Schuur M, Henneman P, van Swieten JC, Zillikens MC, de Koning I, Janssens AC, Witteman JC, Aulchenko YS, Frants RR, Oostra BA, van Dijk KW, van Duijn CM. Insulin-resistance and metabolic syndrome are related to executive function in women in a large family-based study. *Eur J Epidemiol.* 2010 Aug;25(8):561-8. https://doi.org/10.1007/s10654-010-9476-y.
12. 12.Zhu L, Spence C, Yang JW, Ma GX. The IDF Definition Is Better Suited for Screening Metabolic Syndrome and Estimating Risks of Diabetes in Asian American Adults: Evidence from NHANES 2011-2016. *J Clin Med.* 2020 Nov 28;9(12):3871. https://doi.org/10.3390/jcm9123871.
13. Okayasu M, Inukai T, Tanaka D, Tsumura K, Shintaki R, Takeda M, Nakahara K, Jimura K. The Stroop effect involves an excitatory-inhibitory fronto-cerebellar loop. *Nat Commun*. 2023 Jan 11;14(1):27. https://doi.org/10.1038/s41467-022-35397-w.
14. Parris BA, Hasshim N, Wadsley M, Augustinova M, Ferrand L. The loci of Stroop effects: a critical review of methods and evidence for levels of processing contributing to color-word Stroop effects and the implications for the loci of attentional selection. *Psychol Res.* 2022 Jun;86(4):1029-1053. https://doi.org/10.1007/s00426-021-01554-x.
15. Nanay B. The Stroop effect and mental imagery. Perception. 2024 Jan;53(1):61-67. https://doi.org/10.1177/03010066231212152.
16. Yates KF, Sweat V, Yau PL, Turchiano MM, Convit A. Impact of metabolic syndrome on cognition and brain: a selected review. *Arterioscler Thromb Vasc Biol.* 2020;40(3):e103–e112.
17. Segura B, Jurado MA, Freixenet N, et al. Mental slowness and executive dysfunctions in patients with metabolic syndrome. *Neurosci Lett.* 2009;462(1):49–53.
18. Wu C, Zhou D, Wen C, et al. Metabolic syndrome and cognitive decline: a large-scale cohort study. *J Clin Endocrinol Metab*. 2021;106(5):e2138–e2147.
19. Aljondi R, Szoeke C, Steward C, et al. Metabolic syndrome and cognitive performance: a cross-sectional study. *Diabetes Metab Syndr Obes.* 2022;15:123–132.
20. Viscogliosi G, Cipriani E, Liguori ML, et al. Metabolic syndrome and cognitive impairment in COPD patients. *Aging Clin Exp Res.* 2020;32(6):1047–1053.
21. Tune JD, Goodwill AG, Sassoon DJ, Mather KJ. Cardiovascular consequences of metabolic syndrome. *Transl Res.* 2017;183:57–70. https://doi.org/10.1016/j.trsl.2017.01.001.
22. Cavalieri M., Ropele S., Petrovic K., et al. Metabolic syndrome, brain magnetic resonance imaging, and cognition // *Diabetes Care.* – 2010. – Vol. 33(11). – P. 2489–2495.
23. Yaffe K., Kanaya A., Lindquist K., et al. The metabolic syndrome, inflammation, and risk of cognitive decline // *JAMA.* – 2004. – Vol. 292(18). – P. 2237–2242.
24. Ktaiche M, Fares Y, Abou-Abbas L. Stroop color and word test (SCWT): normative data for the Lebanese adult population. *Appl Neuropsychol Adult*. 2022 Nov-Dec;29(6):1578-1586. https://doi.org/10.1080/23279095.2021.1901101.
25. Palta P, Schneider ALC, Biessels GJ, Touradji P, Hill-Briggs F. Magnitude of cognitive dysfunction in adults with type 2 diabetes: a meta-analysis of six cognitive domains. *Diabetes Care.* 2014; 37(10): 2850–2858.
26. Parthasarathy V, Frazier DT, Bettcher BM, Jastrzab L, Chao L, Reed B, Mungas D, Weiner M, DeCarli C, Chui H, Kramer JH. Triglycerides are negatively correlated with cognitive function in nondemented aging adults. *Neuropsychology*. 2017 Sep;31(6):682-688. https://doi.org/10.1037/neu0000335.
27. Mehra A, Suri V, Kumari S, Avasthi A, Grover S. Association of mild cognitive impairment and metabolic syndrome in patients with hypertension. *Asian J Psychiatr.* 2020 Oct;53:102185. https://doi.org/10.1016/j.ajp.2020.102185.
28. Boutcher YN, Boutcher SH. Cardiovascular response to Stroop: effect of verbal response and task difficulty. *Biol Psychol*. 2006 Oct;73(3):235-241. https://doi.org/10.1016/j.biopsycho.2006.04.005.
29. Kouvari, M.; D'Cunha, N.M.; Travica, N.; Sergi, D.; Zec, M.; Marx, W.; Naumovski, N. Metabolic Syndrome, Cognitive Impairment and the Role of Diet: A Narrative Review. *Nutrients.* 2022, 14, 333. https://doi.org/10.3390/nu14020333.

JOURNAL OF CLINICAL MEDICINE OF KAZAKHSTAN (E-ISSN 2313-1519)
Original Article DOI: https://doi.org/10.23950/jcmk/18165

Structural and Cognitive Measures Across Childhood, Adolescence, and Adulthood: Associations with Education and Brain Morphometry

Sujatha Nagari[1,2], Zareena Begum Miyajan[3], Kalpana Thondapu[1], Udaya Kumar Pillam[1], Ratna Priyanka Janamala[1]

[1]*Department of Anatomy, Mamata Medical College, Khammam, Telangana, India*
[2]*Research Scholarship, Saveetha Institute of Medical and Technical Sciences (SIMATS University), Chennai, India*
[3]*Department of Anatomy, Saveetha Medical College, Saveetha Institute of Medical and Technical Sciences (SIMATS University), Chennai, India*

Received: 2026-01-10.
Accepted: 2026-03-19.

This work is licensed under a **Creative Commons Attribution 4.0 International License**

J Clin Med Kaz 2026; 23(2): 87-103

Corresponding author:
Sujatha Nagari.
E-mail: kruthika.nagari@gmail.com.
ORCID: 0000-0002-7251-0072.

ABSTRACT

Background: The organization of the human brain shows key characteristics through its cortical thickness and brain volume distribution across different regions, and the way both brain hemispheres display their distinct functions. However, age-stratified neuroimaging data that jointly consider structural asymmetry, education, and cognition within a single population remain limited, especially for South Asian groups.

Methods: The study involved 200 neurologically healthy people from South India who ranged in age from 3 to 90 years. The researchers divided participants into five distinct age groups, which included childhood, adolescence, early adulthood, mid-adulthood, and late adulthood. The research team used a 3.0 Tesla scanner to capture high-resolution T1-weighted MRI scans, which FreeSurfer (v7.3.2) software used to calculate regional cortical thickness and volumetric measures for predefined cortical regions. The researchers measured hemispheric asymmetry through a standardized laterality index. The researchers used the Montreal Cognitive Assessment (MoCA) to measure cognitive performance. The researchers conducted statistical analyses through paired-sample t-tests, which compared hemispheric differences and used Pearson correlation analyses and general linear models that included age, sex, and years of education as covariates.

Results: Across all age groups, significant hemispheric asymmetry was observed in the examined cortical regions ($p < 0.001$). The frontal regions showed permanent leftward volumetric asymmetry, which reached its peak in the rostral anterior cingulate cortex (laterality index = 0.252), inferior frontal gyrus (0.065), and superior frontal gyrus (0.029). The posterior regions exhibited rightward volumetric asymmetry, which reached its peak in the inferior parietal lobule (−0.143) and middle temporal gyrus (−0.089) areas. The researchers found that cortical thickness showed asymmetry, which reached statistical significance, although it produced smaller results than volumetric asymmetry. Age-group comparisons revealed relative stability of regional volumes and cortical thickness across developmental and adult stages. The researchers found that years of education, together with MoCA scores, produced positive effects on cortical thickness and volume in frontal, parietal, and temporal regions.

Conclusions: The age-stratified study shows that regional hemispheric asymmetry remains consistent throughout childhood, adolescence, and adulthood. The study found that volumetric measurements showed stronger lateralization than cortical thickness measurements. The research results show how educational background and cognitive abilities impact brain structure through their effects on cortical development. The research results establish normative reference data for South Indian populations based on age group measurements of cortical asymmetry and morphometric data.

Keywords: Cortical thickness; Brain volume; Hemispheric asymmetry; Age-stratified analysis; Education.

Introduction

The cognitive functioning of people during adulthood and old age results from a complex and ever-changing interplay between their demographic aspects, condition of their brains, and age-related neuroplasticity due to their experiences. One widespread characteristic of cortical morphology during aging is a gradual decline; thus, area-wise specific shrinkages in cortical thickness, volume, and surface complexity are the main aspects of this phenomenon. This shrinkage is particularly pronounced in the frontal, temporal, and parietal regions, which are involved in executive control, memory, and higher-order cognitive processes [1–4]. Large multi-cohort and longitudinal studies have revealed that brain structural changes follow declines in processing speed, executive functions, memory, and global cognition, and simultaneously show a large inter-individual difference that could be due to both nature and nurture factors [2,3,5].

Cortical volume is a combination of the surface area and thickness, which have different developmental and aging processes. Longitudinal MRI studies have revealed that during the transition from late childhood to early adulthood, both cortical volume and thickness undergo a nonlinear decrease, with changes in thickness being the major contributor to the reduction in volume during adolescence [1]. During old age, the thickness and area of the brain continue to decrease, but there is a lot of variation between individuals; changes in thickness and volume, especially, are linked to changes in cognitive skills [2]. Cross-sectional and longitudinal investigations conducted on middle-aged and older persons have revealed that the age-induced reduction in cortical thickness and volume is most evident in the frontal and temporal areas, specifically in the case of the superior and middle frontal gyri, lateral orbitofrontal cortex, temporal gyri, and parietal regions such as the precuneus and postcentral gyrus. Furthermore, these changes are associated with poor performance in memory, working memory, visuomotor coordination, and other areas of cognition [3,4].

The fronto-parietal-temporal networks extending to the anterior cingulate cortex (ACC), inferior and superior frontal gyri, inferior parietal lobule (IPL), and middle temporal gyrus (MTG) are particularly important for executive function, attention control, working memory, and episodic memory [3,4,6]. Longitudinal analyses conducted in specific domains have shown that smaller hippocampal and amygdala volumes and heavier white matter lesions are reliable indicators of a decline in global cognition, executive function, language, and memory, highlighting the role of widespread cortico-limbic networks in cognitive support during aging [6]. Aging has been globally identified as a factor that causes a decline in the coupling between structure and function. This phenomenon was the most pronounced in the sensorimotor area. However, some higher-level cognitive systems can maintain their local coupling, indicating the differential vulnerability of cortical systems, which may explain the variability in cognitive aging trajectories [7].

Hemispheric asymmetry is a primary organizational feature of the human cortex. Multiple large datasets from both pediatric and adult populations show that strong structural asymmetries in terms of cortical volume, thickness, and surface area are not only present in early childhood but are also quite stable throughout the developmental process, albeit with specific patterns per region and metric [8,9]. Usually, there is asymmetry of left-side domination in the frontal and anterior temporal lobes, and right-side domination in the posterior temporal, parietal, and occipital lobes [9]. The data obtained from Pediatric ENIGMA indicate that certain asymmetries are influenced by age to the extent of getting stronger, weaker, or even reversing their direction, and that there are only minor sex differences in the degree and area of asymmetry [8]. Adult lifespan work further shows widespread left > right thickness in the frontal cortices and right > left thickness in the posterior temporal–parietal–occipital regions, with age-by-asymmetry interactions indicating that cortical thinning can proceed more rapidly in one hemisphere than in another in specific territories [9]. Greater normative asymmetry in certain frontal and temporal areas has been associated with enhanced working memory and vocabulary scores, and it has been proposed that structural lateralization may facilitate efficient allocation of cognitive function through the support of different functions [9]. Newer data from studies of older adults living in the community have revealed that significant asymmetry between the anterior cingulate cortex and dorsolateral prefrontal cortex correlates with cognitive decline in selective attention and executive function. Therefore, it appears that the difference in the activity distribution between the two hemispheres constitutes a cognitive risk factor, underscoring this issue [10].

Fractal dimensions, among other cortical complexity measures, also display systematic hemispheric and lobar asymmetries together with thickness and volume, where rightward asymmetry is present at the hemispheric, frontal, parietal, and occipital levels, while leftward asymmetry is observed in the temporal lobes. There are also differences in the patterns of asymmetry between the sexes. Moreover, these characteristics are age-related and can thus provide further insight into conventional morphometric indices when characterizing normal and pathological ageing [11].

Educational attainment is a frequently used indicator of cognitive reserve and is closely connected to high cognitive performance throughout adult life and a lower incidence of dementia in old age [5,12]. Longitudinal studies that have been harmonized among different cohorts reveal that people with a greater number of years of formal education have higher cognitive functioning throughout adulthood, but do not show significantly lower rates of cognitive decline; however, education seems to raise the baseline cognitive level, which is in line with the threshold models of dementia [12]. At the structural level, there was a positive correlation between education and cortical volume and surface area, especially in the frontal and temporal areas, along with higher total brain volume. However, associations with regional cortical thickness are usually modest and vary between studies [1,3,4,13]. Mendelian randomization and polygenic studies have pointed to a connection between education and cortical macrostructures that are partly bidirectional. However, they also proposed that structural change is not the sole factor in the protective effect of education against dementia risk due to other factors [7,12].

In older patients and clinical samples, the influence of genetic or pathological risk factors on cognition can be reduced through education. As illustrated in the case of older individuals, the greater the ADHD polygenic risk, the worse the attention and language performance; however, this is true only for the less educated, suggesting that education has a moderating effect [14]. Similarly, large-scale international cohort studies have shown that each additional year of education results in a slightly slower decline in global screening scores (such as the MMSE), and the effects on domain-specific decline are minor and may vary by domain [5]. Functional neuroimaging studies suggest that education- and IQ-based reserve proxies correspond to task-general, age-invariant activation patterns in the temporal, occipital, and inferior frontal cortices, whereas age-related

compensatory overrecruitment in the prefrontal and parietal areas during episodic encoding is more closely related to brain reserve (e.g., total brain volume) than cognitive reserve proxies [13]. These findings indicate that education is closely related to the structure and activity of the brain; however, its impact on aging is not straightforward, varies by location, and is only to some extent recognized through traditional measures of brain morphology.

One of the main goals of modern cognitive neuroscience is to identify strong structure-cognition links that indicate vulnerability or resilience at an early stage. These links have been articulated through longitudinal MRI studies that investigated both healthy and at-risk adult populations. These studies have revealed a strong connection between individual differences and changes in the anatomical features of the brain (such as thickness, area, and volume), especially in the association regions of the frontal, temporal, and parietal lobes, and cognitive changes, such as those related to memory, executive function, working memory, and processing speed [2–4,6]. Domain-specific studies indicate that the shrinkage of the hippocampus and amygdala, as well as the rise in white matter lesions, are partly responsible for the downregulation of different cognitive functions, such as executive functioning, language, and memory. This implies that different cognitive processes depend on different structural supports and reserves [6]. Different studies focusing on this aspect suggest that global measures (such as whole-brain volume) mainly affect the rate of cognitive change in people with mild cognitive impairment or Alzheimer's disease, whereas regional markers (e.g., hippocampal volume and entorhinal thickness) are more connected to cognitive level than to change speed [15].

The Montreal Cognitive Assessment (MoCA) and other global cognitive screening tools provide the benefit of delivering not only a total cognition score but also subscores akin to the domains estimated to be executive control, working memory, and episodic recall. Studies have shown that MoCA subdomains can significantly separate the causes of early neurocognitive disorders and correlate with particular structural and functional changes. Hence, they are a powerful means for researching structure-function connections in non-demented community-based groups [16]. In addition to studying brain volume, new research in the areas of functional connectivity, cortical iron accumulation, and hypothalamic volume has shown that using different types of measurements together can clarify age-related differences in fluid cognition, network segregation, and homeostatic contributions to cognitive performance that are explained by different factors [17,18]. These findings emphasize a network-level architecture of structural and functional correlates that is multidimensional, supports cognitive function, and proposes various possible pathways for early risk stratification.

Although progress has been made, most large neuroimaging cohorts are from North America, Europe, and East Asia, with very little representation from South Asia, particularly South India. International collaborative research has shown that the extent of age-related cognitive decline and its associated factors, such as gender, education, and APOE genotype, differ among ethnic and geographic groups, most likely due to variations in genetics, health, lifestyle, and educational systems [5]. Similarly, international research on structural complexity and asymmetry, as well as on the coupling of structure and function, reveals not only wide-ranging similarities but also differences that are specific to particular regions, thereby emphasizing the necessity of locally characterizing normative data [7,11]. Diverse cultural and contextual factors influence quality of education, literacy practices, and environmental exposure. Therefore, the propagation of the findings on reserves and education from Western groups to the South Indian population cannot be justified without empirical testing.

On this basis, the present study capitalizes on the heterogeneous lifespan sample of South Indians to test in a single coherent framework the association between demographic factors (age, sex, education), regional cortical volume, cortical thickness, and hemispheric asymmetries in major frontal, parietal, and temporal locales as measured by global and domain-specific cognitive performance as represented by MoCA. By measuring the detailed morphometric parameters of the rostral ACC, inferior and superior frontal gyri, inferior parietal lobule, and middle temporal gyrus in each of the two hemispheres, and by determining the individual variability of such parameters with regard to education and cognition, this study aimed to determine the common distributions and inter-subject differences in regional cortical volumes and thickness across a large age and education range. We quantified the variation in hemispheric volume and thickness of the association cortices, established whether hemispheric asymmetry occurred, and confirmed whether hemispheric asymmetry conformed to canonical left frontal/right parietal-temporal patterns. We identified the strength, geography, and specificity of the relationships between years of education and morphometric parameters and examined education-related changes in brain structure as a putative measure of cognitive reserve. We compared the correlations between regional morphometry and hemispheric asymmetry and global and domain-level cognitive scores, and sought to establish patterns in the structure that would suggest either early cognitive resilience or vulnerability. It can be suggested that the proposed integrated strategy will deliver population-relevant information regarding brain-behavior relationships, improve the understanding of how demographic and experience factors affect cortical structure, and advance the idea of structural homologs that can be employed to inform early risks to the brain in underserved populations.

Methods

Participants

The study used a cross-sectional design to examine 200 participants who had normal neurological function throughout their lives from age 3 to 90. The South Indian population selected study participants who included both male and female participants who had completed different educational levels, from no formal education to 20 years of schooling. The study recruited participants through Mamata Medical College and Hospital in Khammam, Telangana, India, which included students, hospital referrals, and community outreach program enrollees. The structured questionnaires collected demographic data, which included information about age, sex, years of education, and all pertinent medical conditions. The researchers divided study participants into five age groups, which included childhood (3–10 years), adolescence (11–17 years), early adulthood (18–39 years), mid-adulthood (40–59 years), and late adulthood (≥60 years). The research used this stratification method to conduct age-based analyses, which included descriptive and inferential statistics while keeping medical data separate for pediatric and adult populations.

The study used a rigorous screening process to identify and remove from the study people who had neurological,

psychiatric, or cognitive disorders. The screening procedures used structured clinical interviews together with medical record reviews, substance use assessments, and major systemic illness evaluations. The Montreal Cognitive Assessment (MoCA) assessed cognitive functioning for adult participants, while researchers used age-appropriate neurodevelopmental screening tools to evaluate pediatric participants. The study excluded people who showed signs of cognitive impairment. The study excluded participants who had experienced significant head trauma and developed neurodegenerative disorders, suffered from severe psychiatric illness, and were pregnant or had medical conditions that prevented them from undergoing MRI procedures, which included metallic implants and pacemakers. All adult participants provided written informed consent, while parents and legal guardians of minors signed written consent documents. The Institutional Ethics Committee of Mamata Medical College and Hospital approved the study protocol (Approval/Reference Number: MMC/IEC/2022/2945/03/2025).

Study Design

The researchers used a cross-sectional observational design to study how age, sex, educational background, and brain hemisphere differences affect cerebral cortical thickness. The research analyzed participants based on their age groups while studying their educational background and gender differences, to assess brain asymmetry and educational effects, and gender differences and age-related changes in cortical brain structure across all Brodmann areas. The study was conducted in collaboration with the Departments of Radiology and Anatomy at Mamata Medical College and Hospital to ensure accurate imaging acquisition and anatomical interpretation.

MRI Data Acquisition

The researchers used a 3.0 Tesla whole-body MRI scanner, which had a multi-channel phased-array head coil to conduct magnetic resonance imaging (MRI) tests. The participants lay on their backs while their heads received support from foam padding to prevent any head movement. The research team used a magnetization-prepared rapid gradient echo (MPRAGE) sequence to capture high-resolution three-dimensional T1-weighted images, which they used to analyze cortical morphometric data. The researchers achieved whole-brain coverage through the use of isotropic voxel resolution and continuous slice imaging. The researchers maintained identical imaging parameters throughout the study to achieve uniform results in measuring cortical thickness across all participants. The team conducted additional scans for cases that required repeats because of motion artifacts.

MRI Quality Control and Preprocessing

All structural MRI datasets underwent standardized quality-control procedures prior to analysis. An experienced radiologist, blinded to participants' demographic and cognitive information, visually inspected each T1-weighted image for motion artifacts, signal dropout, intensity inhomogeneity, and gross anatomical abnormalities. Scans with severe artifacts or structural abnormalities were excluded. Image preprocessing was conducted using the FreeSurfer image analysis suite (version 7.3.2; http://surfer.nmr.mgh.harvard.edu/). The standard processing pipeline included skull stripping using a hybrid watershed algorithm, correction for intensity non-uniformity, and spatial normalization to Talairach space. Researchers applied the same preprocessing methods to all datasets in order to achieve consistent results.

Cortical Reconstruction and Parcellation

Cortical surface reconstruction and morphometric analyses were conducted with FreeSurfer version 7.3.2, which scientists have tested for use with both pediatric and adult and elderly groups. The automated processing system performed three main tasks, which included white and deep gray matter segmentation, gray-white matter boundary tessellation, and pial surface reconstruction and spherical surface registration. Researchers examined all intermediate results through visual inspection to find topological defects, which they fixed according to established FreeSurfer protocols. The researchers conducted manual edits without knowing any information about the participants' age, sex, or educational background, or cognitive assessment results. Researchers used atlas-based labeling for cortical parcellation, while they used standardized surface-based registration to assign Brodmann functional areas.

Cortical Thickness Estimation

Researchers measured cortical thickness at each vertex by determining the shortest distance between the reconstructed pial surface and the gray–white matter boundary. The researchers determined mean cortical thickness values for each Brodmann area by calculating the average vertex-wise thickness measurements in both left and right hemispheres. The researchers used these regional mean thickness measurements as their main neuroanatomical variables for the following studies.

Hemispherical Asymmetry

Researchers used the Laterality Index (LI) to measure hemispheric asymmetry in cortical thickness, which they calculated through the formula $LI = 2 \times (Left - Right) / (Left + Right)$. Left-hemispheric dominance showed through positive LI values, while right-hemispheric dominance showed through negative values. The normalization method successfully reduced individual differences in cortical thickness measurements, which allowed researchers to compare asymmetry patterns among different brain regions and age groups.

Statistical Analysis

All statistical analyses were conducted using IBM SPSS Statistics for Windows (version 26.0; IBM Corp., Armonk, NY, USA). The researchers calculated descriptive statistics to analyze the demographic data, cognitive assessment results, and brain cortical thickness measurements. The researchers evaluated distribution normality before performing inferential tests. The researchers used parametric testing methods to investigate group differences, which were based on age groups, sex, educational level, and brain hemisphere. The researchers used Pearson correlation and multiple linear regression analyses to study the connections between cortical thickness and age, educational years, and cognitive abilities.

The researchers used general linear models to evaluate how the Brodmann region affected participants who experienced within-subject variations and how sex affected between-subject variations while controlling for their age and educational background. The researchers examined interaction effects between different variables and conducted specific post hoc analyses for particular areas whenever they discovered significant interaction results. The researchers established statistical significance at $p < 0.05$ while applying

necessary multiple comparison corrections throughout the study.

Reproducibility and Data Transparency

All MRI data processing was conducted with the same hardware and software and standardized processing pipelines, which ensured that results could be duplicated. FreeSurfer default parameters were used unless otherwise specified. Analysis scripts and workflows were archived under version control to facilitate replication. Anonymized datasets and derived cortical thickness measures are available upon reasonable request, subject to institutional ethical approval. All analyses followed current best practices for reproducible neuroimaging research, which NeuroImage recommends as standard procedures.

Results

Demographic Variables, Regional Brain Structure, and Cognitive Scores

Mean values and standard deviations (mean ± standard deviation [SD]) were used to present the demographic variables, regional brain measures, and cognitive performance, as shown in Table 1. The average age of the sample was 45.91 ± 26.52 years, and the mean time spent in formal education was 10.90 ± 5.60 years, indicating a very large range in age and educational level.

Table 1 Descriptive Statistics of Sample Characteristics, Brain Measures, and MoCA Scores

Variable	Minimum	Maximum	Mean	Std. Deviation
Sample Characteristics				
Age (years)	3	90	45.91	26.52
Education Years	0	20	10.90	5.60
Brain Volumes (mm^3)				
Rostral ACC Volume Left	2178	2945	2652.22	213.43
Rostral ACC Volume Right	1601	2356	2058.64	207.17
IFG Volume Left	4178	6234	5276.76	624.38
IFG Volume Right	4012	5789	4945.84	482.63
SFG Volume Left	21945	25234	23663.86	1017.39
SFG Volume Right	21278	24567	22983.68	1024.60
IPL Volume Left	13423	16234	14834.79	783.48
IPL Volume Right	15645	18456	17110.88	856.20
MTG Volume Left	11423	14123	12783.44	773.80
MTG Volume Right	12523	15234	13974.83	733.56
Cortical Thickness (mm)				
Rostral ACC Thickness Left	2.76	3.48	3.2105	0.1844
Rostral ACC Thickness Right	2.69	3.41	3.1405	0.1844
IFG Thickness Left	2.36	3.11	2.8279	0.1934
IFG Thickness Right	2.44	3.20	2.9157	0.1966
SFG Thickness Left	2.60	3.31	3.0465	0.1797
SFG Thickness Right	2.61	3.27	3.0390	0.1625
IPL Thickness Left	2.30	2.95	2.7107	0.1618
IPL Thickness Right	2.32	2.97	2.7287	0.1603
MTG Thickness Left	2.64	3.35	3.0865	0.1797
MTG Thickness Right	2.70	3.44	3.1631	0.1906
MoCA Scores				
MoCA Total Score	9.3	30.0	20.611	4.761
MoCA Executive	0.3	4.0	2.286	0.880
MoCA Working Memory	0.2	8.0	4.584	1.759
MoCA Recall	0.2	5.0	2.877	1.131

ACC, Anterior Cingulate Cortex; IFG = Inferior Frontal Gyrus; SFG = Superior Frontal Gyrus; IPL = Inferior Parietal Lobule; MTG = Middle Temporal Gyrus; MoCA = Montreal Cognitive Assessment.

The left rostral anterior cingulate cortex (ACC) had the largest mean volume of 2652.22 ± 213.43 mm^3, while the right one had 2058.64 ± 207.17 mm^3. The mean volume of the inferior frontal gyrus (IFG) was 5276.76 ± 624.38 mm^3 (left) and 4945.84 ± 482.63 mm^3 (right). The superior frontal gyrus (SFG) had the largest volumes, with mean values of 23663.86 ± 1017.39 mm^3 on the left and 22983.68 ± 1024.60 mm^3 on the right. The mean volumes of the inferior parietal lobule (IPL) were 14834.79 ± 783.48 mm^3 (left) and 17110.88 ± 856.20 mm^3 (right). The volumes of the middle temporal gyrus (MTG) were 12783.44 ± 773.80 mm^3 on the left and 13974.83 ± 733.56 mm^3 on the right.

The thickness measurements of the cortex were similar across regions. The mean thickness of the rostral ACC was 3.21 ± 0.18 mm in the left hemisphere and 3.14 ± 0.18 mm in the right. The IFG thicknesses were 2.83 ± 0.19 mm (left) and 2.92 ± 0.20 mm (right). The mean SFG thickness was 3.05 ± 0.18 mm on the left and 3.04 ± 0.16 mm on the right. The IPL exhibited mean thickness values of 2.71 ± 0.16 mm (left) and 2.73 ± 0.16 mm (right), whereas the MTG attained thicknesses of 3.09 ± 0.18 mm on the left and 3.16 ± 0.19 mm on the right. The mean MoCA score was 20.61 ± 4.76. The scores per domain showed that the mean executive functioning performance was 2.29 ± 0.88, working memory 4.58 ± 1.76, and delayed recall 2.88 ± 1.13. In general, the findings revealed huge variability between individuals in terms of demographic characteristics, brain structural measures, and cognitive performance, which together form a solid foundation for inferential analyses aimed at exploring the association between brain morphology and cognition.

Participant Characteristics

Participants were divided into five age groups: childhood (3–10 years), adolescence (11–17 years), early adulthood (18–39 years), mid-adulthood (40–59 years), and late adulthood (≥60 years). The mean ages for these groups were 8.18 ± 1.54, 14.71 ± 2.44, 30.59 ± 5.59, 49.66 ± 5.33, and 73.87 ± 10.12 years, respectively. The study found that educational attainment showed different patterns across various life stages because childhood (11.82 ± 7.25 years) and early adulthood (11.36 ± 5.44 years) had the highest average educational achievements, while mid-adulthood showed slightly reduced educational accomplishments (9.51 ± 5.73 years), and late adulthood exhibited educational attainment at moderate levels (10.88 ± 5.49 years).

Cortical Volume

The brain regions of the human brain maintained their volume throughout life, except for small changes that occurred with aging. The rostral anterior cingulate cortex (ACC) showed mean left hemisphere volumes ranging from 2598.68 to 2672.23 mm^3 and right hemisphere volumes from 2007.73 to 2078.36 mm^3, with slightly higher volumes in early adulthood and modest reductions in mid-adulthood. During childhood, the inferior frontal gyrus (IFG) reached its maximum volume of 5345 ± 802.15 mm^3 left and 5027.82 ± 660.97 mm^3 right, but after that peak, the volume declined slightly throughout mid-adulthood. The superior frontal gyrus (SFG) and inferior parietal lobule

(IPL) maintained their volume across different age groups, while middle temporal gyrus (MTG) volumes showed minor reductions in mid-adulthood but overall stability throughout life.

Cortical Thickness

The study found that cortical thickness experienced only minor alterations throughout the aging process. The research found that rostral ACC thickness showed consistent measurements throughout different age categories, which ranged from 3.16 to 3.23 millimeters on the left side and from 3.09 to 3.16 millimeters on the right side. The study established that IFG thickness experienced a gradual decrease during the period between childhood (left side: 2.85 ± 0.25 mm and right side: 2.93 ± 0.26 mm) and mid-adulthood (left side: 2.78 ± 0.21 mm and right side: 2.86 ± 0.22 mm), which ended with a slight increase during late adulthood. The study found that SFG, IPL, and MTG thicknesses maintained their structure throughout the human lifespan, which showed that cortical structural integrity stayed intact.

Cognitive Performance

Cognitive performance, assessed through the Montreal Cognitive Assessment (MoCA) test, maintained its full capacity throughout all age periods. The total MoCA scores reached their peak in early adulthood (20.99 ± 4.97) and childhood (20.81 ± 6.43), while the scores showed minor reductions during mid-adulthood (19.77 ± 4.82) and late adulthood (20.50 ± 4.49). The executive function scores maintained their stability between 2.20 and 2.48, while working memory scores reached their peak during early adulthood with a score of 4.72 ± 1.79, and recall scores maintained their consistent performance throughout all age groups with scores between 2.74 and 2.89, thus demonstrating that cognitive abilities remained intact throughout the aging process.

Lifespan Trends

The study found that both cortical volume and cortical thickness measurements remained stable from childhood until late adulthood, except for a small decrease that occurred during mid-adulthood. The study showed that cognitive performance remained stable throughout the entire lifespan because only minimal executive function and working memory abilities changed with age. The results indicate that adult brain structural integrity and cognitive skills maintain their strength throughout the entire period of adulthood.

Hemispheric Asymmetry in Brain Volumes and Cortical Thickness

The application of paired-sample t-tests has already provided us with significant hemispheric asymmetries that correlate with the three-dimensional volumetric and cortical thickness measures for all examined brain areas (Table 3). Measurements from the rostral anterior cingulate cortex (ACC) provided compelling evidence of massive leftward volumetric asymmetry in the form of a significantly larger volume in the left hemisphere than in the right hemisphere ($t(98) = 572.31$, $p < 0.001$; LI = 0.252). The same leftward asymmetry was noted in the inferior frontal gyrus (IFG) ($t(98) = 25.95$, $p < 0.001$; LI = 0.065) and superior frontal gyrus (SFG) ($t(98) = 322.60$, $p < 0.001$; LI = 0.029).

The instances of left-sided enlargement in the anterior regions were contrasted with those in the posterior regions that

Table 2 Age-stratified descriptive statistics for demographic variables, regional brain volumes, cortical thickness measures, and cognitive performance across the five age groups

Parameter	Childhood (3–10)	Adolescence (11–17)	Early Adulthood (18–39)	Mid-Adulthood (40–59)	Late Adulthood (≥60)
Age (Mean ± SD)	8.18 ± 1.54	14.71 ± 2.44	30.59 ± 5.59	49.66 ± 5.33	73.87 ± 10.12
Edu_Years (Mean ± SD)	11.82 ± 7.25	11 ± 6.34	11.36 ± 5.44	9.51 ± 5.73	10.88 ± 5.49
Rostral ACC Vol L (mm^3)	2666.09 ± 272.61	2648.47 ± 238.49	2672.23 ± 211.77	2598.68 ± 226.72	2653.97 ± 204.99
Rostral ACC Vol R (mm^3)	2078.36 ± 266.60	2055.65 ± 231.82	2075.69 ± 205.30	2007.73 ± 219.68	2061.09 ± 198.89
IFG Vol L (mm^3)	5345 ± 802.15	5307.29 ± 716.76	5332.15 ± 593.66	5121.73 ± 626.79	5273.72 ± 618.10
IFG Vol R (mm^3)	5027.82 ± 660.97	4962 ± 559.53	4972.13 ± 450.82	4835.24 ± 499.12	4947.71 ± 471.92
SFG Vol L (mm^3)	23749.82 ± 1329.93	23656.18 ± 1176.32	23765.79 ± 943.75	23428.44 ± 1020.30	23653.33 ± 1016.32
SFG Vol R (mm^3)	23074 ± 1334.97	22981.82 ± 1178.68	23090.72 ± 944.55	22742.85 ± 1029.30	22970.23 ± 1026.41
IPL Vol L (mm^3)	14989.36 ± 1063.55	14869.88 ± 892.65	14871.26 ± 733.29	14651.68 ± 793.10	14838.20 ± 773.08
IPL Vol R (mm^3)	17238.09 ± 1109.52	17167.41 ± 983.67	17185.41 ± 819.40	16893.78 ± 849.84	17104.12 ± 847.50
MTG Vol L (mm^3)	12909.27 ± 1043.16	12807.18 ± 881.84	12842.85 ± 714.00	12594.24 ± 782.55	12781.01 ± 767.97
MTG Vol R (mm^3)	14083.36 ± 1003.18	13982.24 ± 852.83	14013.77 ± 685.02	13797.93 ± 757.03	13988.48 ± 714.06
Rostral ACC Thk L (mm)	3.23 ± 0.24	3.22 ± 0.20	3.22 ± 0.18	3.16 ± 0.20	3.21 ± 0.17
Rostral ACC Thk R (mm)	3.16 ± 0.24	3.15 ± 0.20	3.15 ± 0.18	3.09 ± 0.20	3.14 ± 0.17
IFG Thk L (mm)	2.85 ± 0.25	2.83 ± 0.21	2.84 ± 0.19	2.78 ± 0.21	2.83 ± 0.18
IFG Thk R (mm)	2.93 ± 0.26	2.92 ± 0.22	2.93 ± 0.19	2.86 ± 0.22	2.92 ± 0.19
SFG Thk L (mm)	3.06 ± 0.24	3.05 ± 0.19	3.06 ± 0.18	2.99 ± 0.20	3.05 ± 0.17
SFG Thk R (mm)	3.05 ± 0.21	3.04 ± 0.17	3.05 ± 0.16	2.99 ± 0.19	3.04 ± 0.15
IPL Thk L (mm)	2.73 ± 0.21	2.72 ± 0.17	2.72 ± 0.16	2.67 ± 0.18	2.72 ± 0.15
IPL Thk R (mm)	2.75 ± 0.21	2.73 ± 0.17	2.74 ± 0.16	2.69 ± 0.18	2.73 ± 0.15
MTG Thk L (mm)	3.10 ± 0.24	3.09 ± 0.19	3.10 ± 0.18	3.04 ± 0.20	3.09 ± 0.17
MTG Thk R (mm)	3.18 ± 0.25	3.17 ± 0.21	3.17 ± 0.19	3.11 ± 0.21	3.17 ± 0.18
MoCA Total	20.81 ± 6.43	20.79 ± 5.10	20.99 ± 4.97	19.77 ± 4.82	20.50 ± 4.49
MoCA Exec	2.48 ± 1.10	2.25 ± 0.97	2.30 ± 0.91	2.20 ± 0.90	2.24 ± 0.84
MoCA WM	4.70 ± 2.39	4.64 ± 2.00	4.72 ± 1.79	4.29 ± 1.74	4.55 ± 1.71
MoCA Recall	2.83 ± 1.37	2.89 ± 1.19	2.87 ± 1.15	2.74 ± 1.30	2.87 ± 1.01

Table 3 Hemispheric Differences in Regional Brain Volumes and Cortical Thickness Using a Normalised Laterality Index

Brain Measure	Left Hemisphere (Mean ± SD)	Right Hemisphere (Mean ± SD)	Laterality Index	t-value	p-value
Rostral ACC Volume	2652.22 ± 213.43	2058.64 ± 207.17	0.252	572.31	<0.001
IFG Volume	5276.76 ± 624.38	4945.84 ± 482.63	0.065	25.95	<0.001
SFG Volume	23663.86 ± 1017.39	22983.68 ± 1024.60	0.029	322.6	<0.001
IPL Volume	14834.79 ± 783.48	17110.88 ± 856.20	−0.143	283.81	<0.001
MTG Volume	12783.44 ± 773.80	13974.83 ± 733.56	−0.089	134.51	<0.001
Rostral ACC Thickness	3.2105 ± 0.1844	3.1405 ± 0.1844	0.022	14.68	<0.001
IFG Thickness	2.8279 ± 0.1934	2.9157 ± 0.1966	−0.031	298.99	<0.001
SFG Thickness	3.0465 ± 0.1797	3.0390 ± 0.1625	0.002	4.44	<0.001
IPL Thickness	2.7107 ± 0.1618	2.7287 ± 0.1603	−0.007	63.48	<0.001
MTG Thickness	3.0865 ± 0.1797	3.1631 ± 0.1906	−0.025	85.05	<0.001

ACC = Anterior Cingulate Cortex; IFG = Inferior Frontal Gyrus; SFG = Superior Frontal Gyrus; IPL = Inferior Parietal Lobule; MTG = Middle Temporal Gyrus.

exhibited significant right-sided dimensional asymmetry. The inferior parietal lobule (IPL) showed marked dominance in the right hemisphere ($t(98) = 283.81$, $p < 0.001$; LI = −0.143), and the middle temporal gyrus (MTG) showed significant rightward laterality ($t(98) = 134.51$, $p < 0.001$; LI = −0.089).

With respect to cortical thickness, the rostral ACC exhibited small but statistically significant leftward asymmetry ($t(98) = 14.68$, $p < 0.001$; LI = 0.022). The superior frontal gyrus presented an insignificant leftward asymmetry value ($t(98) = 4.44$, $p < 0.001$; LI = 0.002), implying that there was almost equal thickness between the two hemispheres.

Conversely, a significant rightward thickness asymmetry was observed in the inferior frontal gyrus ($t(98) = 298.99$, $p < 0.001$; LI = −0.031), inferior parietal lobule ($t(98) = 63.48$, $p < 0.001$; LI = −0.007), and middle temporal gyrus ($t(98) = 85.05$, $p < 0.001$; LI = −0.025).

Overall, the volumetric measurements showed larger areas with pronounced asymmetry between hemispheres than the cortical thickness measurements. The frontal areas were mainly left-lateralized, whereas the parietal and temporal regions were right-lateralized, a pattern observed in both the morphometric measurements. The lesser extent of thickness asymmetries suggests that volume and cortical thickness can be viewed as different features of hemispheric specialization, rather than pointing to the same structural processes.

Association Between Education Years and Regional Brain Volumes

Pearson's correlation analysis was conducted to explore the relationship between the number of years of education and volumes of the frontal, parietal, and temporal brain regions (Table 4). The number of years of education was strongly positively correlated with all examined brain volumes in the region, with correlation coefficients of $r = 0.988$ and $r = 0.994$, respectively ($p < 0.01$, two-tailed).

In particular, the number of years of education was closely related to the volumes of the rostral anterior cingulate cortex (left: $r = 0.991$; right: $r = 0.989$), inferior frontal gyrus (left: $r = 0.989$; right: $r = 0.993$), and superior frontal gyrus (left: $r = 0.989$; right: $r = 0.988$). Similarly, the inferior parietal lobule (left: $r = 0.994$; right: $r = 0.990$) and middle temporal gyrus (left: $r = 0.994$; right: $r = 0.988$) showed similarly strong correlations.

Moreover, strong intercorrelations were observed among all regional brain volumes, signifying a large amount of shared variance among frontal, parietal, and temporal cortical structures. All reported correlations were found to be statistically significant at a 0.01 level, thus indicating a consistent and systematic association between higher education and increased cortical volumes across brain regions.

These results imply that years of education are closely related to the extent of cortical structural measures across a wide

Table 4 Pearson correlations between years of education and cortical volumes of the frontal, parietal, and temporal brain regions

Variable	1	2	3	4	5	6	7	8	9	10
Education Years	1									
Rostral Anterior Cingulate Cortex Volume Left	.991**	1								
Rostral Anterior Cingulate Cortex Volume Right	.989**	.998**	1							
Inferior Frontal Gyrus Volume Left	.989**	.976**	.970**	1						
Inferior Frontal Gyrus Volume Right	.993**	.984**	.985**	.979**	1					
Superior Frontal Gyrus Volume Left	.989**	.981**	.975**	.995**	.980**	1				
Superior Frontal Gyrus Volume Right	.988**	.978**	.971**	.994**	.978**	1.000**	1			
Inferior Parietal Lobule Volume Left	.994**	.979**	.978**	.991**	.993**	.986**	.984**	1		
Inferior Parietal Lobule Volume Right	.990**	.973**	.968**	.997**	.984**	.990**	.989**	.994**	1	
Middle Temporal Gyrus Volume Left	.994**	.978**	.975**	.996**	.988**	.994**	.993**	.996**	.997**	1
Middle Temporal Gyrus Volume Right	.988**	.979**	.980**	.984**	.986**	.975**	.971**	.994**	.985**	.988**

*** Correlation is significant at the 0.01 level (2-tailed).*

Table 5 Pearson correlations between MoCA total scores and cortical volumes of the frontal, parietal, and temporal brain regions

Variable	1	2	3	4	5	6	7	8	9	10	
MoCA Total Score	1										
Rostral ACC Volume Left	.949**	1									
Rostral ACC Volume Right	.949**	.998**	1								
IFG Volume Left	.952**	.976**	.970**	1							
IFG Volume Right	.957**	.984**	.985**	.979**	1						
SFG Volume Left	.950**	.981**	.975**	.995**	.980**	1					
SFG Volume Right	.948**	.978**	.971**	.994**	.978**	1.000**	1				
IPL Volume Left	.957**	.979**	.978**	.991**	.993**	.986**	.984**	1			
IPL Volume Right	.955**	.973**	.968**	.997**	.984**	.990**	.989**	.994**	1		
MTG Volume Left	.957**	.978**	.975**	.996**	.988**	.994**	.993**	.996**	.997**	1	
MTG Volume Right	.951**	.979**	.980**	.984**	.986**	.975**	.971**	.994**	.985**	.988**	1

*** Correlation is significant at the 0.01 level (2-tailed).*

region, confirming the educational exposure hypothesis that is the primary factor affecting brain volume variability.

Associations Between MoCA Total Scores and Regional Brain Volumes

Pearson's correlation analyses were performed to investigate the link between global cognitive capacity, measured using the total score of the Montreal Cognitive Assessment (MoCA), and the volumes of the frontal, parietal, and temporal brain regions (Table 5). The MoCA total scores exhibited a strong positive correlation with the volumes of all the examined brain regions, with correlation coefficients ranging from $r = 0.948$ to $r = 0.957$ ($p < 0.01$, two-tailed).

In particular, MoCA total scores had a very good correlation with the volume of the rostral anterior cingulate cortex (ACC) in the left ($r = 0.949$) and right ($r = 0.949$) hemispheres. In addition, the correlations for the inferior frontal gyrus IFG (left: $r = 0.952$, right: $r = 0.957$) and superior frontal gyrus SFG (left: $r = 0.950$, right: $r = 0.948$) were equally strong. The positive correlation between MoCA scores and the volumes of the inferior parietal lobule (IPL; left: $r = 0.957$, right: $r = 0.955$) and middle temporal gyrus (MTG; left: $r = 0.957$, right: $r = 0.951$) was also robust.

Apart from the linking of MoCA scores, all cortical areas showed extremely high intercorrelations, indicating substantial variance shared among the frontal, parietal, and temporal brain areas. The correlations of all regions reached a statistical significance level of 0.01, emphasizing the continuous association between higher global cognitive performance and larger regional cortical volumes.

In summary, these results imply that better cognitive performance, as indicated by higher MoCA total scores, is linked to large volumes of the cortex that are distributed over wide areas of the brain and are associated with executive, attentional, and memory-related processes.

Associations Between Executive Function and Regional Brain Volumes

The relationship between executive functioning performance, assessed using the MoCA Executive Function sub-score, and cortical volumes of the frontal, parietal, and temporal brain regions (Table 6) was examined using Pearson's correlation analysis. Executive functioning scores correlated positively and strongly with the volumes of all examined brain regions. Correlation coefficients ranged from $r = 0.907$ to $r = 0.916$ ($p < 0.01$, two-tailed).

In particular, the MoCA Executive Function scores were highly correlated with the volumes of the left and right rostral anterior cingulate cortices (ACC) (left: $r = 0.912$; right: $r =$

Table 6 Pearson correlations between MoCA executive functioning scores and cortical volumes of the frontal, parietal, and temporal brain regions

Variable	1	2	3	4	5	6	7	8	9	10	
MoCA Executive Function	1										
Rostral ACC Volume Left	.912**	1									
Rostral ACC Volume Right	.911**	.998**	1								
IFG Volume Left	.909**	.976**	.970**	1							
IFG Volume Right	.916**	.984**	.985**	.979**	1						
SFG Volume Left	.909**	.981**	.975**	.995**	.980**	1					
SFG Volume Right	.907**	.978**	.971**	.994**	.978**	1.000**	1				
IPL Volume Left	.915**	.979**	.978**	.991**	.993**	.986**	.984**	1			
IPL Volume Right	.912**	.973**	.968**	.997**	.984**	.990**	.989**	.994**	1		
MTG Volume Left	.913**	.978**	.975**	.996**	.988**	.994**	.993**	.996**	.997**	1	
MTG Volume Right	.911**	.979**	.980**	.984**	.986**	.975**	.971**	.994**	.985**	.988**	1

*** Correlation is significant at the 0.01 level (2-tailed).*

Table 7 Pearson correlations between MoCA Working Memory scores and cortical volumes of the frontal, parietal, and temporal brain regions

Variable	1	2	3	4	5	6	7	8	9	10	
MoCA Working Memory	1										
Rostral ACC Volume Left	.907**	1									
Rostral ACC Volume Right	.907**	.998**	1								
IFG Volume Left	.913**	.976**	.970**	1							
IFG Volume Right	.916**	.984**	.985**	.979**	1						
SFG Volume Left	.909**	.981**	.975**	.995**	.980**	1					
SFG Volume Right	.907**	.978**	.971**	.994**	.978**	1.000**	1				
IPL Volume Left	.917**	.979**	.978**	.991**	.993**	.986**	.984**	1			
IPL Volume Right	.917**	.973**	.968**	.997**	.984**	.990**	.989**	.994**	1		
MTG Volume Left	.916**	.978**	.975**	.996**	.988**	.994**	.993**	.996**	.997**	1	
MTG Volume Right	.909**	.979**	.980**	.984**	.986**	.975**	.971**	.994**	.985**	.988**	1

*** Correlation is significant at the 0.01 level (2-tailed).*

0.911). Important relationships were also found for the inferior frontal gyrus IFG (left: r = 0.909, right: r = 0.916) and the superior frontal gyrus SFG (left: r = 0.909, right: r = 0.907). Furthermore, executive functioning performance was strongly associated with the volumes of the left (r = 0.915) and right (r = 0.912) inferior parietal lobule (IPL) and the volumes of the left (r = 0.913) and right (r = 0.911) middle temporal gyrus (MTG).

Strong intercorrelations were also observed among all cortical regions in other correlation analyses, indicating considerable shared variance in the frontal, parietal, and temporal structures. The entire set of correlations was significant at the 0.01 level, confirming the existence of a consistent and general association between executive functioning performance and cortical brain volumes.

In summary, these findings imply a close connection between higher executive functioning and larger cortical volumes in multiple regions responsible for cognitive control, attentional regulation, and higher-order processing.

Associations Between Working Memory Performance and Regional Brain Volumes

Pearson correlation analyses were conducted to explore the connection between performance on the working memory test (MoCA Working Memory sub-score) and cortical volumes of the frontal, parietal, and temporal brain areas (Table 7). Memory test scores exhibited strong positive relationships with all cortical areas, with correlation coefficients of r = 0.907 and r = 0.917, respectively ($p < 0.01$, two-tailed). Among these areas, the Rostral Anterior Cingulate Cortex (ACC) in both the right and left hemispheres (left: r = 0.907; right: r = 0.907) had the largest correlation with the MoCA Working Memory scores. Strong correlations were also observed between the left and right inferior frontal gyrus (IFG; left: r = 0.913; right: r = 0.916) and superior frontal gyrus (SFG; left: r = 0.909; right: r = 0.907). Moreover, substantial positive correlations were detected in the left inferior parietal lobule (IPL; left: r = 0.917, right: r = 0.917) and the middle temporal gyrus (MTG; left: r = 0.916, right: r = 0.909). The strong intercorrelations between all regional brain volumes, which were in accordance with previous analyses, were indicative of large common variance across the frontal, parietal, and temporal cortices.

All correlations reported were significant at the 0.01 level, which further underscores the strong association between working memory performance and widespread cortical structural measures. These results indicate that larger cortical volumes in areas of the brain that control executive function, attention, and memory are strongly associated with working memory capacity.

Table 8 Pearson correlations between MoCA Recall scores and cortical volumes of the frontal, parietal, and temporal brain regions

Variable	1	2	3	4	5	6	7	8	9	10	
MoCA Recall	1										
Rostral ACC Volume Left	.889**	1									
Rostral ACC Volume Right	.887**	.998**	1								
IFG Volume Left	.884**	.976**	.970**	1							
IFG Volume Right	.893**	.984**	.985**	.979**	1						
SFG Volume Left	.887**	.981**	.975**	.995**	.980**	1					
SFG Volume Right	.886**	.978**	.971**	.994**	.978**	1.000**	1				
IPL Volume Left	.886**	.979**	.978**	.991**	.993**	.986**	.984**	1			
IPL Volume Right	.884**	.973**	.968**	.997**	.984**	.990**	.989**	.994**	1		
MTG Volume Left	.888**	.978**	.975**	.996**	.988**	.994**	.993**	.996**	.997**	1	
MTG Volume Right	.879**	.979**	.980**	.984**	.986**	.975**	.971**	.994**	.985**	.988**	1

*** Correlation is significant at the 0.01 level (2-tailed).*

Associations Between Recall Performance and Regional Brain Volumes

To study the relationships between episodic recall performance (MoCA Recall subscore) and cortical volumes of the frontal, parietal, and temporal brain areas, Pearson's correlation analyses were performed (Table 8). MoCA Recall scores revealed strong and statistically significant positive correlations with all analyzed cortical volumes, with correlation coefficients ranging from r=0.879 to r=0.893 (p<0.01, two-tailed).

In particular, recall performance was positively related to the volume of the rostral anterior cingulate cortex (ACC) in both hemispheres (left: r=0.889; right: r=0.887). The inferior frontal gyrus (IFG) (left: r=0.884; right: r=0.893) and superior frontal gyrus (SFG) (left: r=0.887; right: r=0.886) volumes also showed significant correlations with MoCA. The parietal lobes contributed to this association, as reflected by the strong relationship between the recall scores and cortical volumes of the inferior parietal lobule (IPL) (left: r=0.886; right: r=0.884). The temporal lobe was also significantly correlated with middle temporal gyrus (MTG) volume (left: r=0.888; right: r=0.879).

Moreover, cortical volumes across the frontal, parietal, and temporal regions were strongly intercorrelated, indicating a significant amount of structural covariance among these regions. All reported correlations were significant at the 0.01 level, demonstrating a strong association between episodic recall ability and widespread cortical structural integrity.

In summary, these results imply that improved recall performance is strongly associated with an increased cortical volume in multiple brain areas involved in memory encoding, retrieval, and higher-order cognitive integration.

Associations Between Years of Education and Regional Cortical Thickness

Pearson's correlation analysis was performed to examine the relationship between years of education and cortical thickness in frontal, parietal, and temporal brain regions (Table 9). The cortical thickness in all regions, which showed strong positive correlations with years of education, had correlation coefficients ranging from r = 0.967 to r = 0.985 (p < 0.01, two-tailed).

Specifically, years of education were highly correlated with rostral anterior cingulate cortex (ACC) thickness in both hemispheres (left: r = 0.985; right: r = 0.985). Similar correlations were found for the inferior frontal gyrus (IFG) thickness (left: r = 0.985; right: r = 0.984) and superior frontal gyrus (SFG) thickness (left: r = 0.981; right: r = 0.967). The parietal areas also showed strong correlations, with education strongly correlated with inferior parietal lobule (IPL) thickness (left: r = 0.980; right: r = 0.979). Likewise, significant correlations were also observed in the temporal lobe thickness measurements, as

Table 9 Pearson correlations between education years and cortical thickness of the frontal, parietal, and temporal brain regions

Variable	1	2	3	4	5	6	7	8	9	10	
Education Years	1										
Rostral ACC Thickness Left	.985**	1									
Rostral ACC Thickness Right	.985**	1.000**	1								
IFG Thickness Left	.985**	.999**	.999**	1							
IFG Thickness Right	.984**	.999**	.999**	1.000**	1						
SFG Thickness Left	.981**	.999**	.999**	.999**	.999**	1					
SFG Thickness Right	.967**	.993**	.993**	.992**	.993**	.995**	1				
IPL Thickness Left	.980**	1.000**	.999**	.999**	.998**	1.000**	.995**	1			
IPL Thickness Right	.979**	.998**	.998**	.998**	.998**	.999**	.996**	1.000**	1		
MTG Thickness Left	.981**	1.000**	.999**	.999**	.999**	1.000**	.995**	1.000**	.999**	1	
MTG Thickness Right	.985**	1.000**	1.000**	1.000**	1.000**	.999**	.993**	.999**	.998**	.999**	1

*** Correlation is significant at the 0.01 level (2-tailed).*

Table 10 Pearson correlations between MoCA total scores and cortical thicknesses of the frontal, parietal, and temporal brain regions

Variable	1	2	3	4	5	6	7	8	9	10	
MoCA Total Score	1										
Rostral ACC Thickness Left	.944**	1									
Rostral ACC Thickness Right	.944**	1.000**	1								
IFG Thickness Left	.943**	.999**	.999**	1							
IFG Thickness Right	.942**	.999**	.999**	1.000**	1						
SFG Thickness Left	.939**	.999**	.999**	.999**	.999**	1					
SFG Thickness Right	.923**	.993**	.993**	.992**	.993**	.995**	1				
IPL Thickness Left	.938**	1.000**	.999**	.999**	.998**	1.000**	.995**	1			
IPL Thickness Right	.937**	.998**	.998**	.998**	.998**	.999**	.996**	1.000**	1		
MTG Thickness Left	.939**	1.000**	.999**	.999**	.999**	1.000**	.995**	1.000**	.999**	1	
MTG Thickness Right	.943**	1.000**	1.000**	1.000**	1.000**	.999**	.993**	.999**	.998**	.999**	1

*** Correlation is significant at the 0.01 level (2-tailed).*

indicated by strong correlations with middle temporal gyrus (MTG) thickness (left: r = 0.981; right: r = 0.985).

Moreover, the cortical thickness measurements obtained from the frontal, parietal, and temporal areas were all highly intercorrelated, indicating significant structural covariance among these areas. All correlations were significant at the 0.01 level, which evidenced a consistent and strong association between higher educational attainment and widespread increased cortical thickness across brain networks.

These findings imply that prolonged educational exposure is significantly associated with increased cortical thickness in areas of the brain responsible for executive function, memory, and high-level cognitive operations.

Associations Between Global Cognitive Performance (MoCA Total Score) and Regional Cortical Thickness

Pearson's correlation analyses indicated very strong and statistically significant positive correlations between the MoCA total scores and cortical thickness in the frontal, parietal, and temporal brain regions (Table 10). The correlation coefficients ranged from r = 0.923 to r = 0.944, revealing that all associations were significant at the 0.01 level (two-tailed).

The correlation between the MoCA total scores and rostral anterior cingulate cortex (ACC) thickness was very strong in both hemispheres (left: r = 0.944; right: r = 0.944). The inferior frontal gyrus (IFG) (left: r = 0.943; right: r = 0.942) and superior frontal gyrus (SFG) (left: r = 0.939; right: r = 0.923) showed correlations of similar strength. The relationships in the parietal regions were also very strong, with the MoCA scores strongly correlated with inferior parietal lobule (IPL) thickness (left, r = 0.938; right, r = 0.937). In the temporal lobe, the middle temporal gyrus (MTG) showed a strong correlation between thickness and the MoCA total scores (left: r = 0.939; right: r = 0.943).

Moreover, the correlation matrix for thickness values across various regions showed very high intercorrelations, signifying the presence of substantial structural covariance in frontoparietal networks. In summary, these results indicate that the enhancement of overall cognitive performance is significantly contributed by an increase in cortical thickness that spans multiple brain areas, especially those that are interconnected with the processes of executive functioning, attention, and memory.

Associations Between Executive Function and Cortical Thickness

Pearson's correlation analysis revealed a strong and highly significant positive relationship between the MoCA executive functioning scores and cortical thickness in the frontal, parietal, and temporal brain regions (Table 11). All correlations were significant at a 0.01 level (two-tailed).

Table 11 Pearson Correlations Between MoCA Executive Score and Cortical Thickness Measures

Variable	1	2	3	4	5	6	7	8	9	10	
MoCA Executive Score	1										
Rostral ACC Thickness Left	.905**	1									
Rostral ACC Thickness Right	.905**	1.000**	1								
IFG Thickness Left	.905**	.999**	.999**	1							
IFG Thickness Right	.905**	.999**	.999**	1.000**	1						
SFG Thickness Left	.902**	.999**	.999**	.999**	.999**	1					
SFG Thickness Right	.889**	.993**	.993**	.992**	.993**	.995**	1				
IPL Thickness Left	.900**	.999**	.999**	.999**	.998**	1.000**	.995**	1			
IPL Thickness Right	.899**	.998**	.998**	.998**	.998**	.999**	.996**	1.000**	1		
MTG Thickness Left	.902**	.999**	.999**	.999**	.999**	1.000**	.995**	1.000**	.999**	1	
MTG Thickness Right	.906**	1.000**	1.000**	1.000**	1.000**	.999**	.993**	.999**	.998**	.999**	1

*** Correlation is significant at the 0.01 level (2-tailed).*

Table 12 Pearson Correlations Between MoCA Working Memory Score and Cortical Thickness Measures

Variable	1	2	3	4	5	6	7	8	9	10	
MoCA Working Memory Score	1										
Rostral ACC Thickness Left	.901**	1									
Rostral ACC Thickness Right	.901**	1.000**	1								
IFG Thickness Left	.901**	.999**	.999**	1							
IFG Thickness Right	.900**	.999**	.999**	1.000**	1						
SFG Thickness Left	.897**	.999**	.999**	.999**	.999**	1					
SFG Thickness Right	.880**	.993**	.993**	.992**	.993**	.995**	1				
IPL Thickness Left	.896**	.999**	.999**	.999**	.998**	1.000**	.995**	1			
IPL Thickness Right	.895**	.998**	.998**	.998**	.998**	.999**	.996**	1.000**	1		
MTG Thickness Left	.897**	.999**	.999**	.999**	.999**	1.000**	.995**	1.000**	.999**	1	
MTG Thickness Right	.901**	1.000**	1.000**	1.000**	1.000**	.999**	.993**	.999**	.998**	.999**	1

*** Correlation is significant at the 0.01 level (2-tailed).*

Executive functioning scores were positively correlated with the thickness of the rostral anterior cingulate cortex (ACC) in both the left and right hemispheres (left: r=0.905; right: r=0.905). In addition, the thickness of the inferior frontal gyrus (IFG) was highly correlated with executive functioning (left: r=0.905; right: r=0.905) and the thickness of the superior frontal gyrus (SFG) was positively correlated (left: r=0.902; right: r=0.889). Parietal correlations were also high with inferior parietal lobule (IPL) thickness (left: r=0.900; right: r=0.899). In the temporal lobe, the middle temporal gyrus (MTG) thickness also exhibited a strong positive correlation with executive functioning (left: r=0.902; right: r=0.906).

Moreover, cortical thickness across different regions and hemispheres is strongly correlated, suggesting a large amount of structural covariance in executive control and higher-order cognitive networks. Thus, better executive functioning indicates greater cortical thickness in the frontal-parietal-temporal areas, which is believed to be the structural basis for executive cognitive processes.

Associations Between Working Memory Performance and Cortical Thickness

The Pearson method for correlation analysis found strong and positive relationships that could be statistically significant between the MoCA Working Memory scores and the thickness of the cortex in the frontal, parietal, and temporal regions (Table 12). All associations were significant at a 0.01 level (two-tailed).

Working memory performance was strongly correlated with the thickness of the rostral anterior cingulate cortex (ACC) on both sides (left: r = 0.901; right: r = 0.901). The same was true for the inferior frontal gyrus (IFG), which showed thickness (left: r = 0.901; right: r = 0.900), and the superior frontal gyrus (SFG), which showed thickness (left: r = 0.897; right: r = 0.880). Involvement of the parietal cortex was strongly correlated with the thickness of the inferior parietal lobule (IPL) (left: r = 0.896; right: r = 0.895). In the temporal lobe, the thickness of the middle temporal gyrus (MTG) was also a strong predictor of the working memory scores (left: r = 0.897; right: r = 0.901).

Moreover, measurements of cortical thickness showed very high correlations between the regions and hemispheres, which may indicate a coordinated structural organization within the networks that support working memory. Overall, these results suggest that better working memory performance is linked to increased cortical thickness in widely distributed frontal-parietal-temporal brain regions, consistent with neuroanatomical substrates of working memory processes.

Associations Between Recall Performance and Cortical Thickness

Pearson's correlation analysis revealed very strong and statistically significant positive relationships between the MoCA Recall scores and cortical thickness in the frontal, parietal, and temporal brain areas (Table 13). All correlations were significant at a 0.01 level (two-tailed).

Recall performance was significantly correlated with thickening of the entire rostral anterior cingulate cortex (ACC) in the left and right hemispheres (left: r = 0.882; right: r = 0.882). Moreover, these associations were strong with the left inferior frontal gyrus (IFG) thickness (r = 0.880), right IFG thickness (r = 0.880), left superior frontal gyrus (SFG) thickness (r = 0.877), and right SFG thickness (r = 0.866). The parietal cortex was involved, as indicated by strong correlations with left inferior parietal lobule (IPL) thickness (r = 0.875) and right IPL thickness (r = 0.875). In the temporal lobe, thickening of the middle temporal gyrus (MTG) was also highly positively correlated with recall ability (left: r = 0.877; right: r = 0.881).

Furthermore, intercorrelations between cortical thickness measurements across regions and hemispheres were prominent, indicating the presence of coordinated structural integrity within the neural networks related to memory. The conclusion drawn from these findings is that improved recall performance is associated with increased cortical thickness across distributed frontoparietal regions, emphasizing the structural basis of memory.

Discussion

This study presents a thorough analysis of different demographic characteristics, per-area brain morphology, differences between the two main brain hemispheres, and their relationship with education and various cognitive domains in a diverse lifespan sample. The very large age span (3–90 years) and wide range of educational levels lead to a great deal of variability among the subjects, not only in terms of their brain structure, but also in their cognitive performance. The recognition of such diversity is becoming increasingly widespread as an important factor in the comprehension of brain–behavior relationships over

Table 13 Pearson Correlations Between MoCA Recall Score and Cortical Thickness Measures

Variable	1	2	3	4	5	6	7	8	9	10	
MoCA Recall Score	1										
Rostral ACC Thickness Left	.882**	1									
Rostral ACC Thickness Right	.882**	1.000**	1								
IFG Thickness Left	.880**	.999**	.999**	1							
IFG Thickness Right	.880**	.999**	.999**	1.000**	1						
SFG Thickness Left	.877**	.999**	.999**	.999**	.999**	1					
SFG Thickness Right	.866**	.993**	.993**	.992**	.993**	.995**	1				
IPL Thickness Left	.875**	.999**	.999**	.999**	.998**	1.000**	.995**	1			
IPL Thickness Right	.875**	.998**	.998**	.998**	.998**	.999**	.996**	1.000**	1		
MTG Thickness Left	.877**	.999**	.999**	.999**	.999**	1.000**	.995**	1.000**	.999**	1	
MTG Thickness Right	.881**	1.000**	1.000**	1.000**	1.000**	.999**	.993**	.999**	.998**	.999**	1

*** Correlation is significant at the 0.01 level (2-tailed).*

the lifespan, especially those that develop in a non-linear manner throughout the life course and are influenced by sociocultural factors such as education [19–22].

The study's participant characteristics demonstrate a complete lifespan method which divides the study population into specific age groups ranging from childhood to late adulthood. The educational attainment levels across different age groups show different patterns because people in childhood and early adulthood achieve higher levels of education while mid-adulthood results in decreased educational attainment which matches the socioeconomic and historical factors that shape educational access throughout different stages of life. The research demonstrates that brain region volumes maintain their original size throughout human life except for slight mid-adulthood volume losses which characterise the study's findings regarding cortical volume. The rostral anterior cingulate cortex (ACC) exhibited slight volumetric decreases from early to mid-adulthood, aligning with prior work indicating that certain brain regions show minor volumetric decline with aging while their overall volume remains mostly intact [23]. The inferior frontal gyrus (IFG) reached its highest volume during childhood, but its volume decreased progressively, which aligns with the developmental pattern of cortical maturation that precedes subsequent pruning and stabilization of volume [24]. The superior frontal gyrus (SFG), inferior parietal lobule (IPL), and middle temporal gyrus (MTG) regions maintained consistent volume measurements which showed different aging patterns because of their distinct cortical aging mechanisms [25].

The research showed that cortical thickness results matched the volume measurements, which demonstrated that aging produced only minor changes in both measurements. The study found that rostral ACC thickness maintained constant values through different age groups, which demonstrated that the ACC maintains its structural integrity throughout aging process and assists in sustaining cognitive ability [26]. The IFG thickness decreases steadily from childhood until mid-adulthood before showing a minor increase during late adulthood, which indicates that each region develops through different processes that may help people age [27]. The research shows that SFG, IPL, and MTG thickness remains stable throughout a person's life because emerging evidence shows that certain important brain regions related to cognition maintain their thickness despite the typical age-related decline of cortical thickness [28].

The Montreal Cognitive Assessment (MoCA) test results demonstrated that cognitive abilities remained stable for all age groups, though younger adults and older children showed higher performance than the remaining age groups, who exhibited results between these two peaks. The executive function and recall score stability demonstrates that older adults maintain their cognitive abilities throughout their entire life span [29]. Working memory reaches its highest point during early adulthood when cognitive control abilities reach their complete development but then start to decline after that stage. The cognitive performance patterns observed in this study show that healthy aging leads to minor cognitive decline which affects specific areas while the person maintains their brain structure and neural functions [23,25].

The documented lifespan trends demonstrate that both cortical volume and thickness maintain complete stability from childhood to late adulthood. The maintained cognitive function shows preserved cortical structural integrity, which demonstrates that adult brain morphology allows healthy individuals to keep their cognitive abilities throughout their life. This challenges the traditional view that aging invariably leads to substantial cortical atrophy and cognitive decline, suggesting instead a more nuanced pattern where specific regions and functions remain robustly preserved or compensated for [26,30].

The research results demonstrate that researchers must examine specific brain regions because they impact both brain development and cognitive abilities during the aging process. The research needs to adopt longitudinal studies with neurobiological markers to investigate how healthy cognitive aging mechanisms work and to explain the subtle structural changes discovered in this study [24,31].

The brain regional volumes and cortical thickness values of the current sample mostly followed the established normative patterns. The larger volumes of the frontal regions indicate the importance of the prefrontal cortices in the organization of the human brain, while the cortical thickness values were mostly around the same range (~2.7–3.2 mm), which is what major population imaging studies have shown that thickness is less variable between individuals than volume measures [19,32]. The wide distributions of age, education, and MoCA scores thus create a robust descriptive base for studying the relationships between the structural differences in the frontal, parietal, and temporal association cortices and cognitive variability throughout the lifespan [22,33].

During the study, large and consistent robust hemispheric asymmetries were observed in all the cortical regions. The frontal part of the brain, particularly the ACC, IFG, and SFG, showed left-sided volumetric asymmetry, whereas the parietal-temporal areas of the IPL and MTG showed right-sided asymmetry. This pattern was similar to the findings from large-scale normative and consortium-level datasets that reported a greater left-hemisphere extent in the medial and lateral prefrontal cortices and relatively larger right lateral parietal and temporal association areas [34–37].

The asymmetry patterns differed significantly between the volume and cortical thickness measurements. Although frontal volumes were mainly left-lateralized, thickness asymmetries were more region-specific, and a reversal in direction occurred in some areas, especially in the inferior frontal, parietal, and temporal cortices. This dissociation reinforces the view that volume, area, and thickness are influenced by developmental, genetic, and evolutionary factors [32,36,38]. Therefore, structural asymmetry is suggested to be a fundamental and genetically determined characteristic of cortical organization rather than simply a reflection of the total brain size [36,39]. Thus, the largely normative asymmetry profile observed in this study might provide a valuable reference framework for future studies exploring deviations related to cognitive decline or psychiatric conditions [40–42].

The current analysis found strong positive correlations between years of education and both regional cortical volume and cortical thickness across frontal, parietal, and temporal regions. However, the correlations are directionally in accordance with the cognitive reserve theories, but the strength of the associations is much more than what has been reported in a number of large cross-sectional and longitudinal studies where education has shown small and diffuse relationships characterized by brain morphometry, often more strongly with total surface area or intracranial volume than with mean cortical thickness [20,32,43–45].

Moreover, longitudinal evidence is growing, suggesting that education does not have a significant impact on the rate of cortical atrophy but rather raises the cohort's level of cognitive

and structural measures (higher intercepts) without changing the slopes of decline [46–48]. Similarly, education appears to influence the relationship between age and the brain in a complex, region-specific manner, sometimes postponing decline while being correlated with steeper late-life loss rather than having a simple monotonic effect on cortical volume or thickness [46]. Thus, the near-perfect correlations found in this study are difficult to relate to established evidence, and they strongly imply that there is a possibility of inflation because of the shared variance with age, cohort effects, intracranial volume, or global cortical measures.

The MoCA total scores were found to have strong positive correlations with both the regional cortical volume and cortical thickness in the ACC, IFG, SFG, IPL, and MTG. From an anatomical perspective, this is a plausible scenario and corresponds with extensive research that has established the notion that global cognitive screening scores reflect the integrity of brain regions, particularly the distributed networks of fronto-parieto-temporal regions, rather than isolated points [33,48,49]. Atrophy of the aforementioned three regions (frontal, parietal, and temporal) has been linked to age-related declines in cognitive function due to aging (demonstrated by MoCA total and subdomain scores in executive, visuospatial, and memory performance) [33,48,50].

Moreover, in cases of neurodegenerative disorders and individuals at risk, it has been found that performance on the MoCA test is positively associated with gray matter volume or is reflected by cortical thickness in the temporal, parietal, and frontal areas, and is also considered a very sensitive indicator of the degeneration of the entire network [49,51,52]. Hence, the regional distribution of MoCA–structure correlations observed in this study is not different from the prevailing theories of global cognition. Nevertheless, the extremely large effect sizes uniformly exceed the usual findings, which are typically modest once the demographic and global brain measures are controlled [3,53,54].

The MoCA subscores for executive function and working memory exhibited robust positive associations with cortical volume and thickness in the ACC, lateral frontal gyri, IPL, and MTG. This observation aligns with the cognitive control network theory, which underscores the frontoparietal network and pivotal role of the ACC in modifying task requirements [55,56]. Structural and functional imaging studies, much clearer in their findings, have consistently pointed to the integrity of the above-mentioned regions as a reason for good performance in executive and working memory tasks at the network level rather than single-region resolution [29,48,57].

In contrast, most large-sample studies have reported small-to-moderate correlations between structures and cognitive functions, with some even indicating that executive tests show almost no association with cortical thickness after controlling for age, education, and global measures [58–60]. The very strong correlation between executive functioning and working memory across all regions examined in the current study is most likely indicative of a prevailing global cortical integrity factor rather than region-specific effects, thus reinforcing the argument that a general factor of cortical atrophy is responsible for the decline in several cognitive domains [61].

The ability to recall episodic memories was highly correlated with both the volume and thickness of the frontal, parietal, and temporal cortical association regions. This agrees with recent studies showing that the brain areas involved in the distortion of memory work and even monitoring the context need to be connected through networks that include medial temporal regions, as well as frontal, parietal, and cingulate areas [62–64]. In all studies of healthy aging, subjective cognitive impairment, and early stage Alzheimer's disease, the cortical thickness and volume in the superior frontal, inferior parietal, posterior cingulate, and temporal regions have been repeatedly associated with recall and delayed memory performance [54,60,65,66].

However, earlier studies have shown that memory–structure relationships can be complicated and sometimes even reversed, especially in older adults, which is in line with neural efficiency or compensatory models [67,68]. Thus, the extremely large and generally positive correlations between recall and structure found in this study deviate from the intricate coexisting literature and hint at a rise again, which is a result of shared global or demographic variance being the most likely cause.

In every case, cortical volume and thickness measurements were strongly correlated with each other, and their relationships with educational level and cognitive performance were very powerful. A recent study indicated that the occurrence of such patterns demonstrates global cortical integrity or general atrophy, which tracks aging, disease burden, and global cognition more closely than any single regional measure [3,43,61]. Even though this global factor has biological significance, it still makes regional interpretation difficult and increases bivariate correlations when the covariates are not explicitly modelled.

Neuroimaging data obtained from real-world cases are subject to constraints, such as measurement error, biological variability, and developmental heterogeneity; therefore, the occurrence of correlations that come close to the theoretical maxima is, in most cases, implausible [32,69]. Therefore, the consistency of near-ceiling correlations across education, cortical measures, and multiple cognitive domains strongly suggests unmodeled confounding, shared scaling factors (e.g., head size and global thickness), or analytical dependencies.

Collectively, the current results support a network-based perception of cognition in which the functioning of the executive, working memory, recollection, and overall cognitive performance hinges upon the integrity of the distributed fronto-parieto-temporal system. The interpretation of the findings would, by and large, be in line with the frameworks of cognitive and brain reserves, where higher education implies higher levels of structural and cognitive functioning at a given moment [33,70,71]. Nevertheless, the remarkable size of the marked associations denies strong causal or region-specific implications.

Thus, future analyses must make thorough adjustments for age, sex, intracranial volume, education, and global cortical measurements. Multivariate and latent factor techniques have been applied to separate the global and regional effects [48,61]. The structures of the medial temporal lobe are critical for episodic memory [54,62]. Longitudinal methods were used to determine whether the relatively preserved thickness or volume of a specific region predicted slower cognitive decline [29,65].

Conclusion

In summary, the current research reaffirms the patterns of hemispheric asymmetry that have been widely recognized and simultaneously highlights the usefulness of different ages of people throughout life for the study of brain–cognition relationships. The anatomical distribution of associations between education, the brain, and cognition is in line with current network models, but the extremely high effect sizes across the board are not in agreement with previous literature,

and probably point to global shared variance or methodological inflation. Careful multivariable modelling and longitudinal validation are necessary before making substantive conclusions about regional brain–behavior relationships.

Author Contributions: Conceptualization, S. N., Z. B., K. T; methodology, S. N., K. T., Z. B.; data acquisition, S. N., R. P. J.; MRI segmentation and parcellation, trained MRI technicians under supervision of U. K., K. T., S. N.; statistical analysis, S. N., Z. B., K. T., R. P. J.; writing – original draft preparation, S. N., K. T., U. K.; writing – review and editing, S. N., K. T., Z. B., U. K., R. P. J.; supervision, U. K., K. T., Z. B. All authors have read and agreed to the final version of manuscript.

Disclosures: The authors have no conflicts of interest.

Acknowledgments: The authors express their sincere gratitude to all study participants for their cooperation throughout the research process. The authors also thank the technical staff of the Department of Radiology, Mamata Medical College, Khammam, for their assistance in obtaining MRI data, anatomical guidance, and quality assurance. Appreciation is extended to the neuroanatomy and MRI technicians for their support during segmentation and volumetric analysis.

Funding: None.

Data availability statement: The anonymized MRI results and measurement of cortical thickness and regional brain volume were sent to the relevant author as a reasonable request with the requirements of the Institutional Ethics Committee of Mamata Medical College and in agreement with the institutional data-sharing policy.

Artificial Intelligence (AI) Disclosure Statement: The authors declare no AI Tools used for preparation of this work.

References

1. Tamnes CK, Herting MM, Goddings A-L, Meuwese R, Blakemore S-J, Dahl RE, et al. Development of the Cerebral Cortex across Adolescence: A Multisample Study of Inter-Related Longitudinal Changes in Cortical Volume, Surface Area, and Thickness. *J Neurosci.* 2017;37:3402–12. https://doi.org/10.1523/JNEUROSCI.3302-16.2017.
2. Sele S, Liem F, Mérillat S, Jäncke L. Age-related decline in the brain: a longitudinal study on inter-individual variability of cortical thickness, area, volume, and cognition. *Neuroimage*. 2021;240:118370. https://doi.org/10.1016/j.neuroimage.2021.118370.
3. Singh AD, Kumar M, Swathi BH, Bhargavi P, Godbole A, Khushu S. Age-related cortical changes and cognitive performance in healthy adults. *Brain Cogn.* 2025;187:106306. https://doi.org/10.1016/j.bandc.2025.106306.
4. Cui D, Wang D, Jin J, Liu X, Wang Y, Cao W, et al. Age- and sex-related differences in cortical morphology and their relationships with cognitive performance in healthy middle-aged and older adults. *Quant Imaging Med Surg.* 2023;13:1083–99. https://doi.org/10.21037/qims-22-583.
5. Lipnicki DM, Crawford JD, Dutta R, Thalamuthu A, Kochan NA, Andrews G, et al. Age-related cognitive decline and associations with sex, education and apolipoprotein E genotype across ethnocultural groups and geographic regions: a collaborative cohort study. *PLOS Med.* 2017;14:e1002261. https://doi.org/10.1371/journal.pmed.1002261.
6. Lee W-J, Jung K-H, Park K-I, Chu K, Lee SK. Domain-specific longitudinal associations between brain volume, white matter lesions, and cognitive function changes. *Heliyon*. 2025;11:e42536. https://doi.org/10.1016/j.heliyon.2025.e42536.
7. Esfahlani FZ, Faskowitz J, Slack J, Mišić B, Betzel RF. Local structure-function relationships in human brain networks across the lifespan 2021. https://doi.org/10.1101/2021.05.23.445128.
8. Kurth F, Schijven D, van den Heuvel OA, Hoogman M, van Rooij D, Stein DJ, et al. Large-scale analysis of structural brain asymmetries during neurodevelopment: Associations with age and sex in 4265 children and adolescents. *Hum Brain Mapp.* 2024;45. https://doi.org/10.1002/hbm.26754.
9. Plessen KJ, Hugdahl K, Bansal R, Hao X, Peterson BS. Sex, Age, and Cognitive Correlates of Asymmetries in Thickness of the Cortical Mantle Across the Life Span. *J Neurosci.* 2014;34:6294–302. https://doi.org/10.1523/JNEUROSCI.3692-13.2014.
10. Matsuda S, Doi T, Harada K, Nakakubo S, Katayama O, Sakimoto F, et al. Brain structural asymmetry associated with cognitive impairment in community-dwelling older adults. *Arch Gerontol Geriatr.* 2025;138:105975. https://doi.org/10.1016/j.archger.2025.105975.
11. Nazlee N, Waiter GD, Sandu A. Age-associated sex and asymmetry differentiation in hemispheric and lobar cortical ribbon complexity across adulthood: A UK Biobank imaging study. *Hum Brain Mapp.* 2023;44:49–65. https://doi.org/10.1002/hbm.26076.
12. Lövdén M, Fratiglioni L, Glymour MM, Lindenberger U, Tucker-Drob EM. Education and Cognitive Functioning Across the Life Span. Psychol Sci Public Interes. 2020;21:6–41. https://doi.org/10.1177/1529100620920576.
13. Elshiekh A, Subramaniapillai S, Rajagopal S, Pasvanis S, Ankudowich E, Rajah MN. The association between cognitive reserve and performance-related brain activity during episodic encoding and retrieval across the adult lifespan. *Cortex*. 2020;129:296–313. https://doi.org/10.1016/j.cortex.2020.05.003.
14. Leffa DT, Zhang Y, Wang Y, Teverovsky EG, Jacobsen E, Bellaver B, et al. Association Between the Genetic Risk for Attention-Deficit/Hyperactivity Disorder and Cognitive Function in Older Age: The MYHAT Population-Based Study. *Am J Geriatr Psychiatry*. 2025. https://doi.org/10.1016/j.jagp.2025.10.005.
15. Hosseininasabnajar F, Kakinami L. The longitudinal effects of global and regional brain measurements on cognitive abilities. *Sci Rep.* 2025;15:27846. https://doi.org/10.1038/s41598-025-08152-6.
16. Palmer CE, Zhao W, Loughnan R, Zou J, Fan CC, Thompson WK, et al. Distinct Regionalization Patterns of Cortical Morphology are Associated with Cognitive Performance Across Different Domains. *Cereb Cortex.* 2021;31:3856–71. https://doi.org/10.1093/cercor/bhab054.

17. Xu P, Estrada S, Etteldorf R, Liu D, Shahid M, Zeng W, et al. Hypothalamic volume is associated with age, sex and cognitive function across lifespan: a comparative analysis of two large population-based cohort studies. *EBioMedicine*. 2025;111:105513. https://doi.org/10.1016/j.ebiom.2024.105513.
18. Merenstein JL, Zhao J, Madden DJ. Depthwise cortical iron relates to functional connectivity and fluid cognition in healthy aging. *Neurobiol Aging.* 2025;148:27–40. https://doi.org/10.1016/j.neurobiolaging.2025.01.006.
19. Walhovd KB, Fjell AM, Reinvang I, Lundervold A, Dale AM, Eilertsen DE, et al. Effects of age on volumes of cortex, white matter and subcortical structures. *Neurobiol Aging.* 2005;26:1261–70. https://doi.org/10.1016/j.neurobiolaging.2005.05.020.
20. Ball W, Byars A, Schapiro M, Bommer W, Carr A, German A, et al. Total and Regional Brain Volumes in a Population-Based Normative Sample from 4 to 18 Years: The NIH MRI Study of Normal Brain Development. *Cereb Cortex*. 2012;22:1–12. https://doi.org/10.1093/cercor/bhr018.
21. Mungas D, Reed BR, Farias ST, DeCarli C. Age and education effects on relationships of cognitive test scores with brain structure in demographically diverse older persons. *Psychol Aging.* 2009;24:116–28. https://doi.org/10.1037/a0013421.
22. Pettemeridou E, Kallousia E, Constantinidou F. Regional Brain Volume, Brain Reserve and MMSE Performance in Healthy Aging From the NEUROAGE Cohort: Contributions of Sex, Education, and Depression Symptoms. *Front Aging Neurosci.* 2021;13. https://doi.org/10.3389/fnagi.2021.711301.
23. De Chastelaine M, Srokova S, Hou M, Kidwai A, Kafafi SS, Racenstein ML, et al. Cortical thickness, gray matter volume, and cognitive performance: a crosssectional study of the moderating effects of age on their interrelationships. *Cereb Cortex.* 2023;33:6474–85. https://doi.org/10.1093/cercor/bhac518.
24. Vijayakumar N, Allen NB, Youssef G, Dennison M, Yücel M, Simmons JG, et al. Brain development during adolescence: A mixed-longitudinal investigation of cortical thickness, surface area, and volume. *Hum Brain Mapp*. 2016;37:2027–38.
25. Schilling KG, Archer D, Rheault F, Lyu I, Huo Y, Cai LY, et al. Superficial white matter across development, young adulthood, and aging: volume, thickness, and relationship with cortical features. *Brain Struct \& Funct.* 2023;228:1019–31. https://doi.org/10.1007/s00429-023-02642-x.
26. Petersen M, Nägele FL, Mayer C, Schell M, Rimmele DL, Petersen E, et al. Brain network architecture constrains age-related cortical thinning. *Neuroimage.* 2022;264:119721. https://doi.org/10.1016/j.neuroimage.2022.119721.
27. Frangou S, Modabbernia A, Williams SCR, Papachristou E, Doucet GE, Agartz I, et al. Cortical thickness across the lifespan: Data from 17,075 healthy individuals aged 3–90 years. *Hum Brain Mapp.* 2022;43:431–51. https://doi.org/10.1002/hbm.25364.
28. Karama S, Bastin ME, Murray C, Royle NA, Penke L, Muñoz Maniega S, et al. Childhood cognitive ability accounts for associations between cognitive ability and brain cortical thickness in old age. *Mol Psychiatry.* 2013;19:555–9. https://doi.org/10.1038/mp.2013.64.
29. Dominguez EN, Stark SM, Ren Y, Corrada MM, Kawas CH, Stark CEL. Regional Cortical Thickness Predicts Top Cognitive Performance in the Elderly. *Front Aging Neurosci.* 2021;13. https://doi.org/10.3389/fnagi.2021.751375.
30. Cox SR, Bastin ME, Ritchie SJ, Dickie DA, Liewald DC, Muñoz Maniega S, et al. Brain cortical characteristics of lifetime cognitive ageing. *Brain Struct Funct.* 2017;223:509–18. https://doi.org/10.1007/s00429-017-1505-0.
31. Lotter LD, Saberi A, Hansen JY, Misic B, Paquola C, Barker GJ, et al. Regional patterns of human cortex development correlate with underlying neurobiology. *Nat Commun.* 2024;15. https://doi.org/10.1038/s41467-024-52366-7.
32. Potvin O, Mouiha A, Dieumegarde L, Duchesne S. P3-277: Morphometric Cortical Normative Data Throughout Aging. *Alzheimer's Dement.* 2016;12. https://doi.org/10.1016/j.jalz.2016.06.1940.
33. Rangus I, Teghipco A, Newman-Norlund S, Newman-Norlund R, Rorden C, Riccardi N, et al. The Influence of Structural Brain Changes on Cognition in the Context of Healthy Aging: Exploring Mediation Effects Through gBAT—The Graphical Brain Association Tool. *Hum Brain Mapp.* 2024;45. https://doi.org/10.1002/hbm.70038.
34. Allen JS, Damasio H, Grabowski TJ. Normal neuroanatomical variation in the human brain: An MRI-volumetric study. *Am J Phys Anthropol.* 2002;118:341–58. https://doi.org/10.1002/ajpa.10092.
35. Goldberg E, Roediger D, Kucukboyaci NE, Carlson C, Devinsky O, Kuzniecky R, et al. Hemispheric asymmetries of cortical volume in the human brain. *Cortex*. 2013;49:200–10. https://doi.org/10.1016/j.cortex.2011.11.002.
36. Kong X-Z, Mathias SR, Guadalupe T, Glahn DC, Franke B, Crivello F, et al. Mapping cortical brain asymmetry in 17,141 healthy individuals worldwide via the ENIGMA Consortium. *Proc Natl Acad Sci.* 2018;115. https://doi.org/10.1073/pnas.1718418115.
37. Hardisty A, Addink W, Glöckler F, Güntsch A, Islam S, Weiland C. A choice of persistent identifier schemes for the Distributed System of Scientific Collections (DiSSCo). *Res Ideas Outcomes.* 2021;7. https://doi.org/10.3897/rio.7.e67379.
38. Panszczyk D, Dale C, Kurth F, Luders E. Hemispheric asymmetry in language-related brain regions. *Brain Res.* 2025;1857:149606. https://doi.org/10.1016/j.brainres.2025.149606.
39. Dorfschmidt L, White S, Gardner M, Bedford S, Ball G, Edwards AD, et al. Charting structural brain asymmetry across the human lifespan 2025. https://doi.org/10.1101/2025.07.21.665924.
40. Fang J, Li J, Liu D, Liu C, Li Y, Zhu W, et al. Investigating the correlation between cortical lateralization and personality traits in young Chinese adults through structural magnetic resonance imaging. *Quant Imaging Med Surg.* 2025;15:6981–91. https://doi.org/10.21037/qims-2025-271.
41. Li Q, Zhao W, Palaniyappan L, Guo S. Atypical hemispheric lateralization of brain function and structure in autism: a comprehensive meta-analysis study. *Psychol Med.* 2023;53:6702–13. https://doi.org/10.1017/S0033291723000181.
42. Qin P, Bi Q, Guo Z, Yang L, Li H, Li P, et al. Microstructural asymmetries of the planum temporale predict functional lateralization of auditory-language processing. *Elife*. 2024;13. https://doi.org/10.7554/eLife.95547.3.
43. Hoagey DA, Rieck JR, Rodrigue KM, Kennedy KM. Joint contributions of cortical morphometry and white matter microstructure in healthy brain aging: A partial least squares correlation analysis. *Hum Brain Mapp.* 2019;40:5315–29. https://doi.org/10.1002/hbm.24774.
44. Lange N, Froimowitz MP, Bigler ED, Lainhart JE, Brain Development Cooperative Group. Associations Between IQ, Total and Regional Brain Volumes, and Demography in a Large Normative Sample of Healthy Children and Adolescents. *Dev Neuropsychol.* 2010;35:296–317. https://doi.org/10.1080/87565641003696833.

45. Mitchell BL, Cuéllar-Partida G, Grasby KL, Campos AI, Strike LT, Hwang L-D, et al. Educational attainment polygenic scores are associated with cortical total surface area and regions important for language and memory. *Neuroimage*. 2020;212:116691. https://doi.org/10.1016/j.neuroimage.2020.116691.
46. Nyberg L, Magnussen F, Lundquist A, Baaré W, Bartrés-Faz D, Bertram L, et al. Educational attainment does not influence brain aging. *Proc Natl Acad Sci.* 2021;118. https://doi.org/10.1073/pnas.2101644118.
47. Steffener J. Education and age-related differences in cortical thickness and volume across the lifespan. *Neurobiol Aging.* 2021;102:102–10. https://doi.org/10.1016/j.neurobiolaging.2020.10.034.
48. Armstrong NM, An Y, Shin JJ, Williams OA, Doshi J, Erus G, et al. Associations between cognitive and brain volume changes in cognitively normal older adults. *Neuroimage*. 2020;223:117289. https://doi.org/10.1016/j.neuroimage.2020.117289.
49. Kritikos M, Rama T, Zubair V, Huang C, Christodoulou C, Chen APF, et al. Gray Matter Volume Associations with Montreal Cognitive Assessment Domains in an ADNI Cohort of Early-Onset Mild Cognitive Impairment and Alzheimer's Disease. *J Dement Alzheimer's Dis.* 2025;2:24. https://doi.org/10.3390/jdad2030024.
50. DeJong NR, Jansen JFA, van Boxtel MPJ, Schram MT, Stehouwer CDA, van Greevenbroek MMJ, et al. Brain structure and connectivity mediate the association between lifestyle and cognition: The Maastricht Study. *Brain Commun.* 2024;6. https://doi.org/10.1093/braincomms/fcae171.
51. Chen B, Zhou H, Liu X, Yang W, Luo Y, Zhu S, et al. Correlations of gray matter volume with peripheral cytokines in Parkinson's disease. *Neurobiol Dis.* 2024;201:106693. https://doi.org/10.1016/j.nbd.2024.106693.
52. Li R, Zeng K, Liu J, Yang Z, Wang Y. Choroid plexus enlargement correlates with cognitive impairment and brain atrophy in patients with temporal lobe epilepsy. *Neuroscience.* 2025;588:84–91. https://doi.org/10.1016/j.neuroscience.2025.09.046.
53. Couvy-Duchesne B, Frouin V, Bouteloup V, Koussis N, Sidorenko J, Jiang J, et al. Grey-Matter Structure Markers of Alzheimer's Disease, Alzheimer's Conversion, Functioning and Cognition: A Meta-Analysis Across 11 Cohorts. *Hum Brain Mapp.* 2025;46. https://doi.org/10.1002/hbm.70089.
54. Ossenkoppele R, Smith R, Ohlsson T, Strandberg O, Mattsson N, Insel PS, et al. Associations between tau, Aβ, and cortical thickness with cognition in Alzheimer disease. *Neurology.* 2019;92. https://doi.org/10.1212/WNL.0000000000006875.
55. Tabassi Mofrad F, Schiller NO. Distinct connectivity patterns in clusters of inferior parietal cortex: from a cognitive control hub to modulating cortical areas. Neuroscience. 2025;580:62–8. https://doi.org/10.1016/j.neuroscience.2025.06.034.
56. Di X, Zhang H, Biswal BB. Anterior cingulate cortex differently modulates frontoparietal functional connectivity between resting-state and working memory tasks. *Hum Brain Mapp.* 2020;41:1797–805. https://doi.org/10.1002/hbm.24912.
57. Fatemi M, Daliri MR. Genetic effect on working memory activation pattern and structural properties of cortical gray matter. Sci Rep. 2025;15:21096. https://doi.org/10.1038/s41598-025-07959-7.
58. Owens MM, Duda B, Sweet LH, MacKillop J. Distinct functional and structural neural underpinnings of working memory. *Neuroimage*. 2018;174:463–71. https://doi.org/10.1016/j.neuroimage.2018.03.022.
59. Morris VL, Owens MM, Syan SK, Petker TD, Sweet LH, Oshri A, et al. Associations Between Drinking and Cortical Thickness in Younger Adult Drinkers: Findings From the Human Connectome Project. *Alcohol Clin Exp Res.* 2019;43:1918–27. https://doi.org/10.1111/acer.14147.
60. Youn H, Choi M, Lee S, Kim D, Suh S, Han CE, et al. Decreased Cortical Thickness and Local Gyrification in Individuals with Subjective Cognitive Impairment. *Clin Psychopharmacol Neurosci.* 2021;19:640–52. https://doi.org/10.9758/cpn.2021.19.4.640.
61. Cox SR, Harris MA, Ritchie SJ, Buchanan CR, Valdés Hernández MC, Corley J, et al. Three major dimensions of human brain cortical ageing in relation to cognitive decline across the eighth decade of life. *Mol Psychiatry.* 2021;26:2651–62. https://doi.org/10.1038/s41380-020-00975-1.
62. Ma J, Zheng M-X, Wu J-J, Xing X-X, Xiang Y-T, Wei D, et al. Mapping the long-term delayed recall-based cortex-hippocampus network constrained by the structural and functional connectome: a case-control multimodal MRI study. *Alzheimers Res Ther.* 2023;15:61. https://doi.org/10.1186/s13195-023-01197-7.
63. Snytte J, Fenerci C, Rajagopal S, Beaudoin C, Hooper K, Sheldon S, et al. Volume of the posterior hippocampus mediates age-related differences in spatial context memory and is correlated with increased activity in lateral frontal, parietal and occipital regions in healthy aging. *Neuroimage.* 2022;254:119164. https://doi.org/10.1016/j.neuroimage.2022.119164.
64. Zhao S, Sang F, Liu C, Wang F, Liu J, Chen C, et al. Age-related enhancement of the association between episodic memory and gray matter volume in medial temporal and frontal lobes. *Behav Brain Funct.* 2024;20:10. https://doi.org/10.1186/s12993-024-00237-y.
65. Rolls ET, Wirth S, Deco G, Huang C, Feng J. The human posterior cingulate, retrosplenial, and medial parietal cortex effective connectome, and implications for memory and navigation. *Hum Brain Mapp.* 2023;44:629–55. https://doi.org/10.1002/hbm.26089.
66. Swierkot A, Rajah MN. Cortical thickness in right frontal and left lingual gyri differentially mediate episodic memory for spatial contextual details across the adult lifespan 2018. https://doi.org/10.1101/289447.
67. Van Petten C, Plante E, Davidson PS., Kuo TY, Bajuscak L, Glisky EL. Memory and executive function in older adults: relationships with temporal and prefrontal gray matter volumes and white matter hyperintensities. *Neuropsychologia*. 2004;42:1313–35. https://doi.org/10.1016/j.neuropsychologia.2004.02.009.
68. Gautam P, Cherbuin N, Sachdev PS, Wen W, Anstey KJ. Relationships between cognitive function and frontal grey matter volumes and thickness in middle aged and early old-aged adults: The PATH Through Life Study. *Neuroimage*. 2011;55:845–55. https://doi.org/10.1016/j.neuroimage.2011.01.015.
69. Raz N, Gunning-Dixon F, Head D, Rodrigue KM, Williamson A, Acker JD. Aging, sexual dimorphism, and hemispheric asymmetry of the cerebral cortex: replicability of regional differences in volume. *Neurobiol Aging.* 2004;25:377–96. https://doi.org/10.1016/S0197-4580(03)00118-0.
70. Heo D, Kim M-S, Lee Y-J, Kim S-K, Kim YS, Sung W, et al. Unravelling the interplay: brain regional atrophy and neuropsychological function in early Alzheimer's disease. *Front Aging Neurosci.* 2025;17. https://doi.org/10.3389/fnagi.2025.1508849.
71. Kim H-B, Kim S, Um YH, Wang S-M, Kim REY, Choe YS, et al. Modulation of associations between education years and cortical volume in Alzheimer's disease vulnerable brain regions by Aβ deposition and APOE ε4 carrier status in cognitively normal older adults. *Front Aging Neurosci.* 2023. https://doi.org/10.3389/fnagi.2023.1248531.

JOURNAL OF CLINICAL MEDICINE OF KAZAKHSTAN (E-ISSN 2313-1519)
Original Article DOI: https://doi.org/10.23950/jcmk/18012

Impact of Nanocellulose-Based Biocomposite Implantation on Rodent Behavior in the Elevated Plus Maze Test

Madina Rashova[1,2], Saule Akhmetova[2], Berik Tuleubaev[1], Zhanerke Bolat[3], Ulzhalgas Mukhtarkhan[4], Kamila Tazabekova[5], Ivan Lavrinenko[5], Vitaliy Feoktistov[1]

[1]*Department of Surgical Diseases, Karaganda Medical University, Karaganda, Kazakhstan*
[2]*Department of Biomedicine, Karaganda Medical University, Karaganda, Kazakhstan*
[3]*School of Biomedicine, Karaganda Medical University, Karaganda, Kazakhstan*
[4]*School of Medicine, Karaganda Medical University, Karaganda, Kazakhstan*
[5]*Nazarbayev Intellectual School, Karaganda, Kazakhstan*

Received: 2026-01-17.
Accepted: 2026-02-25.

This work is licensed under a **Creative Commons Attribution 4.0 International License**

J Clin Med Kaz 2026; 23(2): 104-108

Corresponding author:
Madina Rashova.
E-mail: rourke_m@mail.ru.
ORCID: 0009-0001-7892-7768.

ABSTRACT

Introduction: For application in regenerative medication, the biomaterial used in implants should have both structural and biological compatibility along with long-term safety with respect to the central nervous system. Nanocellulose (NC) is a promising biomaterial when it comes to biocompatibility, mechanical strength, and modifiability. However, there is a limited data on its long-term behavioural effects. Assessment of animal behaviour is an important aspect of preclinical safety evaluation.

Methods: The six-month in vivo study was conducted using 20 male rats divided into an experimental group with intramedullary implantation of a nanocellulose-based biocomposite and a control group with an autologous blood clot. The elevated plus maze test was used to assess the behavioural activity, which includes anxiety-related behaviour, exploratory activity, emotional responses, and locomotor function.

Results: No statistically significant differences were observed between the experimental and control groups for any of the analysed behavioural parameters. The animals exhibited comparable levels of anxiety, emotional state, and locomotor activity, with no signs of increased stress or neurotoxic effects. The findings show the implantation of the nanocellulose-based biocomposite does not cause adverse long-term behavioural effects in rats, supporting its biocompatibility and behavioural safety.

Conclusion: These findings are consistent with current concepts of nanocellulose biocompatibility and support the potential for its further application in regenerative medicine and tissue engineering.

Keywords: nanocellulose, toxicity, biocomposite, bone, elevated plus maze.

Introduction

Assessment of the biocompatibility and safety of novel biomaterials is a key stage in preclinical research, especially when they are intended for use as implantable materials [1, 2]. Along with morphological, biochemical, and histological methods, the analysis of the behavioral responses in laboratory animals is important, as it allows the identification of possible long-term neurotoxic or stress-induced effects of experimental interventions [3].

Nanocellulose is regarded as a promising material for use in regenerative medicine and tissue engineering due to its biocompatibility, mechanical strength, porosity, and modifiability. It is used for tissue regeneration, the creation of dressings, targeted drug delivery

and the production of implants [4, 5]. However, the implantation of permanent biomaterials may potentially influence the overall physiological state of the organism, including the central nervous system, which requires a comprehensive in vivo safety assessment [6].

Behavioral tests in rodents are a sensitive tool for detecting changes in emotional state, anxiety, and motor activity. One of the most widely used methods is the elevated plus maze test, based on the natural conflict between an animal's desire for exploratory activity and its avoidance of open spaces. Analysis of the results of this test allows us to assess the level of anxiety, locomotor activity, and stress response in animals [7].

Hypothesis: Implantation of nanocellulose-based biocomposite does not cause an increase in anxiety-like behavior in rats in the elevated plus maze (EPM) test compared to the control group.

Aim: to evaluate behavioral responses in rats following implantation of a nanocellulose-based biocomposite using the elevated plus maze test.

Methods

Surgical procedure

The production of nanocellulose and the fabrication of a biocomposite incorporating calcium phosphate were conducted in collaboration with the Department of Physical and Colloid Chemistry. The number of animals is determined by the recommended groups from GOST for assessing the biological effect of chronic toxicity. The surgical intervention was performed on 20 male rats. The animals were divided into two experimental groups, with 10 rats in each group.

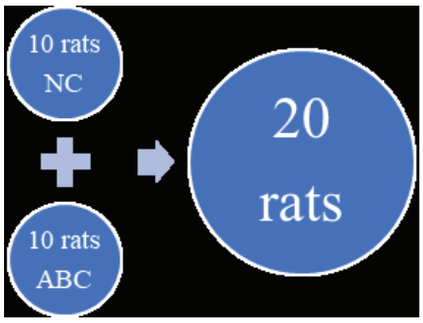

Figure 1 – Research design

Anesthesia was performed with Tiletamine (0.1 mg/kg). Implantation was performed in the middle third of the left femur. The first group included animals that underwent intramedullary implantation of nanocellulose into the femur (Figure 2). In the second group, the bone defect was filled with an autologous blood clot (ABC).

Figure 2 – Filling a defect in the femur with a nanocellulose-based biocomposite

All procedures related to animal housing, experimental manipulations, and analysis of the data obtained complied with the established standards of GOST ISO 10993-11—2021 and GOST ISO 10993-6—2021. The study was approved by a meeting of the local bioethics committee.

Elevated Plus Maze test

The study was conducted to assess the chronic toxicity of nanocellulose biocomposite. The observation period was 6 months. Prior to euthanasia, all animals underwent the elevated plus maze (EPM) test, which consists of two open arms and two dark closed arms arranged perpendicularly (Figure 3).

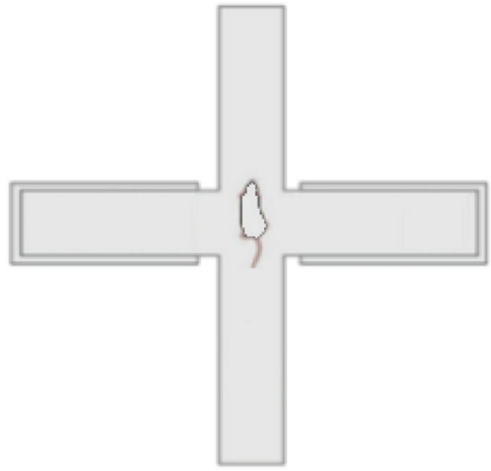

Figure 3 – Base of the elevated plus maze test: A – open arms, B – closed arms

Before each test, the maze was cleaned and wiped with alcohol. The camera was positioned to ensure full coverage of the maze. Before starting the video recording, animal identification was documented by displaying a card indicating the experimental group and the individual rat number.

Each animal was placed at the intersection of the open and closed arms, in the center of the maze, with its muzzle facing the open arm. The duration of video recording was five minutes. After completion of the test, the animal was removed and the maze was cleaned. A test protocol was completed, including the assessment of a range of parameters related to locomotor activity, anxiety and vegetative responses.

In the present study, the elevated plus maze test was used to assess the behavioral responses of rats six months after implantation of the nanocellulose-based biocomposite. The choice of a long-term observation period was determined by the need to identify potential chronic or delayed effects that may not be evident during the early postoperative period.

Statistical analysis

Statistical analysis of the study results was performed using STATISTICA 6.0 software (StatSoft, USA). Quantitative data were analyzed using standard methods of variation statistics. The results are presented as median and interquartile range. Differences between groups were considered statistically significant at $p < 0,05$. For pairwise comparisons, the nonparametric Mann–Whitney U test was also applied.

Results

There were no seizures during dynamic observation. The parameters assessed in the elevated plus maze (EPM) test are presented in Table 1.

Comparative analysis of rat behavior in the elevated plus maze 6 months after the intervention revealed no pronounced differences between the groups across all studied parameters.

The latency to leave the central platform was identical in both groups, indicating no differences in baseline locomotor activity or orienting responses. The total time spent on the central platform, as well as in the closed and open arms of the maze, did not differ significantly, suggesting a comparable level of anxiety in animals from both groups (Figure 4A, B).

Indicators of exploratory activity, including the number of entries into closed arms and the centre, remained within physiological limits and did not differ between groups. A similar pattern was observed for the number of entries into open arms and the number of head dippings, indicating no effect of the intervention on anxiety-related or risk-associated behaviors (Figure 4C).

Markers of emotional tension (grooming behavior, number of fecal boli, and rearings) also showed no significant intergroup differences (Figure 4D). The absence of increased defecation and grooming in open arms indicates a lack of pronounced stress exposure. The number of squares crossed in both open and closed arms was comparable between groups, reflecting preserved locomotor activity.

Table 1 Behavioral responses in the elevated plus maze test

Parameter	Group 1 (NC) Me [Q1; Q3]	Group 2 (ABC) Me [Q1; Q3]	Mann–Whitney test
Latency to leave the central platform, s	0 [0; 0]	0 [0; 0]	p > 0.05
Total time spent on the central platform, s	0,5 [0; 1]	1 [0; 1]	p > 0.05
Total time spent in closed arms, s	280 [269; 300]	294 [283;299]	p > 0.05
Total time spent in open arms, s	13 [0; 20]	3 [0; 8]	p > 0.05
Number of entries into closed arms, times	4 [1; 4]	1 [1; 3]	p > 0.05
Number of entries into center, times	5 [0; 6]	1,5 [0; 2]	p > 0.05
Number of entries into open arms, times	1 [0; 2]	1 [0; 1]	p > 0.05
Number of head dippings in open arms, times	3 [0; 3]	0,5 [0; 2]	p > 0.05
Grooming in open arms, times	-	-	-
Grooming in closed arms, times	3 [3; 3]	3 [2; 5]	p > 0.05
Number of rearings in open arms, times	-	-	-
Number of rearings in closed arms, times	9 [7; 10]	5 [3; 9]	p > 0.05
Number of fecal boli (defecations), times	0 [0; 1]	0 [0; 0]	p > 0.05
Number of squares crossed in open arms, times	6 [0; 6]	1,5 [0; 4]	p > 0.05
Number of squares crossed in closed arms, times	18 [3; 29]	9 [5; 16]	p > 0.05

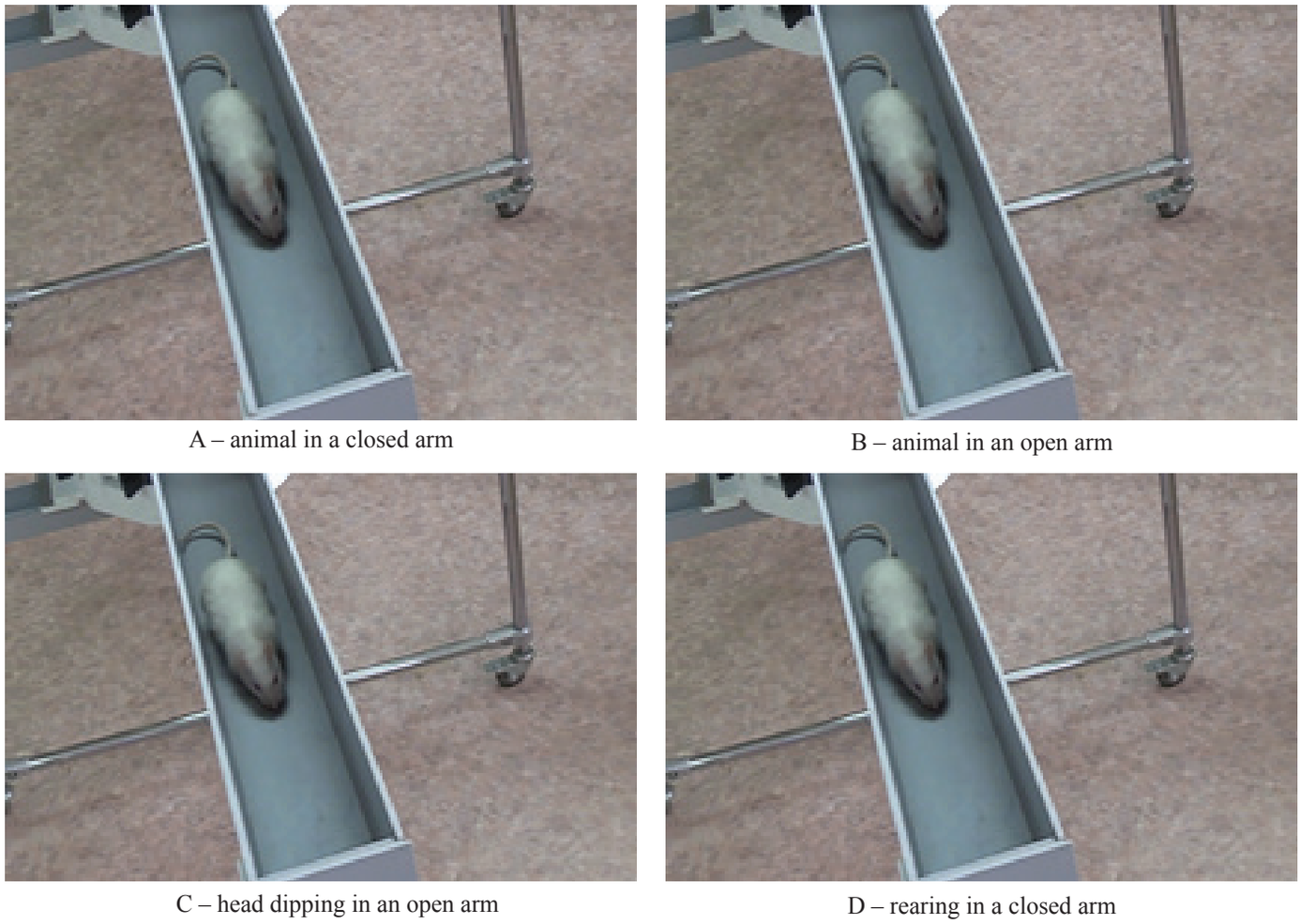

A – animal in a closed arm

B – animal in an open arm

C – head dipping in an open arm

D – rearing in a closed arm

Figure 4 – Selected behavioral responses in the elevated plus maze test

The obtained data indicate that the investigated intervention does not exert a significant effect on anxiety levels, emotional state, or motor activity of rats at long-term follow-up. The absence of statistically significant differences ($p > 0.05$) across key test parameters confirms the behavioral safety and lack of neurotoxic effects of the nanocellulose-based biocomposite.

Discussion

The elevated plus maze test is a validated method for assessing anxiety, emotional state, and locomotor activity in laboratory animals and is widely used to detect potential neurotoxic and behavioral effects of experimental interventions [7, 8, 9]. In the present study, this test was used to evaluate the long-term behavioral consequences of implantation of a nanocellulose-based biocomposite.

The results demonstrate the absence of a pronounced effect of the tested material on rat behavioral responses 6 months after implantation. Key anxiety-related parameters—time spent in open and closed arms and the number of entries into open arms—did not show statistically significant differences between the experimental and control groups. This suggests the absence of both anxiogenic and anxiolytic effects of the biocomposite implantation [10, 11, 12].

The lack of differences in latency to leave the central platform and total time spent in the maze center indicates that the intervention did not affect baseline locomotor activity or exploratory behavior. Comparable values for the number of squares crossed in open and closed arms further confirm the preservation of overall locomotor function and the absence of motor impairments that could confound anxiety assessment. These findings are consistent with previously published data [10, 12].

Markers of emotional tension, including grooming frequency, number of defecations, rearings, and head dippings, also did not differ significantly between groups. These parameters are considered additional indicators of stress response, and their stability suggests the absence of chronic stress or discomfort at long-term observation points. This is particularly important for evaluating the biocompatibility of implantable materials, as emphasized by multiple authors [10, 12, 13, 14].

It should be noted that quantitative fluctuations in individual parameters were variable and accompanied by relatively high standard deviations, which is characteristic of behavioral testing. However, the absence of statistically significant differences allows these variations to be interpreted as individual variability rather than effects of the experimental intervention, in agreement with the literature [15].

Conclusion

Thus, the results of behavioral testing in the elevated plus maze confirm the absence of adverse effects of the nanocellulose-based biocomposite on the central nervous system, anxiety level, and locomotor activity of rats at long-term follow-up after implantation. These findings are consistent with current concepts of nanocellulose biocompatibility and support the potential for its further application in regenerative medicine and tissue engineering.

Limitations

Therefore, the obtained results are preliminary and should be viewed with caution. This study has several limitations that should be considered when interpreting the findings. First, the sample size ($n = 10$ per group) was consistent with commonly used designs in experimental behavioral neuroscience; however, it may have provided limited statistical power, particularly for detecting small effect sizes. The use of the nonparametric Mann–Whitney U test, although appropriate given the distribution of the data, may further reduce sensitivity compared to parametric approaches.

Accordingly, the possibility of a type II error (β-error) cannot be excluded. The absence of statistically significant differences ($p > 0.05$) does not definitively rule out the presence of subtle between-group effects that may not have been detectable within the current sample size. Second, behavioral parameters in the Elevated Plus Maze test are characterized by inherent inter-individual variability, which may increase dispersion and reduce the ability to identify modest group differences. Third, behavioral assessment was conducted at a single post-implantation time point. Potential transient or delayed neurobehavioral effects could therefore remain undetected.

Future studies with larger sample sizes, predefined effect size assumptions, and longitudinal behavioral assessment are warranted to further validate the present findings. Further histological examination of the organs for toxicity is planned.

Author Contributions: Conceptualization, M. R., S. B., T. B., V. F.; methodology, M. R., S. B., V. F.; formal analysis, S. B., T. B.; resources, T. B.; conducting an experiment, M. R., U. M., I. L., Z. B., K. T.; animal observation and video analysis, M. R., U. M., I. L., Z. B., K. T.; writing – original draft preparation M. R.; writing – review and editing, S. B., T. B.; visualization, M. R., I. L.; supervision, S. B.; funding acquisition, T. B.; statistical analysis and translation, M. R., Z. B., K. T., I. L. All authors have read and agreed to the published version of the manuscript.

Disclosures: The authors have no conflicts of interest.

Acknowledgments: None.

Funding: None.

Data availability statement: The corresponding author can provide the data supporting the study's conclusions upon request.

Artificial Intelligence (AI) Disclosure Statement: The authors declare no AI Tools used for preparation of this work.

References

1. Dec P, Modrzejewski A, Pawlik A. Existing and Novel Biomaterials for Bone Tissue Engineering. *International journal of molecular sciences.* 2022; 24(1): 529. https://doi: 10.3390/ijms24010529
2. Aijaz M, Ahmad S, Alam S. Regenerative Medicine Unveiled: Principles, Technologies, and Clinical Breakthroughs in Tissue Regeneration. *J CLIN MED KAZ.* 2025;22(5):105-18. https://doi.org/10.23950/jcmk/16880

3. Casarrubea M, Roy, V, Sorbera, Magnusson MS, Santangelo A, Arab A, Crescimanno G. Temporal structure of the rat's behavior in elevated plus maze test. *Behavioural brain research.* 2013; 237: 290-299. https://doi:10.1016/j.bbr.2012.09.049
4. Khan A, Wang B, Ni Y. Chitosan-Nanocellulose Composites for Regenerative Medicine Applications. *Current medicinal chemistry.* 2020; 27(28): 4584-4592. https://doi:10.2174/0929867327666200127152834
5. Rashova M, Amirkhanova Z, Akhmetova S, Tuleubaev B, Turebekova D, Koshanova A, Vinokurov V. Assessment of Antibacterial and Antifungal Activity of a Biocomposite Based on Nanocellulose in Vitro. *J CLIN MED KAZ.* 2025; 22(3): 53-7. https://doi.org/10.23950/jcmk/16328
6. Tambe S, Kumar R, Amin P, Mishra M, Gupta M, Govarthanan K, Narasimhan A, Gupta P. Current aspects of organoid technology for biomaterial toxicity analysis. *Future Med Chem*. 2023; 15(7): 579-582. https://doi:10.4155/fmc-2023-0043
7. Knight P, Chellian R, Wilson R, Behnood-Rod A, Panunzio S, Bruijnzeel AW. Sex differences in the elevated plus-maze test and large open field test in adult Wistar rats. *Pharmacol Biochem Behav.* 2021; 204: 173168. https://doi:10.1016/j.pbb.2021.173168
8. Hilton JR, Simpson SR, Sherman ER. Reactivity to conditioned threat cues is distinct from exploratory drive in the elevated plus maze. Eur J Neurosci. 2023; 57(1): 54-63. https://doi:10.1111/ejn.15870
9. Biedermann SV, Roth L, Biedermann D, Fuss J. Reliability of repeated exposure to the human elevated plus-maze in virtual reality: Behavioral, emotional, and autonomic responses. *Behav Res Methods*. 2024; 56(1): 187-198. https://doi:10.3758/s13428-022-02046-5
10. Kraeuter AK, Guest PC, Sarnyai Z. The Elevated Plus Maze Test for Measuring Anxiety-Like Behavior in Rodents. *Methods Mol Biol.* 2019; 1916: 69-74. https://doi:10.1007/978-1-4939-8994-2_4
11. Danduga RCSR, Kola PK. Elevated Plus Maze for Assessment of Anxiety and Memory in Rodents. *Methods Mol Biol.* 2024; 2761: 93-96. https://doi:10.1007/978-1-0716-3662-6_8
12. Walf AA, Frye CA. The use of the elevated plus maze as an assay of anxiety-related behavior in rodents. *Nat Protoc.* 2007; 2(2): 322-328. https://doi:10.1038/nprot.2007.44
13. Anderson JM, Rodriguez A, Chang DT. Foreign body reaction to biomaterials. *Semin Immunol.* 2008; 20(2): https://doi:10.1016/j.smim.2007.11.004
14. Williams DF. The plasticity of biocompatibility. Biomaterials. 2023; 296: 122077. https://doi:10.1016/j.biomaterials.2023.122077
15. Hurst JL, West RS. Taming anxiety in laboratory mice. *Nat Methods.* 2010; 7(10): 825-826. https://doi:10.1038/nmeth.1500

JOURNAL OF CLINICAL MEDICINE OF KAZAKHSTAN (E-ISSN 2313-1519)
Original Article DOI: https://doi.org/10.23950/jcmk/18054

Study of Serum microRNA-217 Expression Pattern in Different Stages of Diabetic Kidney Disease – a Cross-sectional Study

Ponnudhali Doraiwamy[1], Lakshmi Prabha Sivalingam[2], Priya K. Dhas[3], Nagarajan Palaniappan[4]

[1]*Department of Biochemistry, Vinayaka Missions' Kirupananda Variyar Medical College and Hospital, Vinayaka Missions Research Foundation (DU), Salem, Tamil Nadu, India*
[2]*Department of Biochemistry, KMMC Medical College and Hospital, Muttom, Kanyakumari, Tamil Nadu, India*
[3]*Department of Biochemistry, Vinayaka Missions' Kirupananda Variyar Medical College & Hospital, Vinayaka Missions Research Foundation (DU), Salem, Tamil Nadu, India*
[4]*Department of Nephrology, Govt. Mohankumaramangalam Medical College and Hospital, Salem-1, Tamil Nadu, India*

Received: 2026-02-02.
Accepted: 2026-03-08.

This work is licensed under a **Creative Commons Attribution 4.0 International License**

J Clin Med Kaz 2026; 23(2): 109-114

Corresponding author:
Nagarajan Palaniappan.
E-mail: naganudhali@gmail.com.
ORCHID: 0009-0002-6841-7307.

ABSTRACT

Background: Diabetic kidney disease (DKD) represents the leading cause of end-stage renal disease worldwide, affecting 30-40% of patients with type 2 diabetes mellitus (T2DM). Some microRNAs (miRNAs), like miRNA-217 are upregulated in Diabetic Kidney Disease (DKD), and known to play a key role in Diabetes Mellitus & its complications. Recent studies have shown miRNA 217 to be involved in the development of DKD, by promoting renal inflammation, angiogenesis and fibrosis.

Aim and objectives: To assess the miR217 expression levels in DKD patients with differing stages of albuminuria, compared to normoalbuminuric Diabetes mellitus -II patients & to identify its role as a predictive biomarker of DKD.

Methodology: This analytical cross-sectional study recruited 135 participants aged 40-65 years from a Govt medical college Hospital in Tamil Nadu. Participants includedT2DM patients (n=34) & DKD patients & healthy controls(n=35). Fasting serum samples were collected & miRNA-217 extraction and qRT-PCR quantification was done & Fold change was calculated, along with the baseline clinical parameters (age, BMI, HbA1c, lipids, urea, creatinine, eGFR, UACR).

Statistical analyses like Kruskal-Wallis tests, Spearman's correlations & ROC curves were computed using Jamovi software version 2.6.44

Results: Serum miRNA-217 expression was markedly elevated in DKD patients with microalbuminuria (39.36 ± 76.24 fold change) & macroalbuminuria (64.32 ± 109.23 fold change) compared to Diabetes mellitus -II patients with normoalbuminuria (2.29 ± 4.77, P=0.027).MiRNA-217 correlated positively with UACR (ρ=0.472, p<0.001) and was able to discriminate DKD from Diabetes-II, with 59% sensitivity & 90% specificity, ROC analysis yielded AUC 0.738 (p<0.001).

Conclusion: Serum miRNA-217 exhibits progressive up-regulation in accordance with stages of DKD severity, with moderate diagnostic utility. miRNA-217 could be a potential biomarker for early DKD detection and risk stratification, warranting longitudinal studies in larger populations for further validation and establishment of these findings.

Keywords: microRNA 217, miRNA 217, Diabetic Kidney Disease, DKD, UACR.

Introduction

Diabetic Kidney Disease (DKD) is a microvascular complication affecting 30–40% of patients with diabetes, and it is the leading cause of chronic kidney disease and end-stage renal disease (ESRD) worldwide (1,2). DKD develops through complex pathogenic mechanisms triggered primarily by sustained hyperglycemia, which induces metabolic and hemodynamic alterations, including glomerular hyperfiltration, glomerulosclerosis, tubulointerstitial inflammation, and fibrosis (2,3).

MicroRNAs (miRNAs) are endogenous, small non-coding RNAs that regulate gene expression post-transcriptionally by targeting messenger RNAs. They play crucial roles in maintaining cellular homeostasis and are involved in various biological processes, such as proliferation, differentiation, and immune response regulation. Dysregulation of miRNAs contributes to the development and progression of several diseases, including cardiovascular diseases, cancer, autoimmune disorders, infectious diseases, Diabetic Kidney Disease (DKD), and neurodegenerative conditions. Their altered expression can serve as diagnostic biomarkers and therapeutic targets, highlighting their potential in disease diagnosis and treatment strategies (4–7).

Many microRNAs have been implicated in the pathogenesis and progression of DKD, though with varying results. One such microRNA, miRNA-217, has been identified to play a crucial role in the pathogenesis and progression of DKD. miRNA-217 is found to promote angiogenesis and renal fibrosis by inhibiting the expression of SIRT1, a protein that protects against oxidative stress, apoptosis, and fibrosis, thereby leading to the development of DKD (8).

Upregulation of miR-217 expression could be an important molecular mediator in DKD, and increasing levels could indicate the progression of disease (9). There are very few human studies on miR-217 levels in Diabetic Kidney Disease carried out in the Indian population. This study is an attempt to identify the variations in miR-217 levels in different stages of severity of DKD and to assess its diagnostic utility as a candidate biomarker for DKD in a small population in South India.

Methods

Study Design and Participants

This is an analytical cross-sectional study conducted in 135 participants aged 40–65 years attending the Diabetology OPD in a Government Medical College Hospital in Salem, Tamil Nadu. The study included 35 healthy non-diabetic controls with normal renal function and 100 patients with type 2 diabetes mellitus (T2DM) categorized by urinary albumin/creatinine ratio (UACR) into normoalbuminuria (<30 mg/g, n=34), microalbuminuria (30–300 mg/g, n=33), and macroalbuminuria (>300 mg/g, n=33).

Patients with type 2 Diabetes Mellitus and Diabetic Nephropathy were included in the study. Healthy non-diabetic controls without any comorbid illness formed the control group. Individuals with malignancies, chronic renal, liver, or cardiac diseases, urinary tract infections, renal stones, recent nephrotoxic drug use, co-existing comorbid conditions such as ischemic heart disease, hypertension, other diabetic complications, or recent NSAID or hormonal treatment were excluded from the study. Institutional Ethical Committee approval was obtained prior to the commencement of the study, and written informed consent was obtained from all participants before enrollment.

Laboratory Analysis

Fasting blood and urine samples were collected. Five millilitres of venous blood were drawn from each participant and divided into two parts: one for biochemical tests and the other for RNA extraction. Two millilitres were collected in fluoride-containing tubes, another 2 mL in EDTA-containing tubes, and the remaining portion was left for 10 minutes to clot and then centrifuged at 3000 rpm for 5 minutes. The first part for biochemical tests was used immediately, while the second part was stored for miRNA detection. Serum was separated and stored in RNase/DNase-free tubes at −80°C until RNA isolation.

Clinical and laboratory assessments included comprehensive demographic data collection, including age, sex, and relevant medical history. Renal function was evaluated using the estimated glomerular filtration rate (eGFR) calculated using the CKD-EPI formula, and the urinary albumin-to-creatinine ratio (UACR) was measured from spot urine samples to classify the stages of diabetic nephropathy. Additional biochemical parameters assessed included fasting blood glucose, HbA1c, lipid profile, serum urea, and creatinine levels using the fully automated analyzer (EM200) and HbA1c analyzer (TOSOH).

MiRNA Extraction (Qiagen Kit)

MiRNAs were isolated using a miRNA extraction kit. The collected serum was mixed with 300 µl of binding buffer solution, and then ethanol was added to precipitate total RNA and eluted in nuclease-free water. Total RNA was then incubated with miRNA wash solutions without preamplification, and purified small RNA molecules were eluted in 50–100 µl of sterile RNase-free water supplied with the kit. The samples were stored at −80°C until used.

Primer Design and Positive Controls

Three primers were designed each for miR-217 and miR-423-5p, which was used as an endogenous control. One forward primer (5'-AACACGTGTACTGCATCAGGAAC-3'), Universal reverse primer (5'-GCGAGCACAGAATTAATACGAC-3'), Universal reverse transcriptase primer (5'-GCGAGCACAGA ATTAATACGACTCACTATAGGTTTTTTTTTTTTVN-3'). Synthetic oligonucleotides for miR-217-5p and miR-423-5p were ordered for optimization.

cDNA Synthesis and miR-217 Amplification

After RNA extraction, samples were converted into cDNA using the PolyA method, employing PolyA enzyme, RT enzyme, and universal RT primer. Quantitative real-time polymerase chain reaction (qRT-PCR) was employed to quantify miRNA-217 levels using specific primers and BioRad SsoAdvanced SYBR Green Supermix on a QuantStudio 8 RT-PCR system. Normalization was performed using the endogenous control miRNA-423-5p to correct for expression levels across the control and DKD groups (10). Fold change of miR-217 in all samples was calculated using the Livak method 2^(−ΔΔCt) (11). Quality control included assessment of RNA concentration and purity by spectrophotometry (NanoDrop method) and verification of PCR efficiency and specificity through melt curve analysis.

Statistical Analysis

Descriptive statistics of baseline parameters and group comparisons of miR-217 and other parameters were performed using non-parametric tests (Kruskal-Wallis), which are appropriate given the non-normal distribution of miRNA fold-change data. Correlation analyses employed Spearman's rank

correlation to evaluate associations between miRNA-217 levels and clinical parameters such as UACR and glycemic indices. Receiver operating characteristic (ROC) curve analysis was performed to assess the diagnostic accuracy of miRNA-217 as a diagnostic biomarker of Diabetic Nephropathy. Data analysis was performed using Jamovi software version 2.6.44. A post-hoc power analysis was conducted using the observed AUC of 0.738, with $\alpha = 0.05$ and a case-to-control ratio of 66:34 (DKD:DM-II), which yielded a post-hoc power of approximately 80%, suggesting adequate statistical power to detect the observed diagnostic effect for the primary biomarker outcome.

Table 1 Baseline Characteristics of the Study Participants

S. No	Parameter	Healthy Controls (Mean ± SD)	Diabetes Mellitus-II (Mean ± SD)	Diabetic Kidney Disease (Mean ± SD)
1	N	35	34	66
2	Age (years)	51.27 ± 10.75	52.91 ± 10.29	56.35 ± 9.59
3	BMI	23.21 ± 5.28	26.37 ± 4.95	24.41 ± 5.10
4	Duration of Diabetes	—	5.86 ± 5.7	7.52 ± 7.0
5	FBS (mg/dl)	79.73 ± 16.47	159.79 ± 79.26	173.42 ± 87.70
6	HbA1c (%)	5.54 ± 0.85	8.60 ± 2.25	8.77 ± 2.64
7	Urea (mg/dl)	25.03 ± 5.82	24.58 ± 9.14	29.72 ± 17.94
8	Creatinine (mg/dl)	0.93 ± 0.18	1.09 ± 0.37	1.40 ± 0.76
9	T. Cholesterol	172.17 ± 31.59	184.84 ± 50.13	174.4 ± 48.29
10	Triglycerides	158.52 ± 67.77	175.98 ± 90.58	184.70 ± 96.19
11	HDL	41.07 ± 7.83	47.79 ± 30.68	44.06 ± 9.85
12	LDL	99.40 ± 32.89	115.82 ± 43.82	94.02 ± 39.41
13	eGFR (ml/min)	80.60 ± 22.25	70.06 ± 15.52	60.63 ± 24.04
14	UACR	13.55 ± 9.19	15.14 ± 8.3	1087.8 ± 2320.22
15	miRNA-217 expression	—	2.29 ± 4.77	46.70 ± 87.38

Results

Participant Characteristics and Baseline Parameters

The study included 35 healthy controls, 34 patients with Diabetes Mellitus-II (DM-II), and 66 patients with Diabetic Kidney Disease (DKD) who were further divided into those with microalbuminuria (n=33) and macroalbuminuria (n=33), totalling 135 participants. The mean age of the participants was 54.1 years and all groups were age-matched (p=0.15). The baseline characteristics of the Diabetes Mellitus-II and DKD groups are presented in Table 1. The glycemic indices — fasting blood sugar (FBS) and HbA1c — were significantly different among all four groups (p<0.001), as shown in Figure 1. Similarly, the renal parameters — urea and creatinine — were significantly different among the groups (p=0.006, p<0.001, respectively). The estimated glomerular filtration rate (eGFR) was significantly lower in patients with DKD, with the most pronounced decline observed from the normoalbuminuria to the macroalbuminuria group (p<0.001). While lipid parameters such as total cholesterol and LDL were significantly different among the groups (p=0.002, p<0.001), serum HDL and BMI showed no significant change, as given in Table 2.

MiRNA-217 Expression in Diabetes Mellitus-II and DKD

In patients with DKD, miRNA-217 expression increased progressively from the normoalbuminuria to the macroalbuminuria group (Table 2), the difference being statistically significant (p=0.008). miRNA-217 expression (fold change) was significantly elevated in DKD patients with microalbuminuria (39.36 ± 76.24 fold change) versus Diabetes Mellitus-II patients with normoalbuminuria (2.29 ± 4.77, p=0.027), and among DKD patients with macroalbuminuria (64.32 ± 109.23 fold change) versus Diabetes Mellitus-II patients with normoalbuminuria (2.29 ± 4.77, p=0.017). No significant difference was found between the micro- and macroalbuminuria groups (p=0.803). The large standard deviations relative to the mean miRNA-217 fold-change values are reflective of the inherent inter-individual biological variability in circulating miRNA expression, which is well-documented in serum miRNA biomarker studies and is a recognized characteristic of miRNA quantification in heterogeneous clinical populations (21,23).

Table 2 Comparison of miR-217 and Other Parameters Across Study Groups

S. No	Parameters	Healthy Controls (Mean ± SD)	DM-II Normoalbuminuria (Mean ± SD)	DKD Microalbuminuria (Mean ± SD)	DKD Macroalbuminuria (Mean ± SD)	P-value
1	Age (years)	51.27 ± 10.75	52.91 ± 10.29	56.02 ± 9.70	56.21 ± 9.57	0.15
2	BMI	23.21 ± 5.28	26.37 ± 5.00	24.34 ± 5.64	24.59 ± 3.76	0.070
3	Duration of Diabetes	—	5.86 ± 5.7	7.43 ± 7.16	7.75 ± 6.76	0.017
4	FBS (mg/dl)	79.73 ± 16.47	159.79 ± 79.26	161.63 ± 81.30	201.95 ± 98.04	<0.001
5	HbA1c (%)	5.54 ± 0.85	8.60 ± 2.25	8.41 ± 2.66	9.62 ± 2.48	<0.001
6	Urea (mg/dl)	25.03 ± 5.82	24.58 ± 9.14	25.57 ± 10.96	39.79 ± 26.31	0.006
7	Creatinine (mg/dl)	0.93 ± 0.18	1.09 ± 0.37	1.21 ± 0.51	1.85 ± 1.04	<0.001
8	T. Cholesterol	166.07 ± 21.84	172.77 ± 30.05	176.48 ± 39.10	214.17 ± 49.56	0.002
9	Triglycerides	158.52 ± 67.77	175.98 ± 90.58	176.84 ± 81.31	203.32 ± 125.3	0.784
10	HDL	41.07 ± 7.83	47.79 ± 30.68	43.78 ± 8.84	44.74 ± 12.16	0.546
11	LDL	92.95 ± 25.54	98.45 ± 37.61	101.96 ± 32.80	132.88 ± 32.84	<0.001
12	eGFR (ml/min)	80.6 ± 22.25	70.06 ± 15.52	66.9 ± 23.25	45.47 ± 19.01	<0.001
13	UACR	13.55 ± 9.19	15.14 ± 8.3	101.15 ± 64.77	3476.5 ± 3258.8	<0.001
14	miRNA-217 expression	—	2.29 ± 4.77	39.36 ± 76.24	64.32 ± 109.23	0.008

Table 3 ROC Curve Summary

	AUC	Std. Error	95% CI Lower	95% CI Upper	P
miRNA-217	0.738	0.0658	0.609	0.867	<0.001

Cut-off	Sensitivity	Specificity	PPV	NPV	Accuracy	Youden's Index
2.95	59%	90%	92%	52.94%	69.5%	0.490

Non-parametric statistical tests were therefore employed throughout, as these do not assume normality of distribution and are robust to such variability. miRNA-217 expression showed a strong positive correlation with UACR (Spearman's rho = 0.472, p<0.001), indicating a significant association with increasing albuminuria severity (Table 3).

miRNA-217 as a Diagnostic Biomarker of DKD

ROC curve analysis for miRNA-217 showed an area under the curve (AUC) of 0.738 (95% CI: 0.609–0.867, p<0.001), indicating moderate to good diagnostic accuracy for distinguishing between DKD and Diabetes Mellitus-II without DKD. At a cut-off of 2.95 fold change, miRNA-217 demonstrated 59% sensitivity, 90% specificity, 92% positive predictive value (PPV), and 52.94% negative predictive value (NPV), with an overall accuracy of 69.5%. While the sensitivity of 59% is modest, the high specificity of 90% and PPV of 92% suggest that miRNA-217 may be particularly valuable as a confirmatory or rule-in biomarker when used adjunctively alongside established clinical markers such as UACR and eGFR, rather than as a standalone screening test.

Discussion

The present study was conducted in a small South Indian population with 135 participants, consisting of 35 healthy non-diabetic controls (Group 4), 34 individuals with Diabetes Mellitus-II (Group 1 — normoalbuminuria), and 66 individuals with DKD further divided into Group 2 (microalbuminuria, n=33) and Group 3 (macroalbuminuria, n=33).

In this cross-sectional study, serum miRNA-217 was significantly upregulated in the micro- and macroalbuminuria groups compared to those with normoalbuminuria (p=0.008) and showed a positive correlation with UACR (p<0.001), implicating its plausible relationship with albuminuria status. Our findings are similar to those of Shao et al., who proposed that serum miR-217 levels steadily increased in individuals presenting with microalbuminuria and macroalbuminuria compared to those with normoalbuminuria (9). Although the glycemic indices — fasting blood glucose (FBG) and HbA1c — were significantly elevated in participants with Diabetes Mellitus and Diabetic Kidney Disease compared to healthy controls (p<0.001), they did not correlate with miR-217 levels.

It is acknowledged that diabetes duration showed a significant difference across groups (p=0.017), representing a potential confounder. However, given the limited sample size of this study, formal multivariable regression analysis incorporating multiple covariates was not feasible. Age, on the other hand, was not significantly different across the four groups (p=0.15, Table 2), thereby minimizing its confounding potential. Future studies with larger sample sizes should incorporate multivariable regression models to adjust for duration of diabetes and other potential confounders.

miRNA-217 has been implicated in the pathogenesis of Diabetic Kidney Disease by inactivating sirtuin 1 (SIRT1), a member of the silent information regulator 2 family of NAD-dependent deacetylases that function as transcriptional regulators (12). Gene polymorphisms in the gene encoding Sirtuin 1 have been found to be associated with the development of Diabetic Nephropathy (13,14). Many mechanisms have been proposed to explain the renoprotective role of SIRT1. Hasegawa et al. reported that downregulation of SIRT1 upregulates the expression of Claudin-1 protein, thereby contributing to albuminuria in DKD (15,16). Claudin-1 is an integral component of the tight junction, and an increase in its levels results in podocyte effacement and albuminuria (17). miR-217 has been found to directly act on the 3'UTR of the SIRT1 gene and significantly inhibit the expression of SIRT1, thereby acting as a negative regulator of SIRT1 (18). This explains the probable mechanism underlying our findings of upregulation of miR-217 in patients with both micro- and macroalbuminuria, while showing no change in normoalbuminuric Diabetes patients.

SIRT1 also deacetylates and inactivates Hypoxia-Inducible Factor-1α (HIF-1α), which plays a significant role in promoting renal fibrosis and renal sclerosis (19). Shao et al. showed that miRNA-217 is markedly upregulated, leading to suppression of SIRT1, activation of HIF-1α, and subsequent induction of profibrotic and pro-inflammatory mediators including CTGF, endothelin-1, fibronectin, TGF-β1, and VEGF; while gene silencing of miRNA-217 attenuated these responses (20). These observations provide evidence that miRNA-217 is an upstream regulator of the SIRT1/HIF-1 axis, a pathway implicated in tubular hypoxia, interstitial fibrosis, and albuminuria seen in Diabetic Nephropathy (19,21). Similar work in podocytes has demonstrated that high-glucose conditions elevate miRNA-217 and that specific inhibition of miRNA-217 restores PTEN expression, enhances autophagic flux, and mitigates podocyte injury and insulin resistance (7).

The present findings suggest that serum miRNA-217 expression increases with advancing albuminuria, along with a significant decline in eGFR from the normoalbuminuric DM-II group to the DKD group with macroalbuminuria (p<0.001) and between the micro- and macroalbuminuria groups (p=0.005). However, no significant correlation was found between miR-217 and eGFR. According to Loredana Fiorentino et al., miRNA-217 was found to be upregulated in diabetic mouse kidneys and mesangial cells treated with high glucose (22). miRNA-217 has been found to be increased in DKD patients and was positively correlated with ln(albumin-creatinine ratio), HbA1c, HOMA-IR, and HIF-1α, while showing a negative correlation with SIRT1 (9).

The large standard deviations observed in miRNA-217 fold-change values across all groups are consistent with the well-documented inter-individual biological variability inherent to circulating miRNA measurements in clinical populations (21,23). This variability is further attributable to differences in disease heterogeneity, metabolic status, and comorbid burden among participants. The use of non-parametric statistical methods (Kruskal-Wallis and Spearman's correlation) was specifically chosen to account for this non-normal distribution, and results were statistically significant despite this variability, underscoring the robustness of the observed associations.

Given the cross-sectional design of this study, the term "predictive biomarker" has been intentionally avoided throughout the revised manuscript. miRNA-217 is herein described as a diagnostic biomarker and a candidate for risk

stratification. The observed 59% sensitivity, while modest for a standalone screening tool, is complemented by the high specificity of 90% and PPV of 92%, suggesting that miRNA-217 may function best as a confirmatory or adjunct biomarker in combination with established clinical markers such as UACR and eGFR. These findings are exploratory in nature and require validation in prospective longitudinal studies.

To assess the role of miRNA-217 as a diagnostic biomarker of DKD, ROC curve analysis was performed, which showed that serum miRNA-217 could discriminate DKD from T2DM without nephropathy ($p<0.001$) with moderate sensitivity and high specificity. As the miR-217 levels correlate with DKD severity, its levels could be utilized for the early detection and monitoring of DKD progression, enabling timely clinical intervention. This study emphasizes the important role played by miRNA-217 in the pathophysiology of DKD, highlighting its potential as an emerging diagnostic biomarker. Given the very limited number of human studies relating miR-217 to DKD, the present findings could represent an important milestone in advancing miRNA research directed towards DKD diagnosis and management. These results require validation in further longitudinal studies in larger populations.

Limitations

The limitations of the present study include the smaller sample size, absence of an a priori power calculation, lack of longitudinal follow-up of Diabetes and DKD patients, and the inability to perform multivariable regression analysis to adjust for potential confounders such as diabetes duration due to the limited sample size. Furthermore, the cross-sectional design precludes any causal or temporal inference regarding the role of miRNA-217 in DKD progression. The modest sensitivity of 59% limits its standalone clinical application as a screening biomarker.

Scope for Future Study

Prospective longitudinal studies in larger populations are warranted to validate the diagnostic utility of serum miRNA-217 in DKD. Multivariable regression analyses adjusting for key confounders including diabetes duration, hypertension, and medications should be incorporated. SIRT1 levels can be measured and their relationship with miR-217 expression in type 2 Diabetes and DKD patients can be assessed to further elucidate the mechanistic pathway.

Conclusion

Serum miRNA-217 levels have been found to be upregulated in type 2 diabetes patients and increase progressively with DKD severity, correlating positively with albuminuria — a key marker of kidney damage. With only a few studies available, the present study is an attempt to assess the role of miR-217 in DKD as a diagnostic biomarker, while future studies in larger populations are needed to establish its exact role in DKD pathogenesis. Once proven, miRNA-217 silencing could prove to be a novel therapeutic strategy to alleviate the inflammation and fibrotic changes seen in DKD, thereby extending the treatment protocol beyond conventional glycemic and blood pressure control. This targeted approach appears promising and could arrest or slow kidney damage and improve clinical outcomes in patients with Diabetic Nephropathy.

Author Contributions: Conceptualization, N.P. and P.D.; methodology, P.D., L.P.S. and P.K.D.; validation, P.D. and P.K.D.; formal analysis, P.D. and L.P.S.; investigation, P.D., L.P.S. and N.P.; resources, N.P.; data curation, P.D. and L.P.S.; writing – original draft preparation, P.D.; writing – review and editing, P.D., L.P.S., P.K.D. and N.P.; visualization, P.D. and P.K.D.; supervision, N.P.; project administration, N.P.; funding acquisition, N/A. All authors have read and agreed to the published version of the manuscript.

Disclosures: The authors have no conflicts of interest.

Acknowledgments: The authors thank all participants who contributed to this study and the laboratory staff for their technical assistance.

Funding: None.

Data availability statement: The datasets generated during and/or analyzed during the current study are available from the corresponding author on reasonable request.

Artificial Intelligence (AI) Disclosure Statement: The authors declare no AI Tools used for preparation of this work.

References

1. Gu HF. Genetic and Epigenetic Studies in Diabetic Kidney Disease. *Front Genet.* 2019; 10: 507. https://doi.org/10.3389/fgene.2019.00507
2. Alicic RZ, Rooney MT, Tuttle KR. Diabetic Kidney Disease: Challenges, Progress, and Possibilities. *Clin J Am Soc Nephrol*. 2017; 12 (12): 2032-2045. https://doi.org/10.2215/CJN.11491116
3. DeFronzo RA, Reeves WB, Awad AS. Pathophysiology of diabetic kidney disease: impact of SGLT2 inhibitors. *Nat Rev Nephrol*. 2021; 17 (5): 319-334. https://doi.org/10.1038/s41581-021-00393-8
4. Paul P, Chakraborty A, Sarkar D, Langthasa M, Rahman M, Bari M, Singha RS, Malakar AK, Chakraborty S. Interplay between miRNAs and human diseases. *J Cell Physiol.* 2018; 233 (3): 2007-2018. https://doi.org/10.1002/jcp.25854
5. Romakina VV, Zhirov IV, Nasonova SN, Grachev VG, Safronova EM, Tereshchenko SN. Circulating microRNAs as potential biomarkers of myocardial fibrosis in patients with heart failure. *Kardiologiia*. 2018; (1): 66-71. https://doi.org/10.18087/cardio.2018.1.10083
6. Latini A, Ciccacci C, Novelli G, Borgiani P. Polymorphisms in miRNA genes and their involvement in autoimmune diseases susceptibility. *Immunol Res.* 2017; 65 (4): 811-827. https://doi.org/10.1007/s12026-017-8937-8
7. Kimura M, Kothari S, Gohir W, Camargo JF, Husain S. MicroRNAs in infectious diseases: potential diagnostic biomarkers and therapeutic targets. *Clin Microbiol Rev.* 2023; 36 (4): e0001523. https://doi.org/10.1128/cmr.00015-23

8. Samadi M, Aziz SG, Naderi R. The effect of tropisetron on oxidative stress, SIRT1, FOXO3a, and claudin-1 in the renal tissue of STZ-induced diabetic rats. *Cell Stress Chaperones.* 2021; 26 (1): 217-227. https://doi.org/10.1007/s12192-020-01170-5
9. Shao Y, Ren H, Lv C, Ma X, Wu C, Wang Q. Changes of serum Mir-217 and the correlation with the severity in type 2 diabetes patients with different stages of diabetic kidney disease. *Endocrine*. 2017; 55 (1): 130-138. https://doi.org/10.1007/s12020-016-1069-4
10. Wong L, Tsang YS, Kenny R, Lyburn M, McMahon LP. MiR-423-5p as Optimal Endogenous Control for Quantification of Circulating MicroRNAs in Patients With CKD. Kidney Int Rep. 2023; 8 (10): 2150-2152. https://doi.org/10.1016/j.ekir.2023.07.018
11. Qureshi R, Sacan A. A novel method for the normalization of microRNA RT-PCR data. *BMC Med Genomics.* 2013; 6 Suppl 1 (Suppl 1): S14. https://doi.org/10.1186/1755-8794-6-S1-S14
12. Michishita E, Park JY, Burneskis JM, Barrett JC, Horikawa I. Evolutionarily conserved and nonconserved cellular localizations and functions of human SIRT proteins. *Mol Biol Cell.* 2005; 16 (10): 4623-4635. https://doi.org/10.1091/mbc.e05-01-0033
13. Maeda S, Koya D, Araki SI, Babazono T, Umezono T, Toyoda M, Kawai K, Imanishi M, Fukatsu A, Yasuda M, Kasuga M, Nishio Y, Haneda M. Association between single nucleotide polymorphisms within genes encoding sirtuin families and diabetic nephropathy in Japanese subjects with type 2 diabetes. *Clin Exp Nephrol.* 2011; 15 (3): 381-390. https://doi.org/10.1007/s10157-011-0418-0
14. Tang K, Sun M, Shen J, Zhou B. Transcriptional Coactivator p300 and Silent Information Regulator 1 (SIRT1) Gene Polymorphism Associated with Diabetic Kidney Disease in a Chinese Cohort. *Exp Clin Endocrinol Diabetes.* 2017; 125 (8): 530-537. https://doi.org/10.1055/s-0043-103966
15. Chuang PY, Xu J, Dai Y, Jia F, Mallipattu SK, Yacoub R, Gu L, Nadkarni GN, Shu L, Klotman PE, He JC. In vivo RNA interference models of inducible and reversible Sirt1 knockdown in kidney cells. *Am J Pathol.* 2014; 184 (7): 1940-1956. https://doi.org/10.1016/j.ajpath.2014.03.016
16. Schelling JR. Tubular atrophy in the pathogenesis of chronic kidney disease progression. *Pediatr Nephrol*. 2016; 31 (5): 693-706. https://doi.org/10.1007/s00467-015-3169-4
17. Wang W, Sun W, Cheng Y, Xu Z, Cai L. Role of sirtuin-1 in diabetic nephropathy. *J Mol Med (Berl).* 2019; 97 (3): 291-309. https://doi.org/10.1007/s00109-019-01743-7
18. Xiao H, Liu Z. Effects of microRNA 217 on high glucose induced inflammation and apoptosis of human retinal pigment epithelial cells (ARPE 19) and its underlying mechanism. *Mol Med Rep.* 2019; 20 (6): 5125-5133. https://doi.org/10.3892/mmr.2019.10778
19. Matoba K, Kawanami D, Okada R, Tsukamoto M, Kinoshita J, Ito T, Ishizawa S, Kanazawa Y, Yokota T, Murai N, Matsufuji S, Utsunomiya K. Rho-kinase inhibition prevents the progression of diabetic nephropathy by downregulating hypoxia-inducible factor 1α. *Kidney Int.* 2013; 84 (3): 545-554. https://doi.org/10.1038/ki.2013.130
20. Shao Y, Lv C, Wu C, Zhou Y, Wang Q. Mir-217 promotes inflammation and fibrosis in high glucose cultured rat glomerular mesangial cells via Sirt1/HIF-1α signaling pathway. *Diabetes Metab Res Rev.* 2016; 32 (6): 534-543. https://doi.org/10.1002/dmrr.2788
21. Fukami K, Yamagishi S, Ueda S, Okuda S. Novel therapeutic targets for diabetic nephropathy. *Endocr Metab Immune Disord Drug Targets.* 2007; 7 (2): 83-92. https://doi.org/10.2174/187153007780832118
22. Szostak J, Gorący A, Durys D, Dec P, Modrzejewski A, Pawlik A. The Role of MicroRNA in the Pathogenesis of Diabetic Nephropathy. *Int J Mol Sci.* 2023; 24 (7): 6214. https://doi.org/10.3390/ijms24076214

CONTENTS

(E-ISSN 2313-1519)
JOURNAL OF CLINICAL MEDICINE OF KAZAKHSTAN

Vitorino Modesto dos Santos, Kin Modesto Sugai, Rafael Campos Nunes
ST-ELEVATION MYOCARDIAL INFARCTION AND ALCOHOL MIXED WITH ENERGY DRINK 4

Aytan Shirinova, Chingiz Asadov, Aypara Hasanova, Zohra Alimirzoyeva
16-YEAR EPIDEMIOLOGIC STUDY OF CHRONIC MYELOID LEUKEMIA IN AZERBAIJAN: CLINICAL AND MOLECULAR INSIGHTS 6

Nurlan R. Utelbayev, Marina A. Morenko, Aleksandr N. Pampura, Kseniya V. Shnayder, Madina R. Gatauova, Nadezhda A. Mayevskaya, Zhanat N. Abdikadyr, Adil A. Zhamankulov, Yerlan Suleimenov, Alexey Balas
THE REGION-SPECIFIC LANDSCAPE OF SENSITIZATION TO RESPIRATORY ALLERGENS IN THE POPULATION OF KAZAKHSTAN ACCORD BASED ON MOLECULAR DIAGNOSTICS 19

Thirunavukkarasu Jaishankar, Preetha Madhan, Sarguru Datchanamurthi, Kalaiselvi Vairavan Pillai Subbammal, Rhona Madhan
EVALUATION OF SERUM GROWTH DIFFERENTIATION FACTOR-15 (GDF-15) AS A NON-INVASIVE BIOMARKER FOR DISEASE SEVERITY AND PAIN INTENSITY IN ENDOMETRIOSIS: A HOSPITAL BASED CASE-CONTROL STUDY 31

Murat B. Zhumabayev, Karlygash S. Kabdenova, Khalka B. Baubekova, Yerlan U. Umbetzhanov, Zhandos K. Burkitbayev, Asima S. Izmailova, Assemgul S. Kassenova
ANESTHETIC MANAGEMENT DURING PIPAC: CLINICAL AND PRACTICAL ASPECTS 39

Seda Sertel Meyvaci, Yusuf Secgin, Taha Gokmen Ulger, Tuba Taslamacioglu Duman, Beyza Celik, Sena Demiroglu
DETERMINATION OF BODY MASS INDEX USING MACHINE LEARNING REGRESSION METHODS FROM BODY COMPOSITION PARAMETERS 45

Saule Nukusheva, Almagul Saduova, Aman Berkinbay, Samal Aliyeva, Dana Zauytbek, Akerke Azanbai, Aygerim Ayazova, Araylim Abduali, Aiya Slamhan, Anel Daber
CYTOGENETIC CHARACTERISTICS AND TREATMENT OUTCOMES OF CONGENITAL ACUTE LEUKEMIA IN CHILDREN IN KAZAKHSTAN: RETROSPECTIVE STUDY 51

Leela Pattapu, Priya K. Dhas, K.P. Mekhala, Ponnudhali D, Chakrapani Cheekavolu
MULTI-BIOMARKER STRATIFICATION OF CORONARY ARTERY DISEASE IN DIABETIC AND NON-DIABETIC PATIENTS: ADIPONECTIN, INFLAMMATION, AND INSULIN RESISTANCE 57

Arailym Abilbayeva, Tair Nurpeissov, Balaussa Seitkhan, Nuray Shaktay
BIOINFORMATICS ANALYSIS IDENTIFYING KEY GENES AND SIGNALING PATHWAYS INVOLVED IN THE EGG ALLERGY IN YOUNG CHILDREN: A RETROSPECTIVE STUDY 64

Sibel Yücetürk, Nurten Özçalkap, Ayşe Çuvadar, Yeter Çuvadar Baş
THE EFFECT OF POSTMENOPAUSAL THERAPEUTIC INTERVENTIONS ON SEXUAL FUNCTION: A META-ANALYSIS STUDY 72

Dinara B. Nemetova, Mira B. Zhunisova, Karlygash Zh. Sadykova, Gulnaz O. Nuskabayeva, Ugilzhan B. Tatykayeva, Aziza T. Dzhurabekova, Dilbar N. Aidarbekova
THE STROOP TEST AS A TOOL FOR ASSESSING COGNITIVE DYSFUNCTION IN PATIENTS WITH METABOLIC SYNDROME 79

Sujatha Nagari, Zareena Begum Miyajan, Kalpana Thondapu, Udaya Kumar Pillam, Ratna Priyanka Janamala
STRUCTURAL AND COGNITIVE MEASURES ACROSS CHILDHOOD, ADOLESCENCE, AND ADULTHOOD: ASSOCIATIONS WITH EDUCATION AND BRAIN MORPHOMETRY 87

Madina Rashova, Saule Akhmetova, Berik Tuleubaev, Zhanerke Bolat, Ulzhalgas Mukhtarkhan, Kamila Tazabekova, Ivan Lavrinenko, Vitaliy Feoktistov
IMPACT OF NANOCELLULOSE-BASED BIOCOMPOSITE IMPLANTATION ON RODENT BEHAVIOR IN THE ELEVATED PLUS MAZE TEST 104

Ponnudhali Doraiwamy, Lakshmi Prabha Sivalingam, Priya K. Dhas, Nagarajan Palaniappan
STUDY OF SERUM MICRORNA-217 EXPRESSION PATTERN IN DIFFERENT STAGES OF DIABETIC KIDNEY DISEASE – A CROSS-SECTIONAL STUDY 109